THE SURFACE CHARACTERISATION OF POLYMER LATICES PREPARED WITH SPECIFIC SURFACE GROUPS

ALAN ROY GOODALL

This thesis is submitted as partial fulfulment for the degree of Doctor of Philosophy, Council for National Academic Awards. The work reported in this thesis was carried out in the Department of Physical Sciences, Trent Polytechnic, Nottingham, and in the Organic and Physical Protection Division, Chemical Defence Establishment, Porton Down, Salisbury.

November, 1976.

TO

My Mother and Father

and C.E.P.

ACKNOWLEDGEMENTS

I would like to gratefully acknowledge the continued help and guidance given to me during the course of this work by Dr. J. Hearn and Dr. M.C. Wilkinson. I would like to thank both Trent Polytechnic and the Chemical Defense Establishment, Porton Down, for provision of funding and facilities. My thanks also go to Mrs. J. Waldron who kindly undertook the typing of this Thesis.

PLATE LEGENDS

CONTENTS

SYNOPSIS

Several detailed aspects of the preparation and characterisation of polystyrene latices produced in the absence of added soap have been studied.

Kinetic experiments have been carried out at varying temperatures. These studies showed that the rate of polymerisation per particle was directly proportional to the particle radius and that growth did not appear to occur solely within the particles, nuclei being continuously formed in the aqueous phase which undergo heterocoagulation with the primary particles.

The presence of 'anomalous particles' has been confirmed and investigated. Their formation is due to the removal of monomer from the particles prior to electron microscopy. The monomer concentration within the particles is heterogenous, this heterogeneity is probably due to the presence within the particles of a region of low molecular weight (~1000) material which arises during particle nucleation.

Particle nucleation is thought to occur via either a precipitation or micellisation process involving free radical oligomers of ~500 molecular weight. It is demonstrated that if this is the case and these nuclei are stable, they can become unstable on further growth. Coagulation then occurs until stability is regained. An initial decrease in number of particles ml^{-1} has been observed in all reactions studied using electron microscopy. A similar decrease has also been observed in reactions followed using laser light scattering.

It was found that steam stripping was an efficient technique for removing monomer and benzaldehyde from latices, these moieties being present even after prolonged dialysis. Benzaldehyde was found to be capable of initiating styrene polymerisation in the presence of light to produce a latex, and also the presence of benzaldehyde within a latex could result in the incorporation onto the particle surfaces of weak acid groupings.

The use of potassium peroxydiphosphate as an initiator for emulsion polymerisation has been studied. It was found incapable of initiation when used alone. In the presence of heavy metal ions latices were produced stabilised by phosphate groups. When used in conjunction with sodium metabisulphite latices were produced predominantly stabilised by sulphonate groups. Sulphonate and phosphate groups were found to be much more stable to hydrolysis than sulphate groups.

CHAPTER I

A. EMULSION POLYMERISATION IN SOAP CONTAINING SYSTEMS.

1) Emulsion polymerisation

The term emulsion polymerisation, if rigorously applied, should only be used to describe systems in which a monomer emulsion, produced by agitation in the presence of surface-active agents, undergoes polymerisation to produce a suspension of polymer particles of colloidal dimensions, i.e. a latex; the continuous medium in nearly all cases being water. However, it has also been applied to other systems in which the product is a latex but the initial system is not an emulsion, e.g. the polymerisation of water-soluble monomers such as acrylonitrile and vinyl acetate, whose polymers are insoluble; and more recently to the polymerisation of water-insoluble monomers in the absence of added surface-active agents. Hence, a wider definition of emulsion polymerisation could be: that process whereby a monomer dispersed in water undergoes polymerisation to produce a dispersion of polymer particles of colloidal dimensions.

That emulsion polymerisation is not merely the polymerisation of monomer droplets is evinced from the fact that the emulsified monomer droplets are seldom less than 1 μm diameter, whereas the polymer particles produced are of the order of 0.1 μm diameter. If the product of the polymerisation is a suspension of relatively large particles then the process is termed a suspension polymerisation. Although the definitions sometimes overlap, suspension polymerisation shows similar characteristics to the polymerisation of bulk monomer where the aqueous phase plays a minor role (1).

2) Industrial Application

Large tonnages of polymers are now produced industrially by emulsion polymerisation, since it has the advantage that the rate of reaction can be increased without the subsequent decrease in molecular weight apparent in other systems. In bulk, suspension and solution polymerisations the rate of reaction $\left(-\frac{d[M]}{dt}\right)$ and the molecular weight of the polymer formed are inversely related. An increased rate of polymerisation due to an increase in the rate of radical production results in an increased rate of termination and hence a decrease in the molecular weight. In emulsion systems however, the polymerisation occurs in a large number of physically isolated regions, and hence it is possible for the rate of reaction and the molecular weight to increase simultaneously. The dispersions formed are also easier to handle than the products from other polymerisation systems, and any heat generated within the system is easily dissipated via the aqueous phase. The industrial process is complex, involving as it does an overlap of technologies between polymer chemistry and surface chemistry. Typical industrial systems contain not only monomer, water, initiator and emulsifier, but usually a mixture of several emulsifiers, activators, buffers, chain-transfer agents and other additives in order to produce a product with the desired properties. Monomers commonly employed include: a) acrolein, b) acrylonitrile, c) butadiene and its derivatives, d) chloroprene, e) ethylene, f) isoprene, g) methyl acrylate and other acrylate esters, h) methyl methacrylate and other methacrylate esters, i) vinyl acetate and other vinyl esters, j) vinyl chloride, k) vinylidene chloride, l) styrene and its derivatives and various co-polymer mixtures of the above.

The mechanisms of polymerisation vary from monomer to monomer, some form polymers in which the monomer is

insoluble (vinylidene chloride), others where it is soluble (styrene), and others which form precipitating polymers such as acrylonitrile.

3) Monodisperse Latices

Using the system of emulsion polymerisation it is possible to produce latices having very narrow size distributions (standard deviation <2%), the size of which can be varied by altering the reaction conditions. The Dow Chemical Company (Midland, Michigan) has been producing commercially monodisperse polystyrene and polyvinyltoluene latices for about twenty years. Wachtel and LaMer (2) have used the term monodisperse to describe sols having a co-efficient of variation in the mean of the diameter of <10%. Monodisperse latices have found applications in a wide variety of scientific fields e.g. a) calibration of instruments and techniques such as light scattering instruments, optical microscopes, Coulter counters and ultracentrifuges, b) medical diagnostic tests for rheumatoid arthritis, trichinosis and human pregnancy etc., c) counting of viruses, d) purification of antibodies, e) determination of the pore sizes of filters and biological membranes, f) investigating the kinetics and mechanism of emulsion polymerisation, and many other uses. However, the use of these latices as model colloids has several drawbacks. In order for the latex to be used as a model colloid it is necessary that the nature and number of the ionogenic surface groupings be known. The presence of adsorbed surfactant at the particle/water interface will affect this and its complete removal is essential. In some cases the removal by dialysis or ion exchange results in the latex undergoing flocculation or coagulation (3,4), and in the cases where removal does not lead to coagulation, the actual process of removal is either lengthy, as in the case of dialysis, or is subject to some doubt, as in the case of removal by ion exchange resin (5).

4) History of Emulsion Polymerisation

The earliest investigations into emulsion polymerisation date from 1910 (6,7) and arose from attempts to simulate the formation of isoprene in the rubber tree. In this early work protective colloids such as gelatin, egg albumin, blood serum and milk were used to stabilise the emulsions, but the reaction times of six weeks were found to be impractical. It was later realised that the polymerisation was catalysed by the decomposition of peroxides formed by the autoxidation of the monomer and it was not until 1926-27 that soap and initiator were employed for the production of synthetic rubber latices (8-10). In 1932 the commercial production of polyvinyl chloride was started at Ludwigshafen (11). Over the last 44 years the amount of polymer produced by emulsion polymerisation has increased considerably, i.e. in 1960 the production of synthetic rubber in Britain was 100,000 tons/year, and in 1970 this had risen to 300,000 tons (12).

Fikentscher (13), in 1938, was the first to express the view that in emulsion reactions the monomer dissolved in the aqueous phase polymerised rather than that present in the emulsified droplets, the dissolved monomer being replenished from the monomer droplets and the rate of polymerisation remaining constant until the droplets disappeared. The Second World War spurred a considerable research and development effort into the commercial production of synthetic rubbers (styrene/butadiene copolymers) and the results of this work were published independently after the war by Yurzhenko et al (14) in the U.S.S.R. and Harkins (15) in the U.S.A. Harkins' (15) qualitative theory of particle formation in these systems containing surfactant above the critical micelle concentration has become generally accepted, and in 1948 Smith and Ewart (16) quantified Harkins' mechanism.

5) Processes Occurring During an Emulsion Polymerisation.

A typical free radical polymerisation proceeds as

follows:

A free radical initiator I undergoes cleavage to produce two free radicals,

$$I \xrightarrow{k_i} 2R^{\bullet} \quad \text{---} \quad (1)$$

These free radicals then react with monomer to form a polymeric radical,

$$R^{\bullet} + M \xrightarrow{k_p} RM^{\bullet} \quad \text{---} \quad (2)$$

$$RM^{\bullet} + nM \xrightarrow{k_p} R(M)nM^{\bullet} \quad \text{---} \quad (3)$$

Competing with the reaction of polymeric radicals with monomer are various termination reactions:

a) Combination :

$$R(M)nM^{\bullet} + R(M)mM^{\bullet} \xrightarrow{k_t} R(M)nMM(M)mR \quad \text{---} \quad (4)$$

b) Disproportionation:

$$R(M)nM^{\bullet} + R(M)mM^{\bullet} \xrightarrow{k'_t} R(M)nM' + R(M)mM'' \quad \text{---} \quad (5)$$

c) Termination with primary radicals ($R^{\bullet}$) can also occur:

$$R(M)nM^{\bullet} + R^{\bullet} \xrightarrow{k_t} R(M)nMR$$

A number of chain transfer reactions are also possible:

a) Transfer to monomer:

$$R(M)nM^{\bullet} + M \longrightarrow R(M)nM' + M^{\bullet} \quad \text{---} \quad (6)$$

b) Transfer to initiator:

$$R(M)nM^{\bullet} + I \longrightarrow R(M)nM' + I^{\bullet} \quad \text{---} \quad (7)$$

c) Transfer to polymer:

$$R(M)nM^{\bullet} + P \longrightarrow R(M)nM' + P^{\bullet} \quad \text{---} \quad (8)$$

6) <u>The Harkins Mechanism</u>

The mechanism of emulsion polymerisation in the presence of surfactant micelles proposed by Harkins (15) can be summarised as follows: initially both emulsifier and monomer are present in three loci (Fig.1.). The emulsifier is present mainly in the form of micelles which are in dynamic equilibrium with emulsifier molecules dissolved in the water, the rest of the emulsifier acts to stabilise the monomer droplets. The monomer is present in solution, as droplets and solubilised in the emulsifier micelles. There are about 10^{18} micelles per millilitre of water at the concentrations usually employed (17), each of

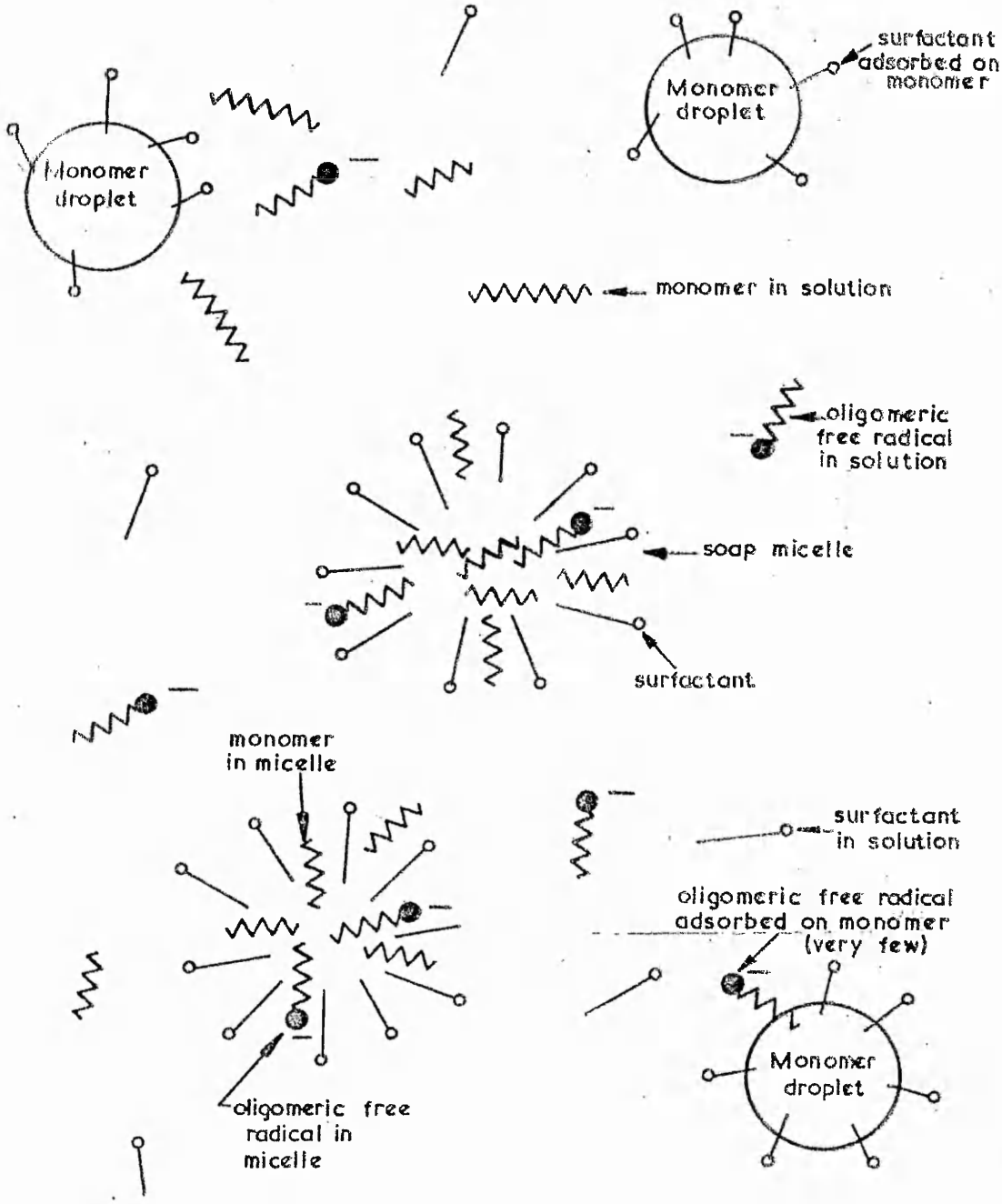

SCHEMATIC DEPICTION OF LOCI OF REACTANTS

FIG. 1

which contains approximately 100 soap molecules (17) and has a diameter of about 5nm (17). The size of the monomer droplets depends on the intensity of the agitation, but they are not usually smaller than 1 - 10 μm, with about 10^{11} of these droplets per millilitre of water for a typical recipe (17).

Upon addition of a free radical initiator, e.g. potassium persulphate, free radicals are formed at a rate dependent upon the temperature. With potassium persulphate at 323 K approximately 10^{13} radicals are formed per millilitre per second at the usual concentrations employed. It is unlikely that these radicals can enter the monomer swollen anionic micelles because of electrostatic repulsions. However, reaction with the monomer dissolved in the water phase results in the formation of free radical oligomers which become surface-active at a certain chain length. The emulsifier in the micelles being in dynamic equilibrium (residence time 0.19 sec. (18)) with that dissolved in the water is then presumably capable of exchange with the new surface-active species.

That the monomer swollen micelles should be the main site of reaction rather than the monomer droplets is seen by comparing the surface areas of the two, where typical formulations contain micelles having a sixty fold advantage in surface area over the droplets.

In the interior of the micelle the free radical end of the oligomer encounters a high concentration of solubilised monomer and chain growth proceeds rapidly. The propagation rate constant, k_p, in persulphate initiated styrene polymerisations at 318 K has been found to be in the range of 120 - 170 l moles^{-1} sec^{-1} (19-22). In the polymerisation of styrene at 323 K a micelle being "stung" by a radical expands in one minute to about 250 times its' original volume. Not all the monomer used in this growth is originally present in the micelle, but diffuses to the particle from the droplets via the water phase. The in-

creased polymer/water interfacial area is stabilised by the adsorption of emulsifier from solution and by the disbanding of soap micelles which have not been "stung" by a free radical. Thus, only a small fraction of the original micelles become growing polymer particles, and the final latex usually contains some 10^{15} particles per millilitre. Harkins reasoned that when all the micelles had disappeared no new particles could be formed.

B. THE KINETICS OF EMULSION POLYMERISATION.

Emulsion polymerisations are usually divided into three intervals:

1) Interval I - during this Interval an initially two phase system (water and monomer) becomes a three phase system due to the formation of polymer particles, Interval I is complete when N, the total number of polymer particles present within the system, becomes constant.

2) Interval II - this lasts from the end of Interval I until the system again consists of two phases: monomer swollen polymer particles and water. During Interval II the number of particles remains constant, as does the monomer concentration within the particles. Gardon (26) has pointed out that the polymer particles will not swell indefinitely even if the monomer was a good solvent for the polymer. As the particles swell, then their interfacial free-energy increases, and at equilibrium the increase in interfacial free-energy is balanced by the free energy of mixing. Indeed, the theories of Gardon (26) and Morton et al (19) and published experimental data (22, 26, 27) indicates that the equilibrium volume fraction of the monomer at saturation is independent of the particle size and is essentially constant during Interval II.

The equilibrium for swelling of the polymer particle by monomer is determined by (28):

$$RT\left(\ln\phi_m + (1 + \frac{1}{m'})\phi_p + \chi\phi_p^2 + \frac{2V_m\gamma}{rRT}\right) = 0 \quad \text{--- (9)}$$

Thus, for constant γ the equilibrium concentration will increase with increasing r, and this increase will be less pronounced the higher the value of χ. However, the increase in r will be accompanied by an increase in γ if no further emulsifier is added. Also, during Interval II it is unlikely that the particle radius will increase by more than a factor of 3, hence the assumption of constant monomer concentration seems reasonable.

3) Interval III - this lasts from the end of Interval II until the end of the reaction, during this period the concentration of monomer dissolved in the polymer and water phases decreases.

C. THEORETICAL TREATMENTS OF INTERVALS I, II AND III.

1) Interval I. Smith and Ewart (16) were the first to formulate theoretical upper and lower limits as to the number of particles generated. These were based upon three assumptions:

a) that the interfacial area, a_s, of a surfactant molecule absorbed on a soap saturated polymer particle was the same as that when it was part of a micelle.

b) that the uptake of free radicals by the micelles and latex particles was governed by the laws of diffusion.

c) that the rate of polymerisation was constant within polymer particles once nucleated.

The upper limit was derived from the basic assumption that free radicals only enter micelles - obviously untrue as evinced by the continued polymerisation after the disappearance of the micelles.

Assuming a constant rate of increase in the volume of each particle, μ, then the surface area of a single particle, a'_{τ^*t}, which was nucleated at time τ^* at a subsequent time t is given by:

$$a'_{\tau^*t} = \left[(4\pi)^{\frac{1}{2}} 3 \int_{\tau^*}^{t} \mu \, d\tau^*\right]^{\frac{2}{3}} = \theta(t - \tau^*)^{\frac{2}{3}}, \quad \text{--- (10)}$$

where $\Theta = \left[(4\pi)^{\frac{1}{2}} 3\mu \right]^{\frac{2}{3}}$

The total polymeric area per unit volume of emulsion, A_p, at time t is thus:

$$A_p = \rho^* \int_0^t a'_{\tau^*,t} \, d\tau^* , \qquad \text{-- (11)}$$

where ρ^* is the rate of entry of free radicals into micelles.

Then;

$$A_p = 0.60 \, \rho^* \, \Theta \, t^{\frac{5}{3}} \qquad \text{-- (11i)}$$

When $A_p = a_s S_s$, where S_s is the weight concentration of surfactant, no micelles remain. Thus, Interval I is complete at a critical time, t_{cr}, where:

$$t_{cr} = \left(\frac{a_s S_s}{0.60 \, \rho^* \Theta} \right)^{\frac{3}{5}} = 0.53 \left(\frac{a_s S_s}{\rho^*} \right)^{\frac{3}{5}} \left(\frac{1}{\mu} \right)^{\frac{2}{5}} \qquad \text{-- (12)}$$

Hence:

$$N = \rho^* t_{cr} = 0.53 \left(\frac{\rho^*}{\mu} \right)^{\frac{2}{5}} \left(a_s S_s \right)^{\frac{3}{5}} \qquad \text{-- (13)}$$

To calculate the lower limit Smith and Ewart (16) assumed that the effectiveness of radical capture per unit area was independent of the size of the species on which the area was located, i.e. particles can capture radicals with the same efficiency per unit area as micelles.

The rate of nucleation is obtained by decreasing ρ^* by the fraction of free radicals which enter polymer particles:

$$\frac{dN}{dt} = \rho^* \left[1 - \left(\frac{Ap}{a_s S_s} \right) \right] \qquad \text{-- (14)}$$

Then,

$$\frac{dN}{dt} = \rho^* - \frac{\rho^* \Theta}{a_s S_s} \int_0^t (t - \tau^*)^{\frac{2}{3}} \left(\frac{dN}{d\tau^*} \right) d\tau^* \qquad \text{-- (15)}$$

Smith and Ewart obtained an approximate solution for this equation:

$$N = 0.370 \left(\frac{\rho^*}{\mu} \right)^{\frac{2}{5}} (a_s S_s)^{\frac{3}{5}} \qquad \text{-- (16)}$$

This was later proved correct by Gardon (29) using a more exact numerical analysis. Thus:

$$N = k\left(\frac{\rho^*}{\mu}\right)^{\frac{2}{5}} (a_s S_s)^{\frac{3}{5}} \qquad \text{--- (17)}$$

where $0.37 < k < 0.53$.

Gardon (29) has argued that the Smith-Ewart lower limit is the true prediction of N, based upon geometrical arguments on the probability of free radicals in solution being captured by particles and micelles at a rate proportional to their surface area. His argument involves the assumption that the absorption rate of free radicals by particles or micelles could be described by collision theory, an assumption also made by Fitch et al (30) i.e.,

$$R_c^* = 4\pi k_a [R^\bullet]_w \sum r_i^2 N_i , \qquad \text{--- (18)}$$

or $R_c^* \alpha r^2$ (proportional to the surface area of the particle). Diffusion theory, however, considers that the absorption of free radicals is influenced by the concentration gradient present around free radical sinks, such as micelles and particles. Assuming irreversible absorption then the first Fickian law (31), given by

$$R_c^* = 4\pi D_w C_w \sum r_i N_i , \qquad \text{--- (19)}$$

assumes that the diffusional path length is much greater than the particle size, i.e. $\rho^* \alpha r$, and the free radical flux per unit area should be expected to be greater for small particles and micelles. Recent results by Fitch et al (32) involving both seeded and perfectly homogenous solution emulsion polymerisations of methyl methacrylate indicate that the process of radical capture is diffusion controlled. A later interpretation of the results for seeded growth lead Fitch (33) to conclude that the collision theory gave a reasonable estimate of the capture rate, but that the mechanism of radical capture was diffusion controlled. LaMer and Reiss (34,35)

showed that growth occurs in some aerosol and hydrosol particle systems by a simple diffusion mechanism.

Smith and Ewart predictions of a constant rate in Interval II, with an average number of free radicals per particle, $\bar{n}$, indicate that there should be a maximum in the rate of polymerisation at the end of Interval I. In their upper limit calculation $\bar{n} = 1$, and although they did not calculate the value of $\bar{n}$ for the lower limit, this has been calculated by Gardon (29) to be ~ 0.67. However, the most careful rate determinations have not exhibited the expected maximum and Gardon has proposed that this is because the predicted maximum is experimentally indetectable. A numerical analysis carried out by Parts et al (36) indicates that it should be detectable.

It has been shown by several workers (37-40) that in some types of emulsion polymerisation free radicals are reversibly absorbed, and are only irreversibly absorbed after the addition of sufficient monomer units to make them either practically insoluble or surface-active. Hansen et al (28,41) have recently applied the second Fickian law to the system of radical capture by polymer particles. The equations they derived indicated that particles containing one radical would tend to absorb radicals at a higher rate from the water phase than micelles or particles containing no radicals. It can be seen that a second radical entering a small particle could be terminated before desorption occurred. They concluded that the average number of free radicals in Interval I would never exceed $\bar{n} = 0.5$, hence the expected rate increase would not occur.

2) Interval II. The two most important parameters of polymerisation reactions are the rate of polymerisation, R_p, and the average degree of polymerisation, $\overline{DP}$. $\overline{DP}$ is the average number of monomer units per polymer molecule. The rate of polymerisation is given by:

$$R_p = k_p [M] [R^\bullet] \quad , \qquad \text{-- (20)}$$

Now:

$$[R^\bullet] = \left(\frac{R_i}{2k_t}\right)^{\frac{1}{2}} \quad , \qquad \text{-- (21)}$$

Thus:

$$R_p = \left(\frac{R_i k_p^{\,2}}{2k_t}\right)^{\frac{1}{2}} [M] \quad , \qquad \text{-- (22)}$$

and:

$$\overline{DP} = 2\frac{R_p}{R_t} = \left(\frac{2k_p^{\,2}}{R_i k_t}\right)^{\frac{1}{2}} [M] \qquad \text{-- (23)}$$

The above two relationships agree well with experimental data for both bulk and solution polymerisations. In emulsion systems, the discrete nature of the reaction loci has to be considered, especially with regard to R_t, which is much lower in emulsion systems because a radical isolated in one particle cannot undergo termination with one in another.

In bulk and solution systems,

$R_t = \frac{-d[R^\bullet]}{dt} = 2k_t [R^\bullet]^2$, which can be rewritten as:

$R_t = 2k_t \frac{n/N_A}{v} \times \frac{n/N_A}{v}$, where n is the number of free radicals in reaction volume v. This equation assumes that a free radical can react with itself as well as with others. In bulk and solution systems n is large and the approximation is valid. However, in emulsion systems n is small and the more accurate expression:

$$R_t = 2k_t \frac{n/N_A}{v} \times \frac{n-1/N_A}{v} \qquad \text{-- (24)}$$

is used, and R_t thus depends on the distribution of the radicals among the particles.

It is usual in emulsion polymerisations to set the rate of reaction equal to the rate of reaction within a single particle multiplied by the total number of part-

icles present:

$$R_p = -\frac{d[M]}{dt} = \frac{k_p [M]_p \bar{n} N}{N_A} \qquad \text{--- (25)}$$

Smith and Ewart (16), and later Haward (42), applied a steady state condition to Interval II, assuming that $[R^{\cdot}]$ remained constant, in order to obtain information on $\bar{n}$ the average number of free radicals per particle. The steady state implies that the rate of formation of particles containing n radicals, N_n, is constant and therefore equals the rate of their disappearance. Particles containing n free radicals are created by three processes, the entry of a free radical into N_{n-1} particles, the exit of a single free radical from N_{n+1} particles, and the termination of two free radicals in N_{n+2} particles. Similar processes in N_n particles result in their disappearance. Hence:

$$N_{n-1}\left(\frac{\rho}{N}\right) + N_{n+1}\left(\frac{k_s S}{N_A}\right)\frac{(n+1)}{v} + N_{n+2}\left(\frac{k_t}{N_A}\right)\left(\frac{(n+2)(n+1)}{v}\right) =$$

$$N_n\left[\left(\frac{\rho}{N}\right) + \left(\frac{k_s S}{N_A}\right)\frac{n}{v} + \left(\frac{k_t}{N_A}\right)\left(\frac{n(n-1)}{v}\right)\right], \qquad \text{--- (26)}$$

This equation can be simplified to give:

$$\alpha N_{n-1} + mN_{n+1}(n+1) + N_{n+2}(n+2)(n+1) = N_n(\alpha + mn + n(n-1)), \qquad \text{--- (27)}$$

where $\alpha = \left(\frac{N_A v}{k_t \tau}\right)$ and $m = \left(\frac{k_s S}{k_t}\right)$,

τ is the interval between successive free radical entries, α is indicative of the radical initiation rate and particle size. m is indicative of the rate of radical transfer out of the particles to the rate of termination within the particles.

In a recent paper by Ugelstad et al (41), the term $\frac{k_s S}{v}$ is replaced by k_d (= the rate constant for desorption of radicals from the particles). The term $\frac{k_s S}{v}$

indicates that the rate of desorption of radicals from a particle should be proportional to the surface area of the particle. Ugelstad et al believe that this is only true in the case of small particles.

Progress in solving this recursion relationship has been made by Stockmayer (43), O'Toole (44) and Gardon (45). Smith and Ewart (16), lacking computer facilities, were forced to calculate solutions for three limiting conditions:

a) Case 1, $\bar{n} \ll 0.5$: the rate of radical entry is much less than the rate of their disappearance ($m \gg \alpha$).

b) Case 2, $\bar{n} \simeq 0.5$: the rate of termination of radicals is faster than the rate of entry and transfer of radicals from the particles is negligibly small ($m \ll \alpha < 1$).

c) Case 3, $\bar{n} \gg 1$: the rate of entry of free radicals is much greater than the rate of loss.

Smith and Ewart considered Case 1 in two different ways:

i) Termination in the water phase dominating. They determined that:

$$\bar{n} = \left(\frac{\rho^{\omega}}{2k_{tw}}\right)^{\frac{1}{2}} a^{*} \frac{V_p}{N} , \qquad \text{--- (27A)}$$

where a^{*} is the distribution coefficient between radicals in particles and in solution $= \left(\frac{[R^{\cdot}]_p}{[R^{\cdot}]_w}\right)$.

Hence,

$$R_p = \frac{k_p [M]_p}{N_A} \left(\frac{\rho^{\omega}}{2k_{tw}}\right)^{\frac{1}{2}} a^{*} V_p . \qquad \text{--- (28)}$$

The situation that termination in the water phase is dominant is improbable in emulsion polymerisations carried out in water. However, it has been observed in nonaqueous emulsion polymerisation (41).

ii) Termination in the particles dominating. They determined that:

$$\bar{n} = \left(\frac{\rho^{\omega} v}{2Nk_s S}\right)^{\frac{1}{2}} , \qquad \text{--- (29)}$$

and thus the rate of reaction is given by:

$$R_p = \frac{k_p [M]_p}{N_A} (\rho^{\omega})^{\frac{1}{2}} \left(\frac{Nv}{2k_s S}\right)^{\frac{1}{2}} \quad \text{--- (30)}$$

Smith and Ewart found that the results generated from Case 2 fitted experimental evidence best. Free radicals enter small particles singly, and the entry of a second free-radical is accompanied by rapid termination, i.e. the time interval between successive free radical entries is long compared with the time taken for two radicals within a single particle to undergo mutual termination ($\bar{n} \simeq 0.5$).

Therefore:

$$[R^{\bullet}] = \frac{N}{2N_A} , \quad \text{-- (31)}$$

and:

$$R_p = k_p [M] \frac{N}{2N_A} , \quad \text{--- (32)}$$

and:

$$\overline{DP} = k_p [M] \frac{N}{\rho N_A} . \quad \text{--- (33)}$$

Thus, the rate of polymerisation is independent of the size of the particle and of the rate of entry of free radicals, and during Interval II remains constant as does $\overline{DP}$, i.e. $\overline{M}_n$ will also remain constant during Interval II.

For Case 3 ($\bar{n} >> 1$), Smith and Ewart only considered the situation where the rate of desorption of radicals was zero, i.e:

$$\bar{n} = \frac{1}{N} \left(\frac{\rho V_p}{2k_t}\right)^{\frac{1}{2}} , \quad \text{--- (34)}$$

and hence:

$$R_p = \frac{k_p [M]_p}{N_A} \left(\frac{\rho V_p}{2k_t}\right)^{\frac{1}{2}} \quad \text{--- (35)}$$

The rate of polymerisation therefore depends upon the square root of the total volume of polymer and a plot of the square root of the percentage conversion versus time should be linear.

Stockmayer (43) obtained a general solution for the Smith and Ewart recursion equation:

$$\bar{n} = \left(\frac{a}{4}\right)\left(\frac{I_{-m(a)}}{I_{1-m(a)}}\right) \quad \text{for } m \leq 1, \qquad -- (36)$$

and,

$$\bar{n} = -\left(\frac{m-1}{2}\right)+\left(\frac{a}{4}\right)\left(\frac{I_{m-2(a)}}{I_{m-1(a)}}\right) \quad \text{for } m \geq 1 \qquad -- (37)$$

I_{-m} etc. are Bessel functions of the first kind, and $a^2 = 8\alpha$ For small values of α, i.e. slow initiation rates or small particles or both, equations 36 and 37 become:

$$\bar{n} = \left(\frac{1-m}{2}\right) + \left(\frac{\alpha}{2-m}\right) \text{ for } m \leq 1, \qquad -- (38)$$

and,

$$\bar{n} = \frac{\alpha}{m} \qquad \text{for } m \geq 1 \qquad -- (39)$$

Equation 38 reduces to Smith and Ewart Case 2 for vanishing m and α.

For large α, i.e. rapid initiation rates or large particle size, the corresponding equation is:

$$\bar{n} = \left(\frac{a}{4}\right) + \left(\frac{1-2m}{8}\right) \qquad -- (40)$$

Stockmayer also considered the case of negligible desorption when $\rho = \rho^{\omega}$ and determined:

$$\bar{n} = \frac{I_{o(a)}}{I_{1(a)}} , \qquad -- (41)$$

which for values of $\alpha > 10$ becomes approximately:

$$\bar{n} = \left(\frac{\alpha}{2}\right)^{\frac{1}{2}} , \qquad -- (42)$$

which is equivalent to the Smith and Ewart Case III.

O'Toole (44) has criticised on physical grounds the solution obtained by Stockmayer when the rate of radical desorption is small but finite ($0 < m < 1$). He obtained:

$$\bar{n} = \left(\frac{a}{4}\right)\left(\frac{I_{m(a)}}{I_{m-1(a)}}\right) , \qquad -- (43)$$

In the cases where a and m are much smaller than unity equation 43 becomes:

$$\bar{n} \simeq \frac{k'_a}{k'_d+2k'_a} \qquad -- (44)$$

where k'_a is the rate constant for capture of polymeric radicals by a zero order absorption from the aqueous phase or intra-particle initiation, and k'_d is the rate constant for the first order desorption or chain stopping transfer of polymeric radicals. It can be seen that when $k'_d \longrightarrow 0$, then $\bar{n} \longrightarrow 0.5$, i.e. Smith and Ewart, Case 2. In the special case where m = 0 then,

$$\bar{n} = \left(\frac{\alpha}{4}\right)\left(\frac{I_{o(a)}}{I_{1(a)}}\right) , \qquad -- (45)$$

so that the rate of polymerisation becomes:

$$-\frac{d[M]}{dt} = \left(\frac{k_p}{N_A}\right) M_p N \left(\frac{\alpha}{2}\right)^{\frac{1}{2}} \left(\frac{I_{o(a)}}{I_{1(a)}}\right) , \qquad -- (46)$$

which can be compared with the Smith and Ewart rate equation for Case 3, where the compartmentalisation of the free radicals is expressed by the factor $\left(\frac{I_{o(a)}}{I_{1(a)}}\right)$.

Gardon (45) has noted that the foregoing theories of Interval II make at least two approximations that could lead to significant error; (i) the steady state approximation may not be valid in that the number of reactive intermediates (free radicals) could vary considerably, and (ii) that in solving the recursion equation v was assumed to be constant, which is not the case as it must increase during the whole of Interval II. However, the necessary requirements for the application of a steady state approximation is not that v should be constant, but that the rate of change of v should be a slow process compared to the rate at which the steady state value of $\bar{n}$, corresponding to a given value of v, is established. It has been calculated (28) that the rate of radical generation during Interval II is an order of magnitude greater than the absolute increase with time of the total number of radicals during Interval II and thus, the above condition is likely to be fulfilled.

Gardon (46) also set out to define the systems to

which the equations related:

i) That all reactants are added at the beginning of the reaction, that a single monomer is used and that the temperature is kept constant.

ii) That the initiator is soluble in the aqueous phase only, and that the half life is much longer than the time of the polymerisation reaction. This overcomes the criticism with regard reactive intermediates stated earlier.

(iii) That micellar soap is used at a concentration such that all the effective radicals are adsorbed into the oil phase.

(iv) That the rate of diffusion of monomer to the particles is greater than its' consumption by polymerisation.

(v) That the soap is an efficient emulsifier for the monomer and that it is adsorbed strongly by the polymer.

(vi) That the polymer is insoluble in the aqueous phase.

(vii) That the monomer is a good solvent for the polymer.

(viii) That the polymer and monomer do not undergo hydrolysis during the reaction.

Gardon applied the more general non-steady state expression for the number of particles containing n radicals:

$$\frac{dN_n}{dt} = \rho \frac{N_{n-1}}{N} + \left(\frac{k_t}{V}\right)(n+2)(n+1)N_{n+2} - \rho \frac{N_n}{N} - \left(\frac{k_t}{V}\right)n(n-1)N_n, \qquad \text{-- (47)}$$

Equation 46 describes the case for negligible desorption. The rate of reaction is given by:

$$-\frac{d[M]}{dt} = \frac{d\,P_v}{dt}\,\frac{d_p}{M_m}, \qquad \text{-- (48)}$$

where P_v is the volume of polymer formed.

and, $$[M]_p = \Phi_M \frac{d_m}{M_m}, \qquad \text{-- (49)}$$

Thus, $$\frac{d\,P_v}{dt} = \frac{k_p}{N_A}\,\Phi_M\,\frac{d_m}{d_p}\,N\,\bar{n} = 2\,\bar{n}\,B, \qquad \text{-- (50)}$$

where $$B = \frac{k_p}{2N_A}\,\frac{d_m}{d_p}\,\Phi_M\,N, \qquad \text{-- (51)}$$

i.e. the Smith and Ewart rate for Case II.

The particle volume is given by, $v = \frac{P_v}{N(1-\Phi_M)}$. --- (52)

Then, eliminating time and v from equation 47 by inserting from equations 50 and 52,

$$2\bar{n}\left(\frac{dN_n}{dP_v}\right) = \left(\frac{\rho}{NB}\right)(N_{n-1}-N_n) + \left(\frac{k_t N(1-\Phi_M)}{BP_v}\right)\left[N_{n+2}(n+2)(n+1) - N_n(n)(n-1)\right] \quad \text{--- (53)}$$

Also, $\bar{n} = \sum n\frac{N_n}{N}$, and $N = \sum N_n$

Gardon solved this equation by introducing the following dimensionless parameters:

$$Z = 0.1297\left(\frac{\rho}{NB}\right)P_v \quad , \quad \text{--- (54)}$$

proportional to conversion.

$$x = 0.698\left(\frac{\rho}{N}\right) \quad \text{--- (55)}$$

proportional to time, and:

$$\Psi = \frac{\left(\frac{k_t N_A}{k_p}\right)\left(\frac{d_p}{d_m}\right)(1-\Phi_M)}{\Phi_M} \quad \text{--- (56)}$$

Then:

$$\frac{\bar{n}df_n}{dZ} = 3.81\,(f_{n-1} - f_n) + \left(\frac{\Psi}{Z}\right)\left[(n+2)(n+1)\,f_{n+2} - n(n-1)f_n\right], \quad \text{--- (57)}$$

where $f_n = \frac{N_n}{N}$, and $\sum f_n = 1$, and $\bar{n} = \sum nf_n$.

Gardon solved the above equations using the boundary conditions that $Z = 0$, $f_o = f_1 = \bar{n} = 0.5$ and $f_n = 0$ $(n \neq 0, 1)$ and found that for all practical purposes the solution was identical to that of Stockmayer (43). Gardon also found that the values of $\bar{n}$ could be predicted with an accuracy of better than 8% by the empirical relationship:

$$\bar{n} = 0.5\left(1 + \left(\frac{4A}{B}\right)^2 P_v\right)^{0.5} \quad , \quad \text{--- (58)}$$

where $A = 0.102 \left[\frac{k_p}{k_t}^{1.94}{}^{0.94}\right] \left(\frac{d_m}{d_p}\right)^{1.94} \left[\frac{\Phi_M}{(1-\Phi_M)}^{1.94}{}^{0.94}\right] \left(\frac{\rho}{N_A}\right)$

Ugelstad and Mork (47) have suggested a simplified expression for $\bar{n}$:

$$\bar{n} = (0.25 + \frac{\alpha}{2}). \qquad -- (59)$$

Comparison of values of $\bar{n}$ calculated from equation 59 between $x = 0 \longrightarrow 100$ deviate by less than 4% from those obtained using the Stockmayer relationship.

According to the Smith and Ewart theory, the molecular weight during Interval II should remain constant. They therefore derived the following equivalent equations:

$$\bar{M}_n = \frac{2BN_A d_p}{\rho}, \qquad -- (60)$$

$$\bar{M}_n = \frac{k_p \Phi_M N d_m}{\rho}, \qquad -- (61)$$

and: $$\bar{M}_n = 0.318 \left[N_A d_p (1-\Phi_M)\right]^{0.4} \left(\frac{d_m k_p \Phi_M a_s S_s}{\rho}\right)^{0.6}, \qquad -- (62)$$

The treatment of Gardon gives:

$$\bar{M}_n = \frac{\frac{4AN_A d_p}{B\rho}}{\left(1 + \left(\frac{4A}{B^2}\right) P_v\right)^{0.5} - 1} \qquad -- (63)$$

Thus, Gardon predicted that during Interval II the molecular weight should increase.

3) Interval III. During this Interval monomer is present both in the particles and dissolved to varying degrees in the aqueous phase. Thus, Interval III could be divided into three sub intervals (37). If the monomer is reasonably soluble in the water, or in the polymer phase, then the supply of monomer could be sufficient for propagation to remain the rate determining step. In fact the last 55% of a styrene polymerisation occurs during Interval III (48). However, as the monomer is consumed the internal

viscosity of the particle becomes very high and the rate of diffusion to the growing free radicals becomes rate determining. A third interval may occur through the changing monomer/polymer ratio within the particles reaching a glass transition point at the temperature of the reaction. This would lead to a virtual stop in the rate of polymerisation because the diffusion of the polymer chains and the monomer is very slow under such glassy conditions (49).

The major problem in determining the kinetic theory of Interval III is the calculation of the decreasing rate of termination with increasing particle viscosity i.e. the gel-effect (50-52). This effect often manifests itself with an increase in the rate of polymerisation during the latter stages of bulk polymerisation where the termination reaction becomes diffusion controlled (49).

A recent kinetic treatment of Interval III has been carried out by Friis and Hamielec (53), who made use of kinetic results from bulk polymerisation to determine k_t as a function of conversion, and used the values in the kinetic treatment of the emulsion polymerisation of methyl methacrylate. In applying the Smith and Ewart (16) equation they neglected radical desorption from the particles. For the bulk polymerisation of methyl methacrylate Balke and Hamielec (54) found that:

$$\frac{k_t^*}{k_p^2} = \left(\frac{k_t'}{k_p^2}\right)_0 \left(\frac{1}{1-x}\right) \exp\left(B'x + Cx^2\right), \qquad \text{--- (64)}$$

where B' and C are constants (-5.48 and -2.72 respectively). The glass transition point of methyl methacrylate at 333 K occurs when there is 10% monomer present (28). Since k_p will be constant up to that point then:

$$k_t^* = (k_t)_0 \left(\frac{1}{(1-x)} \exp B'x + Cx^2\right)^2 \quad 0 < x < 0.9, \qquad \text{--- (65)}$$

To use this equation in emulsion polymerisations x must be

set constant during Interval II, and equal to x_c, the conversion at the end of Interval II. $(k_t)_o$ was set at 3.3×10^6 l moles^{-1} sec^{-1}.

The weight ratio of monomer to polymer in the particles (q) will be constant during Interval II:

$$q_{II} = \frac{1}{x_c} - 1 \quad . \qquad \text{-- (66)}$$

The average particle volume in Interval II is thus:

$$v = \frac{1}{N}\left(\frac{xQ_o}{d_p} + \frac{xQ_o}{d_m}\left(\frac{1}{x_c} - 1\right)\right) \quad , \qquad \text{-- (67)}$$

or:

$$v = \frac{xQ_o}{N}\left(\frac{1}{d_p} + \frac{1}{d_m}\left({}^1/x_c - 1\right)\right) \quad . \qquad \text{-- (68)}$$

In Interval III:

$$v = \frac{Q_o}{N}\left(\frac{x}{d_p} + \frac{1-x}{d_m}\right) \quad , \quad x \geq x_c . \qquad \text{-- (69)}$$

The rate of reaction is thus given by:

$$\frac{dx}{dt} = \frac{k_p \bar{n} [M]_p N M_m}{Q_o N_A} \qquad \text{-- (70)}$$

During Interval II the value of $[M]_p$ is given by:

$$[M]_p = \frac{(1-x_c)d_m}{\left(1-x_c + x_c \frac{d_m}{d_p}\right)M_m} \quad , \; x \leq x_c \; , \qquad \text{-- (71)}$$

and in Interval III by:

$$[M]_p = \frac{(1-x)d_m}{\left(1-x + x_c \frac{d_m}{d_p}\right)M_m} \quad . \qquad \text{-- (72)}$$

From the Smith and Ewart (16) equation, values of $\bar{n}$ could be calculated by applying the values of k_t^* and v, and hence conversion versus time plots determined. Excellent agreement was obtained between calculated results and experimental results obtained by Zimmt (55).

Friis et al (56,57) carried out similar calculations for both vinyl acetate and vinyl chloride emulsion polymerisations and in both cases obtained good agreement between calculated and experimental results. They were also

able to predict the molecular weight development for these two systems.

Apart from the equations relating to the total number of particles formed, the preceding discussion of Intervals II and III should also be applicable to systems containing no added surface-active agents, provided that the system formed is stable, i.e. provided N remains constant.

Medvedev (23) has postulated an alternative theory of emulsion polymerisation.

It has been observed (24,25) that in some cases the total surface area of a latex remained constant during most of the reaction during polymerisation, this and the observation that the rate of polymerisation was constant led Medvedev to propose that the adsorbed emulsifier layer was the principle locus of polymerisation initiation. He also postulated that initiation took place by transfer of initiator to soap in the aqueous phase, which then adsorbed onto the particle and initiated polymerisation. He also stated that the rate of polymerisation was proportional to the square root of both the initiator and emulsifier concentrations.

The possibility of deterministic and stochastic contributions to latex poly-dispersity have been considered by several workers (58,59). The deterministic contribution arises from the formation over an extended period of time, and from dependence of growth on size. The stochastic contribution can be a consequence of the discrete nature of the participating steps.

Saidel and Katz (60) determined both deterministic and stochastic models of emulsion polymerisation to predict the distribution of molecular weights. If the rate of radical entry is much greater than the rate of termination $\bar{n} > 0.5$, then many polymer chains will be growing at the same time within a single particle. Thus, the rate of polymerisation in a single particle at any

instant differs very little from the average rate, and a deterministic approach is valid. When the termination rate is much greater than the rate of entry, $\bar{n} \leq 0.5$, it is unlikely that any particle contains more than one growing polymer chain. Hence there is either one or none growing at any particular time, and average quantities are not adequate to characterise the polymerisation unless the rate of radical entry and polymer growth are uniform with respect to one another. These authors have also extended the stochastic approach in order to treat the case of more than one growing chain per particle (61). However, Min and Ray (62) have shown that even the case with a small number of radicals per particle can be treated in a deterministic fashion.

Saidel and Katz (60) found that the ratio of weight average molecular weight ($\overline{M}_w$) to number average ($\overline{M}_n$) was 2 for the stochastic model and 1.5 for the deterministic.

Brodnyan (63) showed that for a growth process given by:

$$\frac{dv}{dt} = k\, r^x \quad , \qquad \text{--- (73)}$$

when: $x = 3$ a log normal distribution of radii resulted,

$x = 2$ a normal distribution of radii resulted,

$x = 0$ the Smith and Ewart model pertained.

For polystyrene, Ewart and Carr (59) found $x \simeq 2$ and Vanderhoff (64) $x \simeq 2.5$. Brodnyan (63) found that for methyl methacrylate polymerisations, the rate per unit surface area was essentially constant, but a changing particle size distribution from normal to log normal indicated that there were two loci of polymerisation, the surface and the interior of the particles, the dominant one being determined by the ratio of surface to volume.

4) Summary. Smith and Ewart (16) theory predicted that:

a) $N \propto [I]^{2/5} [E]^{3/5}$.

b) Case 2, $\bar{n} = 0.5$.

i) R_p was independant of [I] and v and was constant throughout Interval II as was the molecular weight.

ii) That the conversion versus time curve was linear during Interval II.

c) Case 3, $\bar{n} >> 1$:

i) R_p was independent of N and increased throughout Interval II, being dependent on both [I] and % conversion.

ii) that the percent conversion curve was convex to the time axis, $(\% C)^{\frac{1}{2}} \propto t$.

iii) the molecular weight increased throughout Interval II.

The extensions to the Smith and Ewart theory predicted that:

a) The rate of polymerisation and the molecular weight increased during Interval II.

b) That the conversion versus time curves were convex to the time axis.

D. EXPERIMENTAL EVIDENCE FOR THE THEORIES OF EMULSION POLYMERISATION.

Smith (65,66) did a considerable amount of work to confirm the Smith and Ewart (16) kinetic relationships. By using seeded growth experiments, he determined that the number of particles remained constant over a 70 fold increase in volume and that the polymerisation rate per particle was: (i) independent of particle volume over a 25 fold range, (ii) independent of persulphate concentration over a 16 fold range, and (iii) independent of the number of particles in the range of 2×10^{12} - 2×10^{14}. As predicted by the theory he found that N varied with the 0.6th and 0.4th power of emulsifier and initiator concentrations respectively, and that the rate of polymerisation remained constant over most of the conversion range, indicating that N and the monomer concentration within the particles also remained constant. Using radio-active persulphate he showed that the number of polymer molecules formed depended only on the rate of radical generation and not on the particle number.

Bartholomé et al (21) obtained considerable amount of

experimental evidence to support the Smith and Ewart theory. They followed the rate of reaction by dilatometry and the particle size by electron microscopy and found that after a short initial period the rate of reaction remained constant upto an inflection point, where it decreased in accord with first order kinetics. At high percent conversions a short lived gel-effect was noticed. The conversion versus time curves were interpreted as follows: after particle initiation the rate remained constant due to constant N and constant monomer in polymer ratio; the inflection point occurred when all the remaining monomer was dissolved in the particles and the decrease in rate was due to monomer starvation. R_p and N both varied with the 0.6th and 0.4th of the emulsifier and initiator concentrations respectively. R_p, $[M]_p$, N and $\overline{DP}$ were not influenced by the styrene/water phase ratio over the experimental range. They found the value of $[M]_p$ determined by the inflection point to be 5.5 M, in agreement with Smith (65) and Morton (19) who used equilibrium swelling measurements. Van der Hoff (67) has listed values of $[M]_p$ determined from conversion time curves (Table 1).

TABLE 1

Values for the Saturation Concentration of Styrene in Polystyrene

Latex Particles

Temperature K	$[M]_p$ mole l^{-1}	Reference
298	5.90	(19)
313	5.58	(67)
323	5.15	(67)
323	5.50	(65)
343	4.80	(67)

A plot of the above data gives $[M]_p$ = 5.50 @ 313 K, 5.24 @ 323 K and 4.72 @ 343 K, with an activation energy of

-1 K cal mole $^{-1}$. Bartholomé et al (21) also found that R_p varied linearly with the number of particles present in the system and that $\frac{1}{DP}$ varied linearly with $\frac{1}{R_p}$. k_p the propagation rate constant was found to be 165 l mole^{-1} sec $^{-1}$ at 318 K.

k_t was determined to be 3.6 x 10^3 l mole^{-1} sec^{-1}, a value two to three orders of magnitude less than that found by Saha et al (68) for dilute solutions. Van der Hoff (1) ascribed this lower rate of termination to the much higher viscosity present within the particles, which was confirmed by recent calculations of Gardon (69).

Van der Hoff (1) lists values of the exponents of the Smith and Ewart equation for N. With relatively insoluble monomers the agreement in most cases was good, but with the more water-soluble monomers such as vinyl chloride, methyl methacrylate and vinyl acetate, there were considerable deviations from theory. Indeed it has been postulated (41, 70, 71) that for these more water-soluble monomers the Harkins (15) nucleation model does not hold and that particle nucleation occurs by precipitation of oligomeric chains from solution, and that the micelles only act as surfactant reservoirs. A similar mechanism has also been suggested for the more water-insoluble monomers such as vinyl stearate (72) and styrene (73).

The polymerisation of methyl methacrylate at concentrations below its' saturation solubility displays no abrupt increase in the rate of reaction when the critical micelle concentration is exceeded (74). Similar experiments involving the more water-insoluble monomer styrene showed that when the surfactant was increased above the critical micelle concentration there was an increase in both the rate and number of particles formed (67), indicating that nucleation occurs both in micelles and by some other mechanism, the extent depending on the solubility of the monomer (75). However, it should not be assumed that the more water-insoluble the monomer, the

better the agreement with Smith and Ewart predictions. Moore (72) studied the polymerisation of vinyl stearate, solubility 7×10^{-7} moles l^{-1} (76) (cf styrene 3.7×10^{-3} moles l^{-1} (77)), and found that the number of particles generated was independent of the initiator concentration, whilst the rate of polymerisation was almost directly proportional to it. The maximum rate of polymerisation did not vary as the 0.6th power of the emulsifier, but a rather complex relationship was observed. When the monomer was almost completely solubilised in the surfactant micelles, the rate of polymerisation was very slow, but as the number of micelles was reduced and the number of emulsion droplets increased, the maximum rate also increased, reaching a maximum at 0.02 - 0.05 moles l^{-1} of surfactant. It should be noted that the rate of free radical transfer to monomer is two orders of magnitude greater than that of styrene (78), and that the Harkins mechanism of emulsion polymerisation demands that the rate of transfer of monomer from emulsified droplets to the site of reaction through the aqueous phase should be such that it is not the rate-determining step. Although the lower limit of solubility is not known with certainty, Flory (79) has suggested a figure of 10^{-9} moles l^{-1}.

It also appears that significant deviations from theory with the more water-insoluble monomers can arise from differences in the emulsifier used. Gerrens et al (80-82) using 2 - hydroxystearyl sulphate, found excellent agreement with theory, whereas Vanderhoff (202), using the dihexyl ester of sodium sulphosuccinate, found that the number of particles ranged from 1 - 20% of those predicted by theory.

Ewart and Carr (59) found an increase in the average deviation in the cube of the particle diameter with increasing diameter and interpreted this in terms of fluctuations in $\bar{n}$. Roe and Brass (83) found that the rate of polymerisation of emulsion systems was initially constant, but that as the particle size increased a positive devia-

tion from constant rate became apparent, which they ascribed to an increase in $\bar{n}$.

Vanderhoff et al (64,84) reasoned that if Rp remained constant, particles of different sizes should grow at the same rate, and hence smaller particles would tend to catch up in size with bigger ones. This was found to be the case, but the growth of the small particles was much slower than expected. The rate of volume increase depended on the 2.5 power of the particle diameter, whereas Smith and Ewart, Case 2, predicts the zeroth power, and it follows from the model that:

where $k = k_p [M]$

$$Rp = k_p [M] \bar{n} = \frac{dr^3}{dt} = 3r^2 \frac{dr}{dt} = 0.5 K = \text{Constant}, \quad \text{--- (74)}$$

thus the rate of radius increase isinversely proportional to the radius squared, the rate of relative increase in the radius $(\frac{dr}{r})$ is inversely proportional to the radius and the relative growth of the smaller particles is greater than that of the larger particles. Recent experimental results of Goodall et al (85) showed that the rate of surface area increase with time was constant, $(\frac{dr^2}{dt}) = k_1$, hence:

$$R_p = \frac{dr^3}{dt} = 3/2\ k_2 r, \quad \text{--- (75)}$$

and,

$$\bar{n} = k_3 r, \quad \text{--- (76)}$$

or the average number of free radicals is not constant, but increases with increasing particle size as does R_p. These results were obtained for the surfactant free emulsion polymerisation of styrene.

Work by Williams and Bobalek (86) showed that $\bar{M}_n$ increased with increasing % conversion which they attributed to a decrease in the termination rate constant with increasing particle size.

Smith and Ewart, Case III, and the extensions to the Smith and Ewart theory predicts that the conversion versus time curve is convex to the time axis. Gardon (46) lists

some of the experimental investigations which do report convex conversion/time curves; these include the emulsion polymerisation of styrene, butadiene, isoprene, methyl methacrylate, vinyl acetate and methylacrylate. He also listed numerous experimental data showing a non-constant rate during Interval II when initiator or emulsifier concentrations were changed.

It thus appears that provided the Harkins scheme is a true description of the processes occuring during emulsion polymerisation, then the kinetics of Interval II are, in principle, described by either the Smith and Ewart, Case 3, the explicit theory of Stockmayer and O'Toole or the more elaborate computational procedures devised by Gardon. Interval I remains a theoretical stumbling block, and styrene appears atypical compared with other monomers especially in its' behaviour during this period with regards to agreement with Smith and Ewart particle number predictions. The Medvedev theory predicts that $R_p \propto [E]^{0.5}$ $[I]^{0.5}$, which is difficult to differentiate experimentally from the Smith and Ewart equation at the present time. The treatment of Interval III as carried out by Friis et al gives excellent agreement between predicted and experimentally obtained results and appears capable of being applied to a wide range of monomers.

E. FORMATION OF FREE RADICALS IN AQUEOUS SOLUTION.

1) Initiator Decomposition.

Kolthoff and Miller (87) have studied the decomposition of potassium persulphate in water enriched with oxygen 18 at varying pH, and found that in acid solution (0.6 moles l^{-1} $HClO_4$) all the oxygen produced came from the persulphate, whereas in alkaline solution (0.1 moles l^{-1} NaOH) all the oxygen came from the water. They therefore proposed the following reaction schemes:

a) Uncatalysed:

$$S_2O_8^{2-} \longrightarrow 2SO_4^{\cdot-},$$

$$SO_4^{\cdot-} + H_2O \longrightarrow HSO_4^- + OH^{\cdot},$$

$$2OH^{\cdot} \longrightarrow H_2O + \tfrac{1}{2} O_2.$$

(b) Acid catalysed:

$$S_2O_8^{2-} + H^+ \longrightarrow SO_4 + HSO_4^- ,$$

$$SO_4 \longrightarrow SO_3 + \tfrac{1}{2} O_2 ,$$

$$SO_3 + H_2O \longrightarrow H_2SO_4 \text{ (dilute acid)},$$

$$SO_4 + H_2O \longrightarrow H_2SO_5 \text{ (strong acid)}.$$

The observed kinetics could also arise from the chain mechanism proposed by Bartlett and Cotman (88):

$$S_2O_8^{2-} \longrightarrow 2SO_4^{\cdot-} ,$$

$$SO_4^{\cdot-} + H_2O \longrightarrow HSO_4^- + OH^\cdot ,$$

$$OH^\cdot + S_2O_8^{2-} \longrightarrow HSO_4^- + SO_4^{\cdot-} + \tfrac{1}{2} O_2 ,$$

$$SO_4^{\cdot-} + OH^\cdot \longrightarrow HSO_4^- + \tfrac{1}{2} O_2 .$$

An alternative mechanism for the hydrogen ion independant reaction was put forward by Froneaus and Ostman (89):

$$S_2O_8^{2-} + H_2O \longrightarrow HSO_4^- + SO_4^{\cdot-} + OH^\cdot$$

$$SO_4^{\cdot-} + H_2O \longrightarrow HSO_4^- + OH^\cdot$$

$$2OH^\cdot \longrightarrow H_2O + \tfrac{1}{2} O_2$$

Both Kolthoff and Miller (87) and Froneaus and Ostman (89) found that the rate of decomposition in alkaline solution was independent of ionic strength, but that under acid conditions there was a negative salt effect.

Persulphate decomposition reactions have been reviewed by House (90). The half lives of potassium persulphate 1st order uncatalysed decomposition which have been calculated from the data of Kolthoff and Miller are given in Table 2.

TABLE 2

VARIATION IN THE HALF-LIFE OF POTASSIUM PERSULPHATE WITH TEMPERATURE

Temperature K	$t_{\frac{1}{2}}$ minutes
298	2.8×10^6
313	7.6×10^4
323	1×10^4
333	1.9×10^3
343	4.3×10^2
353	1.3×10^2
363	43

Bovey and Kolthoff (91,92) found convincing evidence that the number of radicals produced by the decomposition of persulphate in water was essentially equal to the number formed in an emulsion polymerisation system. They found at 323 K that the total number of free radicals determined from (a) the number of sulphate containing end groups, (b) the rate of radical formation and, (c) the polymer molecular weight was 6.3×10^{12}, 4.2×10^{12} and 8.4×10^{12} respectively. Using styrene monomer, they found that in the presence of emulsifier the rate of initiation was ten times greater than in its absence and they interpreted this in terms of the low solubility of the monomer, only 10% of the SO_4^- free radicals produced reacted with monomer. This conclusion was substantiated by the fact that the rate of initiation with the much more water soluble vinyl acetate was equal to the rate of thermal decomposition of persulphate and was not affected by the emulsifier used (93).

2) Effect of the constituents of emulsion polymerisation on initiator decomposition.

a) Effect of surfactants. Kolthoff and Miller (87) showed that the decomposition of persulphate was affected by the presence of fatty acid soaps, the rate being greater

in the presence of soap, i.e. a four-fold increase being recorded with potassium laurate at 323 K. The persulphate oxidised the soap causing decarboxylation. Similarily, Ivanchov and Yurzhenko (94,95) have studied the rate of decomposition of persulphate and rate of polymerisation of styrene in the presence of a series of fatty acid soaps from formate to palmitate, and reported that the rates were related to each other. Morris and Parts (96) found that sodium dodecyl sulphate and sodium hexadecyl sulphate increased the rate of disappearance of persulphate anions, whereas a fully fluorinated anionic surfactant did not appreciably change the rate of decomposition, presumably because it was particularily resistant to oxidation (37).

It is not thought (67,91,97) that the enhanced rate of decomposition contributes to initiation. Friend and Alexander (98) using the water-soluble monomer acrylamide, found that the rate of polymerisation was not changed by the presence of sodium dodecyl sulphate above and below the critical micelle concentration, or Renex 690 (a non-ionic alkyl phenyl ether of polylethylene glycol). Similar results were obtained using cationic surfactants below the critical micelle concentration. These workers did not determine whether these surfactants affected the overall rate of decomposition of persulphate. Polyacrylamide is soluble in water, hence any extraneous effects caused by surfactant stabilisation of the polymer particles produced with styrene and other monomers was obviated. Allen (97) using ammonium persulphate and methyl methacrylate found constant persulphate efficiency over a range of sodium dodecyl sulphate concentrations below the critical micelle concentration.

b) Effect of monomers and other oxidizable species.

Potassium persulphate is a powerful oxidising agent at the temperatures usually encountered in emulsion polymerisations (99). Morris and Parts (96) and Patsiga (100)

have found that the rate of disappearance of potassium persulphate in the presence of vinyl acetate was accelerated dramatically. A smaller acceleration was induced by methyl acrylate and acrylonitrile. Wilmarth and Haim (101) have discussed the various mechanisms for the chain decomposition of persulphate in the presence of oxidizable additives.

Stürzenhofecker (102) showed that the rate of decomposition of persulphate was accelerated in the presence of hydrocarbons, e.g. styrene, toluene and ethylbenzene, a similar increase was found by Van der Hoff (1) for n-octane and benzene.

F. PARTICLE MORPHOLOGY IN EMULSION POLYMERISATION.

In the theories of emulsion polymerisation discussed so far, it has been tacitly assumed that the monomer was distributed homogenously throughout the particles. Data obtained by Williams et al (86,103-112) led them to question this basic assumption and to propose a core-shell model, wherein the particles consisted of a monomer-rich shell surrounding a polymer-rich core. They studied the persulphate initiated polymerisation of styrene in the presence of surfactant, and determined that Interval II ended at about 30% conversion, but that the rate expressed as percent conversion versus time, remained constant up to 60% conversion (103,108). They determined that Smith and Ewart (16) Case II kinetics were in operation in that initiation perturbation studies did not lead to a change in the rate of reaction. Smith and Ewart, Case II predicts that $\bar{n} = 0.5$ and hence the rate of polymerisation:

$$R_p = k_p N [M]_p \bar{n} = \frac{k_p [M]_p N}{2}, \qquad \text{--- (32)}$$

i.e. independent of [I]. However, $[M]_p$ is decreasing during Interval III, and in order to explain their results they postulated that the monomer was not evenly distributed throughout the particle, but was mainly present in

the surface region. The concentration of monomer within this region being sufficient so that diffusion of monomer was not the rate-determining step.

In order to demonstrate the presence of this proposed core-shell structure they carried out a series of experiments involving the addition of butadiene (0.7 wt % in styrene) to polystyrene seeds (106,108-110). In the first experiment, the butadiene was added to a polymerisation which had proceeded to 20% conversion. At the end of the reaction, a sample of latex was embedded in resin and ultra thin sections were taken and examined in the electron microscope after being treated with osmium tetroxide which stained the unsaturated butadiene repeat unit. The micrographs showed the presence of an unstained core and a stained shell. In order to determine whether the core-shell structure was due to the rate of polymerisation being so great as to prevent particle saturation swelling of the initial polymer spheres, they prepared a polystyrene seed and saturated it with a mixture of butadiene and styrene monomers before initiating the reaction. Again, electron microscopy showed a core-shell structure, indicating that the primary mode of fresh monomer addition was encapsulation rather than swelling. They also demonstrated the core-shell model in experiments utilising tritiated styrene (108).

Napper (113) suggested that their observed results may be due to the presence of charged sulphate groups on the ends of the polymer chains which would effectively anchor the chains at the polymer/water interface. Second stage growth could occur by diffusion of monomer distributed throughout the particle to the periphery thus producing the observed core-shell morphology. In order to assess this, Williams et al (110) carried out polymerisations using benzoyl peroxide initiator, and although the core-shell morphology was still evident, the shell was much thinner than in the case of persulphate initiation,

indicating that some growth had occurred throughout the particle. However, the amount of staining in the central core region due to the presence of butadiene was very slight.

Bradford et al (114) have previously reported that particle heterogeneity occurred during seeded polymerisations, using different monomer mixtures for the production of the seed and further growth.

In an attempt to explain the encapsulation by monomer, Williams et al (111,112) proposed that a polymer molecule in the periphery of the particle would have a low configurational entropy as configurations involving that part of the polymer molecule, which should be in the water phase, were prohibited. A more entropically favoured particle would consist of a central region with a close network of entangled coiled polymer chains and an outer region with a diluted network of polymer chains which would occupy their most favourable conformations.

Gardon (115,116) has heavily criticised Williams et als' interpretation, and his recalculation of their conversion time curves indicated that they were not linear, but convex to the time axis. He also showed that the rates of monomer diffusion within the particles was rapid enough so that concentration gradients would be unlikely even after the monomer droplets had disappeared at relatively high conversions. Both Gardon and Ugelstad et al (28) have criticised Williams et als assumption of Smith and Ewart Case II behaviour on the premise of perturbation studies, these authors determined that the expected rate increase would be very small, and Gardon upon recalculation and statistical analysis of the relevant conversion/time curves, showed that it was likely that an increase in rate had occurred upon the addition of initiator. Gardon also stated that it was doubtful whether the distribution of monomers in a swollen latex particle would be frozen by their conversion to a copolymer in a two

stage emulsion polymerisation. He also criticised Williams' (111,112) thermodynamic arguments in that it was unlikely that the polymer chains would be anchored to the interface by single point attachment.

Further doubt has recently been cast on the results of Williams et al through their use of Triton x - 100 emulsifier, a nonionic octyl phenoxy ethylene oxide. Recently Piirma et al (117,118) have shown that the emulsifier Williams et al used gave very different rates of polymerisation depending upon the ageing of the emulsifier. This was explained by the spontaneous development of peroxides in the emulsifier in contact with air. They also found that there was a very marked chain transfer to the emulsifier, probably caused by the labile benzillic hydrogen of Triton x - 100. Williams and Bobalek (86) reported a marked increase in molecular weight with conversion, which according to Piirma et al was probably due to the emulsifier.

Recently, Wilkinson et al (119,120) and Goodall et al (85,121,122) have produced evidence of an heterogenous particle structure occurring during styrene and styrene-type emulsion polymerisations. Electron microscope studies of surfactant free multi-sampled kinetic runs and seeded growth processes showed the presence of large numbers of particles having nonuniform electron density gradients. They interpreted their results in terms of a void present within the particle which could have been due to the loss of monomer upon evacuation prior to electron microscopy. They proposed that evacuation of particles homogenously swollen with monomer would not result in the deformations observed, and that therefore most of the monomer in the particles was present within a specific region.

G. CHARACTERISATION OF LATEX SURFACES.

In order for a latex to be employed as a model colloid, it is important that the nature and concentration of

the bound surface groups is known. The determination of these parameters involves two stages; the removal of excess electrolyte and emulsifier from the latex and subsequent analysis of the surface groups.

1) The removal of electrolyte and emulsifier from latices. Two techniques are generally used, and which method is the most efficacious and unequivocal has been the subject of a considerable amount of research.

Dialysis can be an exponential process in which total removal is doubtful. Edelhauser (123) found that the rate of dialysis of sodium dodecyl sulphate against water was initially high, but soon dropped off to a virtual standstill without actually reaching equilibrium. Similarly, Force et al (124) found that with a butadiene/styrene copolymer latex, stabilised with Dresinate 214, only about 50% of the emulsifier was removed by dialysis for 160 days. Similar results for the incomplete removal of emulsifier have been reported by other workers (63,125). Vanderhoff et al (3) using atomic absorption spectroscopy showed that even after prolonged dialysis significant amounts of sodium from the sodium dodecyl sulphate used as emulsifier and potassium from the potassium persulphate initiator were still present. On the other hand, Ottewill and Shaw (126,127) using ^{14}C labelled sodium dodecanoate, found that after nine dialyses 98.89% of the total mass originally present was removed. Similarly, Brace (128) found that ^{14}C and ^{35}S radio-tagged sodium dodecylsulphate could be completely recovered when added to a polystyrene latex prepared in the absence of surface-active agent, except for traces of ^{14}C which he attributed to strongly adsorbed dodecanol formed by hydrolysis of sodium dodecyl sulphate.

Ottewill (5) has found that the charge of some colloidal sols was reversed upon treatment with an ion-exchange resin. Schenkel and Kitchener (129) found that deionised water contained a weakly basic polyelectrolyte and warned against its use in experiments involving small surface

areas. Van den Hul and Vanderhoff (3,130,131) have developed a procedure which is capable of cleaning ion-exchange resins to the extent that no leachable impurities are detectable in the deionised water produced. However, several workers have found that even after cleaning, the resins discoloured water upon standing and smelled of amines (48). Roy et al (132), in their studies on the dye partition technique for the estimation of charged groups in polymers, believed that the low results obtained by Van den Hul et al (133) in the analysis of the sulphate end groups in a polystyrene latex using their method was due to some interfering impurities derived from their latex clean-up process. They further suggested that the interfering impurity might be some quarternary or ammonium salts derived from the ion exchange resins used for cleaning the latices. Indeed, Van den Hul et al (130) have stated in a footnote that the effectiveness of the process depends on the particular batch of resin used. However, their results indicated that once a good batch of resins was purified, they were more efficient at removing adsorbed ionogenic species than dialysis (3,130) as illustrated by their experiment involving atomic absorption on an ion exchanged latex, where they found that the amounts of sodium and potassium present in the latex were well below those for the equivalent dialysed latex. In another experiment, using a latex which had been ion exchanged to constant surface charge (3.3 μ C cm^{-2}), Van den Hul et al (3) showed that dialysis did not remove any more material from the latex (surface charge density 3.4 μ C cm^{-2}), they also added five different emulsifiers to samples of the clean latex, above their critical micelle concentrations, and reionexchanged. In all cases the emulsifiers were removed completely (surface charge density after reionexchange 3.4 μ C cm^{-2}). It has been suggested (134) that because of the strong electrostatic interactions which may develop between the colloidal part-

icles and ion exchange resin beads, it is possible that adsorption of the particles may also occur, in which case the concentration and size distribution of the latex may be altered upon treatment.

Other impurities which are often present in the latex at the end of a reaction include monomer and other organic species such as benzaldehyde. Dialysis is not very efficient at removing these due to their low solubility in water (48). Wilkinson (135) and Gultepe (136) have both found that upon steam stripping a well-dialysed latex, an oily layer was present in the distillate having both the odour and molecular weight of styrene. Shaw and Marshall (137) have detected residual amounts of styrene in well-dialysed latices by infra-red spectroscopy. Greene (138) claims that a combination of dialysis against continuously running deionized water for two days combined with absorption into and adsorption onto nonionic bead polymer particles of the organic impurities gave good results. It is likely that ion exchange beads would perform a similar task with regards organic impurities.

At the present time both ion exchange and dialysis are used, although dialysis is usually restricted to the purification of latices produced in the absence of emulsifier. In a recent discussion of polymer colloids, Fitch (139) states that dialysis would appear to be the method of choice.

2) Surface group analysis. The surface groups present on latices usually arise from initiator fragments chemically bound to the ends of the polymer chains, unless an ionogenic monomer such as acrylic acid is used. The groups most commonly encountered are sulphate, hydroxyl and carboxyl. Sulphate groups are produced directly from the persulphate initiator (140). Hydroxyl groups can arise from the use of hydrogen peroxide initiator or, when present in persulphate initiated latices, from either the hydrolysis of surface sulphate groups (141) or the polymerisation by

hydroxyl radicals produced by a side reaction of persulphate with water (87,130,133,141,142), (see decomposition of persulphate.

Hydrolysis of sulphate groups has been demonstrated by Hearn (48) who found that the number of sulphate groups decreased with time for latices stored at elevated temperatures. Hydrolysis has also been shown to occur at room temperature by Chen (143) and Everett et al (144), the latter workers found the rate to be 2.5% per month.

Several techniques have been developed for the quantitative determination of the groups bound to the ends of the polymer chains. These include conductometric (3,141, 145) and potentiometric titrations (133,146,147), colorimetric dye interaction techniques (132,148), X-ray fluorescence analysis (for sulphur) (145), neutron activation analysis (for oxygen and sodium) (138), radiotracer methods (90,149), titration with a surface-active substance of opposite charge until the onset of rapid coagulation (138) or a change in the slope of the equilibrium adsorption isotherm (150) is observed, electrophoresis (127,151) and infra-red spectroscopy (133,137,147). Only the titration and electrophoresis methods give direct information about the surface groups.

A certain amount of controversy has arisen over the surface groups present on latices. This is complicated by the effectiveness of the clean-up process used, especially in the case of latices produced in the presence of emulsifier.

a) Characterisation of latices produced in the presence of emulsifier. Ottewill and Shaw (127,151) showed by electrophoresis the presence of weak acid groups on latices produced using both hydrogen peroxide and persulphate initiators (the latter also produced strong acid groups) in the presence of a variety of emulsifiers and purified using dialysis. Similarly, Hearn (48) showed the presence of both strong and weak acid groups on polystyrene latices

using the conductometric titration technique. He also ion-exchanged one of his latices and found that the strong acid end-group concentration had increased whereas the weak acid contribution had disappeared, which he attributed to impurities leached from the resins. From electrophoresis results Ottewill and Shaw (127,151) determined that the surface dissociation constant (pK_s) of the weak acid was 4.64 and that it appeared to be an integral part of the polymer. Similar results were obtained by Smitham et al (99). Shaw and Marshall (137) compared the infrared spectra of the latices found to contain carboxylic groups with that of a 'standard polystyrene' (Distillers Co. Light scattering standard) and concluded that these spectra had contributions from carboxylic acid groups which they suggested were phenylacetic acid residues or residues with a similar structure. However, in the preparation of these latices no attempt was made to exclude oxygen. On the other hand Van den Hul and Vanderhoff et al (3,133,145,152), using ion-exchange to purify their latices, found only strong acid sulphate groups on polystyrene latices produced using persulphate and a variety of emulsifiers. That ion-exchange was not an inherently unsuitable cleaning technique for carboxyl groups was demonstrated by Van den Hul (130), who produced a polystyrene latex in the presence of acrylic acid using persulphate initiator. After ion-exchange, conductometric titration curves revealed two distinct regions attributable to sulphate and carboxyl groups.

Evidence obtained by Stone-Masui and Watillon (153) indicate that the emulsifier used may affect the type of surface groups produced. They found that latices produced using sodium dodecyl sulphate, sodium dodecyl sulphonate and sodium octadecyl sulphate with persulphate initiator only showed the presence of strong acid groups, whereas those produced using potassium stearate and sodium laurate emulsifiers showed the presence of large amounts of weak

acid groups. These workers used ion-exchange resins to clean up their latices.

Hydroxyl groups cannot be titrated conductometrically, however they can be detected after their oxidation to carboxyl groups using the method of Van den Hul et al (154), and in this way they have been detected on latices produced under a wide range of conditions and using both ion-exchange and dialysis as clean-up procedures.

b) Characterisation of latices produced in the absence of emulsifier. The same groups as mentioned in the previous section have also been found on these latices, but the presence of carboxyl groups is still subject to some conflicting evidence. Goodwin et al (141) and other workers (48,143,144,147) have detected carboxyl groups using dialysis as a clean-up procedure. However, Laaksonen et al (147) found that with two latices produced under identical conditions except for different ionic strength (adjusted with sodium chloride), one exhibited carboxyl groups whereas the other did not. Furusawa et al (155) found only strong acid groups on latices cleaned by ion-exchange, whereas Stone-Masui and Watillon (153) have detected both strong and weak acid groups on latices similarily purified.

In a recent paper, Wu et al (156) have postulated that pH changes occurring during polymerisation and the presence of heavy metal contaminants could be the cause of carboxyl group formation. They found that the addition of 4×10^{-4} moles l^{-1} silver nitrate to one of two otherwise identical reactions resulted in the formation of carboxyl groups on the latex prepared in the presence of silver nitrate, whereas none were present on the latex produced in the absence. Wu et al (156) attributed this to the catalysed oxidation of hydroxyl groups. They also found that with unbuffered reactions, using persulphate initiator, the pH showed a strong decrease during the polymerisation, and correlated this with a higher proportion of hydroxyl end groups which could be oxidised to carboxyl groups.

Similar results have been observed by Ghosh et al (157), who attributed them to an increase in the rate of reaction of sulphate free radicals with water under acid conditions to produce hydroxyl radicals (158). The increase in the number of hydroxyl groups could also be due to the increased rate of hydrolysis of sulphate groups at low pH. Read and Fredell (159) have shown that the rate of hydrolysis of sodium dodecylsulphate increases markedly as the pH decreases.

Wu et al (156) have shown that with potassium dihydrogen phosphate and sodium tetraborate buffer systems, weak acid groups were produced, even though the final pH was 7.0 - 8.7. They attributed this to chain transfer with the electrolyte ion to give a weak acid end-group, especially in the case of sodium tetraborate, where two different weak acid end points were found.

It has been recently reported that the interpretation of titration curves of latices containing both weak and strong acid groups may not be a straightforward procedure. Everett and Gultepe (144) using dialysis as a clean-up technique found that latices produced in surfactant-free systems had both strong and weak acid groups on the surface. On titrating the latices in 10^{-3} moles l^{-1} electrolyte they found that the end-point became difficult to interpret, and varied with the per cent solids, whilst the strong acid end-point remained constant in agreement with Van den Hul et als (3) findings. They also titrated the latices using barium hydroxide, again confirming Van den Hul et als (3) findings of invariant strong acid end-point as compared with sodium hydroxide, but they found that the weak acid was 30 per cent less, presumably due to difficulty in interpretation of the titration curves.

Yates (146) has demonstrated the applicability of potentiometric titrations to determine the pKa of weak acid groups on latices stabilised solely by these groups,

produced using 4, 4' - azobis 4 cyanopentanoic acid as initiator. However, in a paper examining potentiometric titrations as a technique for latex characterisation, Laaksonen et al (147) concluded that it was not possible to make a significant distinction between the effects of carboxyl and sulphate groups on the binding of hydrogen ions from uncertainties in the equivalence point, the concentration of impurities and diffusion potentials. They thought that the electrophoretic method of Ottewill and Shaw (151) was probably the best method for latices with low surface charge densities.

c) Total end-group determination. It is known that the termination of growing polymer chains in the emulsion polymerisation of styrene is predominantly by combination rather than by disproportionation (160-165). Kammarar et al (163) found that the molecular weight calculated from end-group assay, assuming two end-groups per polymer chain, was in excellent agreement with that determined by osmomotry. Hence, there should be two sulphate or other end-groups per polymer chain. Indeed, Smith (149), using potassium persulphate containing radioactive sulphur, found two sulphate end-groups per polymer molecule in polystyrene samples prepared at temperatures between 303 and 363 K. However, Kolthoff et al (87) found great difficulty in reproducing Smiths (149) results, and found between 1.2 and 3.1 sulphur containing groups per chain and suggested the high values arose from the difficulty of completely removing uncombined radioactive sulphur from the polymer.

Due to the ionic nature of the sulphate groups and the water of hydration of the hydroxyl groups, they should tend to remain at the polymer/water interface. Thus, titration data combined with molecular weight data should yield a value of two for the number of end groups per polymer chain. Workers with surfactant-containing systems have found values typically in the range 1 - 1.3 (1,3) per

polymer chain which increased after oxidation of the hydroxyl groups to carboxyl to about 1.6 per polymer chain. On the other hand Hearn et al (48,166), using dialysis to purify their latices, found that the total number of end groups per polymer chain was in the region of 4.5, which Hearn (48) attributed to the spread of molecular weights.

Two methods have been developed for the analysis of end-groups which become buried within the particle during polymerisation.

i) Pallit and co-workers (148) have developed the dye-interaction and partition techniques. In the dye-interaction technique the acid end-groups are detected by allowing the benzene extract of a basic dye to interact with a solution of polymer in benzene. If acid groups are present then a colour change is observed. The optical density of the polymer/dye solution is measured and compared to a calibration curve prepared using an acid having a similar structure to that of the end-groups. In dye-partition, a solution of latex dissolved in either benzene or chloroform is shaken with an equal volume of methylene blue dye dissolved in 0.1 moles l^{-1} hydrochloric acid. The methylene blue interacts with the acidic groups present and is carried into the organic phase. The colour developed is then measured and compared to a calibration curve as above. Dye-interaction is suitable for determining both strong and weak acid groupings, whereas the dye-partition is only suitable for strong-acid determinations. The number of hydroxyls can be determined after their oxidation to carboxyl groups using the pyridine/phthallic anhydride technique (167). Using these techniques, Ghosh et al (157) determined that there were approximately two end groups per polymer chain for persulphate initiated polymers of styrene and methyl methacrylate.

Doubt has been cast on the reproducibility and

accuracy of these dye techniques due to the sensitivity of the colorimetric reagents not only to trace amounts of acid, but also to light and heat. In particular, Bitsch (168) found that the number of sulphate end-groups determined for polystyrene by the dye-partition method was always much lower than that determined by other methods.

ii) Van den Hul and Vanderhoff (130,152) have titrated conductometrically latices dissolved in dioxan/water mixture (80 : 20). They detected the presence of buried sulphate groups, which when combined with their data on surface sulphate and hydroxyl groups took the number of end groups per polymer chain to about 2. They found that the total number of sulphate groups determined by this technique was in good agreement with that by X-ray fluorescence, but, in agreement with Bitsch (168), were always greater than those obtained by the dye-partition method. (see p. 39).

H. EMULSION POLYMERISATION IN THE ABSENCE OF ADDED SOAP.

1) Introduction.

a) Advantages and disadvantages with respect to emulsifier present formulations. The preparation of polymer latices in the presence of added surface-active agents has some advantages in the context of industrial production, namely that the maximum per cent solids-without-coagulation is greater than is possible in surfactant-free systems, and that the rate of reaction is also greater. However, it can be seen from the preceding sections that they have certain disadvantages when used for kinetic studies due to the effect of the emulsifier on initiator decomposition and also the effect of emulsifier as a chain transfer agent, (see earlier Williams core-shell theory). Dunn (169) considers that surfactants in general are difficult to obtain in a pure state. Also the surface characterisation of the latices produced is complicated by the presence of adsorbed emulsifier and the effectiveness of the techniques used to remove it.

The particle diameters produced in the presence of added surfactant in a single stage growth process, are typically < 500 nm, larger particles being produced by a seeded growth process (166), this process apart from being tedious does not readily lend itself to the production of particles > 1 μm. It has been shown (141,170) that using the surfactant-free process particles of diameter in the range of 100 - 1000 nm could be produced easily in a single-stage process. Further, that the cleaning-up of the latices prior to surface characterisation only involved the removal of electrolyte excess monomer and any reaction by-products such as benzaldehyde.

It would be expected that kinetic studies on surfactant-free systems would be less complicated in that the number of variables in the system is reduced. There would be four extrinsic variables: monomer concentration, initiator concentration, temperature and background ionic strength.

Recent evidence by Homola et al (171) indicates that soap-free emulsion polymerisation in the presence of 10% methanol may give reaction rates and maximum per cent solids comparable to those of reactions carried out in the presence of emulsifier.

b) History. The polymerisation of styrene in the absence of added surface -active agent was first recorded by Hohenstein and Mark (172) in 1946, but it was not until 1965 that Matsumoto and Ochi (173) successfully used the process to prepare monodisperse latices. They produced stable latices using potassium persulphate initiator and styrene monomer, and postulated that the particle stability was due to interparticle electrostatic repulsions derived from the presence on the particle surfaces of sulphate groups covalently bound to the polymer chain rather than by adsorption. Since 1965 a number of studies have been made on the preparation of monodisperse poly-

styrene latices without the addition of emulsifying agents (140,141,170,174,175). Hydrogen peroxide was found to give a polydisperse unstable latex at very low conversions under a variety of conditions which Kotera et al (140) interpreted as being indicative of continuous particle coagulation throughout the reaction due to the absence of electrostatic stabilisation of the particles. Similar results were obtained by Dunn and Taylor (176).

2) The effect of the extrinsic variables on the size, surface charge density and molecular weight. Kotera et al (140) studied the effect of monomer and initiator concentrations and found that increasing the monomer concentration led to an increase in the final diameter of the particles. The molecular weights also increased, although the heterogeneity of the polymer produced, as expressed by $\frac{\overline{M}_w}{\overline{M}_n}$ ratios, remained almost the same. The zeta potentials of the latices, as measured by micro-electrophoresis and moving boundary techniques also remained approximately the same, being in the region of 70 - 80mV and 80 - 90 mV, respectively. The above trend of increasing particle diameter was also observed by Goodwin et al (141,170) who quantified the data they obtained into the relationship:

$$\log D = 0.410 \log [M] + 2.780 \text{ at } 358 \text{ K} \quad \text{--- (77)}$$

$$\text{i.e.} \quad D \propto [M]^{.410} \quad \text{--- (78)}$$

It might be expected that in systems where only the monomer concentration was varying, the number of particles per millilitre would remain the same , and hence the relationship should be:

$$D \propto [M]^{.333}. \quad \text{--- (79)}$$

It therefore appears that increasing the monomer concentration leads to a decrease in particle number.

The experiments of Kotera et al (140) involving the variation of initiator concentration were not carried

out at constant ionic strength. They found that increasing the potassium persulphate concentration resulted in an increase in particle diameter, again the zeta potentials of the latices remained in the range of 70 - 80 mV and 80 - 90 mV. No trend in molecular weight with initiator concentration was observed. Goodwin et al (141, 170) later showed that increasing the initiator concentration at constant ionic strength resulted in a decrease in particle size, the molecular weight decreasing with decreasing particle size.

They found:

$$\log D = -0.239 \log [I] + 3.118 \text{ at } 343 \text{ K.} \quad -- (80)$$

Goodwin et al also investigated the effect of ionic strength and found that increasing the ionic strength resulted in an increase in the particle diameter, but that no trend with regards molecular weight was evident. The following relationship between particle diameter and ionic strength was found:

$$\log D = 0.238 \log [I_s] + 3.23 \text{ at } 343 \text{ K.} \quad -- (81)$$

and:

$$\log D = 0.238 \log [I_s] + 3.14 \text{ at } 353 \text{ K.} \quad -- (82)$$

The relationship between temperature and particle diameter was found by Goodwin et al (141,170) to be:

$$\log D = \frac{1173}{T} - 0.578, \quad -- (83)$$

i.e., that increasing the temperature leads to decreasing particle size. They (141,170) also found that the molecular weight ($\bar{M}n$) decreased with increasing temperature. Equations 77,80-83 can be combined to give:

$$\log D = 0.238 \log \left(\frac{[I_s][M]^{1.723}}{[I]} + \frac{4929}{T} \right) - 0.827 \quad -- (84)$$

Goodwin et al (141,170) found that the surface charge densities of the latices produced under a variety of conditions were similar, (although there did appear to be a trend of increasing surface charge density with increasing

ionic strength for latices produced at 353 K), varying between 2 - 8 μ coulombs cm^{-2} and being of the same magnitude as those found by other workers on latices produced in the presence of added surfactant (130).

Goodwin et al (170) have stated that the hydrodynamic conditions appear to be important, with rapid stirring necessary to keep the monomer phase well dispersed, in order to facilitate the transfer of monomer through the water phase to the growing particles. However, Kotera et al (140) found no appreciable difference in the particle sizes produced during chemically and thermally identical reaction, whilst varying the stirrer speed between 200 and 400 r.p.m., presumably these rates of stirring were sufficient to maintain adequate transfer of monomer to the growing particles.

3) Particle nucleation. It would appear that the solubility of the monomer is important in determining the mode of particle nucleation in the absence of added surface-active agents. The solvent power of the water determines the degree of coiling of the polymer chains and hence affects the rate of mutual collision and thus the rate of association or precipitation (1). Also Lim and Kolinsky (177) have shown, in studies on the polymerisation of styrene in solutions of a homologous series of acetic acid esters, that the degree of coiling affected the rate of termination of the macroradicals. Goodall et al (85) have postulated that the structure of the oligomers is important. They detected large amounts of low molecular weight material (ca 1000) in particles removed from a styrene emulsion polymerisation reaction during the early stages, whereas similar samples from methyl methacrylate emulsion polymerisations did not show the presence of this material. These workers interpreted their results in terms of the structure of the oligomeric free radicals. In the case of styrene the oligomers would have the classical surface-active agent structure, a hydrophobic chain with a hydro-

phillic head group, whereas methyl methacrylate oligomers would have a hydrocarbon backbone, each unit of which would contain a $\overset{O}{\overset{\|}{C}}-O-$ grouping. Thus, the styrene oligomers, (M.W. ~500 i.e. 4 - 5 styrene units long in agreement with Vanderhoff et al (3) who postulated that 4-6 monomer units must add to a sulphate free radical in order for it to become surface-active), would tend to micellise at relatively low chain length, i.e. before they became insoluble, whereas methyl methacrylate oligomers would not. Priest (70) found that when a surfactant-free solution polymerisation of vinyl acetate, initiated by persulphate, was quenched at the point of incipient turbidity, the average degree of polymerisation of the polymer formed was about 50, indicating that higher molecular weight oligomers precipitate out and participate in particle nucleation. However, it is thought (37) that the quenching was not immediate and that the actual value should be slightly less.

Several postulates have been advanced to explain the mechanism of particle nucleation in the absence of added surface-active agent.

i) That the growing oligomeric free radicals reach a chain length and concentration at which they micellise (1,121,141), rapid termination would then occur and further growth take place by imbibition of monomer and other oligomeric free radicals. The term micellise as used here is perhaps misleading. A true micelle only exists in a dynamic sense since it continually breaks down and reforms. However, if surface-active free radical oligomers orientate into a micelle, rapid termination would occur and the resultant nucleus is no longer a "true micelle". Both Hearn (48) and Van der Hoff (67) have detected a drop in surface tension prior to turbidity. Recent results of Goodall et al (85,120,121) suggest that a large amount of termination of low molecular weight species occurs in the early stages of the reaction.

French (178) has reported that in systems containing surfactant below the critical micelle concentration the number of particles generated was independent of the initiator concentration, and that the surface tension of the aqueous phase decreased prior to the onset of cloud-ing. These results lead him to suggest that the surface-active oligomeric free radicals built up to a limiting concentration, followed by the formation of micelles and/or particles.

ii) That as the oligomeric free radicals grow they become less soluble. With the addition of each new monomer unit, the total energy of interaction between the growing organic radical and the solution increases, and this energy is de-creased by the organic backbone coiling up. Growth and coiling proceed rapidly until it can be considered that the oligomeric radicals constitute a separate phase, Fitch (33) has described this process as "the homogenous mechanism of particle nucleation". Fitch et al (71) post-ulated two possible mechanisms for termination; that either colloidal macroradicals coagulated prior to termination, a mechanism also proposed by Baxendale (179), or that chain radicals grew to macromolecular dimensions and under-went mutual termination while still in true solution with particle formation and subsequent growth occurring by phase separation and coagulation of these dead species. They suggested that as homogenous kinetics were obeyed beyond the stage where particles were formed that the second mechanism seemed most likely. Opposing views have been expressed in the literature. Evidence for solution termination has been found by Fiquet-Fayard (180), Whitby et al (181), Sheriff and Santappa (182) for methyl meth-acrylate, by Pastiga et al (183) for vinyl acetate and by Crescentini (184) for methyl vinyl pyridine. However, Biswan and Palit (185), Ley et al (186) for methyl meth-acrylate, Dunn and Taylor (176) for vinyl acetate and Dainton et al (187) for acrylonitrile all support the

view in agreement with Baxendale et al that colloidal coagulation regulates the rate of mutual termination.

Fitch (188) argued that the initial rate of particle formation during the emulsion polymerisation of methyl methacrylate equalled the rate of radical generation. Subsequently, soluble oligomers could form new particles by a precipitation process, or be captured by existing particles:

$$\frac{dN}{dt} = R_i - R_c \quad . \qquad \text{-- (85)}$$

Analogous expressions have been postulated by Gatta et al (189) for vinyl chloride and Gardon (46) for micellar systems. Eventually, R_c would approach R_i until $\frac{dN}{dt} = 0$, for a monodisperse preparation $\frac{dN}{dt} = 0$ should be achieved as quickly as possible (190).

$$N = \int_0^{t_{cr}} (R_i - R_c)\, dt \quad , \qquad \text{-- (86)}$$

t_{cr} is the time to reach steady state.

$$R_c = \pi N r^2 L R_i \quad \text{from Gardon (46),}$$

Nr^2 is proportional to the total polymer particle surface area, i.e. $\alpha \frac{v^{\frac{2}{3}}}{N}$. The volume would increase during the period of particle formation according to non-steady state homogenous kinetics. The overall rate of particle formation can then be shown to take the form:

$$\frac{dN}{dt} = R_i \left[\left(1 - (N\pi)^{\frac{1}{3}}\right) \left(\frac{3k_p}{4k_t \rho} [M] \ln (\cosh R_i k_t)^{\frac{1}{2}t} \right)^{\frac{2}{3}} L \right] \qquad \text{-- (87)}$$

In the heterogenous kinetic scheme the growing macroradicals are physically prevented from mutual termination because of the electrostatic forces which stabilise the colloid. Each growing radical is isolated in a polymer/monomer particle. Termination can then only occur by entry into a growing particle, of a primary initiator radical or an oligomeric radical of low molecular weight. Fitch

et al (71,188) found that if no allowance was made for the charge on the particle, then a radical could diffuse to the particle surface 10,000 times faster than the time required to add a single monomer unit, in agreement with Flory (79). However, the charge on the particles provides a substantial potential energy barrier to radical entry and Fitch et al (71) calculated that when this potential energy barrier was taken into consideration, the probability of a successful entry was very much lower than the probability of monomer addition, so that the average radical entering a particle would have several monomer units attached.

Once the initial nuclei are formed, then, in the case of monomers soluble in their polymer, the nuclei imbibe monomer and swell. However, since the nuclei contain only a small number of chains, it is likely that growth will result in loss of colloidal stability. Goodall et al (85, 121) have shown that for polystyrene the initial particles consist mainly of low molecular weight material (ca 1000), but that further growth occurs by the formation of material > 50,000 molecular weight. This would result in a large volume and hence surface area increase but with the addition to the growing particles surface charge of only two charged initiator fragments. Dunn and Chong (191) applied the theory of the stability of lyophobic colloids, D.L.V.O. theory (192,193). The energy of repulsion, V_R, can be obtained from the surface potential:

$$V_R = \frac{\epsilon r \psi_0^2}{2} \ln (1 + \exp (- \kappa H_0). \qquad -- (88)$$

The energy of attraction which promotes the coalescence of particles arises from the intermolecular Van der Waals' forces of attraction, which depend on the polarity, polarisability, etc. of the material. These forces are characterised by the Hamakar constant (194):

$$V_A = -\frac{A}{6} \left(\frac{2r^2}{R^2-4r^2} + \frac{2r^2}{R^2} + \ln \frac{R^2-4r^2}{R^2} \right) \qquad -- (89)$$

In colloidal systems the particles are in a disperse phase so that A must be modified to include the effects of the surrounding medium (195). Ottewill and Walker (4) found 5×10^{-14} erg for the Hamakar constant of aqueous dispersions of polystyrene latices. The resultant energy of interaction, V, can be calculated as a function of distance between particles by adding V_A and V_R. Thus V_{max}, the height of the potential energy barrier preventing particle coalescence, can be obtained. The rate of particle coalescence can be most conveniently characterised by use of Fuch's stability ratio (196). This is the ratio of the rate of slow coalescence hindered by an energy barrier (V_{max}), to the rate which would be observed if the inter-particle forces were entirely attractive.

$$W = \frac{\int_0^{\infty} \exp \frac{V}{kT} \frac{du}{(u+2)^2}}{\int_0^{\infty} \exp \frac{V_A}{kT} \frac{du}{(u+2)^2}} \quad \text{where } u = \frac{H_0}{r} \qquad -- (90)$$

The rate of coagulation (R_{co}) of colloidal dispersion is given by:

$$R_{co} = -\left(\frac{dN}{dt}\right) = \frac{k_0 N^2}{W} . \qquad -- (91)$$

Since W is small for the particles formed by the nucleation process, rapid coagulation occurs until the new entities formed by coalescence of the monomer swollen nuclei attain a radius and surface charge density which is adequate to produce a large value of W, i.e. a large potential energy barrier to coagulation. The magnitude of the particle radius required to achieve an adequate value of W for stabilisation ($R_{co} \longrightarrow 0$) is dependent on the ionic strength of the medium and on the surface charge density.

During the coagulation stage, the number of particles present in the system decreases according to equation 91. The rate, R_{co}, initially large, gradually drops towards zero as W increases. Hence R_n will initially be large, and since coagulation cannot occur until the particles have

been formed, R_{co} will be small. Therefore at this stage $R_n > R_{co}$ and the total rate of particle formation is given by:

$$R_T = \left(\frac{dN}{dt}\right)_T = R_n + R_{co} \quad , \qquad \text{--- (92)}$$

will be positive. As the particle number increases R_{co} will increase until $R_{co} = R_n$, this gives $R_T = 0$, the condition of a maximum on a curve of N against time. However, once nucleation has occurred, $R_n \longrightarrow 0$ and $R_{co} > R_n$, leading to a decrease in N with time. For small W and large N, R_{co} is large but decreases as W increases and N decreases. Eventually, $R_{co} \longrightarrow 0$ and the number of particles in the system becomes constant. The subsequent growth therefore occurs at constant N, and is controlled by the formation of oligomers in solution and their subsequent diffusion and incorporation into the particle. The results of Goodall et al (85,121) for styrene demonstrate this decrease in N with time during the early stages of the reaction. A similar decrease has been noted by French (178) during the polymerisation of vinyl acetate in the presence of emulsifier, even though the emulsifier was present at a concentration above its critical micelle concentration. Goodwin et al (141,170) found that the coagulation stage for styrene was important in controlling particle size. Their results were obtained using 1 : 1 electrolytes to increase the background ionic strength, 2 : 1 and 3 : 1 electrolytes were also employed and these also exhibited the trend expected by coagulation theory, i.e. that the final particle size increased (N decreased), dependent on the valence of the added ions. Similar findings for the more water-soluble monomers have also been reported. Palit and Guha (197) observed a considerable decrease in the rate of polymerisation in aqueous solutions of methyl methacrylate on addition of 0.016 mole l^{-1} of sodium sulphate, whereas addition of magnesium sulphate resulted in a more drastic reduction of the rate.

Baxendale et al (179) have reported that the addition of a trace of cetyl ammonium bromide (.0003%) doubled the rate of polymerisation of the same monomer initiated by the redox combination of hydrogen peroxide and a ferrous salt. Further insight into nuclei coagulation was gained by the observations of Napper and Alexander (198) on the number of particles generated in the polymerisation of vinyl acetate. Addition of .003% anionic surfactant resulted in an increase in the number of particles by a factor of 50, and the same quantity of a cationic emulsifier reduced the number by a factor of 20. It was confirmed experimentally that the latices were anionic so that in the presence of anionic the latices had added stability but were coagulated by cationic surfactant.

I. CONCLUSIONS.

Since the pioneering work by Harkins (15) and Smith-Ewart (16), the theories of emulsion polymerisation in the presence of added soap has been refined (43-47) to the extent that the kinetics of Interval II are well understood, and recent work indicates that application of k_t and k_p values obtained from bulk polymerisations to Interval III kinetics yields results which are in good agreement with experimental data (53,54,56,57). Interval I remains a stumbling block, and the agreement of styrene emulsion polymerisation to the Smith-Ewart treatment appears to be the exception rather than the rule, indeed evidence obtained for methyl methacrylate, vinyl acetate and other monomers has led some workers (70-73) to question whether the micelles play the important role in particle nucleation Harkins attributed to them.

The production of monodisperse latices by Bradford, Vanderhoff and co-workers (64,199-202) and their subsubsequent surface characterisation (3,130,154) indicated that emulsion polymerisation was not only a process applicable to industrial production of polymers, but also one for the production of monodisperse latices for use in

basic scientific research. The preparation of these systems in the absence of added emulsifier (140,173) made them even more attractive for use as model colloids and Goodwin et al (141,170,175) have carried out an appreciable amount of research into the factors controlling particle size and into the characterisation of the surface groupings. Kinetic studies on these systems should also be facilitated due to the absence of any extraneous effects caused by the presence of emulsifier.

DEFINITION OF SYMBOLS USED.

A	Hamakar constant in vacuo.
A_p	Total polymeric area per unit volume of emulsion.
a	$(8\alpha)^{\frac{1}{2}}$.
a^*	The distribution coefficient between radicals in particles and solution.
a'	Surface area of a single particle.
a_s	Interfacial area of a surfactant molecule.
B	$\left(\frac{k_p}{2N_A}\ \frac{d_m}{d_p}\ \Phi_m N\right)$
C_w	Concentration of free radicals in the aqueous phase far from a particle.
D	Particle diameter.
D_w	The free radical diffusion co-efficient in water.
$\overline{DP}$	Average degree of polymerisation.
d_m	Monomer density.
d_p	Polymer density.
$[E]$	Emulsifier concentration.
f_n etc.	Fraction of particles containing n etc. radicals.
H_o	Distance between the surfaces of two particles.
$[I]$	Initiator concentration.
$[I_s]$	Ionic strength.
k	Boltzmann constant.
k_a	Rate constant for the absorption of free radicals by particles or micelles.
k'_a	Rate constant for the capture of polymeric radicals by a zero order absorption or intraparticle initiation.
k'_d	Rate constant for the first order desorption or chain stopping transfer of polymeric radicals.
k_i	Initiation rate constant.
k_o	Rate constant for diffusion controlled coagulation.
k_p	Propagation rate constant.
$(k_p)_o$	
k_s	Rate constant for free radical transfer out of particles.

k_t	Termination rate constant.
k_t^*	Termination rate constant in bulk polymerisation of methyl methacrylate.
$(k_t)_o$	
$k_{t,w}$	Termination rate constant in the aqueous phase.
$k_{1,2,3}$	Constants of proportionality.
L	The diffusive mean free path of oligomeric radicals prior to precipitation.
M_m	Molecular weight of the monomer.
$[M]$	Monomer concentration.
$[M]_p$	Concentration of monomer within the particles.
m	$\left(\frac{k_s S}{k_t}\right)$
m'	The degree of polymerisation.
N	Total number of particles.
N_A	Avagadro's number.
N_i	Number of particles or micelles of type i.
N_n etc.	Number of particles containing n etc. radicals.
n	Number of radicals in a defined volume.
$\bar{n}$	Average number of free radicals per particle.
P_v	The volume of polymer formed.
Q_o	Initial monomer concentration.
q	Weight ratio of monomer to polymer in the particles.
R	Universal gas constant.
R'	Distance between particle centres.
R_c	Rate of oligomeric radical capture by particles.
R_c^*	Rate of capture of radicals.
R_{co}	Rate of coagulation.
R_i	Rate of initiation.
R_n	Rate of particle formation.
R_p	Rate of polymerisation.
R_T	Total rate of particle formation.
R_t	Rate of termination.
$[R^\cdot]$	Total concentration of free radicals.
$[R^\cdot]_p$	Concentration of radicals in the particles.

$[R^{\bullet}]_w$	Concentration of radicals in the water phase.
r	Particle radius.
r_i	Radius of particles or micelles of type i.
S	Particle surface area.
S_s	Weight concentration of surfactant.
T	Temperature.
t	Time.
t_{cr}	Time at the end of Interval I.
u	$\left(\frac{H_o}{r}\right)$
V	Energy of interaction between particles.
V_A	Energy of attraction.
V_P	Total volume of particles.
V_R	Energy of repulsion.
v	Volume of a single particle.
$\bar{V}_M$	Partial molar volume of the monomer in the particles.
W	Fuchs stability ratio.
x	Conversion.
x_c	Conversion at the end of Interval II.
α	$\left(\frac{N_A V}{k_t \tau}\right)$
ϵ	Dielectric constant.
γ	Interfacial tension.
Υ	Reciprocal of the Debye-Hückel thickness.
μ	Rate of increase in the volume of a single particle.
ψ_o	Surface potential.
ρ	Rate of entry of free radicals into particles.
ρ^*	Rate of entry of free radicals into particles and micelles.
ρ^W	Rate of radical production in the aqueous phase.
τ	Time interval between successive free radical entries.
τ^*	Time of nucleation of a particle.

θ	$\left[(4\pi)^{\frac{1}{2}} 3\mu \right]^{\frac{2}{3}}$
Φ_M	Volume fraction of monomer in the particle.
Φ_p	Volume fraction of polymer in the particle.
χ	Flory-Huggin interaction constant.

CHAPTER II

A PREPARATION OF MATERIALS

1) Water. All the water used, unless otherwise stated, was doubly distilled from an all-pyrex glass apparatus, stored in covered pyrex glass aspirators and used within 48 hours of production. The conductance was always < 1.5 μ mho and the surface tension was found to be within the range of 71.8 - 72.0 dynes cm^{-1}, in good agreement with literature values of 71.97 dynes cm^{-1} at 298 K (203).

2) Potassium persulphate. Hopkins and Williams (Chadwell Heath, Essex, England) 'AnalaR' grade potassium persulphate was recrystallised twice from doubly-distilled water. A saturated solution was made up at room temperature and stored at 276 K for ca. 14 hours, the resulting crystals were collected, and the process repeated. The doubly recrystallised sample was dried and stored in a dessicator, (kept in a dark cupboard). The % -O-O- linkage found to be present in the purified sample was > 98%, as determined by back-titration using ferrous ammonium sulphate and ceric sulphate with ferroin indicator (204).

3) Potassium peroxydiphosphate. Potassium peroxydiphosphate, obtained from Polysciences (Paul Valley Industrial Park, Warrington, Pa., U.S.A.), was used as received. The % -O-O- determined as described above was found to be > 95%. This material was also stored in a dessicator in the dark.

4) Sodium metabisulphite. The sodium metabisulphite was B.D.H., (Poole, Dorset, England), "Laboratory reagent" grade and was used without purification.

5) Monomer purification. The styrene and vinyltoluene used in the polymerisations were of laboratory reagent grade, obtained from B.D.H. and Kochlight, (Colnbrook, Bucks., England) respectively. Upon receipt both contained inhibitor in the form of .001% - .002% tert. butyl catechol and some batches of monomer upon purification, were found to have contained significant amounts of polymer.

The monomers were purified by double distillation under a reduced pressure of nitrogen at ca. 293-313 K, the first and last 10% of each distillate being discarded. The purified monomer was stored under nitrogen at 253 K and was redistilled if the storage time was greater than four weeks.

Monomers such as tert-butylstyrene and divinylbenzene used in small amounts in copolymerisation reactions, were used as received and stored under nitrogen at 253 K.

6) Latex preparation. Polymerisations were carried out in either 0.5 or 1 l three necked flasks fitted with a P.T.F.E. moon shaped stirrer in the case of smale scale 0.25 - 0.50 l reactions (Fig.2); or in 2 l flanged reaction vessels fitted with a multi-necked flanged top and an anchor-type stirrer for reactions > 1 l . The stirrer was maintained at a constant distance (1 cm) from the bottom of the flask in all reactions. Both types of reaction vessel were fitted with a condenser and a nitrogen bleed. The rate of stirring for all reactions was kept constant at 360 r.p.m. The reaction vessel, immersed in a water bath at the appropriate temperature $\pm$ 0.1 K was charged with water and monomer and left to equilibrate for $\frac{1}{2}$ hour whilst being bubbled with 'white spot' nitrogen. Five minutes prior to the addition of the initiator, the stirrer was turned on in order to ensure that the water phase was saturated with monomer. In the case of potassium peroxydiphosphate initiated reactions, the sodium metabisulphite activator was added to the flask immediately prior to the addition of the initiator. Unless otherwise stated, all reactions were allowed to proceed for 24 hours.

7) Sample preparation.

a) Sampling technique. Small (1 ml) samples were removed from the large scale reactions using a teat pipette. The stirrer was stopped, the pipette inserted into the centre of the reaction mixture and the sample removed. A fast

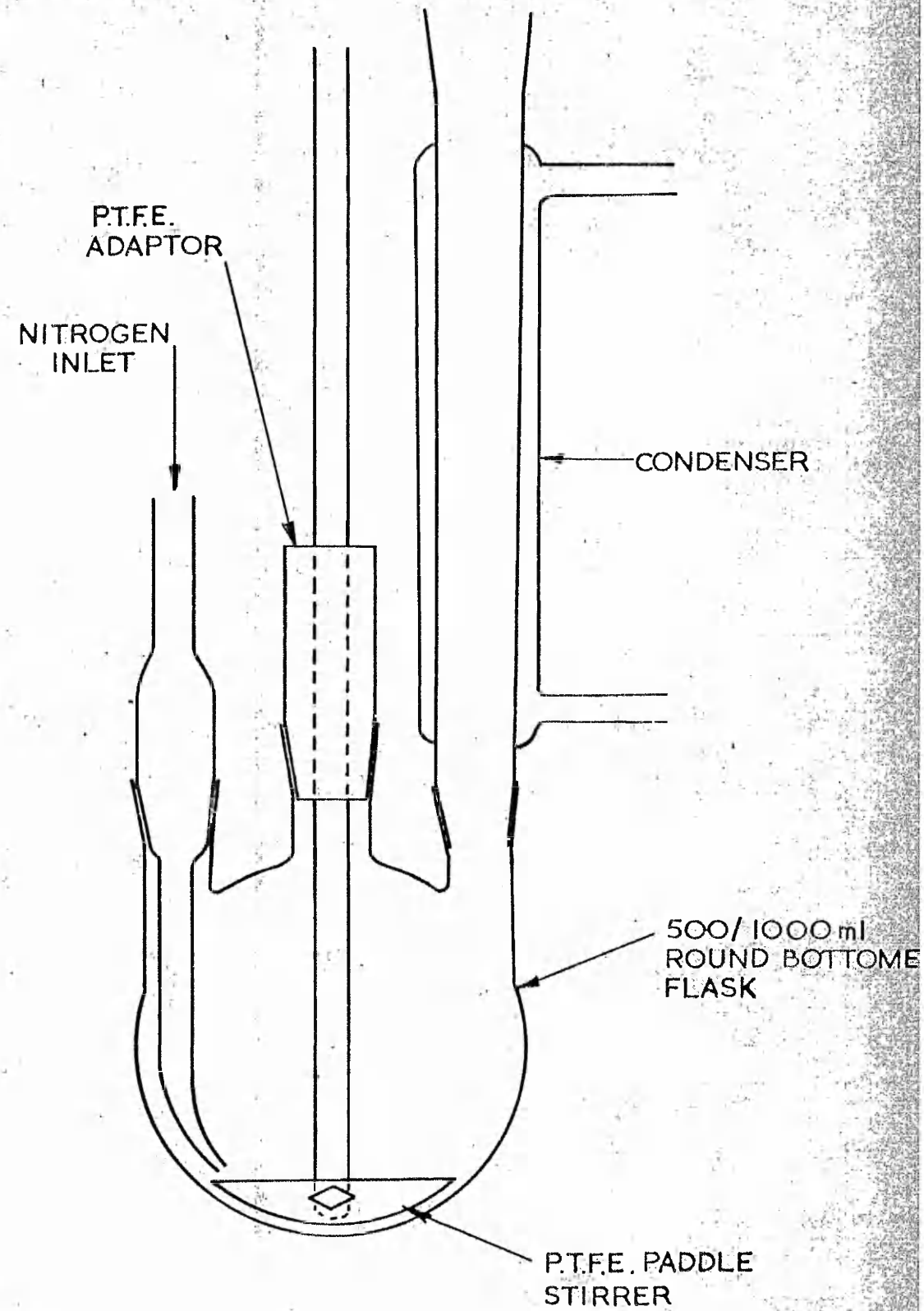

FIG. 2.

APPARATUS USED FOR SMALL SCALE REACTIONS

stream of 'white spot' nitrogen was then passed into the reaction vessel, to expel any air which may have entered, the vessel restoppered and the stirrer restarted. The sampling time was ca. 5 - 10 seconds. Large samples >10 <30 ml were removed using a pipette with a bulb filler, the same procedure was repeated as above, and the sampling time was ca. 10 - 20 seconds. Although every effort was taken to ensure that free monomer was not removed with the sample, a small amount was inevitably present, this was extracted by allowing the sample to stand for ca. 30 seconds during which time it floated to the surface and could be removed using a teat pipette. Samples for electron microscope examination were diluted immediately 100 times with cold water and stored in a cool place. Samples for weights analysis, molecular weight determinations, adsorption experiments and conductometric titration were put on to dialyse against a large excess of cold water as soon as possible after sampling.

b) Dialysis. Dialysis of latices and latex samples removed from reactions was carried out against doubly-distilled water in well boiled-out cellulose Visking tubing, and was continued until the conductance of the dialysate was $<2\ \mu$mho. Dialysis was carried out in covered pyrex-glass aspirators.

c) Freeze drying. The samples were cooled to 238 K and spun rapidly whilst being pumped under vacuum for 17 hours during which time the temperature gradually rose to 273 K.

d) Steam stripping. Steam stripping was carried out under nitrogen at either 373 K at atmospheric pressure, or 353 K under reduced pressure (Fig.3). Steam from doubly distilled water was passed into the latex, which was heated at the appropriate temperature, in order to reduce dilution effects, in a water bath. The extract was passed initially through a water condenser, which removed most of the steam, and then through a cold trap at 77 K which condensed both the organic material and the rest of the

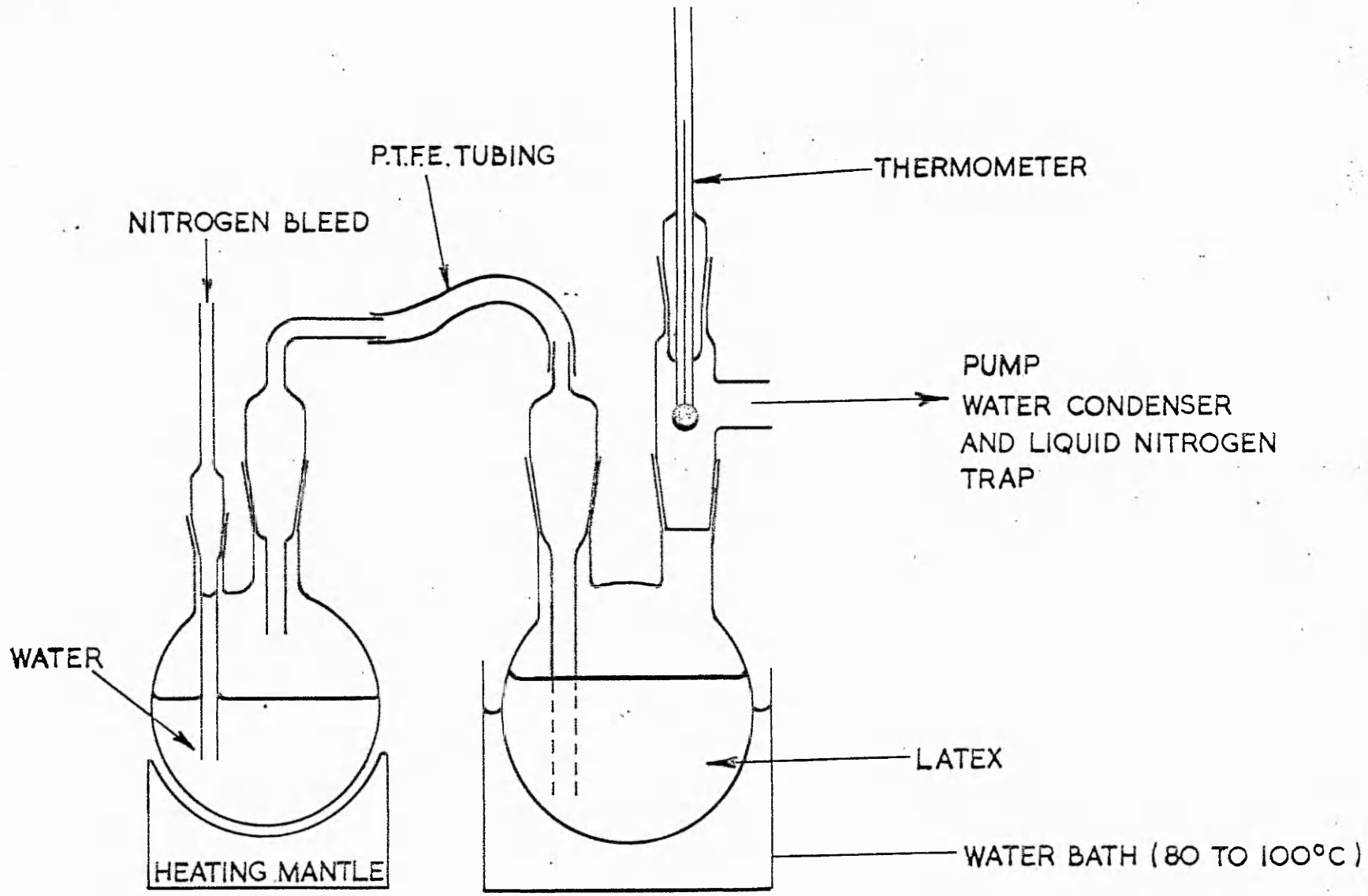

FIG.3.
APPARATUS USED FOR STEAM STRIPPING

water vapour. The extent of steam stripping was calculated from the ratios of the volume of the condensate to the volume of the latex being stripped (i.e. $\frac{1}{2}$: half as much condensate as latex, $\frac{1}{1}$: identical amounts etc.). Both condensates were retained for analysis.

B. TECHNIQUES OF LATEX CHARACTERISATION.

1) Weights analysis. A sample of latex of known weight was placed in a glass sample bottle and heated at 330K in a vacuum oven until a constant weight was attained. A true % solids was then determined from a knowledge of either the amount of electrolyte present in undialysed samples, or from a knowledge of the sample before and after dialysis.

2) Conductometric titrations.

a) Theoretical.

The reaction occurring between a strong acid and a strong base up to the equivalence point can be represented as:

$$H^+ + X^- + M^+ + OH^- = H_2O + M^+ + X^-.$$

The result of the above reaction is the replacement of some hydrogen ions by M^+ ions. The equivalent conductance λ_{H^+} is much greater than that of any other cation, hence up to the equivalence point the conductance decreases. Once the equivalence point has been reached, however, the conductance will increase due to the addition of excess OH^- and M^+ ions to the solution. Before the equivalence point is reached:

$$\frac{1}{R} = \frac{A}{1000l} \left(C_{H^+} \cdot \lambda_{H^+} + C_{M^+} \cdot \lambda_{M^+} + C_{X^-} \cdot \lambda_{X^-}\right). \qquad \text{--- (93)}$$

where: $\frac{l}{A}$ = cell constant

C_{H^+} M^+ X^- = concentration of H^+ M^+ X^- ions.

If the initial solution volume is V_a ml and the concentration is C_a^o equivalents of acid per litre, and if f is the fraction of acid neutralised by the addition of V_b mls of MOH, then:

$$C_{H^+} = (1 - f)\, C_a^o \left(\frac{V_a}{V_a + V_b}\right), \qquad \text{---(94)}$$

$$C_{X^-} = C_a^o \left(\frac{V_a}{V_a+V_b}\right) , \qquad \text{-- (95)}$$

and:

$$C_{M^+} = f\, C_a^o \left(\frac{V_a}{V_a+V_b}\right) \qquad \text{-- (96)}$$

where:

$$f = \frac{V_b\, C_b}{V_a\, C_a^o} .$$

Hence:

$$\frac{1}{R} = \frac{A\, C_a^o}{1000l} \left(\frac{V_a}{V_a+V_b}\right) \left(\lambda_{H^+} + \lambda_{X^-} + \left(\lambda_{M^+} - \lambda_{H^+}\right) f \right) , \qquad \text{-- (97)}$$

then a plot of $\frac{1}{R}\left(\frac{V_a+V_b}{V_a}\right)$ vs V_b will be a straight line of negative slope due to $\lambda_{H^+} > \lambda_{M^+}$. Also, if $V_a >> V_b$ then the dilution factor $\left(\frac{V_a}{V_a+V_b}\right)$ can be ignored and $\frac{1}{R}$ vs V_b will also give a straight line. Beyond the equivalence point, $[H^+] \simeq 0$, there are three ions to carry the current through the solution, then, similarly to above:

$$\frac{1}{R} = \frac{A}{1000l} \left(\frac{V_a}{V_a+V_b}\right) \left(C_a^o \left(\lambda_{X^-} - \lambda_{OH^-}\right) + \frac{C_b}{V_a} \left(\lambda_{M^+} + \lambda_{OH^-}\right) V_b\right) , \qquad \text{-- (98)}$$

and $\frac{1}{R}\left(\frac{V_a+V_b}{V_a}\right)$ vs V_b will give a straight line of positive slope, and when $V_a >> V_b$, $\frac{1}{R}$ vs V_b will also give a straight line. If conductances are measured close to the equivalence point, then a curvature is observed due to the presence of a small concentration of OH^- ions prior to equivalence and to a small concentration of H^+ ions just after the equivalence point.

If a weak acid is titrated against a strong base then at the very beginning of the titration, the reaction:

$$HX + M^+ + OH^- \longrightarrow H_2O + M^+ + X^- ,$$

effectively adds X^- ions to the solution. The resulting increase in the concentration of X^- decreases the concentration of H^+ by nature of the dissociation equilibrium:

$$HX \rightleftharpoons H^+ + X^- .$$

Again a decrease in conductance is observed, the extent of the decrease depending on the pK_a of the weak acid being titrated, the higher the pK_a, the smaller the decrease for acids at the same concentration. As the titration proceeds, the concentration of hydrogen ions is decreased to such a low value that its contribution to the conductance of the solution is negligible. Hence, addition of further MOH only adds more M^+ and X^- ions and thus the conductance increases. Once the equivalence point is reached, the curve becomes identical with the strong acid-strong base curve.

b) Experimental. Conductometric titrations were carried out on extensively dialysed latex samples. Two types of cell were used.

i) A dip-type cell fitted with platinum blacked electrodes (cell constant ~ 1.2) was used in conjunction with a glass cell (maximum capacity 0.1 l), fitted with a water jacket and maintained at constant temperature 298 K. The cell was covered with a close fitting perspex cap, having two small holes for the entry of nitrogen and sodium hydroxide and one large hole for the dip type cell.

ii) A thick walled polyethylene cell with built in graphite electrodes, (Sproule Electronics Ltd., Hitchin, Herts., England), (cell constant 1.0, maximum capacity 10 ml) was also used. As above, this cell was fitted with a cap having two small holes in it, although of course the large hole for the dip-type cell was absent. This cell was not fitted with a constant temperature water jacket, and errors due to temperature changes were negligible. Complete titrations took about 20 minutes.

It was found in practice that both cells gave results identical within experimental error.

In both cases, stirring was facilitated by means of a small PTFE covered magnetic stirrer. The sodium hydroxide (prepared from B.D.H. 'CVS' ampoules) was added using an Agla micrometer syringe (Burroughs Wellcome Ltd.,

Beckenham, England) fitted with a fine bore needle capable of delivering a minimum of 2 μl . The changes in conductance were measured using a Wayne-Kerr Universal Bridge Model 221B (Wayne-Kerr, Bognor Regis, Sussex, England), and the sodium hydroxide made up in freshly boiled out water was standardised against hydrochloric acid (B.D.H. 'CVS' Ampoule). The cell constants were determined periodically using potassium chloride solutions of known concentration.

A sample of filtered latex of known percent solids was pipetted into the cell and bubbled with nitrogen for approximately $\frac{1}{2}$ hour, the nitrogen bleed was then lifted above the surface of the latex and the addition of sodium hydroxide commenced.

The conductance reading after each addition of sodium hydroxide was found to remain constant upon standing on the descending acid leg, however it tended to decrease upon standing on the ascending base leg. The time between the additionsof caustic was thus important and in this work was always measured immediately after the addition of caustic. The total volume of caustic added was 3 - 4 times that required for neutralisation.

3) Potentiometric titrations. Potentiometric titrations were carried out on latices using a Radiometer (Copenhagen) Titrator Type TTlc. In this instrument the chart speed is preset, and is proportional to a change in pH which can be varied. The system works on a bridge principle, as the chart paper advances the bridge becomes unbalanced and base (or acid) is added to the titrant in order to increase (or decrease) its pH such that the system again becomes balanced. The deflection on the instrument is proportional to the volume of acid or base added, the constant of proportionality depending upon the volume set to equal the full scale deflection.

The instrument is fitted with a glass and a calomel electrode, which pass through a nylon cap covering a water

jacketed glass cell (maximum capacity 50 ml). This cap also has three small holes drilled through it for the entry of acid or base, nitrogen and an electronically driven stirrer rod. The base (or acid) is added by means of an electrically driven micrometer screw in contact with the plunger of an all-glass precision ground syringe.

The instrument was calibrated with two standard pH solutions, one at either end of the range of pH values expected to be encountered in the titration. The cell and electrodes were then well rinsed in water before addition of the filtered latex. The latex was bubbled with 'white spot' nitrogen for $\frac{1}{2}$ hour, after which time the nitrogen bleed was raised above the latex surface and the titration cycle initiated.

4) Determination of hydroxyl groups. The procedure of Van den Hul et al (154) was used to convert the surface hydroxyl groups to carboxyl. A sample of latex was heated at 363 K for six hours in the presence of 0.3 g g^{-1} potassium persulphate and 10^{-5}M silver nitrate, in a stirred flask fitted with a condenser. The latices coagulated under this treatment and were filtered using a pyrex sintered glass Buchner funnel (porosity 3). The solid latex was then washed with hot water until the conductance was almost the same as that straight from the stills, and dried in a vacuum dessicator. A known weight of the dry latex was redispersed with the aid of a small amount of ethanol and titrated conductometrically as described above.

5) Gas adsorption.

a) The B.E.T. equation and surface areas. When a highly disperse solid is exposed in a closed space to a gas or vapour, then the solid will adsorb an amount of the gas or vapour, the equilibrium amount adsorbed depending on the equilibrium pressure p, the temperature T and the nature of the gas and of the solid i.e:

$$x = f(p, T, \text{gas}, \text{solid}). \qquad -- (99)$$

For a given gas adsorbed on a given solid at a fixed temperature then:

$$x = f(p)\ T,\ \text{gas},\ \text{solid.} \qquad \text{--- (100)}$$

If the gas is below its critical temperature, i.e. is a vapour, then the form:

$$x = f(P/P_o)\ T,\ \text{gas},\ \text{solid.} \qquad \text{--- (101)}$$

is applicable where P_o is the saturated vapour pressure. Equations 100 and 101 are expressions for the adsorption isotherm. Adsorption isotherms have been measured on a wide variety of solids using a wide range of gases, however most isotherms can be grouped into one of five classes originally proposed by Brunauer, Deming, Deming and Teller (B.D.D.T.) (205) and nowadays commonly referred to as Brunauer, Emmett and Teller (B.E.T.) (206). Both Shaw (127) using krypton and Vanderhoff et al (152) using nitrogen have carried out adsorption isotherms on polystyrene latices. They found that the isotherms obtained were of type II on the B.E.T. classification, typical of multilayer absorption on a non-porous solid.

The B.E.T. equation has proved remarkably successful in the calculation of specific surface areas from Type II isotherms. The B.E.T. equation is derived from the interchange of molecules between the gas phase and the adsorbed layer, and for use in graphical methods takes the following form:

$$\frac{P}{x(P_o-P)} = \frac{1}{x_m C} + \frac{C-1}{x_m C}\,P/P_o \ , \qquad \text{--- (102)}$$

where: x is the uptake of gas at equilibrium pressure P.

P_o is the saturated vapour pressure of the gas,

x_m the monolayer coverage.

C is a constant related to the heat of adsorption.

As the value of C increases, the knee of the isotherm (approximately equal to the monolayer coverage) becomes sharper. A plot of $\frac{P}{x(P_o-P)}$ vs P/P_o gives a straight line

of slope $\frac{C-1}{x_m C}$ and intercept $\frac{1}{x_m C}$, solving this set of simultaneous equations yields x_m. The surface area can then be calculated from a knowledge of the surface area of adsorbing molecule.

This equation is usually only applied to isotherms in the P/P_o range of 0.05 to 0.35, failure of the equation to hold outside these limits is probably due to surface heterogeneity for the lower limit and to the effect of lateral interactions between the adsorbed species for the upper limit neither of which was accounted for in the derivation. Indeed, there is general agreement that the assumptions on which the B.E.T. equation is based are far from valid, and Halsey (207) considers that the equation is simply a mathematical tool to determine the position of the knee of the isotherm curve. The results of Vanderhoff et al (152) and Shaw (127) were obtained using different gasses. Vanderhoff et al found that evacuation of the samples at room temperature for 48 hours resulted in a surface area calculated from a nitrogen isotherm in excess of that calculated from electron microscopy. They attributed this to the latices having either uneven surfaces or a small amount of porosity. On the assumption that the surface would smoothen or the pores close, they heated the latex samples at 393 K for several hours and redetermined the isotherms. This treatment resulted in better agreement between B.E.T. and electron microscope surface areas; the per cent difference between the two was of the order of 12-30%. Shaw (127), on the other hand, using krypton, found excellent agreement between B.E.T. and electron microscope surface areas, however, his results were obtained on a single sample and no details were given with regards sample preparation.

Karnaukhov et al (208-211) have considered the adsorption of gases onto adsorbates consisting of spherical particles. They, (208), showed that for two spheres

touching that:

$$\frac{S}{S_{geom}} = \frac{4\pi R^2 - 2\pi Rr}{4\pi R^2} = 1 - \frac{r}{2R}, \qquad -- (103)$$

where r is the molecular radius of the adsorbing species

R is the particle radius

s is the surface area accessible for adsorption.

This equation takes into account the area of contact between the particles inaccessible to molecules of radius r. For multiple contacts equation becomes:

$$\frac{S}{S_{geom}} = 1 - \frac{nr}{2R}, \qquad -- (104)$$

or, the accessible surface decreases linearly with increasing diameter of the adsorbing species, and depends on the number of contacts n and the particle dimensions R. Thus, for 20 nm particles with a hexagonal close packed array, using nitrogen gas (r = .217 nm) that:

$$\frac{S}{S_{geom}} = 0.87.$$

In the case of small spheres in contact however, it is likely that capillary condensation also takes place which would lead to an increase in the calculated surface area.

b) Experimental. Gas adsorptions were carried out on well - dialysed and freeze-dried latex samples. A gravimetric technique was employed using a Sartorius microbalance (Model 4102) built into a vacuum system of normal design (Fig.4). Experiments were carried out using nitrogen and krypton at 77 K and carbon dioxide at 195 K. Large pressure changes were measured on a mercury manometer constructed out of precision bore tubing using a cathetometer, small pressure changes were measured using a Mcleod guage, again a cathetometer being used to determine the difference in height of the mercury columns. The Sartorius balance on the scale settings used was capable of measuring uptakes of $>5\,\mu g$, the error on reading the scale being $\pm 2.5\,\mu g$.

A sample of latex was placed on the balance pan and left under vacuum (10^{-4} - 10^{-5} torr) overnight at room

FIG. 4.

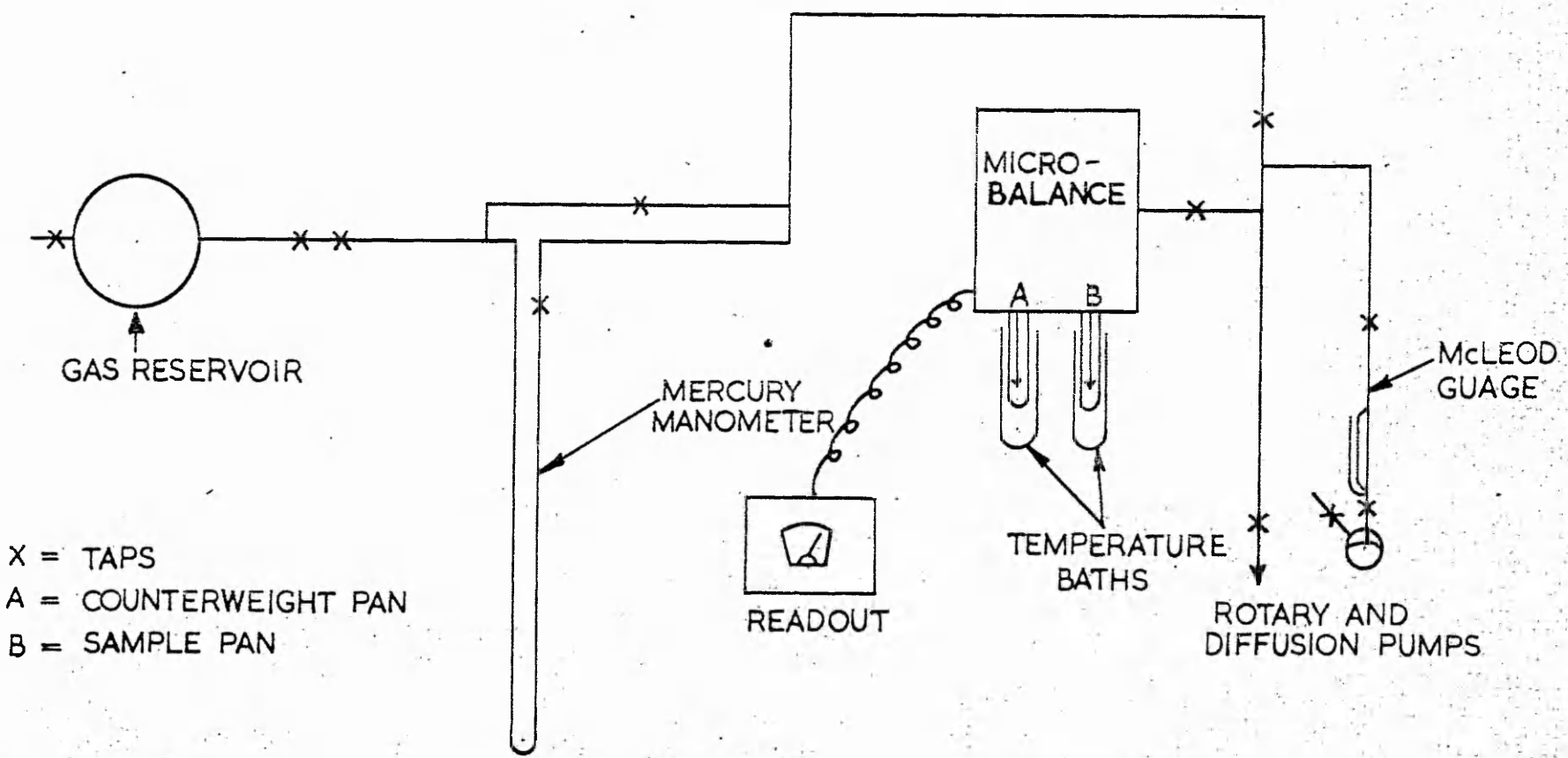

SIMPLIFIED DIAGRAM OF APPARATUS USED FOR GAS ADSORPTION STUDIES

temperature. The sample was then heated using a small circular electric furnace at 343$^{+}_{-}$5 K (glass transition temperature of polystyrene 378 K (212)) for one hour, this time being sufficient for the sample to attain constant weight. (In some cases the sample was heated overnight at 343 $^{+}_{-}$ 0.1 K using a water bath. Isotherms carried out on identical latices treated in either of the ways described above were identical within the limits of experimental error). The sample was then immersed in the temperature bath (liquid nitrogen at 77 K, solid carbon dioxide /methanol at 195 K) and left to equilibrate for $\frac{1}{2}$ hour. Small volumes of gas, dried by passing through a silica gel column, were then allowed into the system and the changes in the weight of the sample and the pressure were measured. Preliminary experiments indicated that the sample weight equilibration time was of the order of 15 minutes, hence readings were taken 40 minutes after each gas addition. Isotherms were plotted and treated using the B.E.T. treatment.

6. Electron microscopy.

a) Background. It has been pointed out by several workers that electron microscopy has certain drawbacks when used to determine the sizes of latex particles.

i) That there appears to be a separation according to size during the sample preparation of polydisperse systems (33,175).

(ii) That the particles tend to aggregate during sample preparation (33).

iii) That they tend to degrade under the electron beam (33,213).

iv) Swelling or contraction of the particles occurs upon exposure to the electron beam (114,213-216).

In the case of monodisperse latices which do not coalesce upon aggregation then neither (i) or (ii) are of importance.

Glaver and Farnham (213) have carried out a study on particle damage caused by the electron beam, they studied

polystyrene, polystyrene/acrylonitrile copolymer (PSAN), polyvinyl chloride (PVC) and polyvinyl acetate (PVAc) latices. They determined that the particle diameters all decreased upon exposure to the beam and that the rate of decrease was rapid during the first few minutes of exposure and then began to level off. For PSAN, PVC and PVAc they found that the maximum decrease in diameter occurred at 80 kV accelerating potential and 20 μ A beam current, (the most intense beam they used), being 12%, 25% and 30% respectively. They explained their results in terms of 'most radio sensitive bonds' in that the carbon-chlorine, C-H (PVC), carbon-nitrile, C-H (PSAN) and carbon-oxygen, C-H (PVAc) were radio sensitive compared to the carbon backbone. The decrease in diameter being due to the formation and resultant diffusion out of the particles of HCl, HCN and CH_3 COOH respectively. In the case of polystyrene however they found a maximum of about 7% decrease which they explained in terms of 'radio insensitivity' of the carbon-carbon bonds, and to the fact that even if the bonds were broken then the benzene residues would not diffuse out of the particle very rapidly. They also found that under beam conditions of 100 kV accelerating potential and 5 μ A beam current the decrease was $< 3\%$ and concluded that: 'the maximum loss from polystyrene was real, but negligibly-small for all but the most precise measurements'.

Other workers (114,214,215) have noticed an increase in diameter upon exposure to the electron beam and attributed this to contamination of the sample. Karamata (215), found ca. 14% increase in diameter of a 340 nm polystyrene latex over a period of 24 minutes.

It would thus appear that, in the case of monodisperse polystyrene latices, if contamination is kept to a minimum and the beam current and accelerating potential kept low that electron microscopy can be used with confidence to determine particle diameters.

b) Transmission electron microscopy (T.E.M.)*. T.E.M. was carried out using a Phillips EM 600 electron microscope. The latex sample was diluted down to ca. 10 ppm and one drop placed onto a 20 μm 'Formvar' coated copper grid and allowed to air dry at room temperature in a dust-free box. Usually, three grids were prepared from each sample, and photographs taken from different regions of each grid. Great care was taken to minimise the effect of beam damage and the operating conditions were chosen such that any beam damage which did occur was minimal, e.g. 80 kV accelerating potential and 3-4 μA beam current. Experiments were carried out to determine the effect of these conditions on latices, by taking photographs of the same grid area after different exposure times, up to 60 minutes, and comparing the particle sizes. It was found that after 60 minutes exposure, a maximum contraction of 4% occurred. Further to this, the focussing of the beam was carried out on an area of the grid adjacent to the area to be photographed, once the beam was focused, this area was moved into the beam and photographed. Thus, the exposure time to the electron beam was reduced to a minimum. Indeed Karamata (215) has used this technique in conjunction with shadowing of the particles and found that the diameter of the particle was identical within experimental error to that determined from the shadow-width.

The electron micrographs were printed onto Ilford stabilisation paper, and the particle size distribution determined by measuring about 250 particles (from different regions of each photograph) if monodisperse (standard deviation $<10\%$) and about 600 if polydisperse.

*I am indebted to Mr. R.A. Cox, C.D.E. Porton, Salisbury, Wilts., for the electron microscopy.

The data thus obtained was analysed by computer to determine the mean and standard deviation. Measurements were carried out using a calibrated eye-piece (Polaron Equipment Ltd., 60/62 Greenhill Cresc., Holywell Industrial Estate, Watford, Hertfordshire, England) measuring to an accuracy of $\pm$ 0.05 mm. The magnification was such that the particles were ca. 1cm diameter on the photographs although limitations were placed on this especially in the case of small particles, when the contrast with the background was not good, in that increasing the magnification on the print resulted in a loss of clarity. The accurate magnification of the prints was determined by measuring the spacings of a carbon replica of a diffraction grating (2160 lines mm^{-1}), a photograph of which was taken at the same magnification as the latex particles.

Some of the latices containing anomalous particles were carbon replicated by drying down a suspension of the latex (1 part in 10^6) at room temperature onto a freshly cleaved mica surface. These were carbon coated by deposition onto the sample of vapourised carbon produced in an electric arc under high vacuum. The carbon film was deposited onto a T.E.M. grid after removing the mica by floating off in water, the grids were then air dried and the polystyrene dissolved away by six hours exposure to the vapour from boiling toluene. The replicas were then examined in the T.E.M.

c) Scanning electron microscopy (S.E.M.). Several samples of latices containing anomalous particles were examined by S.E.M. using a Cambridge Stereoscan (Model IIA, resolution 25 nm). Samples were prepared by placing a drop of the latex dispersion onto a brass surface and evaporating to dryness in a dust free environment at room temperature. The samples were then coated with carbon and gold and scans taken between 0° and 45° to the vertical. As in the T.E.M. examinations experiments were carried out to determine the effects of prolonged beam exposure, 60 minutes, a

maximum contraction of 6% occurred.

d) Statistics of particle size distributions. The diameters of latex spheres are a continuous variable in that they can theoretically have any value, as opposed to a discrete variable which can only take on isolated values, usually positive integral values. The most important discrete distribution is the binomial distribution and the most important continuous distribution is the normal distribution. In order to determine the mean of a normal distribution it is necessary to use the mean of a random sample drawn from a normal population. The mean, $\bar{x}$, is calculated from:

$$\bar{x} = \frac{\sum_{i=1}^{n} x_i}{n} \quad , \qquad \text{-- (105)}$$

where x is the particle diameter,
and n is the sample number.

The standard deviation, σ , is an indication of the sample spread, or polydispersity of the latex, and is often quoted as a percentage of the mean.

$$\sigma = \left[\frac{\sum_{i=1}^{n} (x_i - \bar{x})^2}{n-1} \right]^{\frac{1}{2}} \qquad \text{-- (106)}$$

Another statistical parameter often quoted is the variance, σ^2. Wachtel and LaMer (2) have used the term monodisperse to describe sols with a standard deviation of < 10%.

When the sample mean and the standard deviation are known then the confidence interval for the mean can be determined. The confidence interval defines as a percentage the certainty that the population mean μ is to be found between two limits. It can be shown that if a sample of mean $\bar{x}$ is based on a random sample of size n selected from a normal population with unknown mean μ and unknown variance σ^2, then the random variable

$\frac{\bar{x} - \mu}{\sigma\, n^{-\frac{1}{2}}}$, has a distribution known as the t distribution.

The t distribution depends upon a single parameter known as the number of degrees of freedom, which in this case is equal to n-1. A distribution curve is effectively a probability envelope, the area under the curve at any particular sample size representing the probability of that size occurring, thus the total area under the curve is 1 (100%). The limiting values defining the various probabilities (usually between 90-99%) can be obtained from statistical tables, and are dependent upon n, but as $n \longrightarrow \infty$ the t distribution $\longrightarrow$ normal distribution and the limits become independent of n.

An exact 100 $(1 - \alpha)$ percent confidence interval for μ is given by: $(\bar{x} - t_{\alpha/2}\ \sigma\, n^{-\frac{1}{2}}\ ,\ \bar{x} + t_{\alpha/2}\ \sigma\, n^{-\frac{1}{2}})$,

where $(1 - \alpha)$ is the degree of confidence, (i.e. for a 90% confidence interval $\alpha = 0.1$), and $t_{\alpha/2}$ defines the limits and is tabulated.

For example: 250 latex particle diameters were measured and it was found that $\bar{x}$ = 100 nm and σ = 5 nm, then the 99% confidence interval is (99.19, 100.81), i.e. it is 99% certain that the population mean lies between 99.19 and 100.81 nm. Ottewill and co-workers (141,170, 175) suggest that about 1000 particles should be measured for statistical significance, however, it would appear that with monodisperse samples ($\sigma < 10\%\ \bar{x}$) the number of particles measured can be much less. If the sample size in the above example had been 1000 then the 99% confidence interval would have been (99.59, 100.41), the difference between the two sets of limits being negligible.

7) Molecular Weight Determinations.

a) Membrane Osmometry.*

i) Theoretical.

At constant temperature and pressure the chemical potential of pure solvent will exceed that of solvent in solution, causing the solvent to flow through the membrane into the solution. This flow will continue until the pressure increase due to transfer of solvent is such that the difference in chemical potential is eliminated. This pressure difference is termed the osmotic pressure, Π , and it can be shown that:

$$\Pi \bar{V}_1 = - RT \ln a, \qquad \text{--- (107)}$$

where $\bar{V}_1$ = the partial molar volume of the solvent,

R = the gas constant,

T = the absolute temperature,

a = the activity of solvent in the solution.

For an ideal solution, the solvent activity is equal to the mole fraction. In terms of mole fraction N_2 of solute:

$$N_1 = 1 - N_2 \qquad \text{--- (108)}$$

and $$-\ln N_1 = -\ln (1 - N_2). \qquad \text{--- (109)}$$

If N_2 is small compared to 1, i.e. a dilute solution then:

$$\ln (1 - N_2) \simeq N_2 , \qquad \text{--- (110)}$$

and $$\Pi \bar{V}_1 = RTN_2 . \qquad \text{--- (111)}$$

Under these conditions of dilution, $\bar{V}_1 \simeq V_1$, the molal volume of pure solvent, and $N_2 = \frac{n_2}{n_1}$ where n_2 and n_1 are the number of moles in solution.

*I am indebted to Mr. M.J. Castle, Chemical Defence Establishment, Porton Down, Salisbury, for part of this work.

Thus: $$\Pi \bar{V}_1 = RT \frac{N_2}{N_1} , \quad \text{-- (112)}$$

$$\Pi = RT \frac{N_2}{N_1 \bar{V}_1} , \quad \text{-- (113)}$$

and $$\Pi = RT \frac{C_2}{M_2} , \quad \text{-- (114)}$$

where: C_2 = concentration in grams of solute per litre of solvent,

M_2 = molecular weight of solute.

This equation is only valid at infinite dilution due to both the approximations in the derivation and to the assumption of ideal behaviour. The latter is not the case since the high molecular weight compounds used tend to interact with each other at the concentrations usually employed. Hence it is necessary to determine the osmotic pressure for solutions of various concentrations (10g l^{-1} - 0.8g l^{-1}) and to plot the data obtained such that the value of Π for $C = 0$ can be determined, i.e. plot Π/C vs C then:

$$M_2 = \lim_{C \longrightarrow 0} \frac{RT}{\Pi/C} \quad \text{-- (115)}$$

ii) Experimental.

Molecular weights ($\bar{M}n$) of some of the latices were determined using a Wescan Model 23 recording membrane osmometer, to measure the osmotic pressure between a pure solvent and a solution of known concentration of polymer separated by a semi-permeable membrane. The pressure changes are measured by means of a pressure transducer. The solvent is contained in a closed chamber, one wall of which is a flexible diaphragm, as the solvent diffuses through the rigidly held membrane, the diaphragm distends changing the volume of the chamber. This change in volume is coincident with a corresponding change in pressure caused by the elasticity of the diaphragm.

The polymer solutions were made up in degassed singly

distilled 'Analar' grade toluene, and the membranes, which upon arrival were stored in isopropanol, were conditioned for use with toluene by immersing the membranes in each of the following solutions for two hours:

75% isopropanol/25% toluene.
50% " /50% "
25% " /25% "
0 " /100% "

Gel Permeation Chromatography.*

Molecular weight determinations on some samples were carried out using a Waters Gel Permeation Chromatograph (Model 200). This instrument enables values of both number and weight average molecular weights to be determined, and hence the molecular weight dispersity of the polymer, as well as the actual distribution of molecular weights. The separation of the different molecular weight species involves column chromatography, in which the stationary phase is a heteroporous solvent swollen polymer network. In this work columns containing styrene/divinyl benzene co-polymer beads of 50μm diameter and pore sizes in the range 10^3 - 10^6 Å were used. As the liquid phase containing the polymer sample (usually ½% weight/volume) passes through the column at a known flow rate, the polymer molecules diffuse into all parts of the gel not physically barred to them. The smaller molecules permeate more completely and spend more time in the column, the large molecules permeate less and pass through the column more rapidly. The amount of polymer coming off the column was

*The author is indebted to Messrs J. Paul and D.Hilman, Materials Quality Assurance Directorate, Woolwich Arsenal, London, for this part of the work.

determined using a Differential Refractometer, and the columns calibrated using a series of different molecular weight, anionically polymerised polystyrene standards ($\frac{\bar{M}w}{\bar{M}n} \simeq 1$).

CHAPTER III

A) THE EFFECT OF STEAM STRIPPING ON THE BULK AND SURFACE CHARACTERISTICS OF POLYMER LATICES.

1) INTRODUCTION.

The published studies on the merits of the techniques of dialysis and ion-exchange for the removal of electrolyte and emulsifier from latices has been reviewed earlier (Chapter I). However, their efficiency in removing unreacted monomer and reaction by-products such as benzaldehyde has not been studied extensively (138). Also, the effect of these materials on the surface properties of polymer latices has not been investigated. Shaw and Marshall (137), in their infra-red spectroscopy studies on polystyrene latices, noted the presence of monomer and benzaldehyde in dialysed latices; and it was noted during this work that extensive dialysis (20 changes of doubly distilled water, latex to water ratio 1:100, time period four weeks) did not result in the complete removal of styrene monomer and other organic residues from polystyrene latices, as evinced by the fact that the odour of styrene and benzaldehyde became apparent upon storage.

The effect of the removal of these materials on the bulk and surface characteristics of the latices was determined. The nature of the organic material removed by steam stripping was investigated, as well as the probable effect these residues would have on the surface characteristics of the latices.

2) EXPERIMENTAL.

Steam stripping was carried out (Chapter II) in conjunction with dialysis. Various combinations of steam stripping and dialysis were investigated, such as steam stripping after initial dialysis, and steam stripping after initial dialysis followed by further dialysis. The latices were characterised by conductometric, and in some cases potentiometric titration, after each stage. Where the latex was steam stripped before initial dialysis, it was redialysed before analysis (to remove residual electrolyte).

The steam distillates were collected (see Chapter II) and the water phase titrated conductometrically. The organic phase was extracted using either ether or carbon tetrachloride and analysed using infra-red spectroscopy. In the cases where a separate organic phase of sufficient volume was produced, a molecular weight determination was carried out using gel permeation chromatography (G.P.C.).*

3) DISCUSSION.

a) Effect of Steam Stripping on the Bulk Properties of Latices.

i) Electron Microscopy.

Electron micrographs of latex samples containing small amounts of residual monomer often exhibit bridging between the particles. Steam stripping a sample prior to electron microscopy acts to reduce the amount of bridging, presumably by removing small amounts of residual monomer from the particles (217).

ii) Photon Correlation Spectroscopy.

One of the major problems encountered during particle size determinations using this method, which involves measuring the rate of diffusion of the particles, is the presence of clusters of two or more particles within the latex suspension. These clusters, which are occasionally very difficult to break down, cause the diameter determined by photon correlation spectroscopy to be greater than that

* I am indebted to Mrs. Chittenden of the Chemical Defence Establishment, Porton Down, Salisbury, for the infra-red data, and to Messrs. J. Paul and D. Hilman of the Materials Quality Assurance Directorate, Woolwich Arsenal East, London, for the gel permeation chromatography.

determined from electron micrographs. Samples of both steam stripped and normal polystyrene latices, produced using potassium peroxydiphosphate/sodium metabisulphite initiator system, were supplied to Dr. K. Randall and Capt. D. Munro of the Royal Military College of Science, Shrivenham, Wiltshire, who reported that agreement between diameters determined by electron microscope and photon correlation spectroscopy improved after steam stripping, indicating that this process leads to a reduction in the number of aggregates present in latex suspensions.

b) Effect of Steam Stripping on the Surface Characteristics of the Latices.

Steam stripping was carried out at both 353 K and 373 K (glass transition temperature of polystyrene 378 K (212)) to determine the effect of temperatures close to and below the glass transition temperature. Steam stripping at both these temperatures leads to rapid hydrolysis of the sulphate groups, and their eventual elimination if the process was carried out extensively. The results are summarised in Table 3.

Analysis of the results shows two effects: a) that steam stripping acts to expose otherwise inaccessible acidic material, not necessarily associated with an anomalous region, and b) causes rapid hydrolysis of the surface bound sulphate groups, the duration and temperature of steam stripping being the important factors. For both latices 40 and 296, steam stripping at 373 K after initial dialysis resulted in an increase in the concentration of strong acid. Further dialysis, in the case of 296 and 18A, resulted in a decrease, indicating that some of the acidic material titrated after the first steam stripping was present in the water phase. Steam stripping at 373 K before initial dialysis always resulted in the concentration of the strong acid decreasing; in the case of 54B to zero. Further steam stripping of 296 also resulted in the concentration of the strong acid decreasing to zero, presumably due to the sulphuric acid produced by hydrolysis being carried over in the steam. The steam stripping of latex 296 at 353 K shows similar trends in the eventual

TABLE 3

EFFECT OF STEAM STRIPPING PERSULPHATE INITIATED POLYSTYRENE LATICES

Latex	Treatment	Total strong acid* (μ eq g^{-1})
40	D.	2.64
"	D, SS(373).	3.16
"	SS(373), D.	1.15
296	D.	2.97
"	D, SS(353).	1.89
"	D, SS(373).	3.45
"	D, SS(353), D.	0
"	D, SS(373), D.	0
"	SS(373), D.	0.88
"	SS(373), D, SS(373).	0
"	SS(373), D, SS(373, D.	0
18A	D.	2.98
"	D, SS(373), D.	1.20
54B	D.	3.15
"	SS(373), D.	0

* None of these latices exhibited a weak acid inflection.

D = Dialysis.

SS( ) = Steam stripped.

The steam stripping was carried out on a 1:1 basis.

disappearance of sulphate groups. However, steam stripping after initial dialysis resulted in a decrease in the acid concentration, contrary to the findings at 373 K. This may have been due to acidic material being carried over in the steam at low pressures

The increase in strong acid upon steam stripping at 373 K could be due to exposure of otherwise buried sulphate groups attached to either high or low molecular weight polymer. The diffusion of buried low molecular weight material to the particle surface on steam stripping appears more likely, since isooctane extraction of polystyrene latices produced in the absence of added surfactant always showed the presence of low molecular weight material ($\bar{M}_n \sim 1000$, see Chapter VI). A sample of latex 40 was liquid/liquid extracted with isooctane for 24 hours and re-characterised. The strong acid end point had decreased by 9.5%, indicating that the low molecular weight material does have sulphate end groups attached to it.

It is interesting to note that many latices which had been prepared for several years did not contain any titrateable acid groups, but remained stable after a steam stripping at 373 K, and also after long periods of storage (> one year in the case of 40). These particles cannot be electrostatically stabilised. However, according to Smitham et al (99) hydroxyl groups could contribute to steric stabilisation, by analogy to polyvinyl-alcohol which is a known steric stabiliser. Also, a latex produced by the Dow Chemical Co., was found upon storage to be electrically neutral but very stable, the surface groups being all hydroxyl (139,218).

Although similar results were obtained by steam stripping the latices before and after dialysis, it is thought that steam stripping after dialysis is to be preferred, since further polymerisation and other side reactions could occur between excess initiator still present in an undialysed latex and monomer and other reaction byproducts.

B) HYDROLYSIS OF SULPHATE GROUPS.

1) Introduction.

Several workers have reported the gradual hydrolysis of sulphate groups on polystyrene latices stored at room temperature. Everett and Gultepe (144) have reported the hydrolysis to be 2.5% per month at room temperature, and Chen (143) found strong acid groups in the supernatant after centrifugation of a well-dialysed latex which had been stored for a period of 9 months. Chen showed that dialysis immediately prior to centrifugation resulted in no detectable strong acid groups in the supernatant, proving that the titrateable species of strong acid was water soluble. Hearn (48) has shown that the rate of hydrolysis increased at elevated temperatures.

2) Discussion.

The results described in the previous section show a rapid rate of hydrolysis at elevated temperatures and this was confirmed by controlled experiments at 293 and 343 K (Table 4).

TABLE 4

RATE OF HYDROLYSIS OF LATICES 295 AND 54B STORED AT 293 AND 343 K RESPECTIVELY

Latex	Time (days)	Strong acid* (μ equiv g^{-1})
295A	0	1.78
	27	1.28
	83	0
295B	0	2.90
	30	2.49
	80	0.90
54B	0	3.15
	3	0.76
	9	0.29

* After dialysis.

At 293 K the rate of hydrolysis was of the order 20 - 30% month $^{-1}$, which is considerably greater than 2.5% month^{-1} determined by Everett and Gultepe. The results at 343 K show that within three days the concentration of strong acid groups on the latex had decreased by 76% and after nine days by 91%. It would thus appear that hydrolysis of the sulphate groups is a process which occurs from the very inception of the particles at the beginning of polymerisation, and that it continues at a rate dependent on the temperature. Thus, hydrolysis will be occurring during persulphate initiated polymerisations, which may be evident in the common observation (3,48,141,157) of the presence of hydroxyl groups on the latex particles where their concentration may be greater than that expected by the reaction of persulphate with water to yield OH$^{\bullet}$ (87). It is therefore evident that the reactions should not be continued beyond the time taken to achieve final conversion. For example, Stone-Masui and Watillon (153) have carried out unbuffered reactions at 343 K for 96 hours and found an almost complete absence of strong acid groups. However, when a similar reaction was carried out in the presence of 10^{-3} mole l^{-1} potassium bicarbonate, appreciable amounts of strong acid groups were found. Read and Fredell (219) and Kurz (220) have shown that the rate of hydrolysis of alkyl sulphates increases markedly with decreasing pH. Several workers (133,156) have found that the number of hydroxyl groups produced during a persulphate initiated emulsion polymerisation was dependent upon the pH of the reaction; being less at higher pHs.

All the latices produced during the course of this work with persulphate initiator have exhibited appreciable amounts of strong acid groups, and reactions carried out at temperatures in excess of 333 K were terminated after 24 hours.

Van den Hul, Vanderhoff and co-workers (3,156,152) have carried out a considerable amount of research into the characterisation of polymer latices. They found that their

latices did not undergo any appreciable sulphate hydrolysis, even after extensive periods of storage. However, the latices were prepared using surfactant and it is possible that the surfactant layer around the particles protected the strong acid groups, either reducing or completely preventing hydrolysis.

It is well known that the presence of micelles strongly inhibits certain reactions due to the incorporation into the micelles of one of the reactants. Bunton et al (221) found that Triton X - 114 retarded the rate of hydrolysis of bis - 2, 4 - dinitrophenyl phosphate with OH^-, by incorporation of the former into the micelles, and Fuller and Kurz (222) found that the rate of hydrolysis of ethyl trichloacetate was strongly suppressed in the presence of sodium dodecylsulphate micelles. Similarily the rate of the proton catalysed hydrolysis of N - benzylideneanilene was found to be strongly retarded by the presence of n - hexadecyl trimethyl ammonium bromide micelles (223).

The slow rate of hydrolysis obtained by Everett and Gultepe may be due to their use of a persulphate/metabisulphite initiator system. It is known that metabisulphite is capable of initiating polymerisation in the presence of an oxidising agent with the result that sulphoxy end groups are incorporated onto the latex (224). Warson (225) has proposed the formation of sulphonate radicals in the persulphate/bisulphite initiator system and Palit and co-workers (157,224) have shown that sulphoxy end groups are less susceptable to hydrolysis than sulphate end groups. Hence, the figure of 2.5% $month^{-1}$ obtained by Everett and Gultepe may be much higher, since the total number of hydrolysable groups on the latex particle surface could be considerably less than the total number of acid groups present (see Chapter IV).

3) Effect of Storage on Latices Stabilised Mainly by Sulphoxy Surface Groups.

A sample of latex 52A prepared using the peroxydiphosphate/metabisulphite initiator system (See Chapter IV)

was kept at 343 K for a period of 9 days and a sample titrated (after dialysis) after 3 days and 9 days. The results are shown in Table 5. and Fig. 4A.

TABLE 5

EFFECT OF STORAGE AT 343 K OF LATEX 52A

Time (days)	Strong acid (μ eq g^{-1})
0	5.12
3	4.97
9	5.04

It is evident that latices stabilised mainly by sulphoxy end groups are much more stable to storage at elevated temperatures compared to those stabilised by sulphate end groups (Table 4).

C) ANALYSIS OF STEAM DISTILLATE.

1) Analysis of the Aqueous Phase.

The composition of the distillates varied considerably between latices. In some cases a considerable amount of monomer was observed whereas in others only a small amount was removed. Similarly the odour of benzaldehyde was very strong in some cases but absent in others.

Several samples of the condensate were titrated conductometrically, but no acid groupings were detected; the conductance of the condensate was usually in the range of 2 - 4 μ mho. Samples from the condensates of latices 40 and 18A were shaken with a methanol solution of 2,4 - dinitrophenylhydrazine, and both samples gave a positive reaction (formation of an orange precipitate) indicating the presence of aldehydes and/or ketones (226).

2) Infra-red Spectroscopy of Ether and Carbon Tetrachloride Extracts of the Aqueous Phase.

Several samples which had a strong odour of benzaldehyde, were extracted using either carbon tetrachloride or ether, and analysed using infra-red spectroscopy. The spectra exhibited peaks, characteristic of benzaldehyde

EFFECT OF STORAGE AT 343K ON LATEX 52A

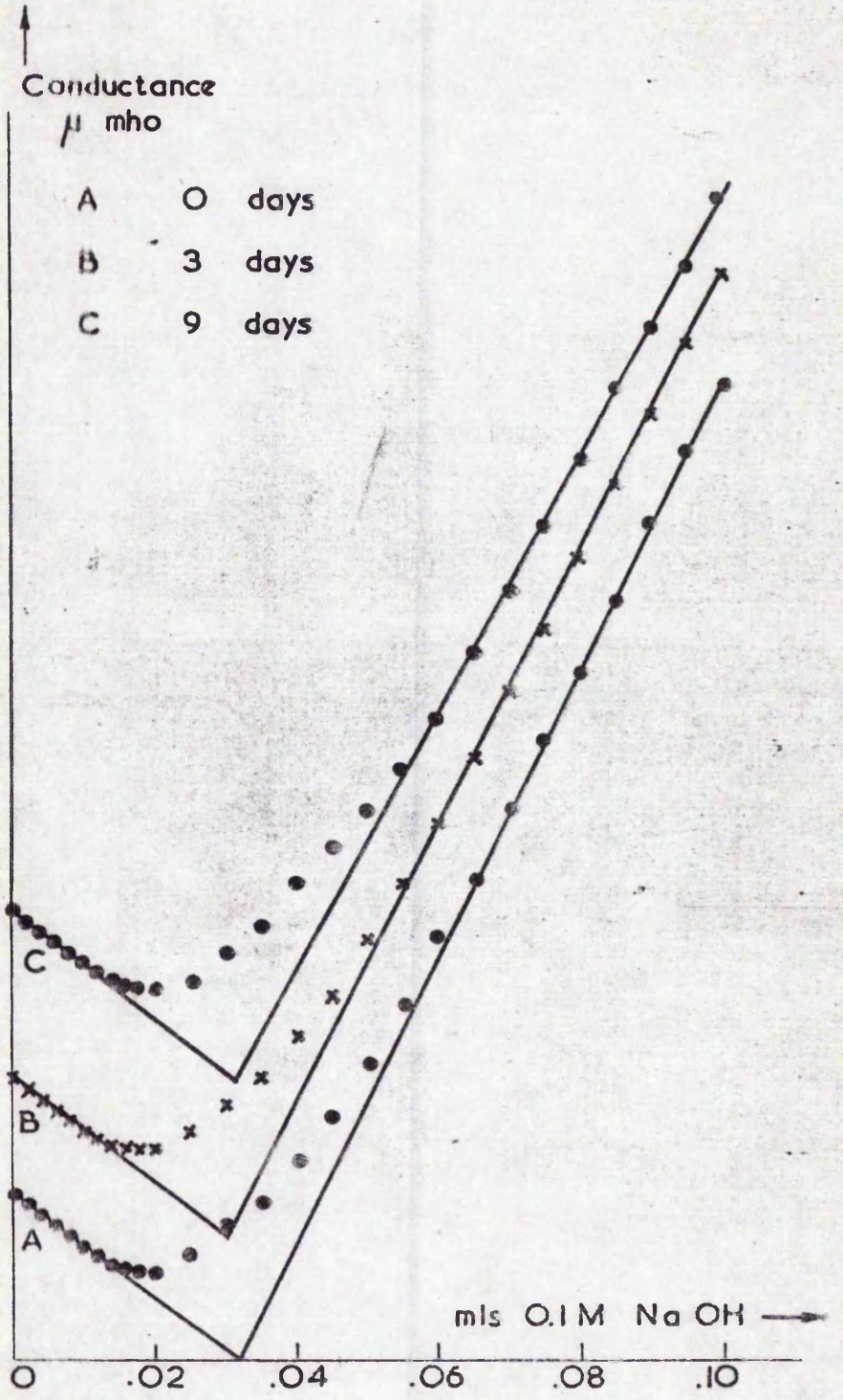

FIG. 4A

which were not apparent in the original latex.

A viscous 'oily layer' separated from a well-dialysed sample of latex 291 after storage for several months. Latex 291 had only been allowed to achieve a small conversion before the reaction was terminated, and all unreacted monomer was separated off. Thus, unreacted monomer from within the latex particle had gradually 'leached' out and some further degree of polymerisation occurred. Analysis of this layer showed the presence of styrene monomer and polystyrene. I.R. analysis, however, revealed the presence of several distinct peaks attributable to benzaldehyde (Fig.5a,b). These were identified by 'spiking' a sample of latex 291 with benzaldehyde and comparing the I.R. with that of a pure sample of benzaldehyde (Table 6). The discrepancy in the C = O group at 1689 cm^{-1} is probably due to the interference from the polystyrene.

TABLE 6

COMPARISON OF WAVENUMBERS OF PURE BENZALDEYDE WITH THOSE ASSOCIATED WITH LATEX 291

	WAVENUMBER (cm^{-1})			
Latex 291	1689	1302	1197	833
Benzaldehyde	1709	1310	1201	833

3) Analysis of the Oil Phase.

This phase always smelled strongly of styrene monomer. A sample was analysed by gel permeation chromatography, and found to consist of styrene monomer only (within the limits of detection of the instrument), no material of higher molecular weight being present.

D) POSSIBLE EFFECTS OF BENZALDEHYDE ON LATEX CHARACTERISATION.

1) Introduction.

It is known that benzaldehyde is easily oxidised to benzoic acid in the presence of oxygen by the following

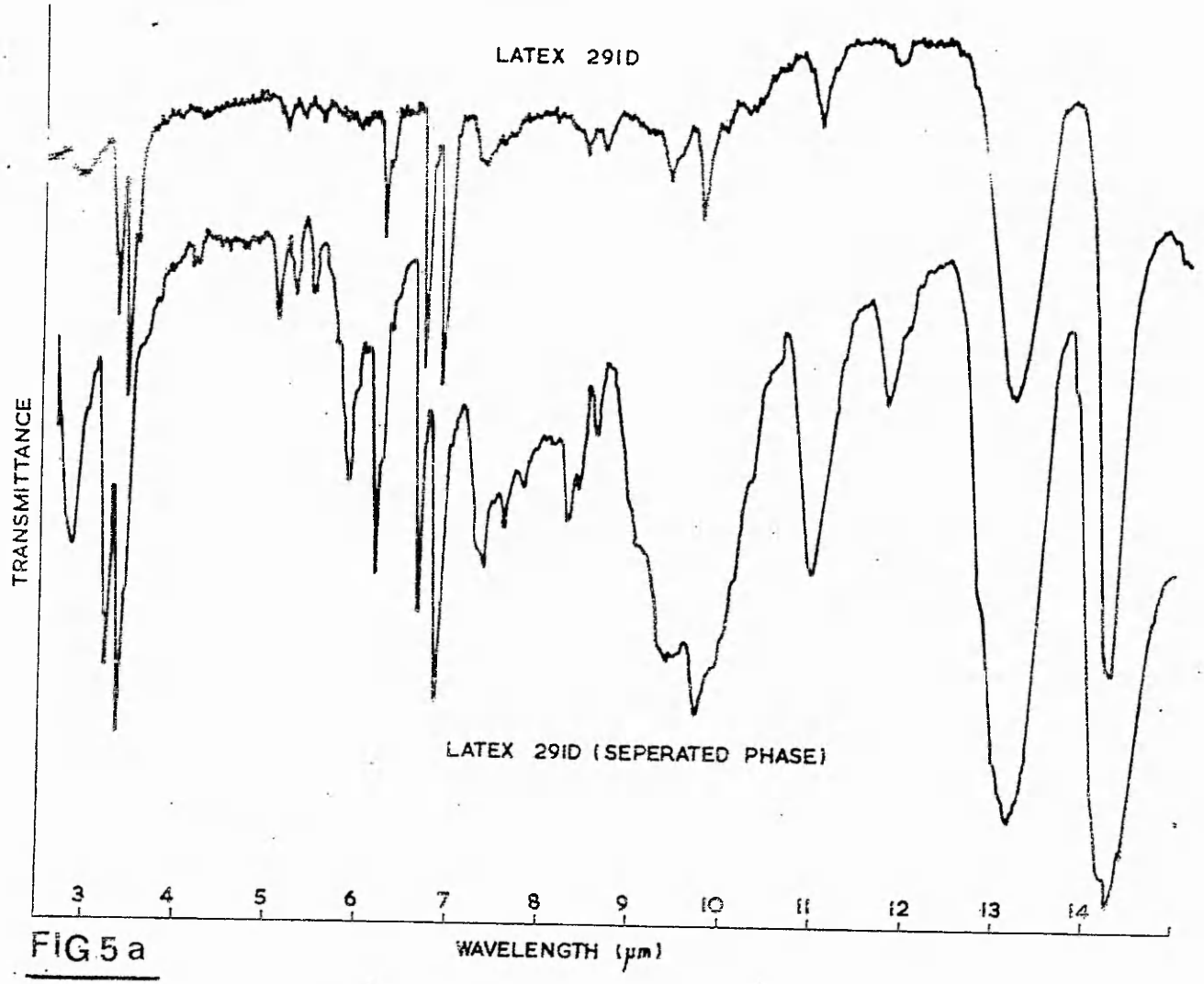
LATEX 291D
LATEX 291D (SEPERATED PHASE)
TRANSMITTANCE
3
4
5
6
7
8
9
10
11
12
13
14
WAVELENGTH (μm)

FIG 5a

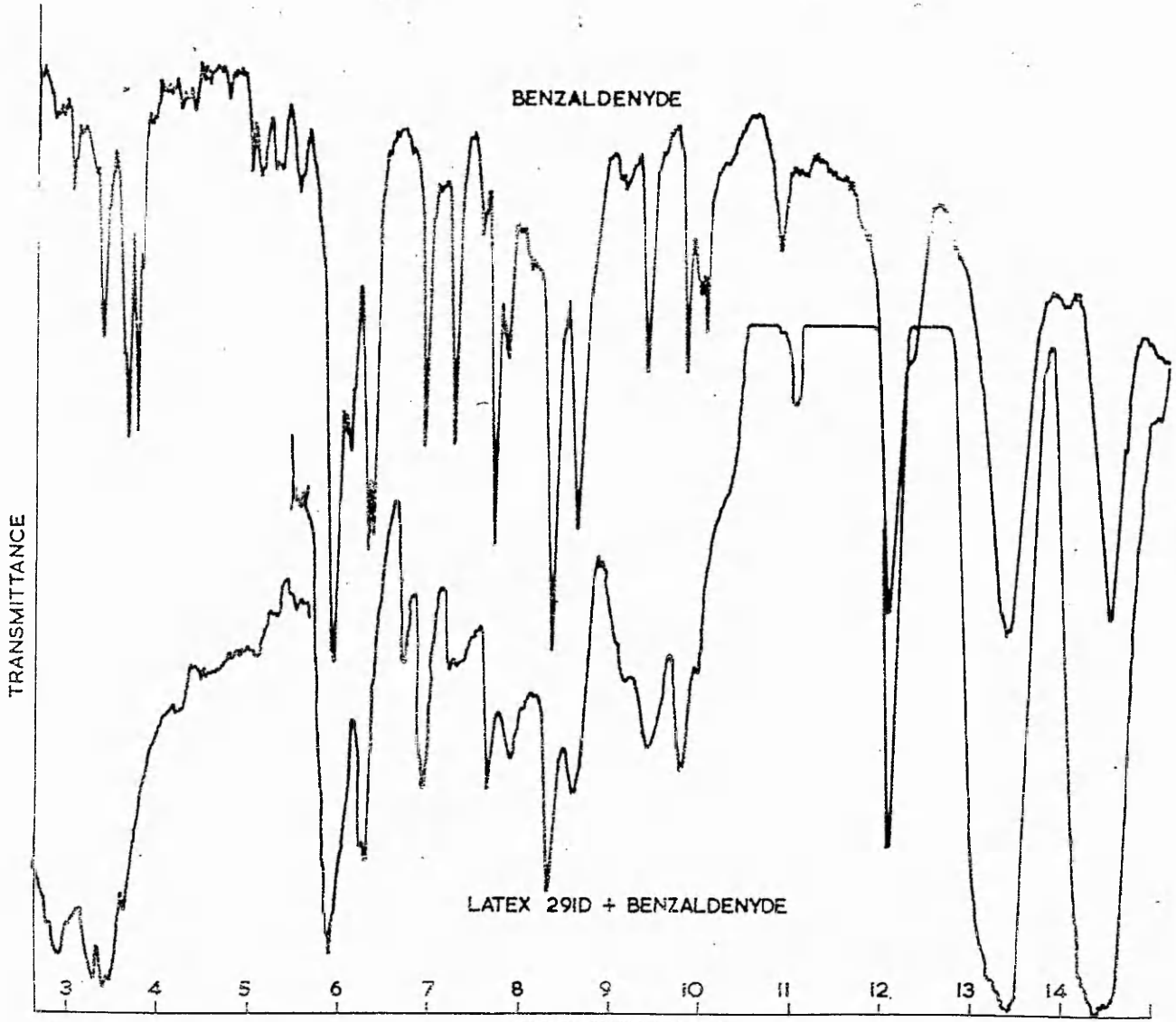
BENZALDENYDE
LATEX 291D + BENZALDENYDE
TRANSMITTANCE
3
4
5
6
7
8
9
10
11
12
13
14
WAVELENGTH (μm)

FIG 5b

per acid mechanism (227):

$$C_6H_5\,CHO + O_2 \longrightarrow C_6H_5\,COOO\,H$$

$$C_6H_5\,COOO\,H \longrightarrow C_6H_5\,CO_2^{\bullet} + \dot{O}H$$

$$C_6H_5\,CO_2^{\bullet} + C_6H_5\,CHO \longrightarrow C_6H_5\,COOH + C_6H_5\,C{=}O$$

$$\dot{O}H + C_6H_5\,CHO \longrightarrow C_6H_5\,C{=}O + H_2O$$

$$C_6H_5\,C{=}O + O_2 \longrightarrow C_6H_5\,COOO^{\bullet}$$

$$C_6H_5\,COOO^{\bullet} + C_6H_5\,CHO \longrightarrow C_6H_5\,C{=}O + C_6H_5\,COOO\,H$$

The reaction being catalysed by light.

If 'in situ' benzoic acid is formed it might be expected that it would be detected by conductometric titration as a 'weak acid'. This would affect the surface charge characteristics, and possibly the stability and extent of interaction with other media.

2) Experimental.

To assess the effect of benzaldehyde and benzoic acid on latices during storage, a small amount of AnalaR grade benzaldehyde (0.5 ml) was added to one 50 ml sample (well-dialysed) of latex 50A, and a small amount of benzoic acid (3 ml of 0.004M) to another. Both samples were preflushed and stored under nitrogen in ground-glass stoppered flasks; no other precautions being taken to exclude oxygen. The flasks (including an untreated sample of 50A) were placed in direct sunlight and titrated every few days. (The samples were not dialysed prior to titration). The results are shown in Figs. 6,7,8. The benzoic acid did not result, as expected, in the formation of a weak acid end point, but acted to increase the apparent strong acid end point. The increase in the apparent strong acid was 25% less than that expected from a knowledge of the amount of benzoic acid present in the sample. It is likely that this discrepancy arises from the difficulty in interpreting the titration curves quantitatively due to the increased curvature at the neutralisation point caused by the benzoic acid. The untreated sample (Fig.7) showed no change upon storage, although the curvature at neutralisation became less presumably due to the hydrolysed sulphate

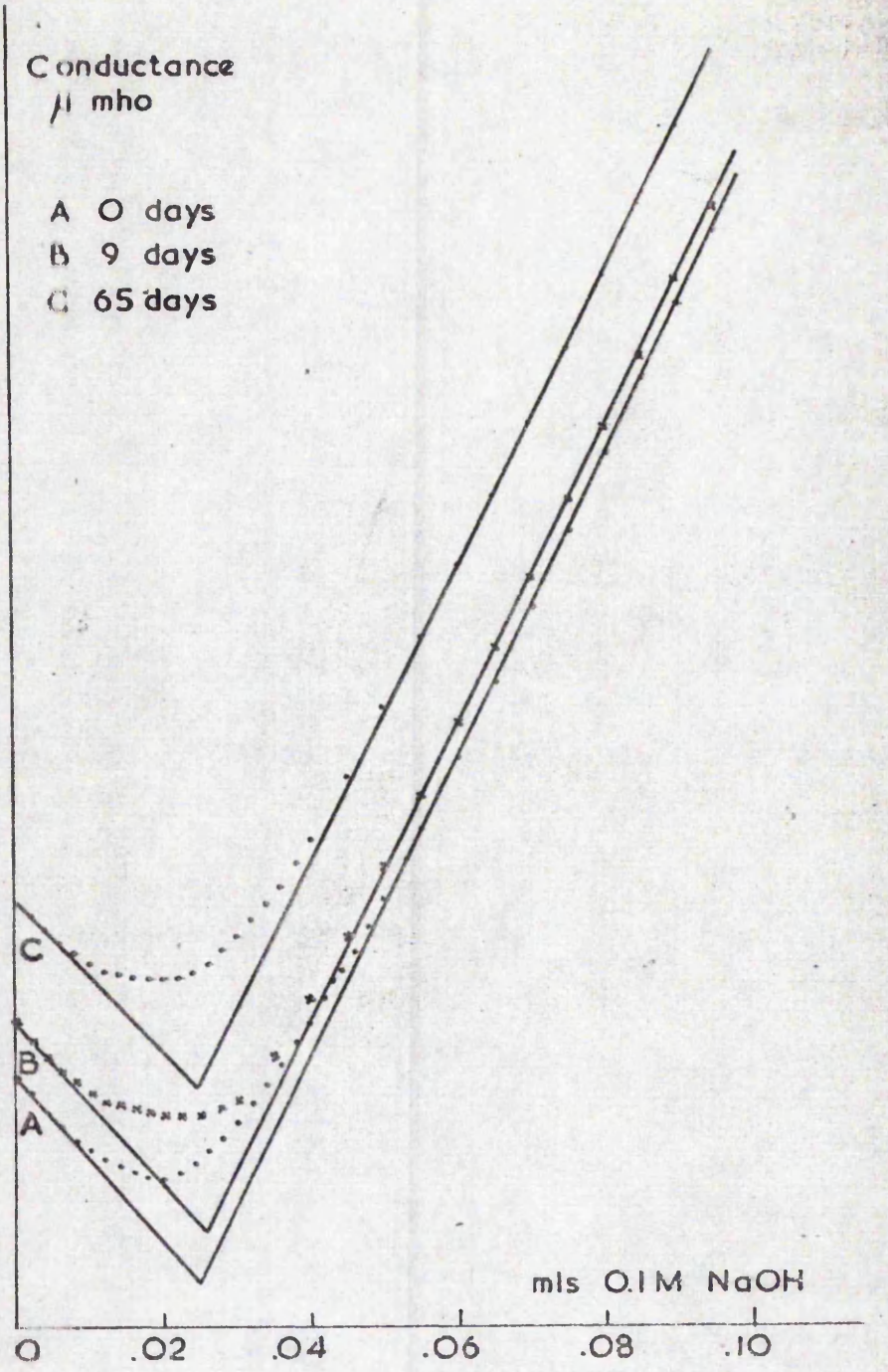

EFFECT OF ADDED BENZOIC ACID ON LATEX 50A TITRATION CURVES WITH TIME

FIG.6.

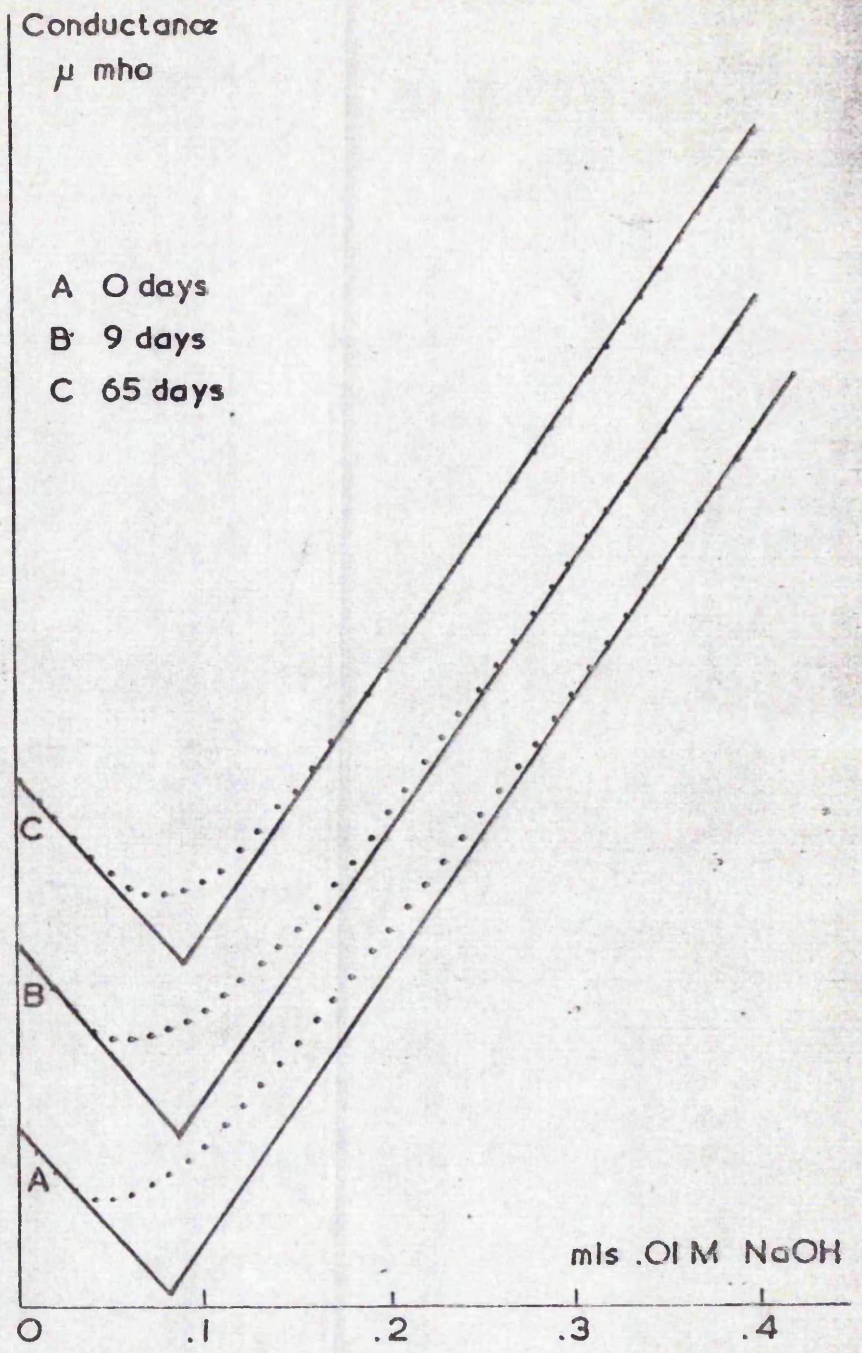

EFFECT OF STORAGE TIME ON LATEX 50A

FIG.7.

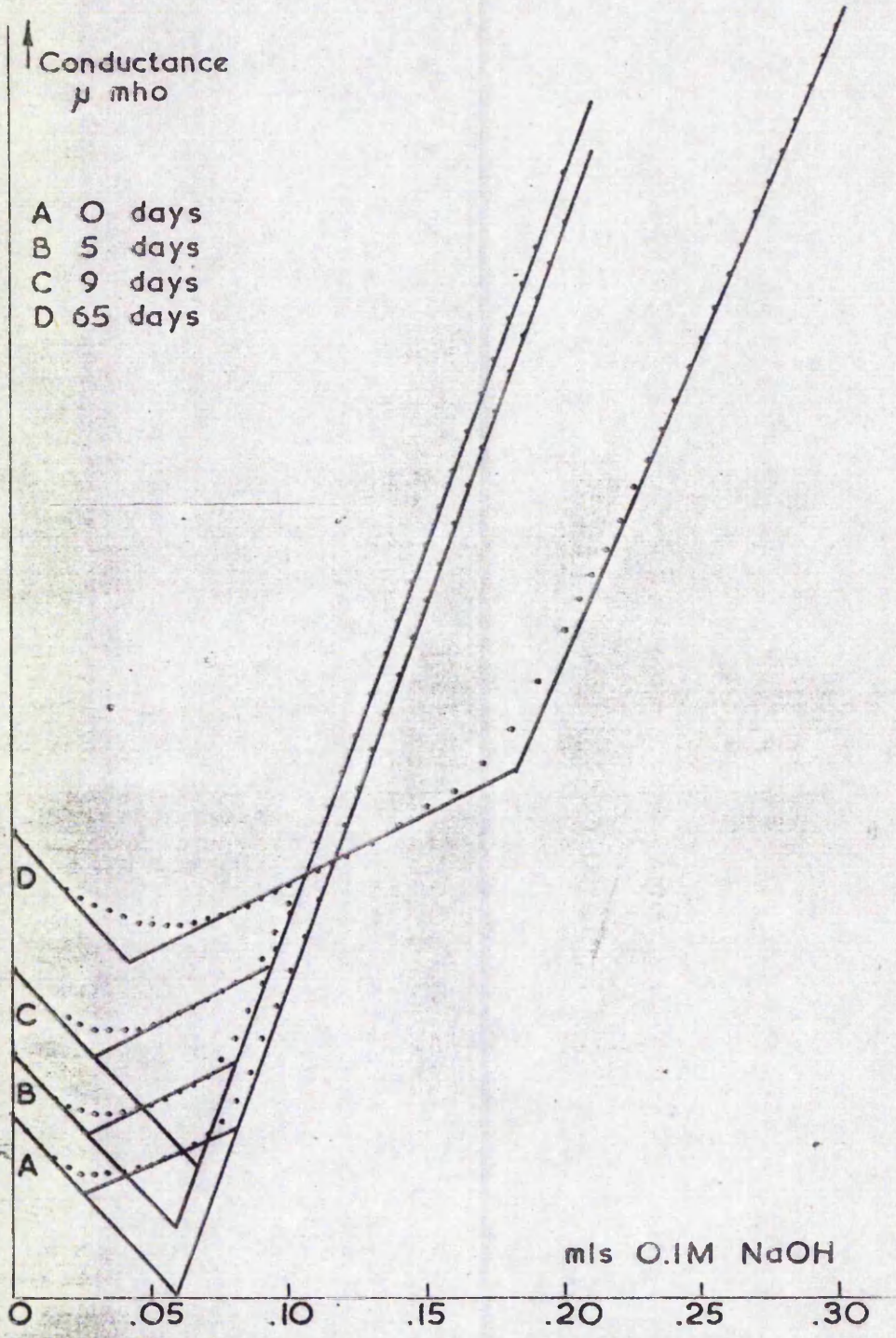

EFFECT OF ADDED BENZALDEHYDE ON LATEX 50A
TITRATION CURVES WITH TIME

FIG.8.

groups present in the aqueous phase. It is thought unlikely that the initial curvature was due to weak acid groups. In the case of benzaldehyde, however (Fig.8), the shape of the curve changed significantly over the period of the experiment. The initial increase in 'strong' acid directly after the addition was due to the small amount of benzoic acid inherently present within the benzaldehyde itself. It can be seen that the number of points at the neutralisation of the strong acid which fall on a straight line increases as the experiment progresses until after two months the titration curve has a distinct inflection on the base leg indicative of weak acid groups.

3) Discussion.

It is known that dilute solutions of weak acids do not behave in the typical 'weak acid manner', Fig. 9. It is thought that benzaldehyde would partition itself between the polymer and water phases with benzoic acid subsequently being formed, (via. oxidation), at the latex particle/water interface. In this situation the benzoic acid may act as a true 'weak acid' due to the presence of strong acid sulphate groups on the particle surface. In solution, however, it acts as a typical dilute weak acid, and in the case of the sample containing added benzoic acid no appreciable adsorption onto the polymer/water interface occurred.

The formation of post-reaction oxidation products, as discussed, could explain a lot of the conflicting data obtained previously with regards the presence and absence of carboxyl groups on polystyrene latex particle surfaces, namely:

a) In latices prepared in the presence of surfactant, then benzaldehyde at the particle/water interface could be protected from oxidation by the adsorbed surfactant layer.

b) Dialysis of polystyrene latices produced in both the absence and presence of surface-active agents usually takes at least two weeks, and no precautions to exclude light and oxygen are usually reported. During dialysis of surfactant-containing systems the protective surfactant

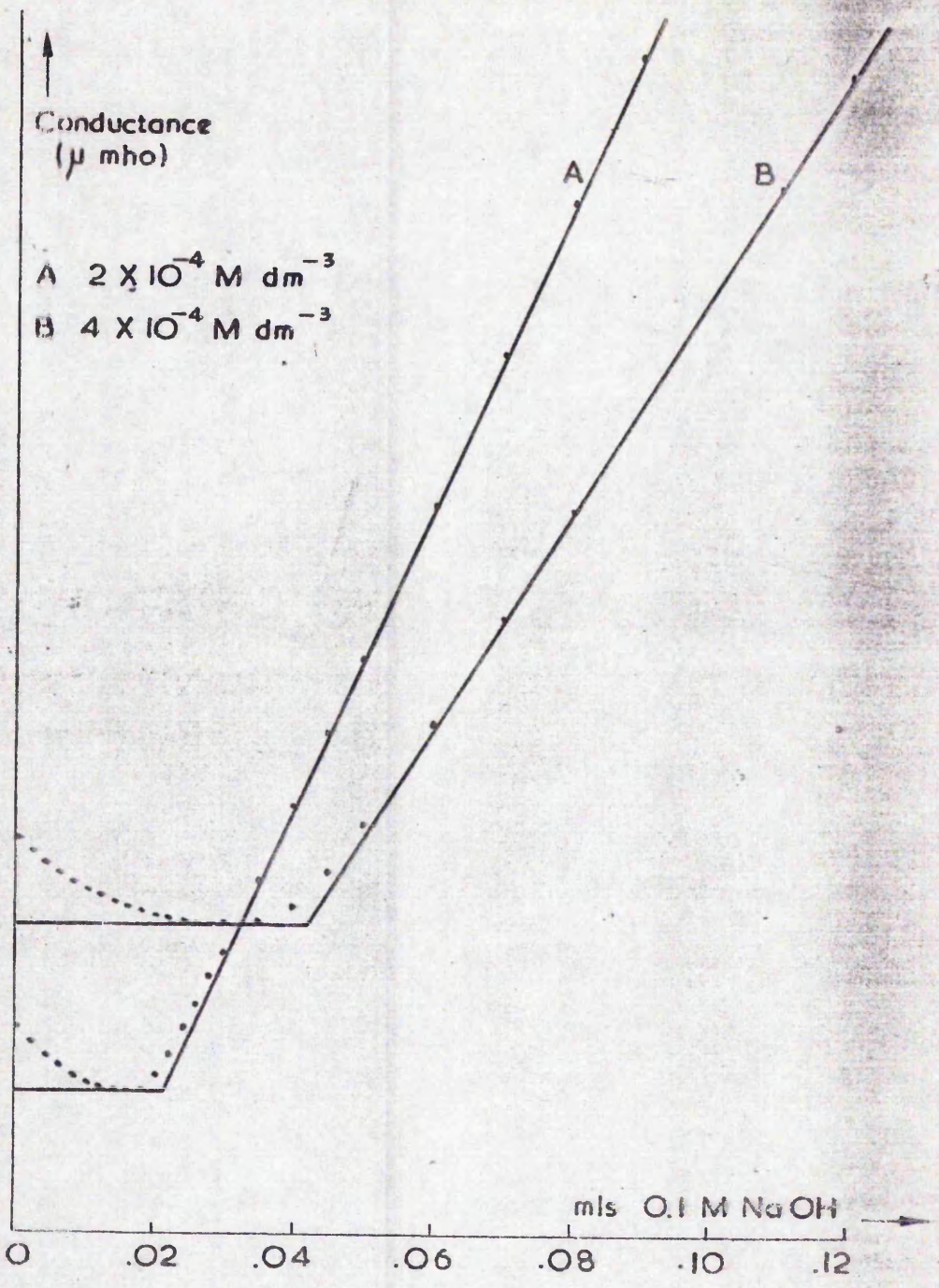

TITRATION OF BENZOIC ACID vs SODIUM HYDROXIDE

FIG.9.

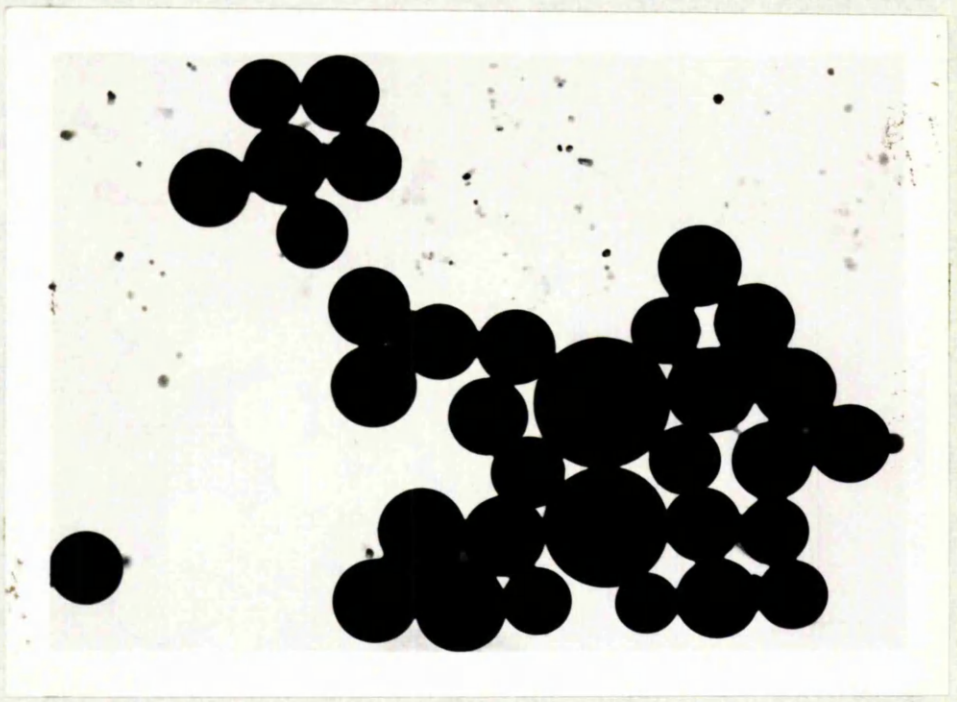

PLATE 1

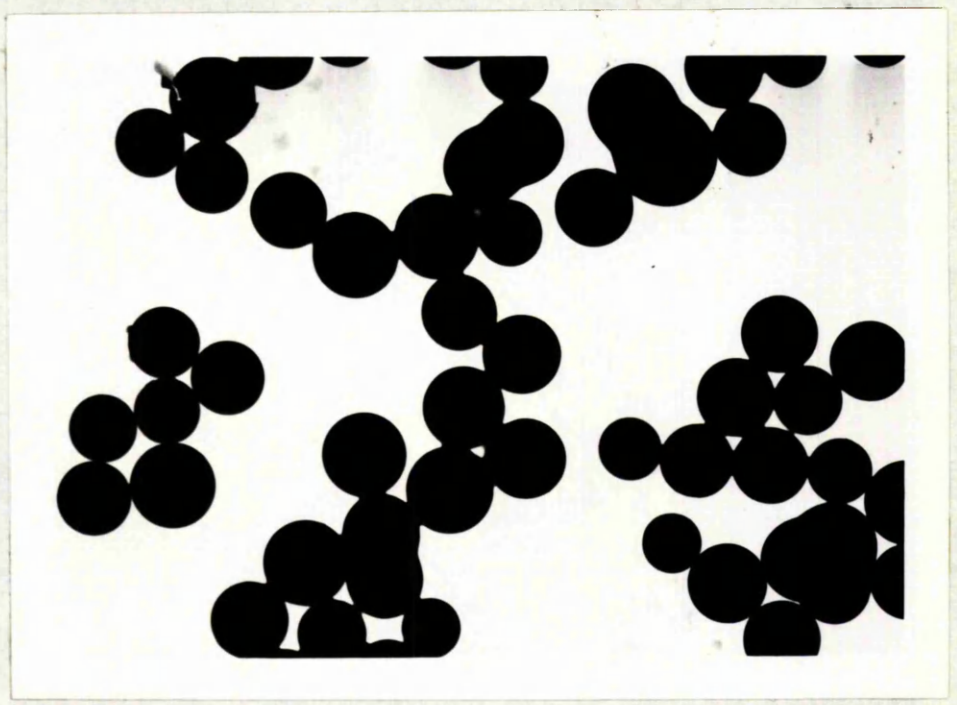

PLATE 2

layer is progressively removed, enabling oxidation of any benzaldehyde to occur. Ion-exchange, however, is a relatively rapid process, and, unless the sample is stored for a considerable period after ion-exchange, appreciable benzaldehyde oxidation is unlikely to occur.

c) Since the oxidation of benzaldehyde is light activated, it would appear that conflicting results could arise from one latex being dialysed in a shady area of the laboratory whereas another was dialysed in a less shaded region.

E) BENZALDEHYDE AS AN INITIATOR FOR POLYMERISATION.

1) Experimental.

It has been found that benzaldehyde promotes the polymerisation of styrene to form a latex in the presence of light either via the free radicals produced during its oxidation or the formation of small amounts of benzophenone. A 1 ml sample of A.R. benzaldehyde was added to a flask containing 10 mls of styrene and 100 mls of water, the flask was flushed with nitrogen and left stoppered and unstirred on a windowsill. After ca. 3 days, the water phase became turbid and after ca. 7 days, the styrene layer had become solid due to bulk polymerisation. The water phase however was found to contain a latex (Plates 1,2) of size 817 $\pm$ 79 nm (Latex 66B). Similar reactions carried out in the dark did not produce any reaction within the same time period. After extensive dialysis the latex was titrated conductometrically.

2) Discussion.

The conductometric titration curve (Fig.10) indicates the presence of weak acid groups on the latex surface, since the presence of undialysed benzoic acid in the water phase would have resulted in a titration curve similar in shape to Fig.9. These groups are presumably due to benzoic acid adsorbed at the polymer/water interface since it is to be noted that none of the free radicals produced during the oxidation of benzaldehyde would result in acid end groups being incorporated onto the ends of the polymer chains.

It has been assumed that in both cases involving benzaldehyde sufficient oxygen diffused past the ground glass

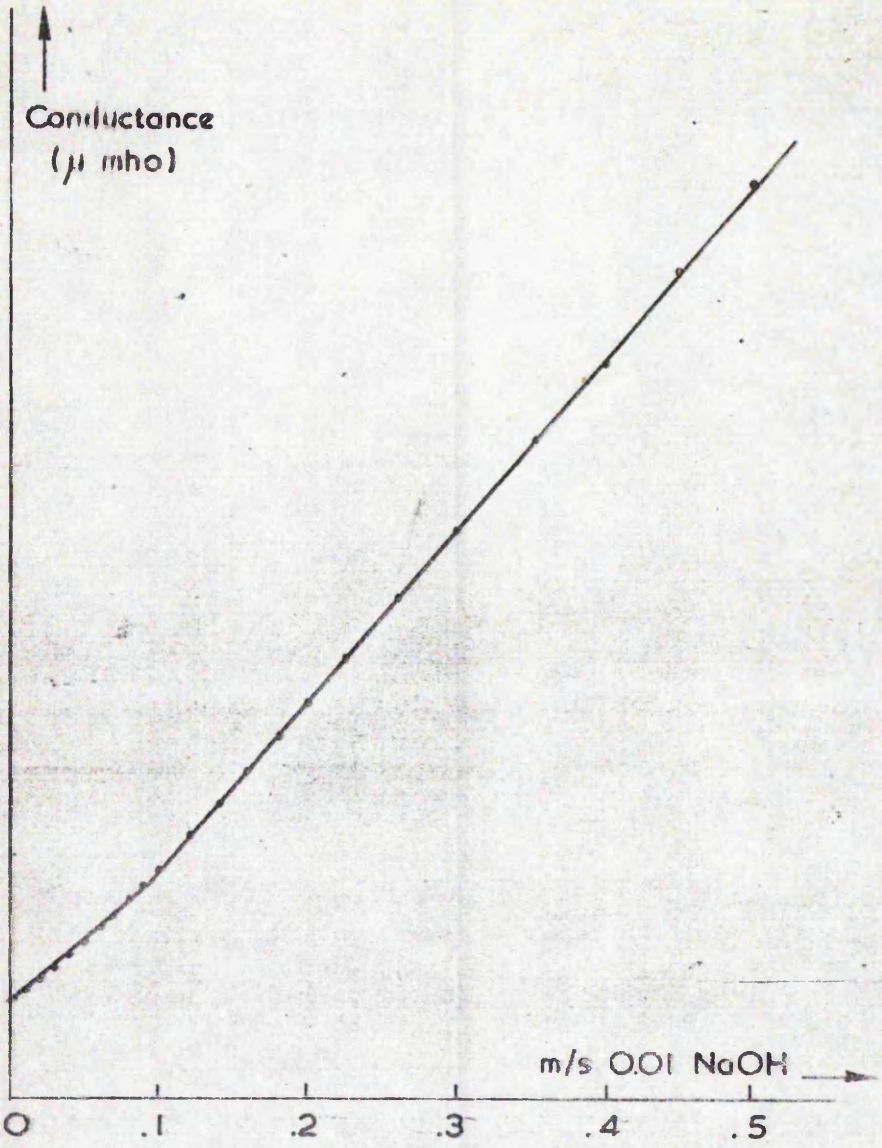

CONDUCTOMETRIC TITRATION OF LATEX 66B

FIG.10

stopper, which was ungreased, to cause oxidation.

F) CONCLUSIONS.

1) It appears that steam stripping is capable of removing excess monomer and other reaction by-products such as benzaldehyde from latices much more efficiently that dialysis. However, in the case of persulphate-initiated latices, the removal also leads to rapid hydrolysis of the surface-bound sulphate groups at the temperatures employed. If steam stripping is to be used as a technique for 'cleaning' persulphate-initiated latices, it should be carried out at low temperatures and pressures, although the overall efficiency of the process may be impaired at temperatures well below the glass transition temperature (378 K).

2) The sulphate groups present on the latex surface are constantly undergoing hydrolysis, an effect which may not be apparent unless the latex is dialysed immediately prior to surface characterisation. This makes these latices unsuitable for use as 'model' colloids (as in electrophoresis and flocculation studies) where a constancy in the nature and number of the surface groups is desired, unless the latex is characterised prior to each experiment, or is stored with surfactant, and the surfactant removed prior to each experiment using ion-exchange.

3) Latices which exhibit neither strong or weak acid groups remain stable, even upon long periods of storage, indicating that stability may be conferred by a steric mechanism involving surface hydroxyl groups.

4) The presence of benzaldehyde, which is likely to be formed in a styrene emulsion polymerisation when an oxidising initiator is used, could have a serious effect on the character of the surface groups, and may have been the cause of the variation in the nature of the surface groups observed by different workers.

5) It would appear that the use of the technique of steam stripping with latices prepared using reducing sulphur compounds such as bisulphite, metabisulphite, sulphurous acid, dithionite etc., activated either by heavy metals or some oxidising initiator such as hydrogen peroxide,

potassium persulphate or potassium peroxydiphosphate, could result in the formation of an 'ideal model colloid' containing neither monomer or any hydrolysable surface groups, and with suitable choice of conditions of preparation (228) they could be formed with the complete absence of hydroxyl surface groups.

CHAPTER IV

POTASSIUM PEROXYDIPHOSPHATE AS FREE RADICAL INITIATOR IN SURFACTANT-FREE EMULSION POLYMERISATIONS

A) LATEX PREPARATIONS USING POTASSIUM PEROXYDIPHOSPHATE INITIATOR IN THE PRESENCE OF ADDED HEAVY METAL IONS.

1) Introduction.

Potassium peroxydiphosphate ($K_4P_2O_8$) has a similar structure to the more commonly used initiator potassium persulphate ($K_2S_2O_8$), and Castrantas et al (229,230) have demonstrated that it will initiate/increase the rate of initiation of soap-added emulsion polymerisation systems when used in conjunction with potassium persulphate and potassium persulphate/sodium metabisulphite. These workers were however primarily concerned with the physical properties of the polymer produced and did not concern themselves with the surface characterisation of the latices.

The work described in this chapter was carried out since it was thought that latices produced using potassium peroxydiphosphate would have the following advantages over persulphate initiated latices:

a) Assuming that the free radicals are produced by the reaction:

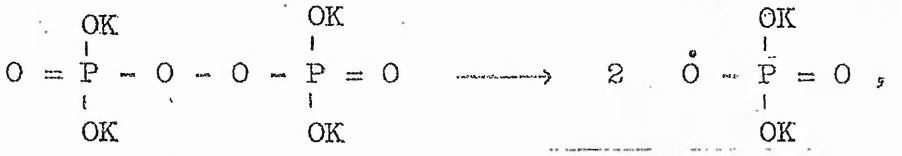

then latices could be prepared having doubly charged phosphate groups on the surface.

b) The amount of monomer oxidation products would be less with peroxydiphosphate, due to the greater stability of the -O-O- linkage. That these oxidation by-products are of importance was shown in Chapter III.

c) A reaction by-product of persulphate-initiated systems is potassium hydrogen sulphate, which results in the final pH of the latices produced in unbuffered reactions being ca. 2.5 - 3.0, under the usual concentrations used. Assuming similar byproducts for potassium peroxydiphosphate, then it would be expected that the reaction would be self-

buffering due to the formation of dipotassium hydrogen phosphate.

2) Preparation.

a) Experimental.

The rate of thermal cleavage of potassium peroxydiphosphate to give free radicals is at least 200 times slower than that of potassium persulphate (231,232). Hence, initiation using this compound alone would not be expected to occur; indeed attempts to produce latices under similar conditions to those used in preparing persulphate latices failed, even after prolonged reaction times (> 72 hours, 343 K). However, it was found that the rate of decomposition to produce free radicals was increased in the presence of heavy metals such as iron (Fe(II)) and silver (Ag(I)), added as ferrous ammonium sulphate and silver nitrate, presumably by the following reaction:

$$M^{n+} + P_2O_8^{4-} \longrightarrow M^{(n+1)+} + PO_4^{\bullet 2-} + PO_4^{3-} ,$$

by analogy to the similar reaction occuring with persulphate (233). A series of polymerisations were carried out to determine the effect of adding varying amounts of these ions to otherwise similar small scale reactions. However, the reproducibility, monodispersity and % conversion obtained with these systems was poor (Table 7).

TABLE 7

PEROXYDIPHOSPHATE INITIATED POLYSTYRENE LATICES PRODUCED IN THE PRESENCE OF ADDED HEAVY METAL IONS

Latex	[I] x 10^3 (mole l^{-1})	[MET.] x10^4 (mole l^{-1})	% Conversion□	Diameter (nm)	% σ	N x 10^{-11} (ml^{-1})	Final pH
20A5	2.92	8.86	12.71	425	10.4	2.7	8.1
20A4	2.84	8.36	18.12	413	18.2	4.2	7.9
20A8	2.85	6.10	12.10	601	8.0	0.9	7.6
20A6	2.92	4.43	2.65	240	11.1	3.2	7.7
20A7	2.84	1.74	7.62	392	10.2	2.1	8.4
20A10	2.93	0.97	1.10	265	12.3	1.0	8.6
20A9	2.85	0.49	0.44	127	7.6	3.5	8.5
20A3	2.90	0.40	3.65	436	4.8	6.3	8.8
32A	1.49	2.25*	-	575	12.7	-	-
32B	1.49	4.50*	-	718	19.8	-	-

□after twenty four hours,

[I] = Initiator concentration,

[MET.] = Concentration of Fe(II),

(* Ag (I)),

Monomer concentration = 0.870 mole l^{-1},

Temperature = 343 K.

b) Discussion.

Although the results are rather scattered, there appears to be a decrease in percent conversion with decreasing Fe(II) concentration. The number of particles ml^{-1} are all of the same order of magnitude, indicating that the initial stages of particle nucleation were probably similar for all the reactions, but that considerable deviations in the rate of radical generation occurred later in the reaction.

The latices produced in the presence of Fe(II) had a dull brown colouration at the end of reaction, presumably due to the presence of hydrated ferric oxide, whereas the latices produced using Ag (I) were primrose yellow in colour, becoming grey upon dialysis - presumably due to the formation of colloidal silver (224). It was impossible to remove these colloidal impurities by normal latex cleaning methods and hence no surface characterisations were carried out on these latices.

An experiment to determine the effect of adding Fe(II) to a persulphate initiated polymerisation under similar conditions to those employed with peroxydiphosphate was carried out ([Styrene] = 0.870 mole l^{-1} , $[K_2S_2O_8]$ = 2.31×10^{-3} mole l^{-1} , [Fe (II)] = 1.12×10^{-4} mole l^{-1}). The percent conversion of the reaction was very low (0.5%) and the particles produced had an unusual morphology (Plate 9 Chapter V).

The low percent conversions observed with both initiator systems were probably due to the initial rate of radical production being very high. Fritzche and Ulbricht (234) determined the second order rate constant for the decomposition of persulphate in the presence of varying amounts of ferrous ammonium sulphate to be of the order of 19 to 24 $l\ mole^{-1}\ sec^{-1}$ at 288 K. Several workers have reported that the persulphate initiated polymerisation of vinyl compounds was greatly accelerated by the presence of oxidisable metal salts (235,236). Rodriguez and Givey (237) observed a 13 - fold increase in the rate of acrylamide polymerisation initiated by persulphate upon addition of 20×10^{-6}

mole l^{-1} Fe (II). This high initiation rate in the case of styrene emulsion polymerisation would probably result in monomer starvation of the water phase coupled with reaction of excess free radicals with more Fe (II):

$$SO_4^{\bullet -} + Fe^{2+} \longrightarrow Fe^{3+} + SO_4^{2-} \quad (238).$$

The overall reaction thus being:

$$S_2O_8^{2-} + 2\ Fe^{2+} \longrightarrow 2\ Fe^{3+} + 2\ SO_4^{2-},$$

as demonstrated by Kolthoff et al (239). A similar effect, but to a lesser extent, would be expected with peroxydiphosphate. However, the concentration of iron present in both systems was considerably less than that of the initiators, indicating that, especially in the case of persulphate, the resulting hydrated ferric oxide acted as an inhibitor to further reaction.

The reaction of silver ions with peroxydiphosphate, again by analogy to persulphate, is probably (240),

$$Ag^{+} + P_2O_8^{4-} \longrightarrow Ag^{2+} + SO_4^{2-} + SO_4^{\bullet -},$$

$$Ag^{2+} + P_2O_8^{4-} \longrightarrow Ag^{3+} + SO_4^{2-} + SO_4^{\bullet -}.$$

It has been suggested that high valency silver ions can initiate polymerisation (240).

B) LATEX PREPARATIONS USING POTASSIUM PEROXYDIPHOSPHATE INITIATOR IN THE ABSENCE OF ADDED HEAVY METAL IONS.

1) Experimental.

Several reactions using peroxydiphosphate as initiator were carried out on a large scale in a reaction vessel fitted with a stainless steel stirrer (composition, Table 8). These reactions were found to proceed to low conversion despite the absence of added heavy metal ions. The results are summarised in Table 9.

TABLE 8

COMPOSITION OF STAINLESS STEEL USED AS STIRRERS

18%	CHROME
9%	NICKEL
0.6%	TITANIUM
0.15%	CARBON
IRON TO 100%	

TABLE 9

POTASSIUM PEROXYDIPHOSPHATE INITIATED LATICES IN THE ABSENCE OF ADDED HEAVY METAL IONS

Latex	[M] (moles l^{-1})	[I] (moles l^{-1})	diameter (nm)	% σ	% Conversion	$Nx10^{-11}$ (ml^{-1})
136	0.963	26.2	486	14	7□	1.11
134	0.963	26.3	503	11	8□	1.13
141	0.963	52.2	636	6	5*	0.35
135	0.963	57.6	565	4	4*	0.41

[M] monomer concentration, [I] initiator concentration,

□ after 42 hours, * after 24 hours.

The large excess of residual monomer was removed from the latex, prior to dialysis, in a separating funnel. The resulting latices were all less dense than water, and floated to the surface upon centrifugation. However, upon either steam stripping or isooctane extraction to remove excess monomer, they all became more dense than water. The removal of this monomer did not affect the particle size, (refer Chapter V and Plates 10 - 12).

Samples of latex 135 and 141 were titrated both conductometrically and potentiometrically (Fig.11). The rate of hydrolysis of the phosphate groups was also determined by heating a sample of latex 135 at 343 K for four days. The sample was then dialysed and titrated (Table 10).

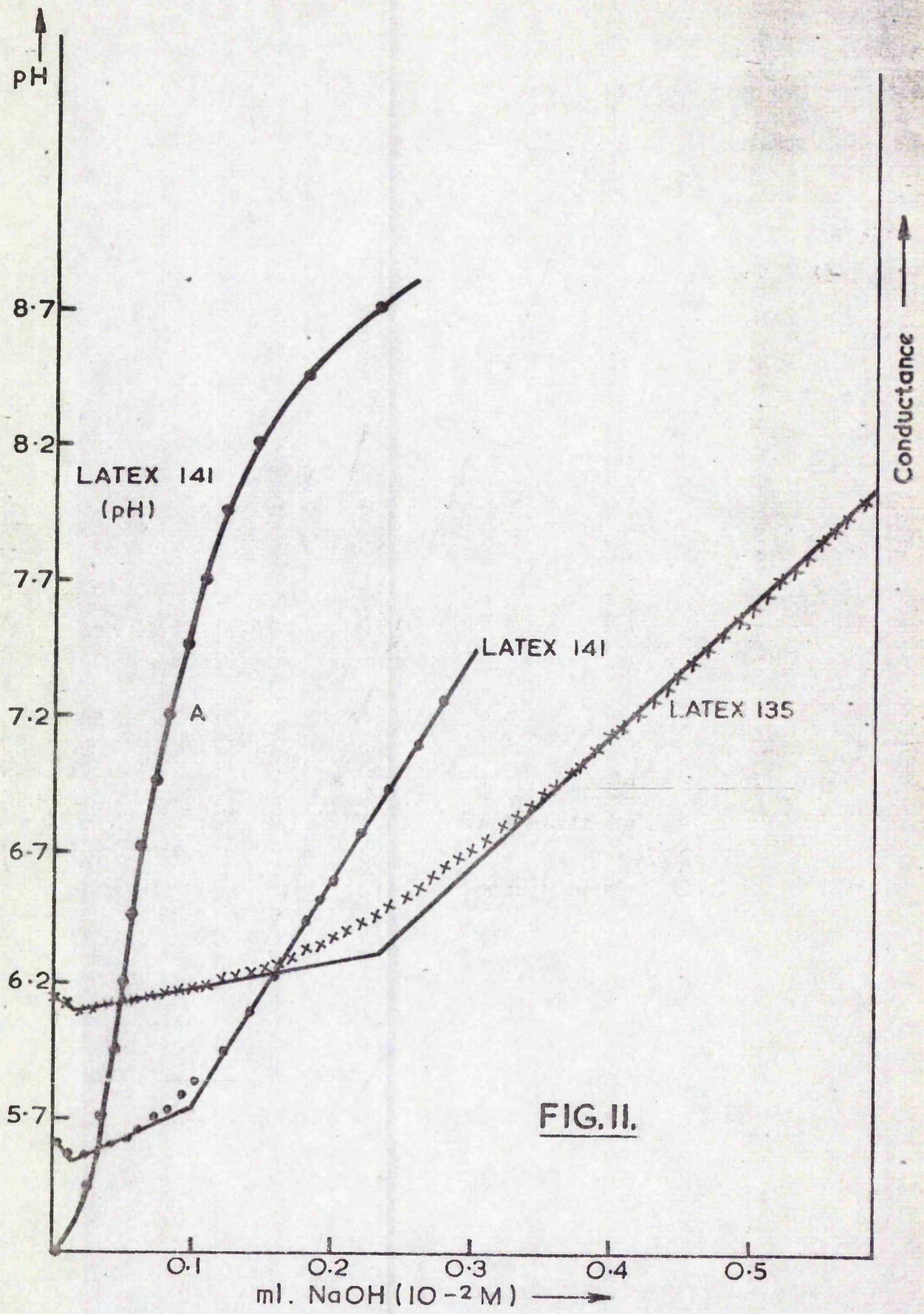
pH
8·7
8·2
7·7
7·2
6·7
6·2
5·7
LATEX 141
(pH)
A
LATEX 141
LATEX 135
Conductance
0·1
0·2
0·3
0·4
0·5
ml. NaOH (10 -2 M)

FIG. II.

TABLE 10

CONDUCTOMETRIC TITRATION RESULTS ON LATICES 135 and 141

CONDUCTOMETRIC TITRATION RESULTS ON LATICES 135 and 141

Latex	End points (μ eq g^{-1})			
	Before heating		After heating (343K)	
	1	2	1	2
135	1.67	10.00	1.06	11.7
141	1.26	9.37	-	-

Latex	Surface charge density (μ C cm^{-2})	
	Before heating	After heating (343K)
135	11.13	12.17
141	11.42	-

2) Discussion.

a) Initiation.

The cause of reaction could be due to:

i) The fact that the volume to vessel wall surface area ratio in a large reaction vessel is greater than in a small one, and hence fewer radicals would be lost to the glass walls. However, identical reactions to the above carried out with a glass stirrer did not produce any reaction.

ii) An increased rate of decomposition into free radicals catalysed by a low concentration of heavy metal ions in solution originating from the stirrer.

iii) The stainless steel surface could act as a catalyst to initiator decomposition.

The latter two seem the most likely explanations since a small scale reaction, carried out in the absence of any added heavy metal ions, but with a piece of stainless steel identical to that of the stirrer dipping into the reaction mixture produced a latex.

b) Surface Characterisation.

The conductometric titration curves (Fig. 11) for these latices appear to show the presence of both strong and weak acid groups, the weak acid group being present in much higher concentrations. It is difficult to determine from the potentiometric titration curve for 141 whether

there is a single end point or two end points. There does appear to be a change in the slope of the curve at A (Fig. 11) although it is not well defined and hence any value of pk_2 obtained would be very tentative. The end groups most likely to be found on these latices are R- PO_4^{2-}, although the presence of carboxyl groups cannot be ruled out completely. Parreira (241) determined the pk values of dodecylphosphoric acid to be 2 $\pm$ 0.1 and 7 $\pm$ 0.1 although the different substituent group encountered in this work would probably alter these. The disparity of the two end points as determined from conductometric titration is probably due to the fact that pk_1 is not sufficiently low that complete ionisation occurs. The surface charge densities are quite high. However, when the double negative charge is taken into account the number of phosphate groups cm^{-2} is of the same order as those found by other workers for sulphate groups (133,141,145,155). As can be seen these groups are stable to hydrolysis at elevated temperatures.

C) LATEX PREPARATIONS USING POTASSIUM PEROXYDIPHOSPHATE INITIATOR IN CONJUNCTION WITH SODIUM METABISULPHITE.

1) Introduction.

Around 1940 workers in several industrial laboratories independently demonstrated that the polymerisation rates which were customary with peroxides could be vastly increased by the use of a combination of oxidising and reducing agents (242). The term 'reduction activation' was initially used (235), but nowadays the reactions are usually termed 'redox catalysis' and 'redox polymerisation'. Since 1940 a large number of these systems have been used for vinyl polymerisations (225).

The mechanism of the reaction between oxidising sulphoxy compounds such as: sodium metabisulphite ($Na_2S_2O_8$), sodium bisulphite ($Na\ HSO_3$), sodium sulphite (Na_2SO_3), sulfurous acid (H_2SO_3), sodium dithionate ($Na_2S_2O_4$), sodium thiosulphate ($Na_2S_2O_3$) etc., with peroxydiphosphate and heavy metal ions has not been previously studied. The following discussion is thus based mainly on analogy to persulphate reaction mechanisms, which it is thought would

be similar to those of peroxydiphosphate albeit more rapid. It is thought that polymerisations involving these systems results in a certain amount of radical generation from the sulphoxy compound and resultant formation of sulphoxy end groups bound to the ends of the polymer chains (157,224,225, 242-245). Mukherjee et al (224) postulated that in cases where polymerisation occurred in the presence of reducing sulphoxy compounds and heavy metal ions that the radical generation could be represented as:

$$Sx\ Oy^{n-} + M^{n+} \longrightarrow Sx\ Oy^{(n-1)-} + M^{(n-1)+}.$$

By the above mechanism it would be possible to incorporate such groups as $-SO_3^-$, $-S_2O_4^-$, $-S_2O_3^-$ etc. onto the ends of the polymer chains.

The exact mechanism of radical formation in the presence of oxidising agents appears to be the subject of some controversy in the literature. For the persulphate /thiosulphate system, Bunn (245) proposed the following mechanism:

$$S_2O_8^{2-} + S_2O_3^{2-} \longrightarrow SO_4^{2-} + \dot{SO}_4^- + \dot{S}_2O_3^-$$

$$\dot{SO}_4^- + S_2O_3^{2-} \longrightarrow SO_4^{2-} + \dot{S}_2O_3^-$$

$$\dot{SO}_4^- + H_2O \longrightarrow H\ SO_4^- + \dot{O}H$$

$$\dot{O}H + S_2O_3^{2-} \longrightarrow OH^- + \dot{S}_2O_3^-$$

$$2\ \dot{S}_2O_3^- \longrightarrow S_4O_6^{2-}$$ (Caros acid, peroxosulphuric acid).

However, Sorum and Edwards (247), in order to explain the pH changes occurring during the reaction, as well as the zero order dependance of the reaction rate on the thiosulphate concentration, postulated that the reaction proceeded as follows:

$$S_2O_8^{2-} \longrightarrow 2\ \dot{SO}_4^-$$

$$\dot{SO}_4^- + H_2O \longrightarrow H\ SO_4^- + \dot{O}H$$

$$\dot{O}H + S_2O_3^{2-} \longrightarrow OH^- + \dot{S}_2O_3^-$$

$$\dot{S}_2O_3^- + S_2O_8^{2-} \longrightarrow SO_4 \cdot S_2O_3^{2-} + \dot{SO}_4^-$$

$$\dot{S}_2O_3^- + \dot{SO}_4^- \longrightarrow SO_4 \cdot S_2O_3^{2-}$$

$$S_2O_3^{2-} + SO_4 \cdot S_2O_3^{2-} \longrightarrow S_4O_6^{2-} + SO_4^{2-}.$$

The outcome of both systems is that in the presence of monomer then -OH, $-S_2O_3^-$, $-SO_4^-$ end groups can be formed.

The case where a sulphoxy compound is used in conjunction with persulphate and a heavy metal has been studied by Berry and Peterson (238) using tetrafluoroethylene. A study of the end groups showed that when bisulphite was the reducing compound then the following reactions occurred in decreasing order of effectiveness:

$$Fe^{2+} + S_2O_8^{2-} \longrightarrow Fe^{3+} + SO_4^{2-} + \dot{SO}_4^-$$

$$Fe^{3+} + H\,SO_3^- \longrightarrow Fe^{2+} + H\,\dot{S}O_3$$

$$S_2O_8^{2-} + H\,SO_3^- \longrightarrow SO_4^{2-} + \dot{SO}_4^- + H\,\dot{S}O_3^-$$

It is important to note that in the above system the Fe (III) acts as a catalyst in the production of free radicals and is continually being regenerated.

Sodium metabisulphite, the sulphoxy compound used in this work, can exist in solution in two forms (248). At high concentrations the equilibrium:

$$Na_2S_2O_5 \rightleftharpoons 2\,Na^+ + S_2O_5^{2-}$$

occurs. Whereas at low concentrations the following equilibria are in operation:

$$Na_2S_2O_5 \rightleftharpoons 2\,Na^+ + S_2O_5^{2-}$$

$$S_2O_5^{2-} + H_2O \rightleftharpoons 2\,H\,SO_3^- \rightleftharpoons 2\,SO_3^{2-} + 2\,H^+$$

It has been remarked that the product sold commercially as sodium hydrogen sulphite may well be the metabisulphite (240).

Thus, by analogy to the above systems the probable radical generation reaction between $P_2O_8^{4-}$ and $S_2O_5^{2-}$ can be summarised as:

$$P_2O_8^{4-} + SO_3^{2-} \longrightarrow PO_4^{2-} + PO_4^{\cdot} + SO_3^{\cdot -}$$

Thereby resulting in the incorporation onto the polymer chains of $-O-PO_3^{2-}$ and $-SO_3^-$ groups. However, the sodium metabisulphite used in this work also contained about 0.01% iron, which at the concentrations used in the reactions would result in their being about 2×10^{-7} moles l^{-1} of iron present within the system, hence an iron catalysed reaction as shown above could also take place.

2) Experimental.

A series of small scale reactions was carried out using the potassium peroxydiphosphate/sodium metabisulphite initiator system. The monomer concentration was varied between 0.168 and 2.011 moles l^{-1}, the temperature between 328 and 368 K and the back ground ionic strength between 27.37×10^{-3} and 208.34×10^{-3}. The latices produced were titrated conductometrically and in some cases potentiometrically. The results are summarised in Tables 11 - 14, and were analysed using the least squares method.

3) Discussion.

a) Variation in particle diameter with monomer concentration.

The experimental and theoretical results from Table 11 were found to fit the following equations (Fig. 12).

Observed $\log d = .403 \log [M] + 2.828$ -- (116)

Theoretical $\log d = .433 \log [M] + 2.857$ -- (117)

The above empirical equations are almost identical to that obtained by Goodwin et al (141,170), i.e.,

$$\log d = 0.410 \log [M] + 2.780 \quad \text{-- (118)}$$

This close similarity is probably fortuitous since Goodwin et al's results were obtained using potassium persulphate initiator at 358 K and a background ionic strenth of 19.2×10^{-3}. The close similarity in form however indicates that the number of particles produced in both systems is almost identical.

It would be expected that N would be invariant with monomer concentration, provided it was sufficient for monomer starvation not to occur during the early stages. If N is invariant with [M] then:

TABLE 11

VARIATION IN PARTICLE DIAMETER WITH MONOMER CONCENTRATION

Latex	[M] (mole l^{-1})	d (nm)	% standard deviation	% Conversion	$Nx10^{-11}$ (ml^{-1})	d^{t*} (nm)	Final pH
44B	0.174	307.3	2.25	98.44	11.08	309.3	7.7
43B	0.348	450.2	2.47	92.04	6.63	462.2	-
42A	0.522	518.7	4.51	78.74	5.58	562.5	7.3
41B	0.696	604.0	1.04	87.67	5.24	631.1	-
42B	0.870	642.9	2.89	75.56	4.85	705.9	7.3
43A	1.044	665.2	6.64	95.19	6.39	676.5	-
44A	1.218	747.4	4.71	82.22	4.54	798.3	7.8
49A	1.566	746.3	4.01	80.74	5.76	802.2	-
49B	2.088	866.1	6.66	73.20	4.45	961.1	-

$^{*}d^{t}$ = Theoretical diameter (100% conversion).

Potassium peroxydiphosphate concentration = 2.31×10^{-3} mole l^{-1}.

Sodium metabisulphite concentration = 2.10×10^{-3} mole l^{-1}.

Temperature = 343 K, Ionic strength = 29.4×10^{-3}.

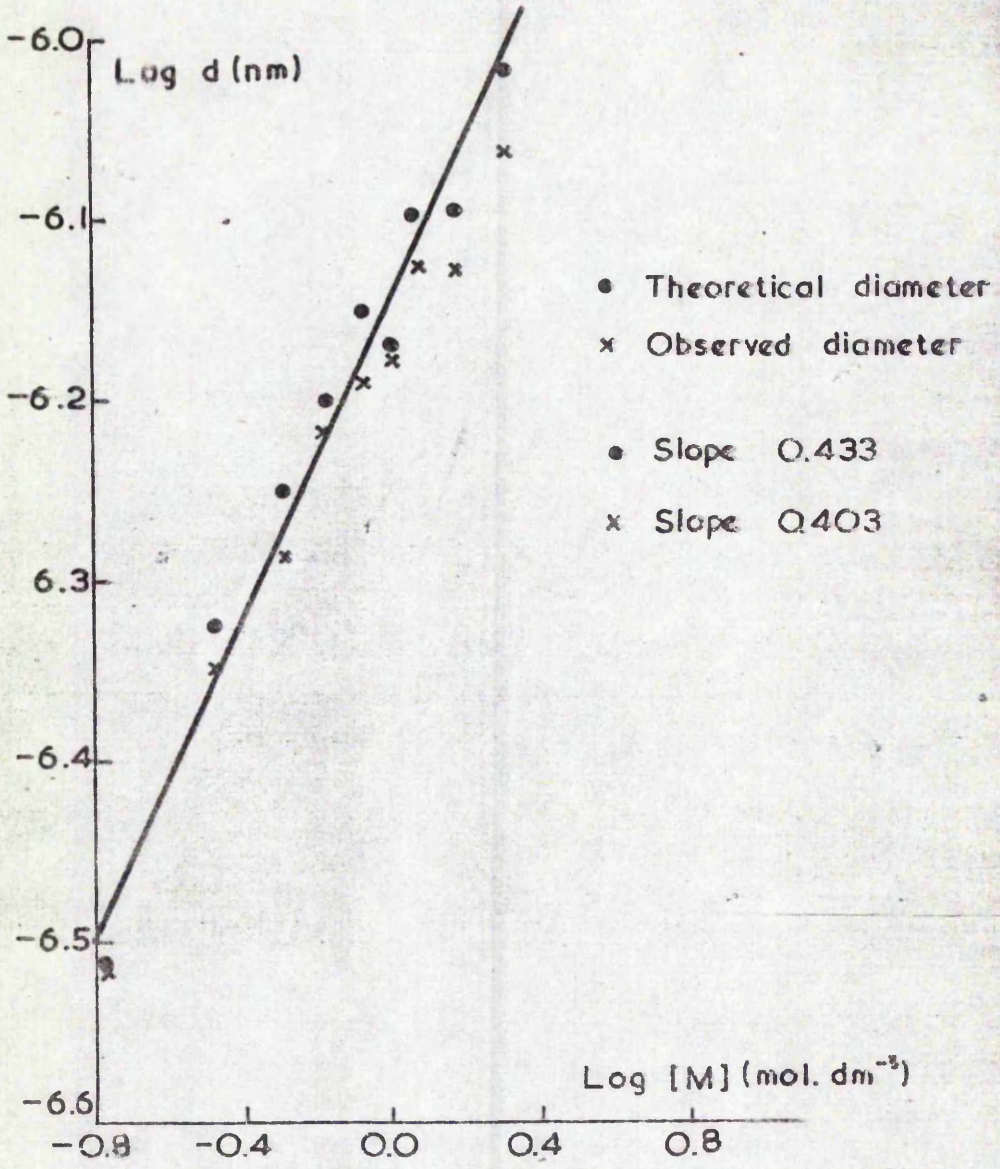

PLOT OF LOG d vs LOG [M] FOR PEROXYDIPHOSPHATE METABISULPHITE LATICES

FIG.12.

TABLE 12

VARIATION IN PARTICLE DIAMETER WITH TEMPERATURE

Latex	Temperature (K)	d (nm)	% Standard deviation	% Conversion	$N \times 10^{-11}$ (ml^{-1})	d^{t}* (nm)
54A	328	829.9	1.96	90.83	2.09	857.3
53B	333	733.6	1.85	91.45	3.05	755.8
53A	338	621.4	2.88	89.72	4.92	644.5
41B	343	604.0	1.04	87.67	5.24	631.1
52B	348	585.6	2.78	94.71	6.21	596.3
52A	353	526.5	1.03	95.07	8.58	535.4
51B	358	520.2	1.04	91.75	8.58	535.4
51A	363	483.9	0.56	95.81	11.14	490.8
50B	368	469.6	4.07	97.62	12.41	473.4

* d^{t} = Theoretical diameter (100% conversion).

Potassium peroxydiphosphate concentration = 2.31×10^{-3} mole l^{-1}.

Sodium metabisulphite concentration = 2.10×10^{-3} mole l^{-1}.

Monomer concentration = 0.696 mole l^{-1}.

Ionic strength = 29.4×10^{-3}.

TABLE 13

VARIATION IN PARTICLE DIAMETER WITH IONIC STRENGTH

Latex	[I] x 10^3	d (nm)	% Standard deviation	% Conversion	N x 10^{-11} (ml^{-1})	d^t * (nm)	Final pH
45A□	27.37	533.5	2.21	76.91	6.67	582.3	7.8
41B	29.40	604.0	1.04	87.67	5.24	631.1	-
45B	29.92	642.9	3.64	76.79	3.81	701.9	7.7
46B	35.71	644.0	14.27	94.42	4.66	656.2	7.6
46A	43.48	605.7	8.39	91.60	5.43	623.6	7.7
47A	56.05	640.1	8.56	92.58	4.65	656.7	8.8
47B	83.59	642.5	1.54	94.20	4.68	655.3	8.2
48A	131.01	666.4	9.98	90.71	4.04	688.2	8.2
48B	208.34	563.3	6.16	27.12	1.99	871.4	7.8

*d^t = Theoretical diameter (100% conversion).

Potassium peroxydiphosphate concentration = 2.31 x 10^{-3} mole l^{-1}.

Sodium metabisulphite concentration = 2.10 x 10^{-3} mole l^{-1}.

Monomer concentration = 0.696 mole l^{-1}.

Temperature = 343 K.

□ Potassium peroxydiphosphate concentration = 2.11 x 10^{-3} mole l^{-1}.

□ Sodium metabisulphite concentration = 2.09 x 10^{-3} mole l^{-1}.

TABLE 14

SURFACE CHARGE DENSITIES AND MOLECULAR WEIGHTS OF PEROXYDIPHOSPHATE/METABISULPHITE INITIATED LATICES

Latex	[M] (moles l^{-1})	T (K)	[I] x 10^3	Surface Charge Density $\mu C\ cm^{-2}$	Molecular Weight* x 10^{-5}
44B	0.168	343	29.40	4.89	1.41
43B	0.335	343	29.40	1.40	7.22
48A	0.503	343	29.40	2.46	4.75
41B	0.696	343	29.40	4.33	3.14
42B	0.838	343	29.40	3.38	4.28
43A	1.006	343	29.40	1.69	11.83
44A	1.173	343	29.40	4.35	3.88
49A	1.508	343	29.40	2.44	6.87
49B	2.011	343	29.40	1.18	16.95
54A	0.696	328	29.40	2.66	7.02
53B	0.696	333	29.40	2.61	6.33
53A	0.696	338	29.40	3.23	4.33
52B	0.696	343	29.40	4.09	3.23
52A	0.696	353	29.40	3.03	3.91
51B	0.696	358	29.40	3.62	3.23
51A	0.696	363	29.40	4.63	2.36
50B	0.696	368	29.40	4.12	2.56
45A	0.696	343	28.21	4.92	2.44
45B	0.696	343	29.92	6.40	2.26
46B	0.696	343	35.71	7.04	2.06
46A	0.696	343	43.48	6.95	1.96
47A	0.696	343	56.05	7.83	1.84
47B	0.696	343	83.59	6.74	2.15
48A	0.696	343	131.01	7.71	1.94
48B	0.696	343	208.34	10.49	1.21

* Determined from titration assuming two acid groups per polymer chain.

$$4/3 \ \pi \ r^3 \ \rho \ N = P_W \qquad \text{--- (119)}$$

where P_W is the weight of polymer formed
N is the total number of particles
ρ is the polymer density.

i.e., $$d = 2\left(\frac{3 P_W}{4 \pi \rho N}\right)^{.333}. \qquad \text{--- (120)}$$

Values of d calculated using the above expression for both the observed (d_A) and theoretical (d_B) (100 conversion) cases are compared with the experimentally observed (d_C) and theoretical (d_D) diameters and with the diameters calculated from equations 116 (d_E) and 117 (d_F) in Table 15.

TABLE 15

COMPARISON OF DERIVED AND EXPERIMENTALLY OBTAINED DIAMETERS

Latex	d_A (nm)	d_C (nm)	d_E (nm)	d_B (nm)	d_D (nm)	d_F (nm)
44B	390	307	332	392	309	337
43B	482	450	440	494	462	456
42A	524	518	518	566	563	543
41B	596	604	582	606	631	615
42B	612	643	636	672	706	677
43A	702	665	685	714	677	733
44A	704	747	729	752	798	784
49A	760	746	806	818	802	874
49B	810	866	905	900	961	990

It can be seen that the values calculated from equations A and B are in better agreement than those calculated assuming N is invariant of monomer concentration. Thus:

$$d_E \propto [M]^{.403}, \qquad \text{--- (121)}$$

and $$d_F \propto [M]^{.433}, \qquad \text{--- (122)}$$

indicating that as [M] increases then N decreases. It is likely that the decrease in N is due to the incorporation of latex particles into the bulk monomer phase. It was noticed in all the multisampled kinetic runs that

as the reaction proceeded, the monomer layer became progressively more viscous, presumably due to both thermally and sulphate free radical initiated bulk polymerisation. A state was eventually reached whereby small droplets of the latex dispersion were incorporated into the viscous monomer phase, by mechanical entrapment. As conversion of monomer to polymer neared 100% this bulk polymer plus the incorporated latex formed a lump on the stirrer. In reactions where the monomer concentration is the only variable, then the greater the monomer concentration the greater the amount of bulk polymer formed due to the increased time needed to achieve 100% conversion, and hence a greater number of latex particles is lost from the reaction. It can be seen from Table 11 that there is a trend of decreasing % conversion to latex with increasing monomer concentration.

b) Variation in Particle Diameter with Temperature.

The experimental and theoretical results from Table 15 were found to fit the following equations (Fig. 13):

$$\text{Observed } \log d = \frac{704}{T} + 0.743 \qquad -- \quad (123)$$

$$\text{Theoretical } \log d = \frac{733}{T} + 0.672 \qquad -- \quad (124)$$

Both of which are similar in form to that obtained by Goodwin et al (141,170):

$$\log d = \frac{1173}{T} - 0.578 \qquad -- \quad (125)$$

From equation 124 the following equation can be derived for the variation of N (ml^{-1}) with temperature, for the system used in this work:

$$\log N = 18.104 - \frac{2199}{T} \qquad -- \quad (126)$$

Results calculated from this equation are plotted in Fig. 14. However, it is to be noted that the formation of coagulum during a reaction will affect this equation. For application to other systems the constants must be recalculated due to the fact that N is not invariant with the monomer concentration. It is to be noted that the form of this equation is very similar to that of the expanded Arrhenius equation, i.e.,

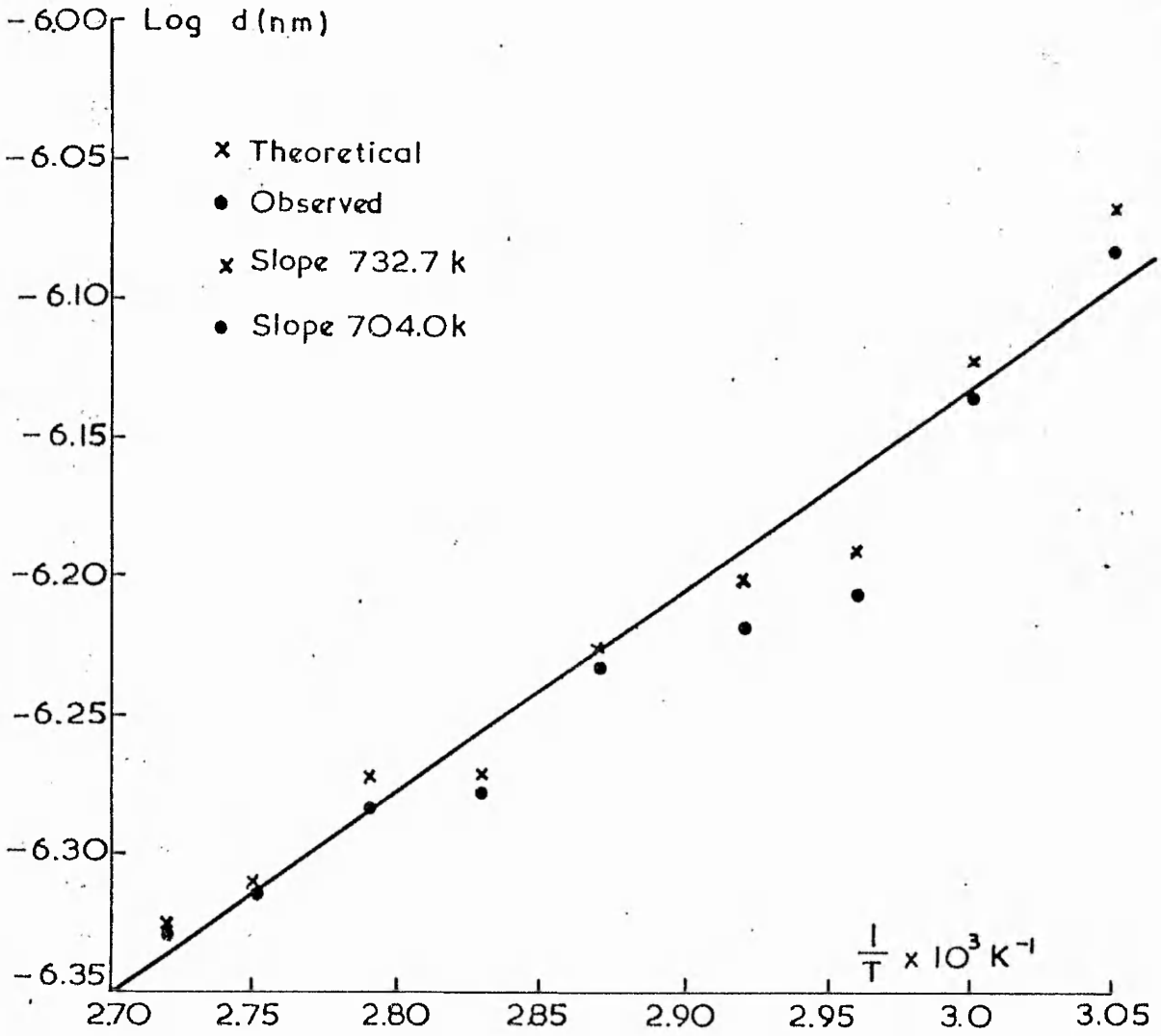

PLOT OF LOG d vs $\frac{1}{T}$ FOR PEROXYDIPHOSPHATE / METABISULPHITE LATICES

FIG.13.

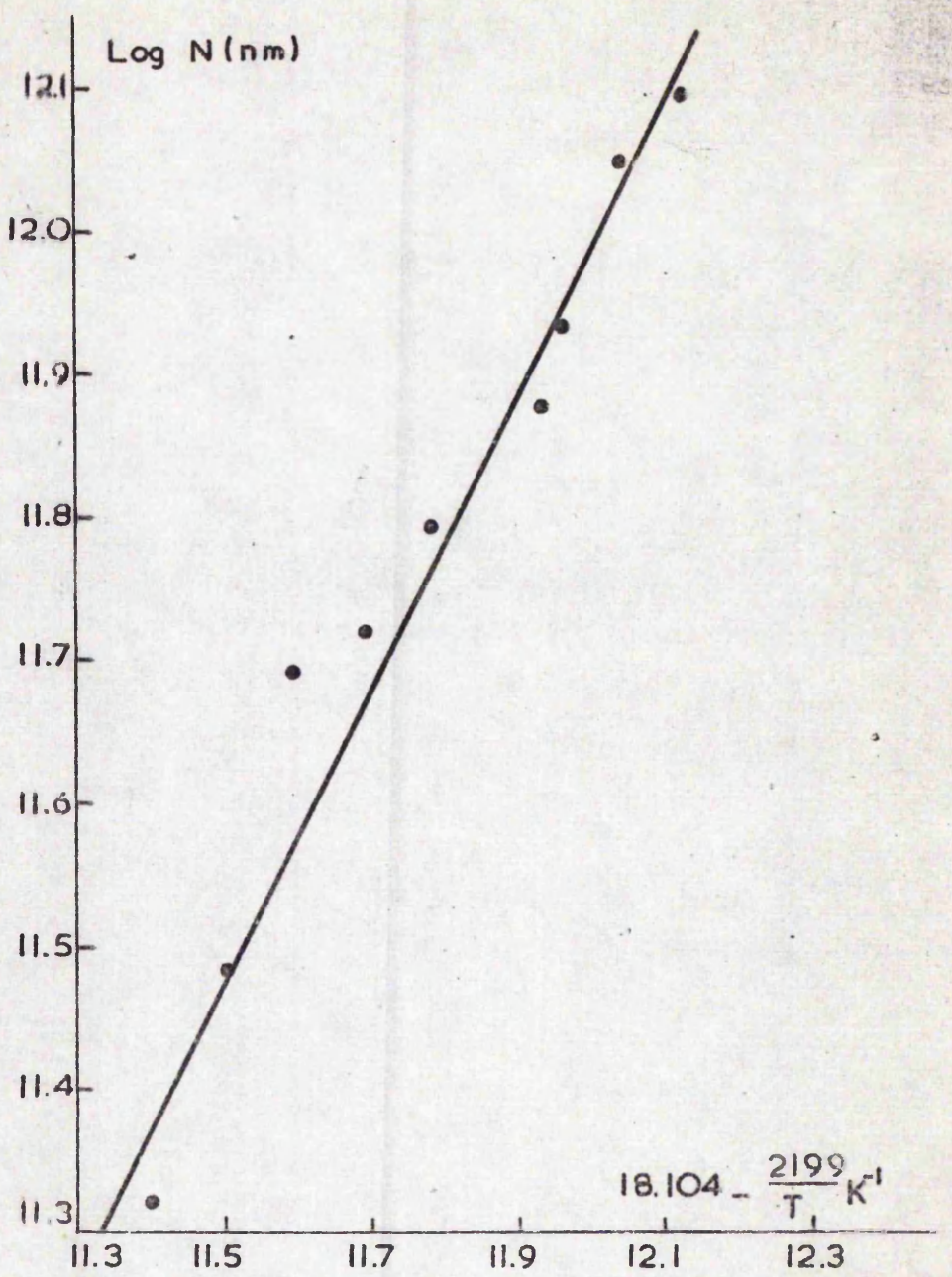

PLOT OF LOG N vs $(18.104 - \frac{2199}{T})$ FOR PEROXYDIPHOSPHATE/METABISULPHITE LATICES

FIG.14.

$$\log k = \log A - \frac{E_a}{2.303\ RT}, \qquad \text{-- (127)}$$

indicating that the total number of particles present at the end of the reaction may be proportional to the rate of formation of free radicals.

The equations for the variation of particle diameter with monomer concentration and temperature can be combined to give:

$$\text{Observed} \quad \log d = 0.202 \left(\log [M] + \frac{1747}{T} \right) + 1.786 \qquad \text{-- (128)}$$

$$\text{Theoretical} \quad \log d = 0.217 \left(\log [M] + \frac{1692}{T} \right) + 1.765 \qquad \text{-- (129)}$$

These equations are plotted in Fig. 15,16 and, as can be seen, give a good representation of the experimental data.

c) Variation in Particle Diameter with Ionic Strength.

The results in Table 13 are very scattered, and no valid line could be drawn through them. However, there does appear to be a trend of increasing theoretical diameter with ionic strength, the observed diameters remaining almost constant over the whole range. These results are in conflict with those obtained by Goodwin et al (141,170) who found, using persulphate initiator, that:

$$\log d = 0.238 \log [I] + 3.23 \text{ at } 343 \text{ K}, \qquad \text{--- (130)}$$

and $$\log d = 0.238 \log [I] + 3.14 \text{ at } 353 \text{ K}. \qquad \text{--- (131)}$$

The reason for the scatter in the results obtained in this work is not readily apparent, since the reactions involving variation in monomer concentration and temperature both gave results which could be fitted to straight lines.

This would indicate that the sodium chloride had an effect on the course of the reaction other than acting as an inert background electrolyte. Although the sodium chloride used was of 'AnalaR' grade it did contain trace amounts of iron and lead which, at the sodium chloride concentration employed, would have been present in the reaction in ca. 4×10^{-8} molar quantities. Both of these

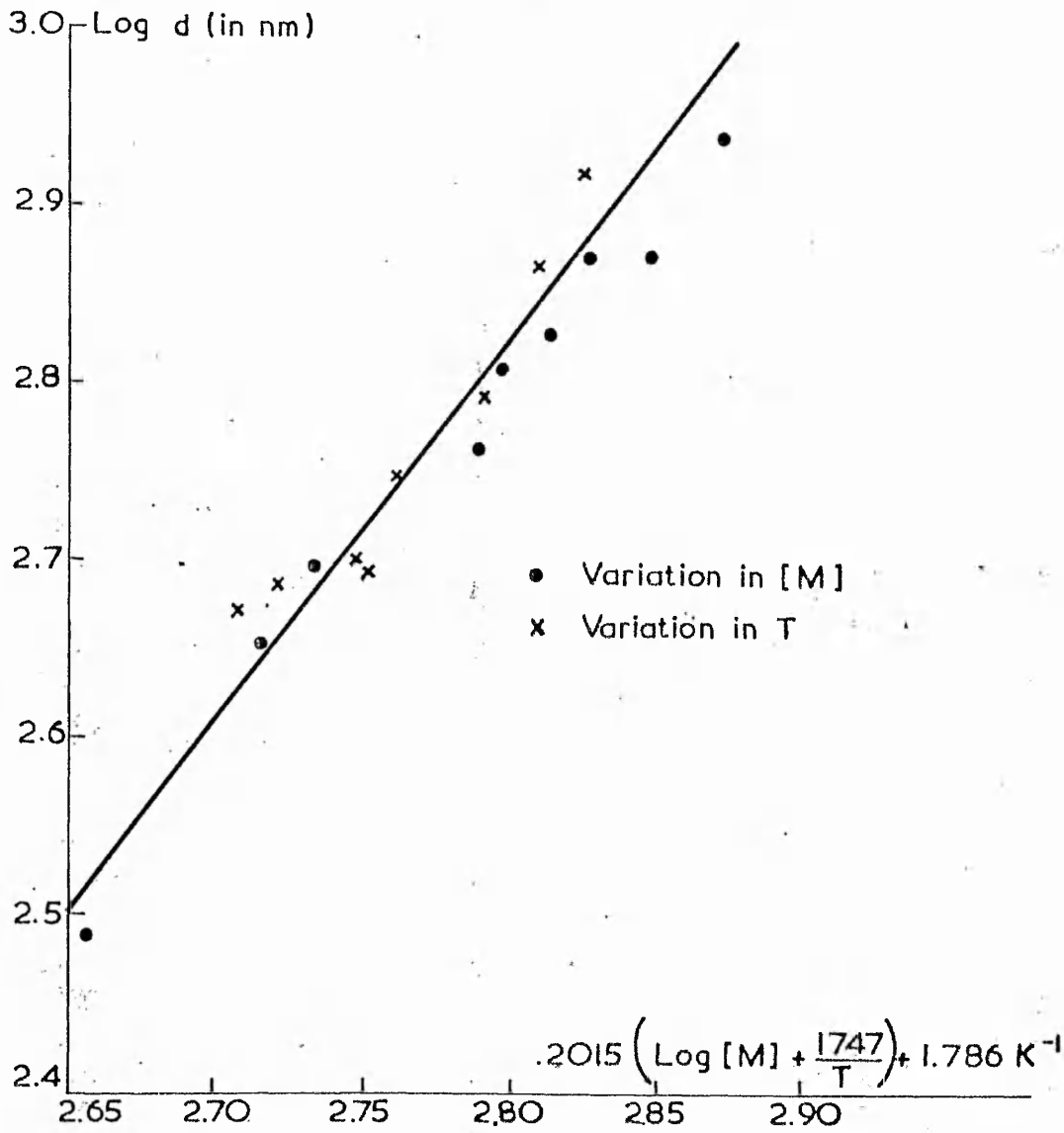

PLOT OF LOG d_{obs} vs $.2015\left(\log [M] + \frac{1747}{T}\right) + 1.786$

FOR PEROXYDIPHOSPHATE/METABISULPHITE LATICES

FIG.15

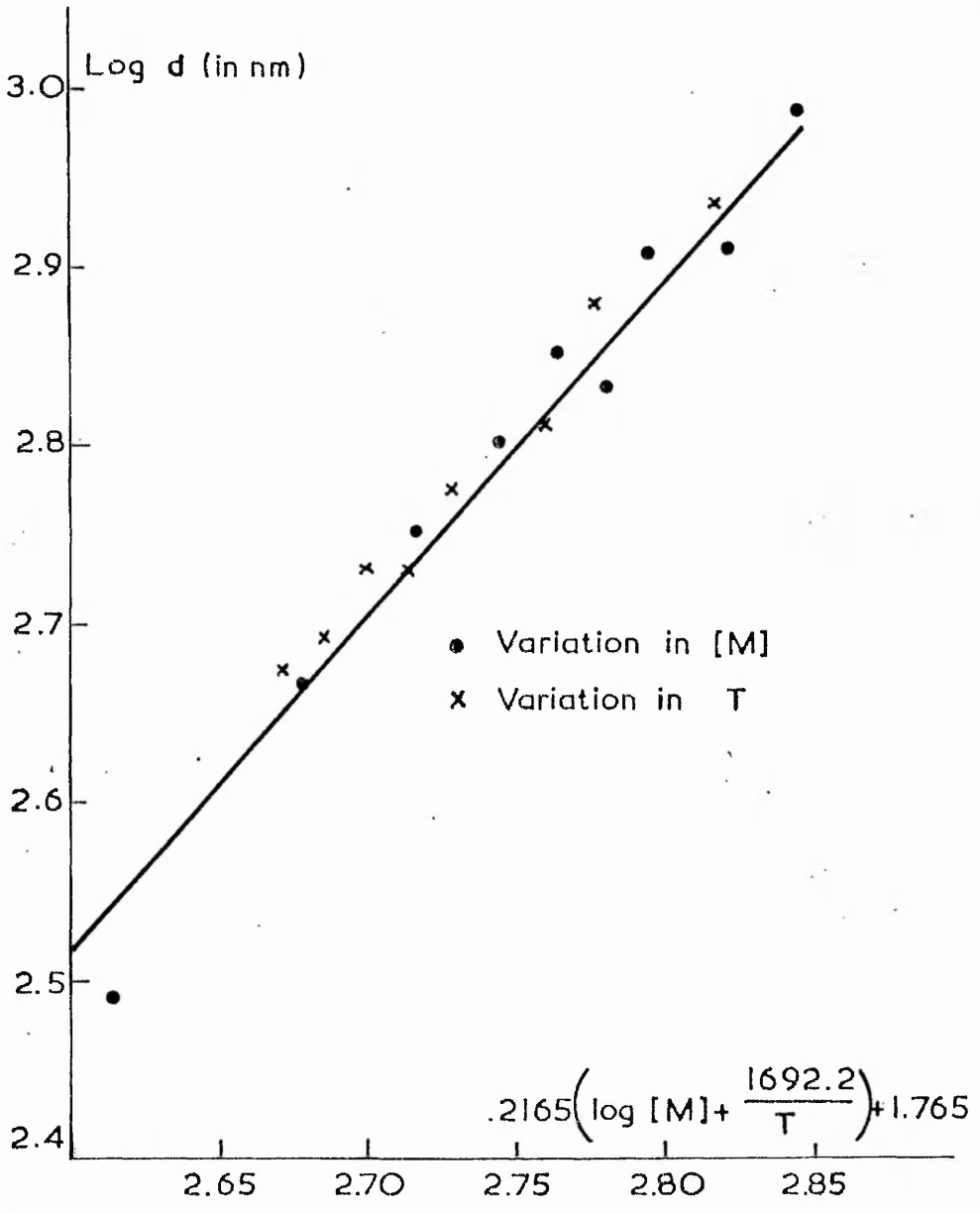

PLOT OF LOG $d_{theor.}$ vs $.2165\left(\log[M]+\frac{1692.2}{T}\right)+1.765$ FOR PEROXYDIPHOSPHATE / METABISULPHITE LATICES

FIG.16.

metal ions would tend to increase the rate of free radical production, especially since they were present in a redox system wherein each oxidation and reduction process resulted in the formation of a free radical. Hence, they would have a much more pronounced effect on the rate of free radical production than if they were introduced into a non-redox system. This increased rate of radical production would result in a larger number of particles being formed which would be counteracted by a decrease due to the higher background ionic strength.

d) Surface Characterisation.

i) Surface Charge Densities.

Both conductometric and potentiometric titration of these latices showed the presence of a single strong acid end point in all cases (Figs. 17,18). The surface charge densities shown in Table 14 vary between 1 and 10 $\mu C\ cm^{-2}$, the majority being in the range 3 to 7 $\mu C\ cm^{-2}$ and similar to those found by other workers for persulphate initiated systems (133,141,145,155). No trends are apparent for the variation of surface charge density with either monomer concentration, temperature or ionic strength, although the charge densities for latices produced with sodium chloride as background electrolyte are greater than those of latices produced in the absence of added electrolyte.

ii) Types of Surface Group.

It would be thought that both strong and weak acid groups would be present at the particle/water interface due to the presence of sulphonate ($-SO_3^-$) and phosphate ($-PO_4^{2-}$) groups. However, the presence of a single strong acid end point indicates that the majority of the groups are sulphonate. This is supported by X-ray fluorescence data* which showed that for latices 44A and 49B the ratio

* I am indebted to Mr. R.H. West of the Royal Military College of Science, Shrivenham, Wiltshire.

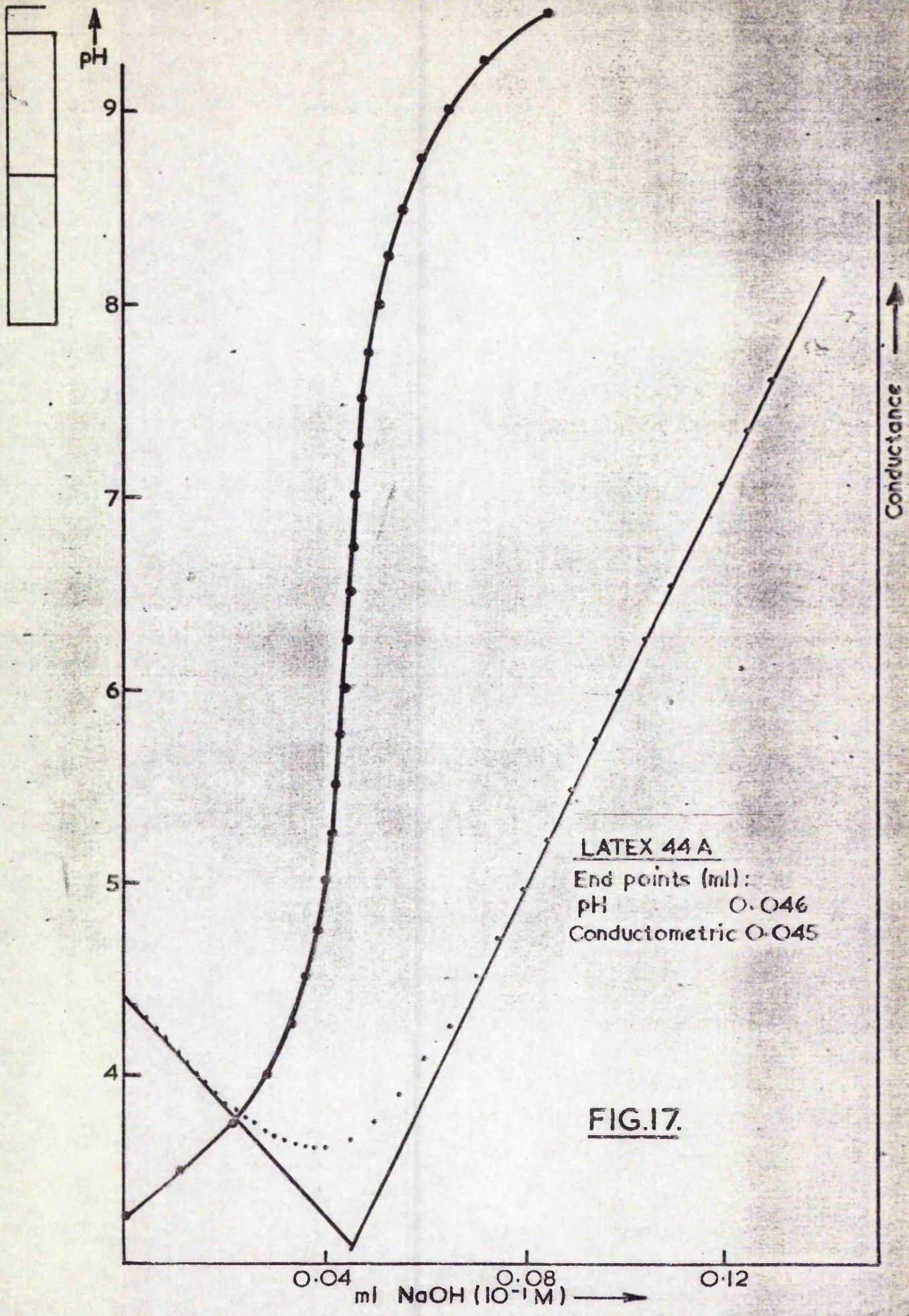
pH
9
8
7
6
5
4
Conductance
LATEX 44 A
End points (ml):
pH 0·046
Conductometric 0·045
0·04
0·08
0·12
ml NaOH (10^{-1} M)

FIG.17.

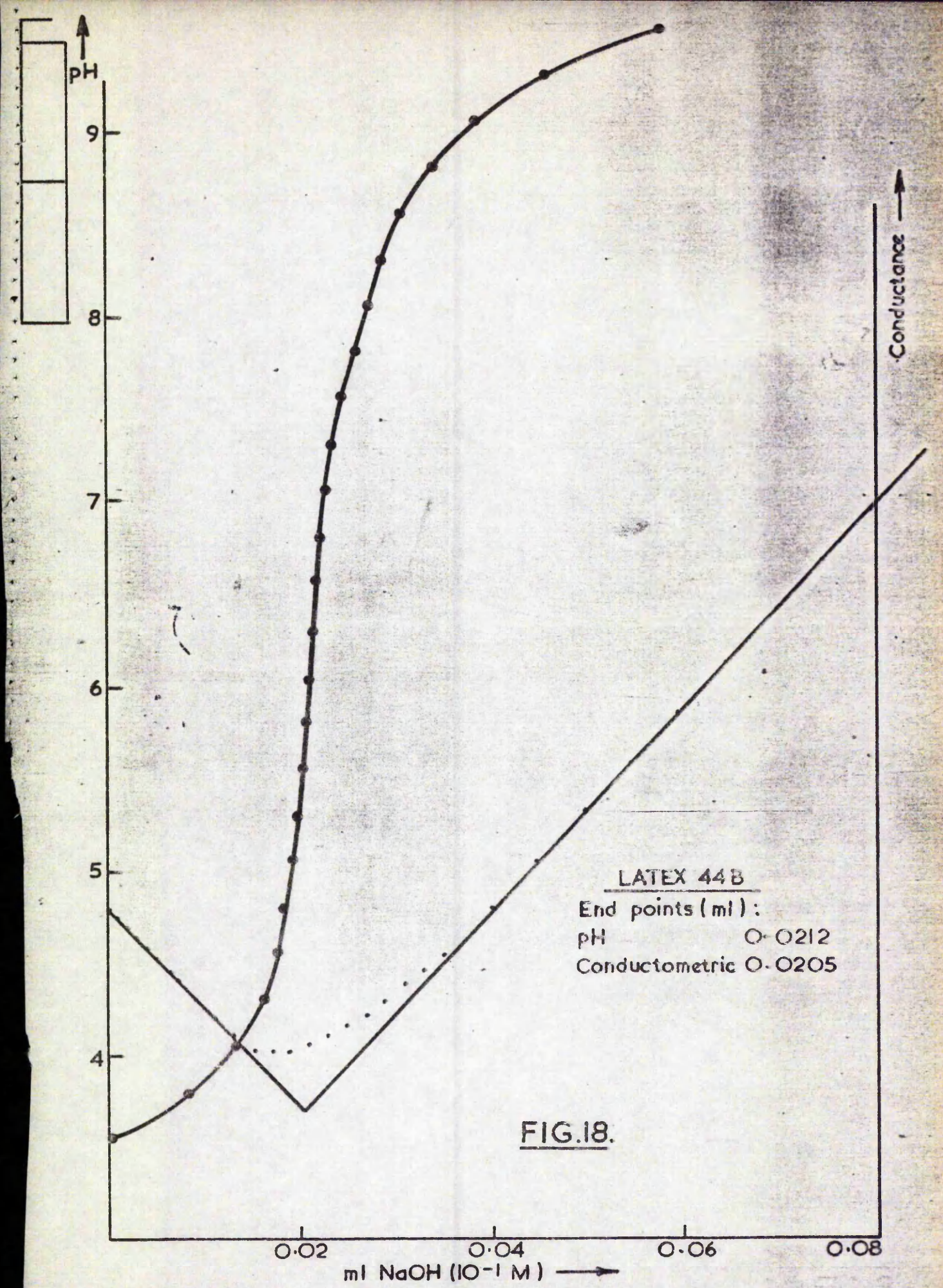
pH
9
8
7
6
5
4
Conductance
LATEX 44B
End points (ml):
pH 0·0212
Conductometric 0·0205
0·02
0·04
0·06
0·08
ml NaOH (10⁻¹ M)

FIG.18.

of sulphur to phosphorous was approximately 10:1. Also, as shown earlier in this section, phosphate groups exhibit two end points. It would thus appear that the majority of the phosphate groups present were either buried or their concentration was such that they were undetectable by the titration techniques used. Smitham et al (99) have suggested that the presence of small amounts of weak acid groups on a latex would be difficult to detect. For similar reasons the presence of carboxyl groups cannot be discounted, although it would be thought that due to the high stability of the peroxide linkage their formation would be unlikely either by oxidation of surface hydroxyl groups or possibly by benzaldehyde formation and its subsequent oxidation.

Several of the latices were oxidised to determine the number of hydroxyl groups present on the surface (Table 16). Where it is evident that all these latices contained surface hydroxyl groups it is unlikely that the presence of these groups is due to hydrolysis since both sulphonate (Chapter III) and phosphate (Chapter IV) groups have been shown to be stable to hydrolysis. It thus appears that these end groups emanate from reaction of a primary free radical, from either the peroxydiphosphate or metabisulphite, with water to produce an hydroxyl free radical.

4) CONCLUSIONS.

a) Potassium peroxydiphosphate as initiator.

It appears that this compound alone is incapable of initiating vinyl polymerisation, presumably due to the high stability of the peroxide linkage.

b) Potassium peroxydiphosphate/heavy metal ions as initiator.

In the presence of relatively large amounts of heavy metal ions polymerisation initiation does occur, although only to produce latices at low conversion and poor monodispersity. The reaction of potassium peroxydiphosphate in the presence of either a solid metal catalyst or very low concentrations of heavy metal ions (stainless steel stirrer) results in the formation (at low conversions) of

TABLE 16

HYDROXYL GROUP CONCENTRATION ON PEROXYDIPHOSPHATE/METABISULPHITE INITIATED LATICES

Latex	Strong acid before oxidation (μeq g^{-1})	After oxidation A Strong acid (μeq g^{-1})	After oxidation B Weak acid (μeq g^{-1})	A & B (μeq g^{-1})	OH concentration (μeq g^{-1})
41B	6.37	0.96	8.62	9.58	3.21
42B	4.16	1.10	6.16	7.26	3.83
44A	5.15	1.05	6.29	7.34	2.19
45A	8.19	1.36	13.00	14.36	6.17
45B	8.84	2.70	15.01	17.71	8.87
46A	10.19	2.56	11.80	13.36	3.17
47B	10.87	1.13	15.02	16.15	5.28

relatively monodisperse latices stabilised by phosphate groups, which appear to be stable to hydrolysis.

c) Potassium peroxydiphosphate/sodium metabisulphite as initiator.

This system is capable of initiating polymerisation to high conversions of monodisperse latices in a reproducible manner. The latices appear to be stabilised mainly by sulphonate groups which titrate conductometrically as strong acid. There is also a small number of phosphate groups present, as well as a considerable number of hydroxyl groups. The sulphonate groups are stable to hydrolysis.

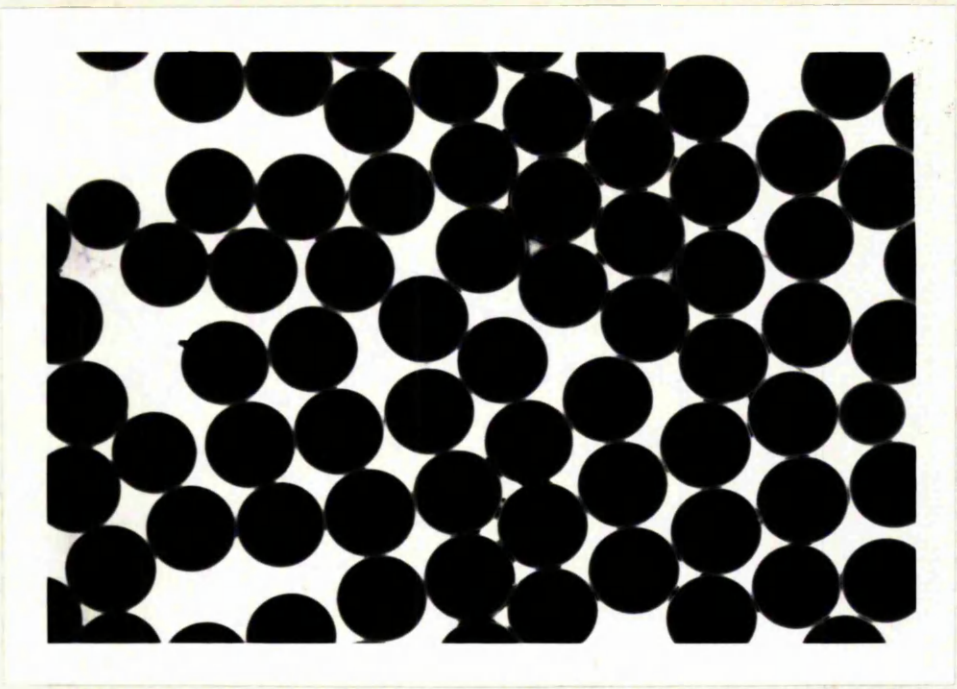

PLATE 3

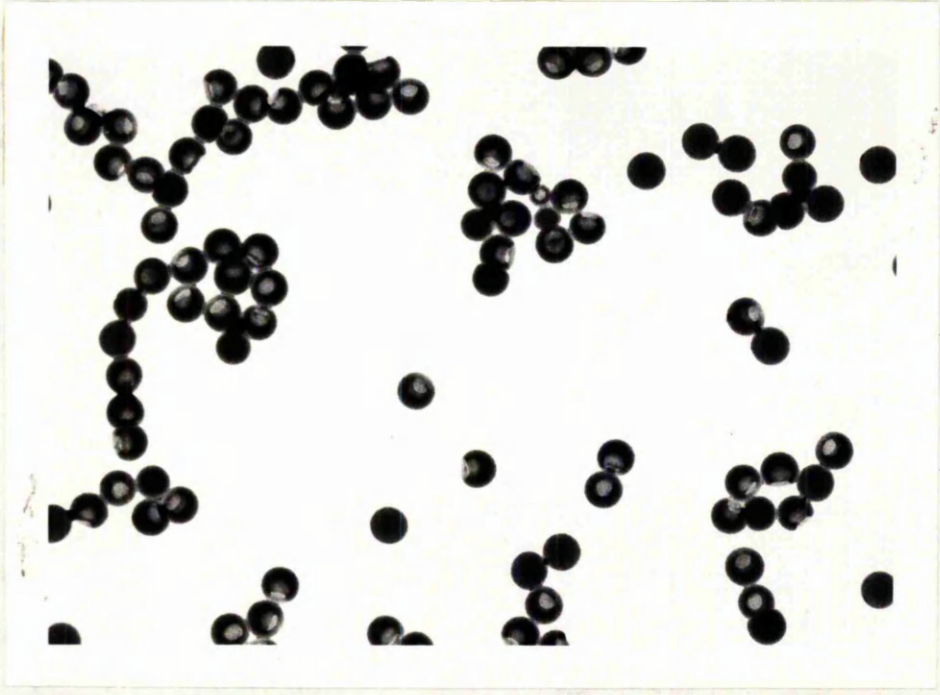

PLATE 4

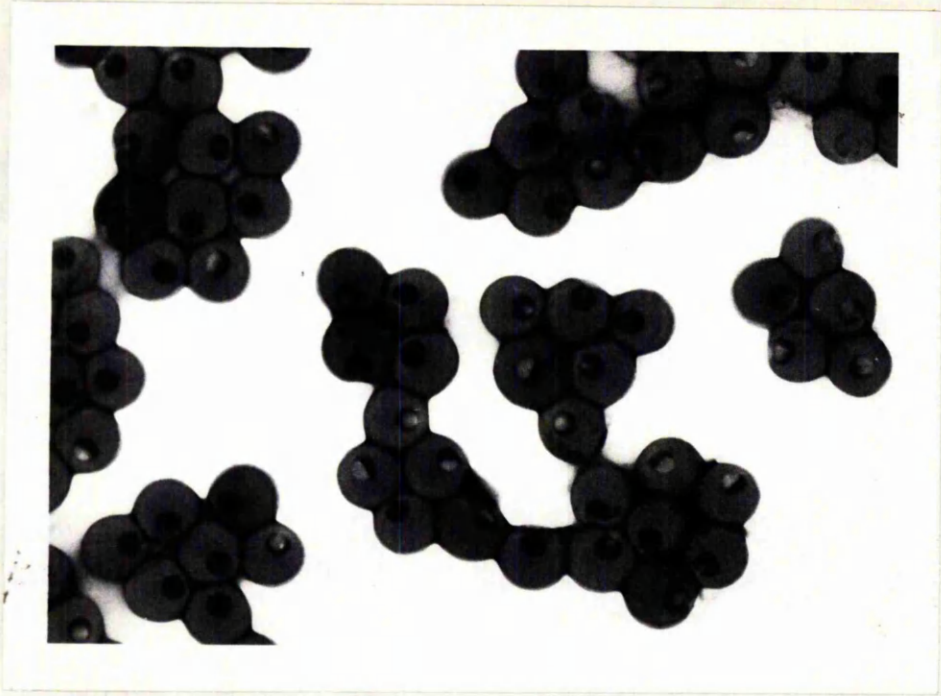

PLATE 5

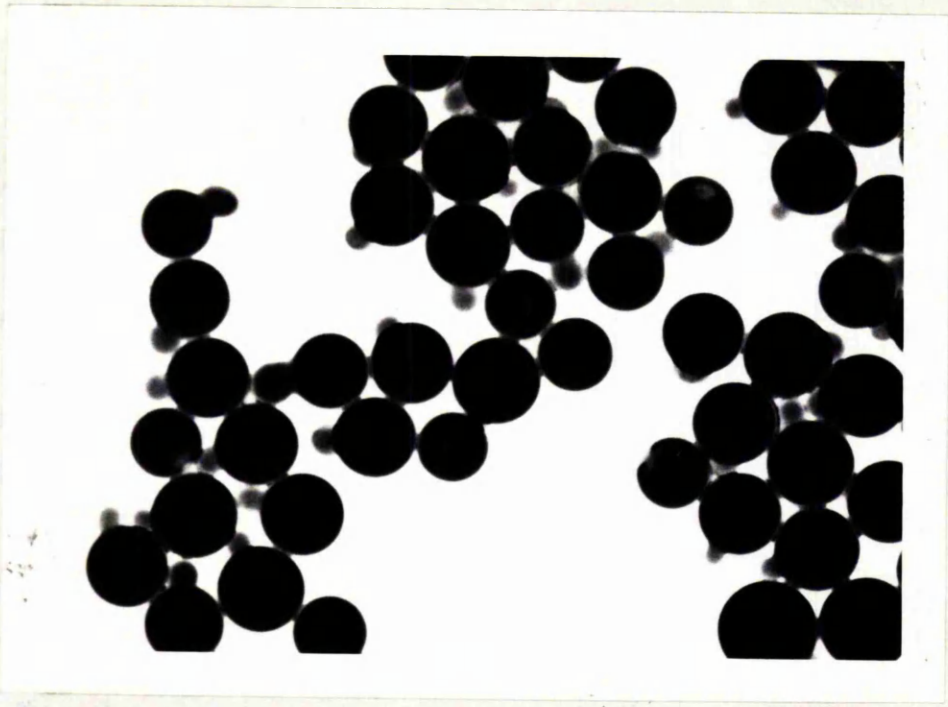

PLATE 6

CHAPTER V

A. ANOMALOUS PARTICLES.

1) DESCRIPTION. The technique of electron microscopy has been used extensively during the course of this work, and from the study of several thousand electron micrographs of latices produced and treated in various ways, it was found that the different particle shapes and electron density gradients observed could be divided into several types.

a) Normal particles (Plates 1,2,3): these appeared completely spherical on the micrographs and, depending on the size of the particles and the beam intensity used in their examination, appeared either uniformly black (low beam intensity and/or large particles) or had a steadily increasing electron density gradient from the periphery to the centre of the particle (high beam intensity and/or small particles).

b) Anomalous particles: these did not exhibit a uniform electron density and/or were not spherical. The loss of sphericity occurred in isolation and was not due to the distortion produced upon exposure to the electron beam of close-packed easily deformed 'normal' particles, which tend to flow together with subsequent loss of sphericity. Several types of anomalous particles have been observed during this work.

i) Anomalous particles type A (Plates 4,13): these appeared almost completely spherical, but exhibited within them a single discrete region of low electron density which was not in accord with the change in electron density observed through 'normal' particles. The region appeared to have an 'inkwell shape', i.e. a narrow neck and wide body.

ii) Anomalous particles type B (Plate 5): these particles were very similar to type A, but had associated with the region of low electron density a region of high electron density, much darker than the rest of the particle.

PLATE 7

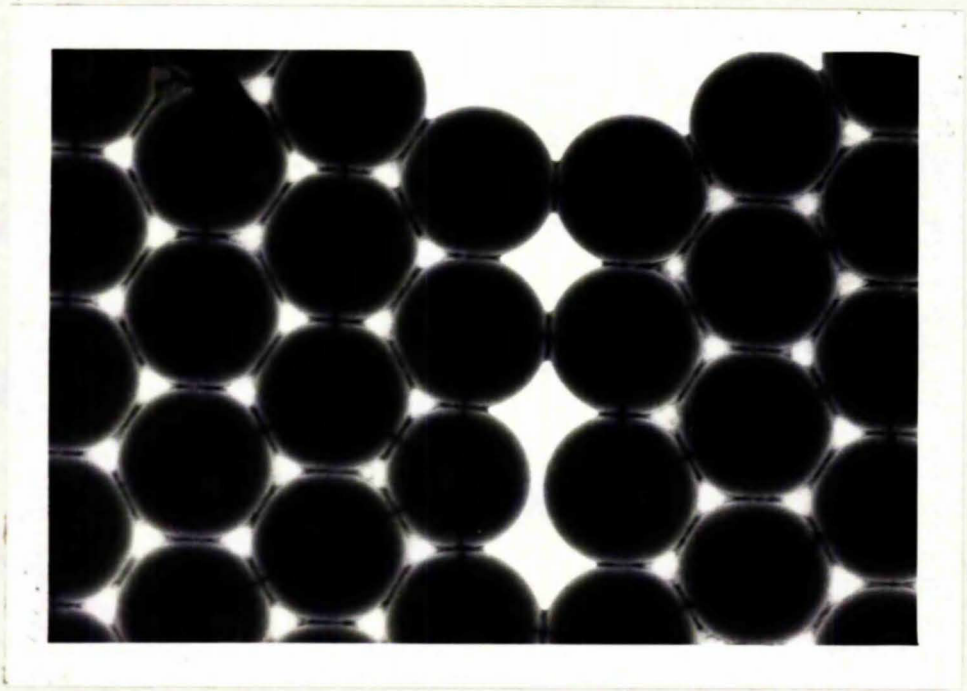

PLATE 8

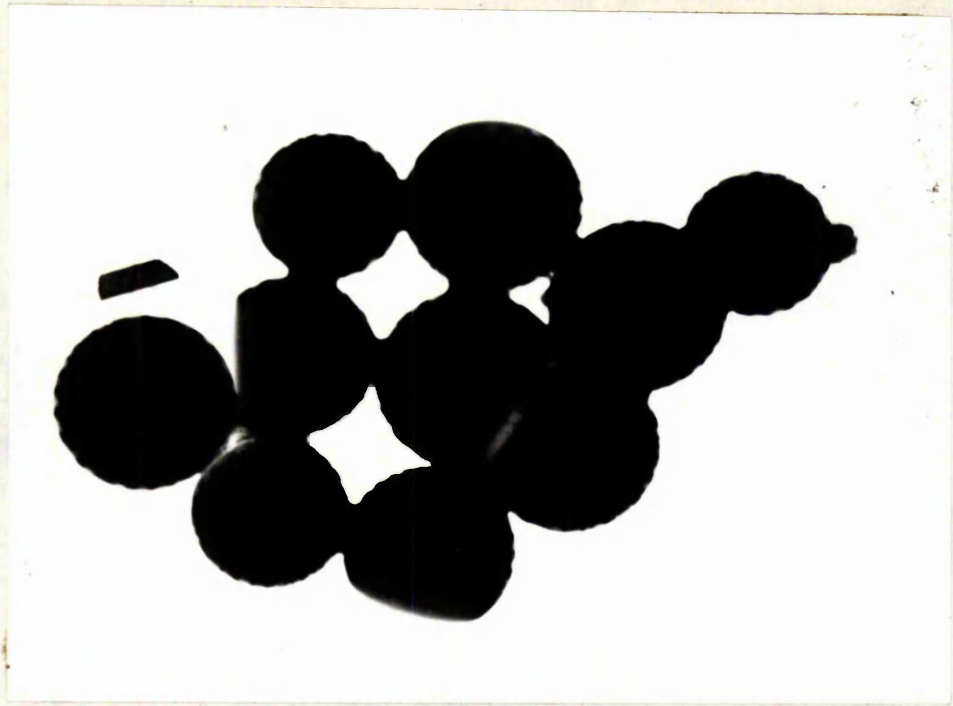

PLATE 9

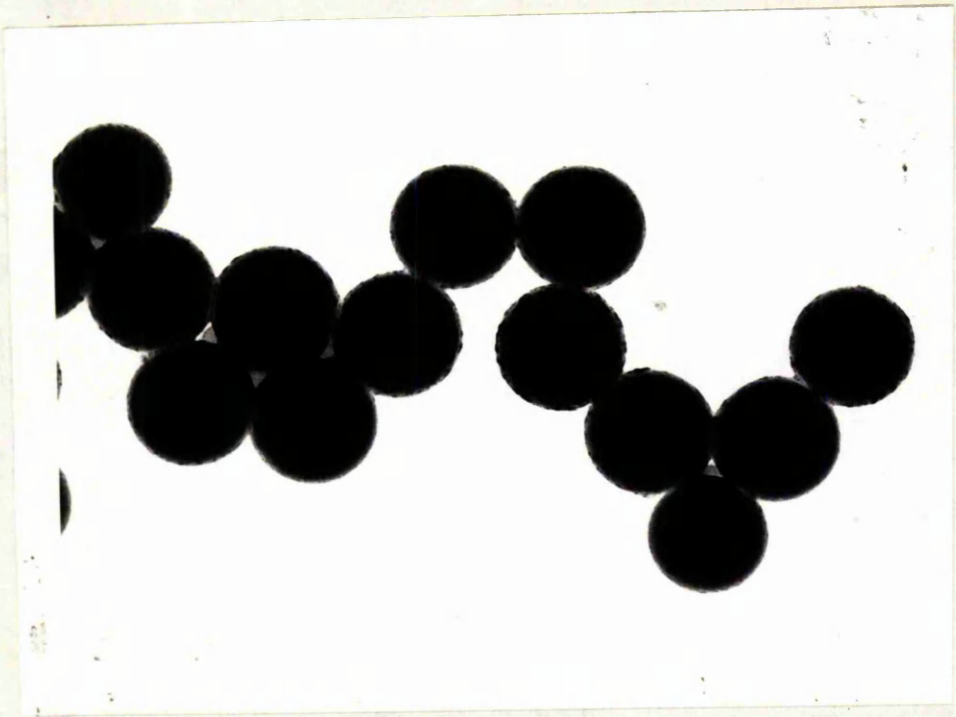

PLATE 10

iii) Anomalous particles type C (Plate 6): these particles exhibited a practically uniform electron density gradient, but had a single spherical or near spherical protruberance on the surface.

iv) Anomalous particles type D (Plate 7): these particles exhibited gross deviations from spherical shape and/or had very large low electron dense regions. The particles appeared either as spheres which had been roughly truncated or as 'shell-like' structures.

v) Anomalous particles type E (Plate 8): these were spherical particles which contained within them a large number of small discrete regions of low electron density.

vi) Anomalous particles type F (Plate 9): these particles appeared, when viewed under the T.E.M., to have a rough spherical outline and to contain a large number of regions of low electron density.

By far the most common in occurrence were types, A,B and C which appeared to be different manifestations of the same phenomena; of these A was the most common. Particles of type D and E were observed less frequently and particles of type F only once.

vii) Another phenomenon often observed was the presence of interparticle bridges (Plates 8,11,12) which appeared as more electron dense regions at the points of contact of the particles either with each other or with the support film. It is likely that these bridges were formed during the drying down of the sample prior to electron microscope examination and, as they were usually observed in undialysed samples it is probable that they were due to the presence of electrolyte.

2) OCCURRENCE. Anomalous particles were usually observed during multi-sampled reactions. However, they were also observed in reactions which had been allowed to proceed for twenty four hours or longer, but which had not achieved maximum conversion. Their appearance during multi-sampled

runs did not affect the sphericity of samples taken at maximum conversion, these particles always appeared normal.

a) Type A: particles of this type were first observed by Cox et al (120) during an electron microscope study of a seeded polystyrene growth process and have been observed during this work (121,122) in all the polystyrene growth processes studied. The presence of these particles has also been confirmed by both Pelton (249) and Ottewill (250). The extent of their occurrence, i.e. the number of samples from a reaction exhibiting the phenomena, varied from reaction to reaction. They were usually observed after about 15 minutes of reaction at 343 K and remained until approximately 50% conversion. The size of the region varied throughout the reaction, (Table 17).

TABLE 17

VARIATION IN THE DIAMETER OF THE LOW ELECTRON DENSE REGION DURING REACTION FOR LATICES 34B, 35A AND 142

Latex sample	Reaction Time (min)	Particle diameter (nm)	Void* diameter (nm)	% Conversion
34B3	30	114	44	0.6
34B4	55	174	93	1.8
34B5	85	208	114	4.4
34B7	185	337	113	17.6
34B8	240	394	121	27.5
34B9	325	412	113	43.6
34B10	465	526	0	71.5
35A4	55	177	30	2.4
35A5	85	205	95	4.3
35A6	115	274	132	5.8
35A7	165	343	225	7.2
35A8	235	560	212	11.3
35A9	295	596	281	19.5
35A10	355	721	271	27.43
35A11	415	790	255	39.7
35A12	475	897	219	41.0
35A13	560	976	104	55.3
35A15	740	1082	0	96.0
142/2	15	70	25	0.8
142/3	30	93	37	1.5
142/4	60	150	52	3.3
142/5	112	209	80	5.8
142/6	175	262	115	12.8
142/7	232	325	99	21.2
142/8	292	365	99	32.3
142/9	342	412	48	47.6
142/10	1440	504	0	90.64

*The diameter was determined by measuring the maximum dimension of the low electron dense region. About 70 were measured for each determination and the maximum variation in any one sample was approximately 20%.

b) Type B: these were always observed in conjunction with Type A, and usually appeared after ~ 25% conversion, they had always disappeared prior to the disappearance of particles of Type A.

c) Type C: these particles were always associated with Type A and were usually observed during the early stages of reaction (up to 20% conversion).

d) Type D: these particles were always preceeded by Type A and were usually observed at temperatures < 333 K (135) although when observed in this work the reaction was at 343 K.

e) Type E: these particles were observed once in the final sample of a peroxydiphosphate initiated latex (latex 135, see Chapter IV) and several times during the polymerisation of vinyl toluene.

f) Type F: these were produced during a styrene emulsion polymerisation initiated by persulphate in the presence of iron (see Chapter IV).

A factor common to the observation of all these types was that the particles were removed from a system containing excess monomer.

3) PRELIMINARY DISCUSSION OF T.E.M. DATA. Several other workers have reported the presence of distorted particles. Rupar and Mitchell (251) reported a range of different effects attributable to loss of monomer from particles under the electron beam, such as gross particle distortion, particle/particle coalescence and inversion effects (water-in-oil to oil-in-water at high monomer concentrations). The oil-in-water inversion at high solids content (> 10%) resulted in encapsulation of water which was subsequently lost upon evacuation. However, the anomalous particles produced during this work were not similar to these. Bradford and Vanderhoff (114) have reported the

presence of non spherical particles during seeded growth processes, similar to Type C in shape. However, they were not associated with particles of Type A, and they attributed their formation to insufficient time being allowed for the monomer to swell the polymer before initiation.

The formation of anomalous particles appears to be a phenomenon isolated to each particle and not caused by the break up of clusters. Also, the type of phenomenon exhibited appears to depend upon the reaction conditions and the percentage conversion. It is unlikely that exposure to the electron beam was the cause of formation since:-

a) They were not isolated to one reaction nor common to all, and in samples exhibiting anomalous particles about 10% of the particles remained unaffected.

b) The size of the electron dense region varied with sample time.

c) The particles did not distort under the electron beam, even after prolonged exposure (30 minutes at 80 kV accelerating potential and 6 μA beam current).

d) There was no evidence on the electron micrographs of extruded polymer which might have been expected if exposure of the low electron dense regions had occurred in the electron beam. Hence it would appear that the phenomenon had already manifested itself prior to exposure to the electron beam. Study of the electron micrographs themselves only gives an indication to the causes of formation of the lower and higher electron dense regions.

The presence of a low electron dense region within a particle is obviously associated with a region containing either material of lower electron density than the surrounding polymer, or to the presence of a void within the particle. The electron density of a sample depends on both its atomic weight and its thickness. Hence it is unlikely that a discrete region of either water or monomer would produce such a pronounced effect. It would thus appear

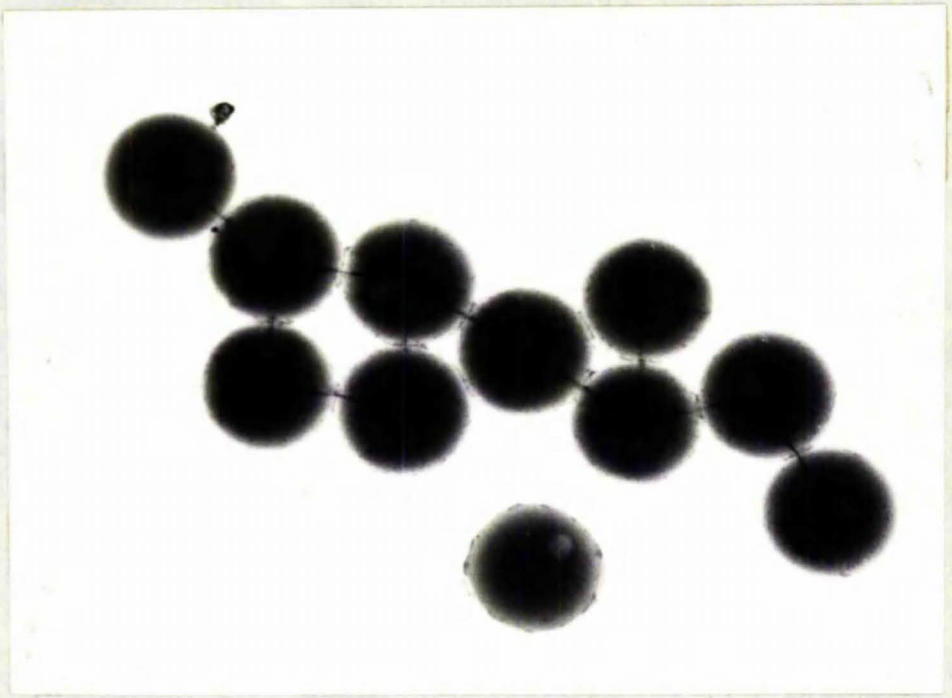

PLATE 11

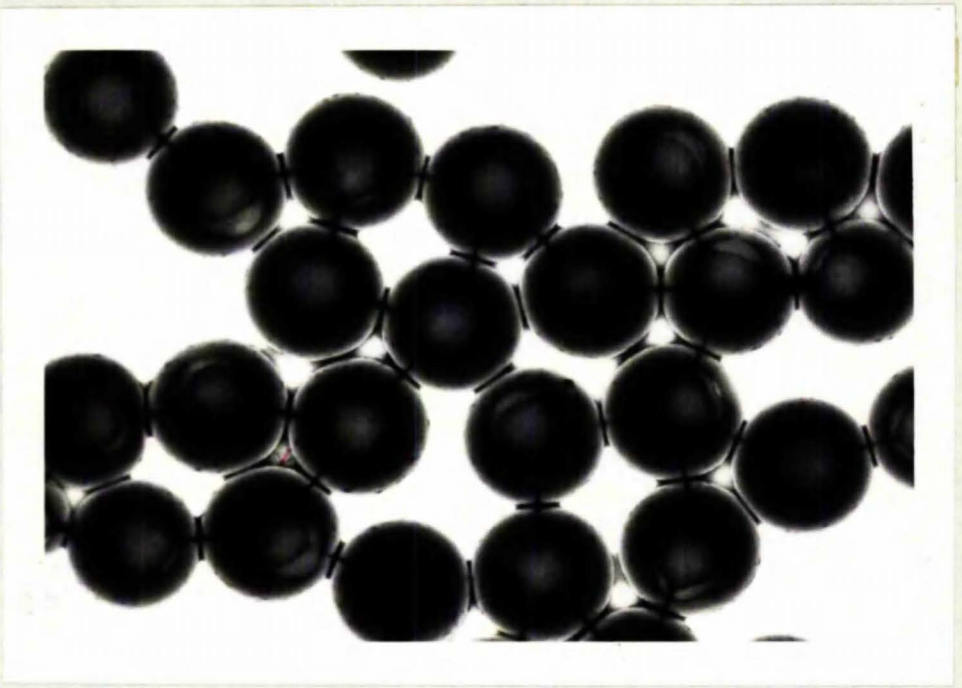

PLATE 12

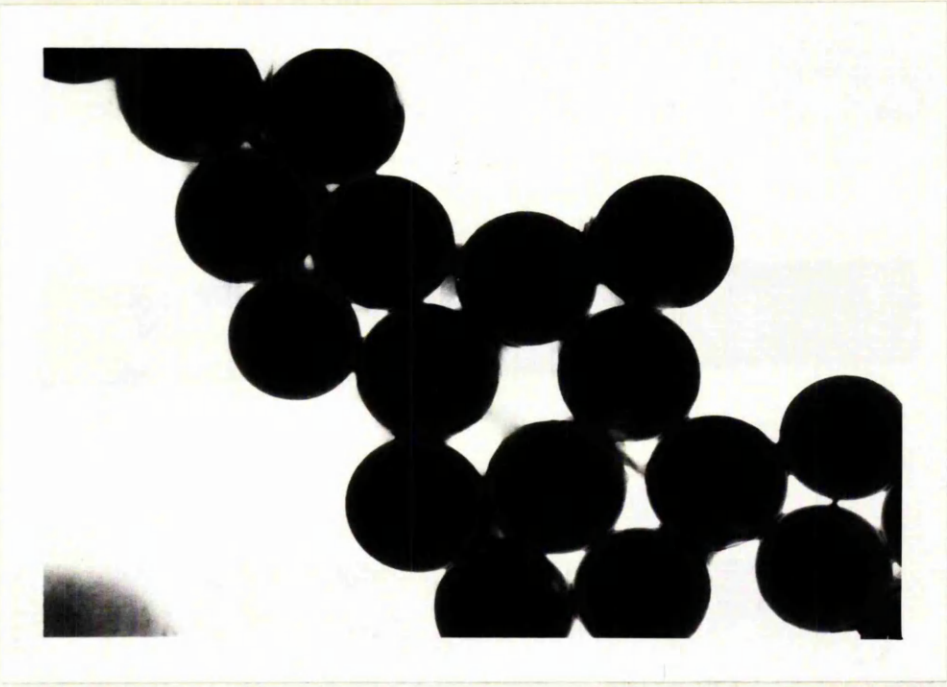

PLATE 13

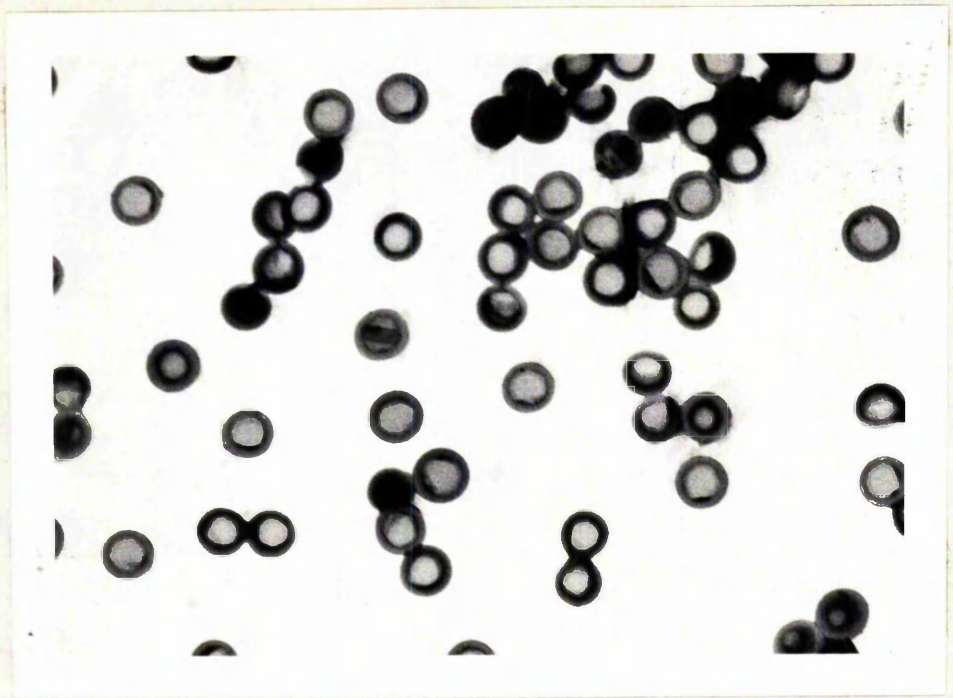

PLATE 14

that the low electron dense regions are due to voids within the particles. These voids would be created by exposure of the sample to vacuum prior to electron microscopy and the volatile material removed from the particle would be either water or monomer. No plausible mechanism is apparent for the inclusion of water into the hydrophobic polymer particles during polymerisation, unless at some stage a non-uniform contraction of the particle had occurred. However, even if a latex particle totally swollen with monomer (ca. 5M) were to have all this monomer polymerised then the contraction caused by the density change upon conversion of monomer to polymer would not be greater than 5% of the swollen volume. Some of the voids were ~ 16% of the total particle volume. Formation by removal of monomer (and perhaps low molecular weight polymer) from the particles upon evacuation is more feasable.

Regions of higher electron density can only be due to the presence of foreign material within the particles, the most likely being electrolyte. However, by consideration of the above and from electron microscopy data alone it appears difficult to explain the presence of electrolyte within the particles. In order to determine the cause of this and the other anomalies, the following series of experiments were carried out.

4) EXPERIMENTAL:

a) Effect of Steam Stripping. An undialysed sample of latex 136, produced using potassium peroxydiphosphate initiator, and not initially exhibiting these regions (Plate 10) was steam stripped and re-examined in the electron microscope. It was found that although the particle diameter remained the same (486 nm), the particles now exhibited anomalous regions within them (Plate 11). This reaction had only proceeded to 7% conversion and hence there were large amounts of monomer present within the particles; steam stripping has been shown to remove this

and any other volatile organic material (see Chapter III) and hence act to expose the region. It is surprising that the initial particles did not appear to exhibit these regions, since evacuation of the sample and subsequent exposure to the electron beam would remove most of the monomer from the particle. This appears to have been the case since both samples were the same size. However, comparison of Plates 10 and 11 , indicates that a higher beam intensity was used for the examination of the steam stripped sample, thus revealing more internal detail. This lack of internal detail coupled with a small anomalous region could be responsible for it not being observed initially.

b) Effect of Isooctane Extraction. An undialysed sample of 136 was isooctane extracted by shaking with isooctane for 24 hours. T.E.M. examination of the separated latex layer showed the presence of a large region of low electron density within each particle; the particle diameter remaining unchanged (486 nm). The extent of these regions was larger than those exposed by steam stripping. Isooctane extraction resulted in the removal of both monomer and low molecular weight material (~1000, see Chapter VI) from latex particles, whereas steam stripping only removed monomer and other volatile material. It thus appears that this low molecular weight material is concentrated within a particular region of the particle (Plate 12).

c) Effect of Stirring a Latex with Monomer. A sample of latex 1B (extensively dialysed), initially not exhibiting anomalous regions (Plate 3), was stirred under styrene monomer for 3 days. Re-examination of the latex with the T.E.M. showed the presence of anomalous regions within the particles (Plate 13). This indicates that the presence of these regions is intimately associated with the particles having been in contact with excess monomer. However, it is unlikely that removal of monomer evenly distributed throughout the particle would result in the

collapse of the particle at a single point. It seems more likely that it would result in an even contraction of the diameter. Samples taken early during polymerisations of styrene in the presence of soap (which were presumably saturated with monomer) did not exhibit these regions (83). This was also the case with monomer saturated samples of methyl methacrylate and vinyl acetate (135). Krieger et al (252), in a study of the kinetics of emulsion polymerisation of the sodium salt of styrene sulphonic acid, did not observe the presence of anomalous regions, neither did Williams and Bobalek (86) in their electron microscope studies of the emulsion polymerisation of styrene in the presence of emulsifier.

d) Effect of γ-irradiation.* If these anomalous regions were due to voids within the particles caused by the removal of monomer from the latex upon evacuation, then γ-irradiation of a sample should polymerise the monomer and the regions should disappear prior to electron microscope examination. To this end a sample of polystyrene latex 37B6 (Plate 14) was irradiated with γ-rays from a Co^{60} source (10^7 rads). The radiation dose estimated for 100% conversion was based on: (i) the pure styrene monomer concentration in 0.3μm diameter spheres, (ii) the oxygen level in monomer in approximate equilibrium with the very slow rate of ingress through the walls of the sphere relative to the dose rate employed.

*The author is indebted to Dr. P. Fydelor, R.M.C.S. Shrivenham, Wiltshire, U.K., for this part of the work.

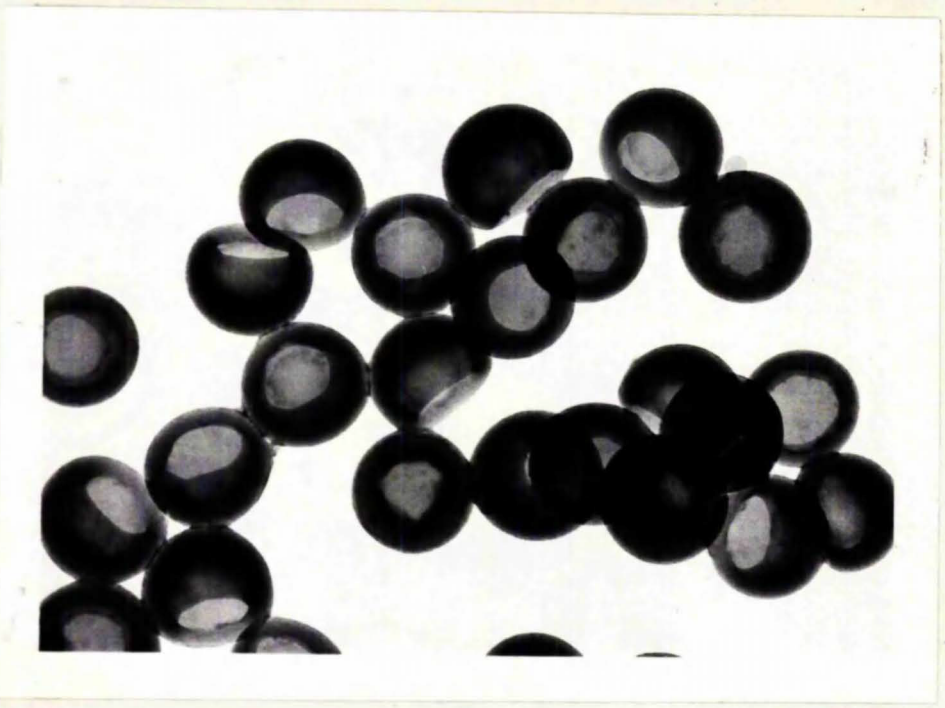

PLATE 15

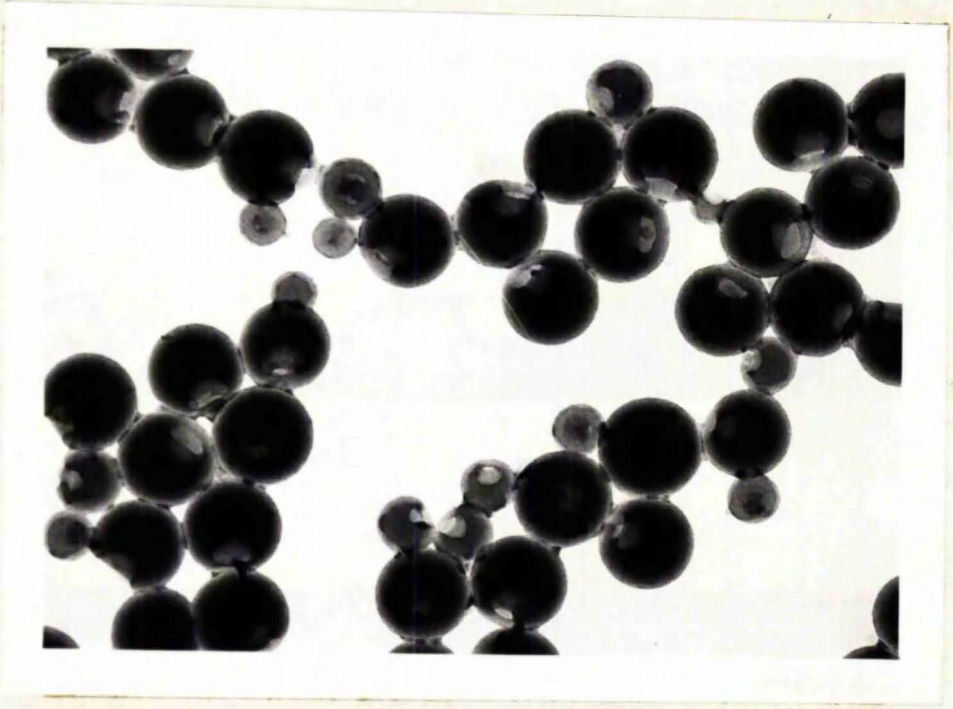

PLATE 16

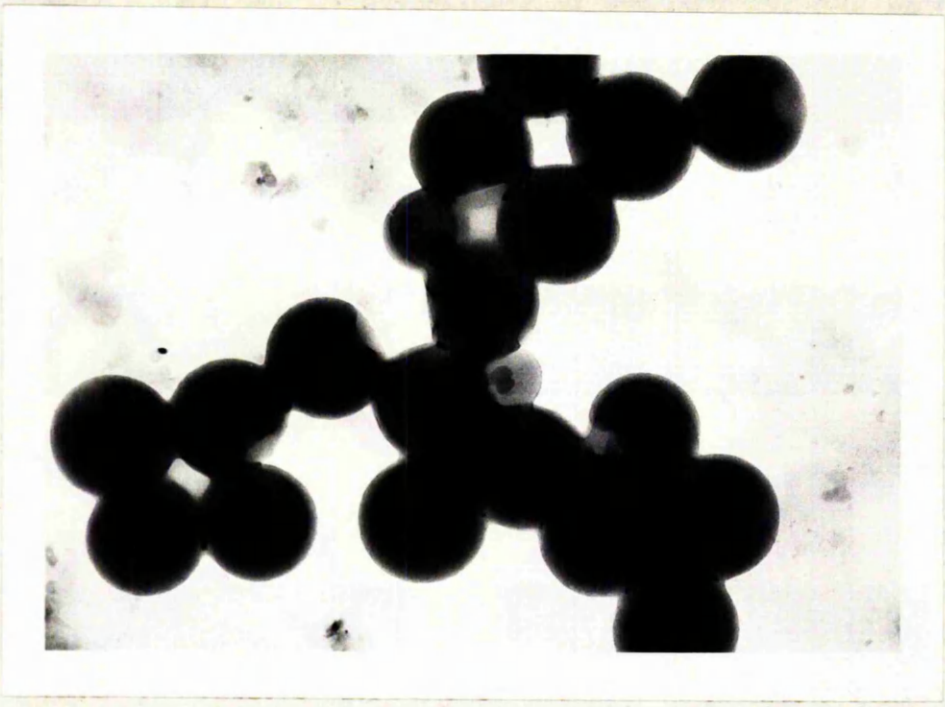

PLATE 17

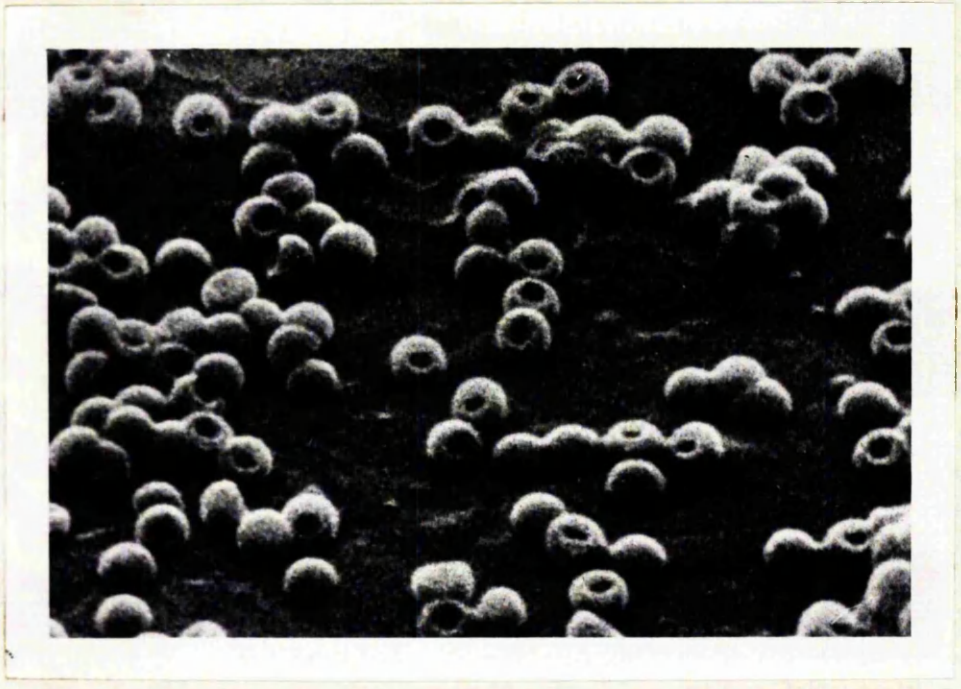

PLATE 18

Examination of the irradiated particles in the T.E.M. showed that the particles still exhibited voids (Plate 15). Although the particles had shrunk by about 6%, the size of the region was about the same as that recorded before irradiation. Thus, it would seem that there was no 'in-situ' monomer present within the latex sample before irradiation. Its absence may have been due to migration out of the particle into the water phase either on storage (nine months) or upon dilution prior to irradiation. Dilution (10^2 - 10^3 times) for irradiation or T.E.M. examination would lead to the monomer concentration within the water phase decreasing by an equivalent factor, whilst that within the particles remained constant. Thus, monomer would be expected to migrate from the particle into the aqueous phase until equilibrium was restored.

d) Effect of Added Electrolyte. It was thought that the more electron dense regions present in some samples (Plate 5) were due to the presence of electrolyte within the voids. If monomer diffused out of the region upon dilution and standing then presumably it was replaced by water. Hence, when the sample was dried down during electron microscope grid preparation, electrolyte could be deposited within the void. In order to test this hypothesis a sample of latex 285 showing only anomalous regions of Type A (Plate 16) was isooctane extracted for 24 hours in order to ensure exposure of these regions whilst in suspension. Electrolyte in the form of potassium persulphate was then added to the sample at a concentration similar to that present during a polymerisation. A sample was then prepared for electron microscopy in the usual way. Upon examination the sample was found to contain particles showing both anomalous regions Type A and B (Plate 17).

The presence of Type B particles was not noticed in all samples, and seemed to occur more frequently in early

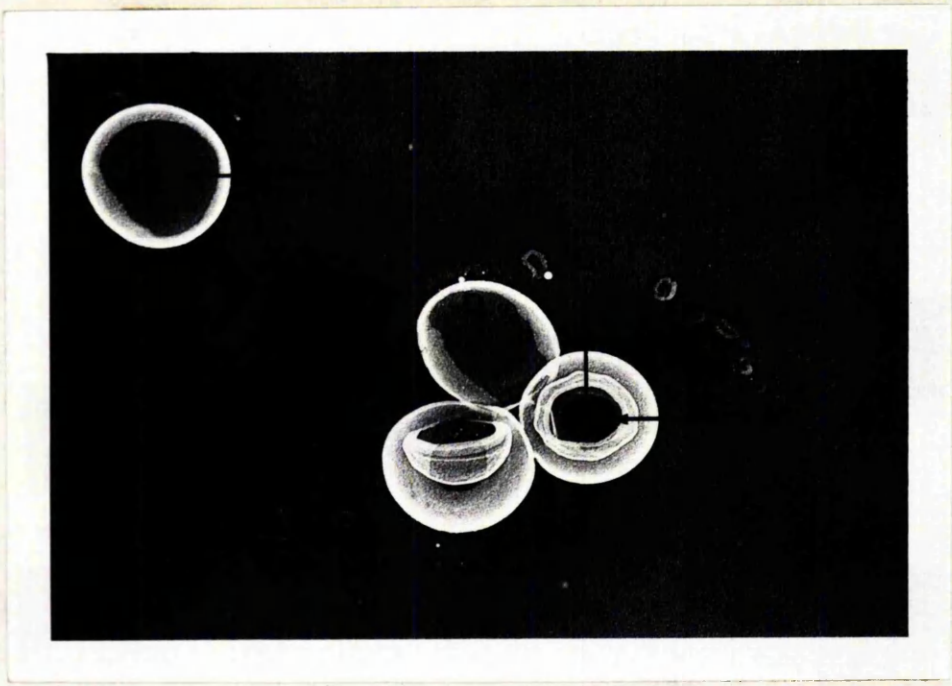

PLATE 19

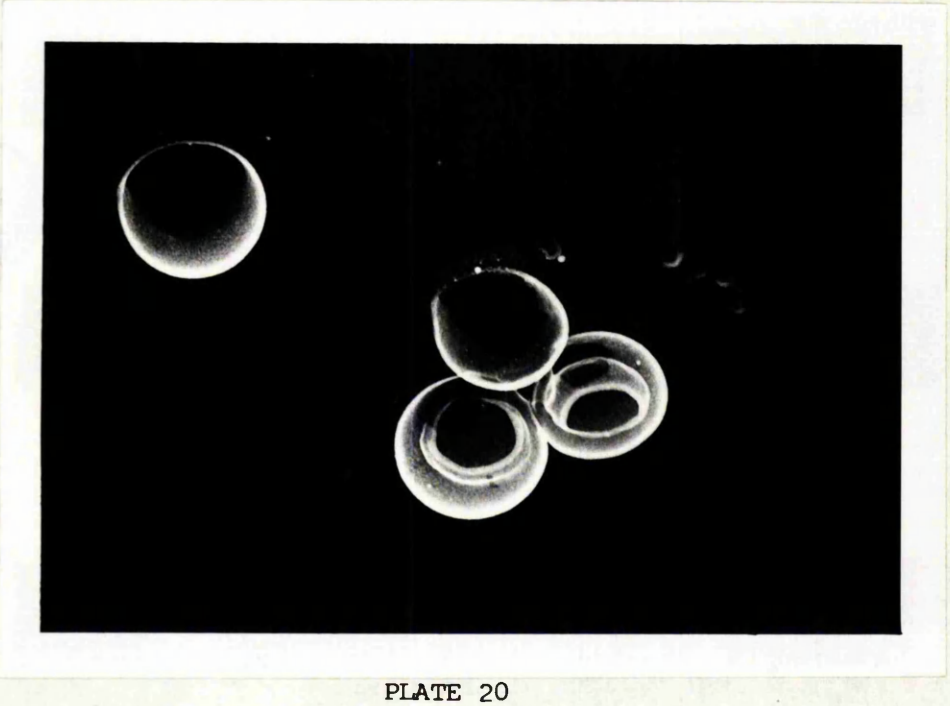

PLATE 20

samples presumably due to: i) variation in dilution of samples before electron microscopy, ii) differences in thickness of the polymer shell surrounding the anomalous region; the thicker the shell then the greater the length of time taken for the monomer to diffuse through it into the water phase, iii) the relative difference in electron density between small and large particles. The large particles would appear much darker than small particles and hence the presence of electrolyte within the voids would be more difficult to observe.

e) Scanning Electron Microscopy (S.E.M.). S.E.M. was used in order to obtain a better understanding of the shapes of the regions. S.E.M. data (Plate 18) supported the T.E.M. data very closely. It also confirmed that the anomalous regions were indeed due to the presence of single voids within the particles, (the slight flattening observed was due to the harsher conditions prevalent in the S.E.M.).

f) Carbon Replication. T.E.M. micrographs of carbon replicas of anomalous particles were taken at both 0° and 45° tilt (Plates 19,20) to aid in interpretation of the particle shape. The small central (dark) region (A) is the area of contact of the particle with the support substrate. This is much smaller than the dark region (boundry D) in the particles arrowed 1, but can be explained by virtue of the fact that these two particles were sitting on the substrate 'void down' before carbon coating. Thus, in this case the void was not replicated. Information on the shape can also be obtained by examining the density of the various regions on the micrograph using the density of the surrounding carbon film as an indication of the number of walls being viewed. For example, with reference to Fig. 19 , only one thickness of carbon is present at F, whereas at E there are three thicknesses (at a tangent through two wall thicknesses and support at 90°).

Multiple wall thicknesses are present which show the

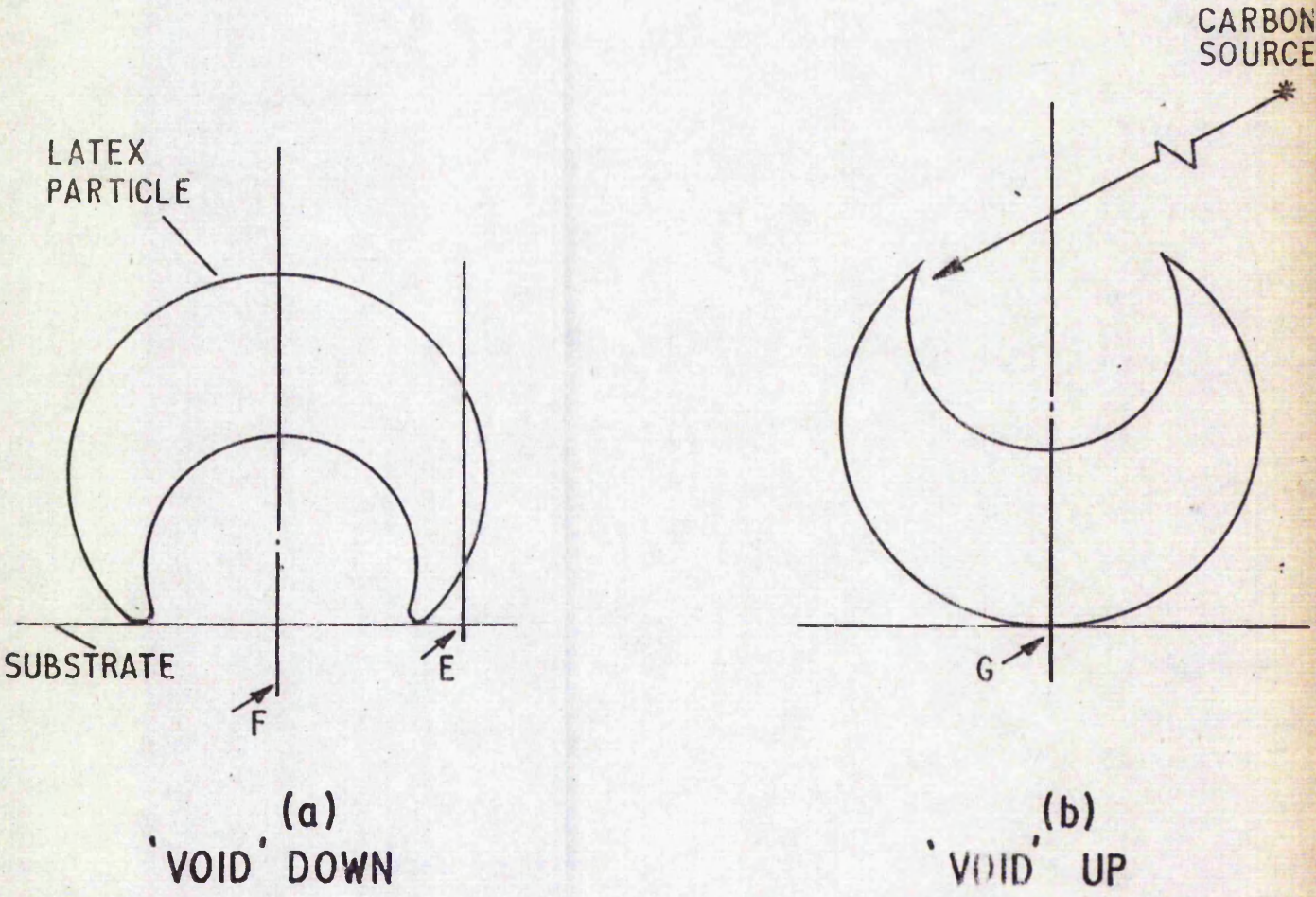

FIG. 19. CARBON REPLICATION OF ANOMALOUS PARTICLE

shape and form of the void. Considering area G (area of contact Fig. 19 b), one would expect to see a single thickness film at this position corresponding to the bottom of the depression. However, this is not the case, and is probably due to the relative geometry between the carbon source and the particles, such that very little carbon was deposited within the void. Carbon replication shows that the void is hemispherical in shape.

g) Nitrogen Gas Adsorption. A series of nitrogen adsorption isotherms was carried out on Freeze-dried samples of latex removed from reaction 34B at various times, in order to determine the existence of voids within the particles. The results are summarised in Table 18 and Figs 20,21 .

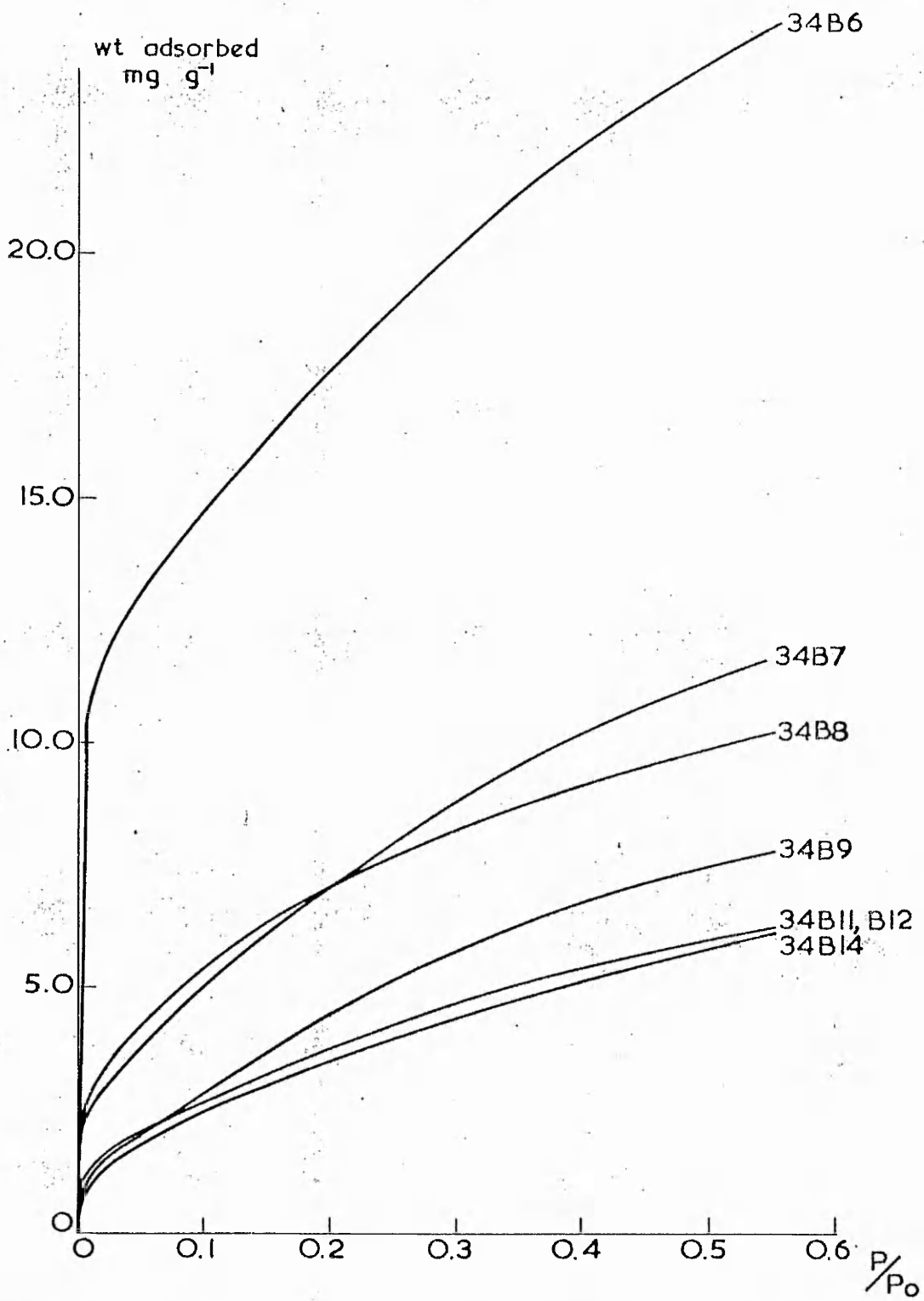

NITROGEN ADSORPTION ISOTHERMS ON 34B SERIES

FIG.20.

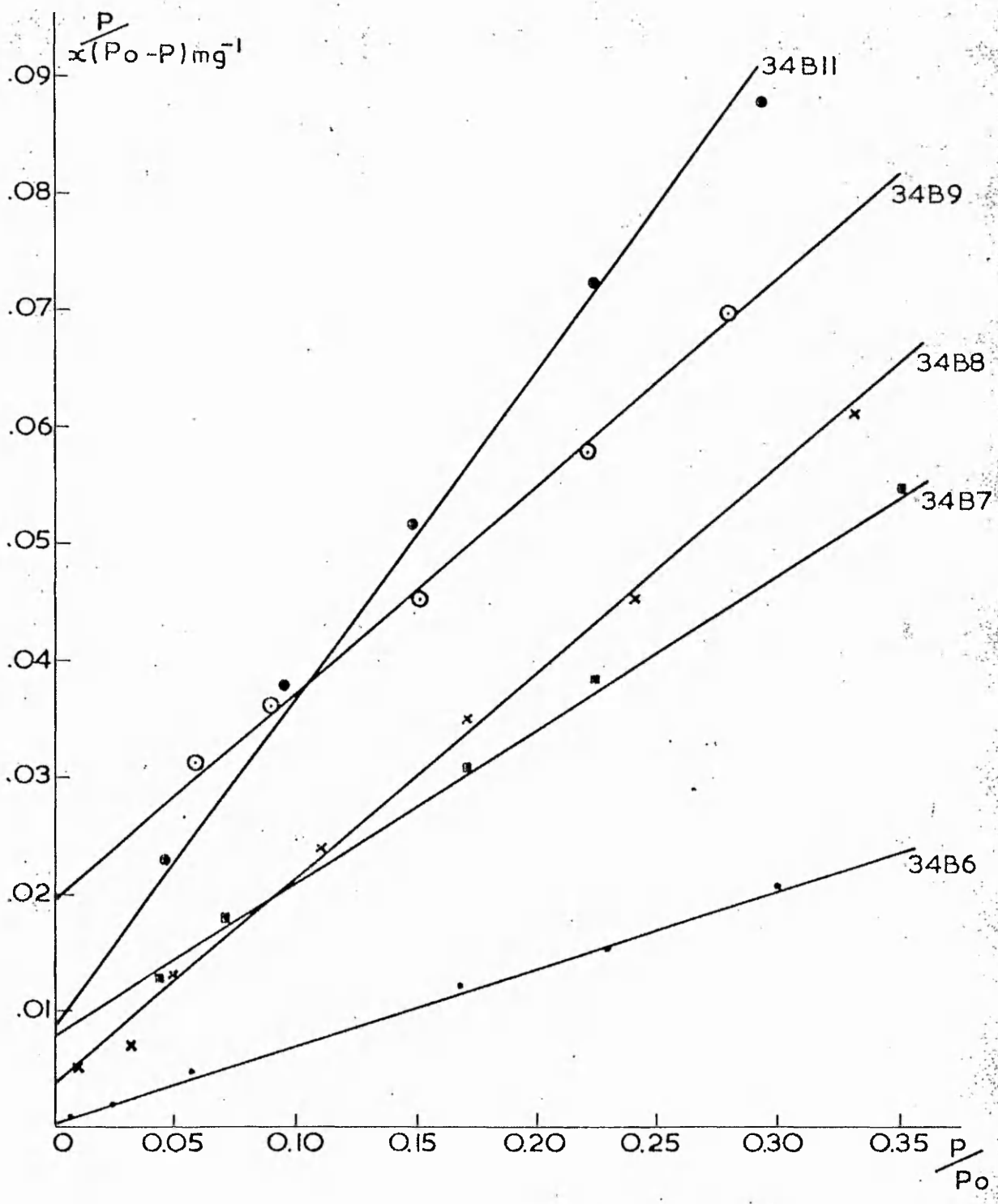

B.E.T. PLOTS FOR NITROGEN ADSORPTION ISOTHERMS ON 34B SERIES

FIG.21.

TABLE 18

a) COMPARISON OF ELECTRON MICROSCOPE (T.E.M.) SURFACE AREAS WITH B.E.T. SURFACE AREAS.

Sample	Particle diameter (nm)	Void diameter (nm)	T.E.M. S.A(M^2g^{-1})	B.E.T. S.A(M^2g^{-1})	$\frac{B.E.T.S.A.-T.E.M.S.A.}{T.E.M.S.A.} \times 100\%$
34B6	244	-	23.4*	50.9	118
34B7	337	113	16.9*	26.0	54
34B8	394	121	14.4*	19.4	35
34B9	412	113	13.9*	16.8	21
34B11	592	-	9.7	11.4	18
34B12	592	-	9.7	11.4	18
34B14	596	-	9.6	10.2	6

* calculated assuming spherical particles with no voids.

18 b) COMPARISON OF T.E.M. AND B.E.T. SURFACE AREAS TAKING INTO ACCOUNT THE PRESENCE OF THE VOID.

Sample	T.E.M.□ S.A(M^2g^{-1})	B.E.T. S.A(M^2g^{-1})	$\frac{\text{B.E.T.S.A.-T.E.M.S.A.}}{\text{T.E.M.S.A.}} \times 100\%$
34B7	17.7	26.0	47
34B8	15.0	19.4	29
34B9	14.3	16.8	17

□Electron microscope surface area calculated from the number of particles per gram and the available surface area per particle, when a hemispherical void is present.
Number of particles g^{-1}:

$$\frac{1}{\frac{1}{3}\pi\rho\,(4R^3 - 2a^3 - (R-(R^2-a^2)^{\frac{1}{2}})^2(2R - (R^2-a^2)^{\frac{1}{2}})}$$

The surface area g^{-1}:

$$\frac{6(R^2 + a^2 + R\,(R^2 - a^2)^{\frac{1}{2}})}{\rho\,(4R^3-2a^3- (R- (R^2-a^2)^{\frac{1}{2}})^2(2R + (R^2-a^2)^{\frac{1}{2}})}$$

where R is the particle radius.
a is the void radius.
ρ is the polymer density.

It can be seen from the data that the earliest samples showed the greatest difference between the B.E.T. and the electron microscope surface areas. This increase is not due to the internal surface of the void (assuming it is smooth) as can be seen from Table 18 b. Sample 36B6 did not exhibit voids, even though samples 34B5 and 34B7 did. The reasons are probably the same as those given earlier for the untreated sample of 136.

5) DISCUSSION.

a) Evidence Against Formation by Exposure to the Electron Beam. From the experimental data it appears that the presence of these regions is not due to evaporation of monomer or particle distortion caused by exposure to the electron beam since:

i) Particles containing very small amounts of monomer prior to grid preparation (i.e. final samples) showed no distortion, even after prolonged exposure to the electron beam.

ii) A sample which had been γ-irradiated prior to T.E.M. examination still exhibited these regions, even though the amount of free monomer within the particles must have been practically zero. Similarly, steam stripping and iso-octane extraction, both of which would considerably reduce the amount of monomer present within the polymer, only had the effect of increasing the size of the region.

iii) Carbon replicas of anomalous particles indicated the presence of a void before exposure to the electron beam.

iv) The deposition of electrolyte within the voids must have occurred before exposure to the electron beam.

b) Evidence Against Formation During Grid Preparation of Samples Exhibiting an Homogenous Monomer Distribution.

It is possible that electron microscope grid preparation could result in their formation. As the sample dries on the grid, the tops of the particles would become exposed to the atmosphere first and evaporation of monomer, evenly distributed throughout the particle, through this small surface region could result in the formation of a depression. However, this appears unlikely since:

i) γ-irradiation, steam stripping and isooctane extraction would all result in there being almost no monomer present to evaporate away.

ii) Deposition of electrolyte within the void could only occur when the void itself was immersed in electrolyte solution.

iii) Carbon replication indicated that after drying down some of the particles were lying void down on the mica surface. Movement of the particles on the mica after drying down cannot account for this, since the presence of a void within a particle would alter the position of its centre of gravity such that if the particles were capable of moving, the void would tend to remain uppermost.

iv) It would be expected that an effect of this type would be apparent in other systems. However, neither polymethylmethacrylate, polyvinylacetate or polystyrene (prepared in the presence of emulsifier) latex samples, removed from reactions before 100% conversion exhibited these regions (83,86,135).

For the reasons given above it is unlikely that evacuation prior to electron microscopy of polystyrene latex particles would result in the formation of a single void if the monomer was evenly distributed throughout the particles.

c) Evidence for an Heterogenous Monomer Distribution within the Particles. The experimental data obtained from γ - irradiation, electrolyte deposition, steam stripping and isooctance extraction indicates that these voids can exist (filled with water) when the particles are still in suspension. The diffusion of monomer or other material out of the particle and into the water phase upon dilution would not be expected to result in the formation of a depression in the particle if this diffusion occurred over the whole of the surface area (i.e. if the monomer were evenly distributed throughout the particle). If the particle contained a discrete region of high monomer concentration then it is likely that diffusion of this monomer from the particle would occur through the thinnest part of the polymer shell separating it from the water phase and this would result in the formation of a cavity on one side of the particle, which would be filled with water.

Diffusion of monomer out of the particle would occur upon dilution in order to re-establish the equilibrium between the monomer concentration in the particle and that in the aqueous phase. The creation of a hemispherical void within the particle would result in an increase in the total surface area of the particle which would be accompanied by an increase in the free-energy of the system. However, this would be counteracted by a lowering of energy due to both the overall decrease in surface area (due to

diffusion of monomer out of the polymer constituting the rest of the particle) and the energy loss on regaining equilibrium. The rate of diffusion of monomer out of the anomalous region would be dependent on the thickness of the polymer shell separating the anomalous region from the water phase. Hence, depending upon both the dilution and the thickness of the polymer shell, the particles upon grid preparation would contain a discrete region of either water or monomer.

The presence of a water-filled void in solution also supports the view that the region of high monomer concentration is not in the centre of the particle, since if this were the case diffusion out of the particle would occur over the whole surface area, resulting in a general contraction, and not in the formation of a single depression.

The thickness of the shell also appears to be important in that if it is too thick then removal of monomer upon evacuation could result in the formation of a protruberance on the particle surface (Plate 6). Rapid removal of monomer from a monomer-rich region would result in the rupture of the shell and it is likely that if the shell was thin, it would fall back into the cavity left by the monomer. If the shell were sufficiently thick then a permanent distortion might occur.

d) Possible Cause for an Heterogenous Monomer Distribution. It is generally accepted that there is an homogenous distribution of monomer throughout latex particles (formed during emulsion polymerisations in surfactant-added systems). Gardon (115) has shown that the diffusion of monomer to the particles is more rapid that its disappearance from the particles due to polymerisation. The assumption of monomer homogeneity, however, must be based on an assumption that even if the molecular weight is heterogenous ($\frac{\bar{M}w}{\bar{M}n} > 1$), the molecular weight of the material present is high. It is interesting here to consider the

equation relating to the swelling of latex particles by monomer:

$$RT\left(\text{as kl}_M \ln \Phi_M + \left(1 - \frac{1}{m}\right)\Phi_P + \chi\Phi_P^2 + \frac{2\bar{V}_M\gamma}{rRT}\right) = 0, \quad -- \ (9)$$

which upon rearrangement gives,

$$\text{as kl}_M \ln \Phi_M = -\left[\left(1 - \frac{1}{m}\right)\Phi_P + \chi\Phi_P^2 + \frac{2\bar{V}_M\gamma}{rRT}\right], \quad -- \ (132)$$

where $\Phi_M = 1 - \Phi_P$.

The effect of m, the degree of polymerisation, is usually discounted. Indeed, for molecular weights in the range 10^5 to 10^6, m is in the range 10^3 - 10^4. However, there is strong evidence for the presence of relatively large amounts of polymer of molecular weight ca. 1000 in samples taken early in the reaction (surfactant-free emulsion polymerisation) and this material is still present in final samples (refer Chapter VI and Figs 29-31). For material of molecular weight ca. 1000, m is about 10, and the term $\frac{1}{m}$ can no longer be neglected. The effect of a significant value of $\frac{1}{m}$ is to make the right hand side of equation 132 less negative and hence lead to an increase in Φ_M.

Isooctane is capable of extracting this low molecular weight material, and isooctane extraction of particles containing anomalous regions leads to an increase in the size of the regions, indicating that the low molecular weight polymer is associated with the regions. (The formation and importance of this low molecular weight material is discussed in Chapter VI).

e) Possible Explanation for the Absence of Anomalous Regions from some Samples. In a number of cases samples taken during polymerisation were found not to exhibit anomalous regions, even though samples taken immediately before and after them did. This indicates that either the monomer present within the region polymerised after sampling, or that the beam intensity used

in the electron microscope was not sufficient to reveal internal detail. Polymerisation of the region is unlikely since the reaction is effectively stopped once the sample is cooled and diluted (the half life for the decomposition of potassium persulphate is 10^6 minutes (87) at room temperature and would be even lower at 276 K - the temperature at which the electron microscope samples were stored). However, further polymerisation cannot be dismissed completely since any one of a number of extraneous effects could have caused further reaction, e.g. accidental exposure to direct sunlight; or the presence of some impurity either within the sampling pipette or sample bottle, or the water added to dilute the sample, which acted as an activator.

f) Possible Reasons for Variation in Size of the Region During Reaction. The growth of the particles is likely to be a surface reaction, as suggested by Napper (113), since the polymer chains are effectively anchored at the interface by the hydrophillic sulphate groups. Also during Interval II the main supply of monomer to the growing free radicals is from the water phase. A growing free radical can migrate through the particles by two mechanisms: the diffusion of the polymer chain itself, or the addition of monomer units. It would be thought that if the molecular weight of the chain is high then its rate of diffusion through the highly viscous medium (10^4 - 10^5 poise (1)) of a polymer particle would be slow. Thus, the prime cause of movement of the free radical through the particle would be by the addition of monomer units. The main supply of monomer is from the aqueous phase and hence the radical would be likely to remain near the surface. Thus, it may be expected that a pocket of high monomer concentration within the particles may well remain unpolymerised during Interval II of the reaction. As the amount of monomer entering the particle from the water phase decreases, then the monomer within the particles becomes the main source for further reaction with the result that

the anomalous region decreases in size and finally disappears.

g) Effect of the Anomalous Regions on the Particle Radius. It may be expected that the presence of a hemispherical void within the particle would result in the measured radius being incorrect, in that its use in volume calculations would not lead to the accurate volume of polymer in the particle, and a correction to R should be necessary. If a sphere of radius R is considered to contain a hemispherical void of radius a then the volume of polymer in the particle is equal to the original volume minus the volume of the void minus the volume of the cap of the void.

$$\text{Original volume} = \tfrac{4}{3}\ \pi\ R^3\ ,$$

$$\text{Volume of the void} = \tfrac{2}{3}\ \pi\ a^3\ ,$$

$$\text{Volume of the cap of the void} = \tfrac{1}{3}\ \pi\ (R-(R^2-a^2)^{\frac{1}{2}})^2\ (2R+(R^2-a^2)^{\frac{1}{2}})$$

Then the volume of polymer in the particle is:

$$\tfrac{1}{3}\ \pi\ (4R^3 - 2a^3-(R-(R^2-a^2)^{\frac{1}{2}})^2\ (2R+(R^2-a^2)^{\frac{1}{2}})$$

The radius of a spherical particle containing no voids which corresponds to this volume, R′, is thus:

$$R' = \frac{1}{4}\ \left[(4R^3 - 2a^3 - (R-(R^2-a^2)^{\frac{1}{2}})^2\ (2R + (R^2-a^2)^{\frac{1}{2}})\right]^{.333}\ .$$

If a theoretical example is considered of a particle of radius 1 containing a void with a radius equal to 1% to 75% of the particle radius, then differences in the observed and calculated radii are shown in Table 19 .

TABLE 19

DIFFERENCES IN OBSERVED AND CALCULATED PARTICLE RADIUS EXHIBITING VOIDS

R	a	R'	$\frac{R - R'}{R} \times 100\%$
1	.75	.893	10.7
1	.50	.974	2.6
1	.25	.997	0.3
1	.20	.999	0.1
1	.15	.999	0.1
1	.10	1	0
1	.05	1	0
1	.01	1	0

Even with a void with a = .75R, then the calculated radius is only 10.7% less than the measured radius, and with a = .5R, the difference is only 2.6%. No samples were found during kinetic runs to have a $>$ .6R, in fact the largest voids usually had a $\sim$.25R, indicating a difference between the calculated and observed radii of 0.3%, which is negligible when one considers that the standard deviation of the particles is usually $>$ 1%.

6) CONCLUSIONS

a) Mode of Formation of Anomalous Particles.

i) The formation of type A anomalous particles appears to be due to the presence of a discrete region within the particles containing monomer at a higher concentration than that distributed throughout the rest of the particle. The monomer within this region is capable of exchanging with water upon dilution, steam stripping or isooctane extraction. The existence of a low electron dense region within the particle is due to the presence of a hemispherical void formed by rapid evaporation of water or monomer out of the particle upon evacuation prior to electron microscopy.

ii) The formation of type B anomalous particles is due to

the deposition of electrolyte within the void, caused by the exchange of monomer originally present with water.

iii) The formation of type C anomalous particles is due to the evacuation of type A particles in which the monomer rich region is covered by a shell of polymer sufficiently thick that permanent distortion occurs upon rapid removal of the monomer.

iv) The formation of type D anomalous particles would appear to be a gross manifestation of type A behaviour. The fact that the reactions in which they were most commonly observed were carried out at a temperature < 333K suggests this, since according to Van der Hoff (67) the solubility of styrene in its polymer when in the form of a latex increases with decreasing temperature. As discussed previously with regards type A, it is unlikely that this phenomenon could occur through the evacuation of homogenously highly swelled particles.

v) Investigations were not carried out on the formation of type E anomalous particles. However, it would appear from the above discussion, that each low electron dense region is due to a void caused by loss of monomer from a region of high monomer concentration. It is interesting to note that particles of this type were usually observed with polyvinyltoluene latices, where it would be expected that the capability of the chains to move relative to each other would be hindered due to the methyl group on the benzene ring.

vi) No positive evidence exists for the mode of formation of type F anomalous particles. However, it is of note that: a) they are likely to consist of polymer of low molecular weight (refer Chapter IV) due to the very rapid initiation rate employed in their formation. (N.B. The low molecular weight polymer is not to be confused with that of molecular weight ca.1000 mentioned earlier). b) The micrographs could be interpreted in terms of 'particles' consisting of an agglomerated mass of smaller particles. The latter explanation seems the most likely.

vii) The existence within the particles of a region of high monomer concentration compared to that in the rest of the particle is probably due to the presence of polymer of molecular weight ~ 1000 in a discrete region.

Gel permeation chromatography (refer Chapter VI) showed that this material was present throughout the reaction. Indeed the formation of anomalous regions within latex particles otherwise not containing them, by exposure of the latex suspension to free monomer, indicates that the underlying cause for the formation of an heterogeneous monomer distribution throughout the particles is still present at the end of reaction and is not solely associated with the growth process.

b) A Possible Explanation for Monomer Heterogeneity.

The presence of an heterogenous monomer distribution within the particles is contrary to the accepted theory (115) of an homogenous distribution. The results of Williams et al (103-112), put forward to support the core-shell theory appear to be explainable in terms of an homogenous monomer distribution. However, several important points arise from the use of emulsifier-free systems:

i) The equilibrium swelling of the particle is determined mainly by the interfacial energy. In the case of a soap-containing system this is considerably decreased by the presence of emulsifier. However in soap-free systems the interfacial energy will be higher, hence it might be expected that the equilibrium volume fraction of monomer to polymer in these systems would be lower.

ii) It has recently been shown by Chung-li et al (175) that 'aged' latex particles (emulsifier-free) when exposed to monomer take a considerable time to swell, the rate appearing to increase as the amount of monomer imbibed increases. Further, the rate of swelling of freshly formed polymer was also slow, so slow in fact as to be unable to account for the rate of growth observed during seeded growth processes. To explain this Chung-li et al (175) postulated the continual formation of small

polymer nuclei, saturated with monomer, in the water phase which then underwent heterocoagulation with the seed particles.

iii) Another important fact is the presence of large amounts of low molecular weight material in the early samples, as will be discussed later (Chapter VI). This material probably arises as a direct consequence of the mode of particle nucleation. Upon coagulation of these initial nuclei and further growth, this low molecular weight material could either: a) diffuse throughout the whole particle, or b) remain as a distinct region within the particle. It it diffuses throughout the particle, then the reason for an heterogenous monomer distribution becomes unclear. However, if it remains together it will do so at one side of the growing particle since each of the chains will have a hydrophillic sulphate group at both ends. Thus, it is possible that the surface of the particle contains a region of high charge density compared to the rest of the particle. With regards imbibition of monomer this particular surface region would have two advantages over the rest of the particle surface:

a) The monomer would be expected to be slightly more soluble in a region containing a large amount of low molecular weight polymer.

b) Preferential swelling of this region due to monomer imbibition would be facilitated due to the high surface charge density and the associated lowering of the interfacial energy.

The presence of this region of high surface charge might also be expected to have consequences with regards the rate of entry of charged oligomeric radicals in that the rate of ingress of these radicals would be slower than over the rest of the particle surface due to the greater charge repulsion. Hence a subsurface region of relatively high monomer concentration could remain essentially unpolymerised until the supply of monomer to the growing particles through the water phase began to decrease.

CHAPTER VI

KINETIC STUDIES

A) Introduction.

Since the observation of Matsumoto and Ochi (173) that styrene and other monomers would undergo polymerisation in the absence of added emulsifier to produce stable monodisperse latices, a number of studies have been carried out upon these systems (140,141,170) to date, however, studies have been concerned solely with the variation of the final particle diameter with the reaction parameters such as temperature, background ionic strength etc. (141, 170), and with the surface characterisation of the latices produced (141, 153). In the case of styrene, no kinetic studies on the reaction have been reported. It might be anticipated that kinetic studies on these systems would be less complicated than in the presence of emulsifier, which it is known can affect the course of the reaction (117).

B) Reproducibility of Reactions.

For a system to be studied kinetically, it is necessary that the reaction be reproducible. In order to determine whether the emulsion polymerisation of styrene in the absence of added surfactant was a reproducible process, six identical small scale reactions were carried out. The diameters of the latices produced (final samples) were determined using electron microscopy and the surface charge densities determined by conductometric titration. In some cases the number of hydroxyl groups was also determined by the oxidation technique of Van den Hul and Vanderhoff (133). The results are summarised in Table 20.

TABLE 20

a) REPRODUCABILITY OF REACTIONS

Latex	Diameter (nm)	σ (%)	Conversion (%)	N (ml^{-1}) $x10^{-12}$	d (100%)* (nm)
15A	483	2	92.12	1.35	496
15B	474	1	93.45	1.44	485
16A	485	1	89.69	1.29	503
16B	470	1	91.20	1.45	484
17A	469	3	96.51	1.54	475
17B	482	2	89.01	1.31	501

*diameter at 100% conversion.

b) SURFACE CHARGE DENSITIES

Latex	Sulphate groups (μeq g^{-1})	Carboxyl groups (μeq g^{-1})	Surface Charge density (μC cm^{-2})	Hydroxyl groups (μeq g^{-1})
15A	2.84	4.72	6.16	-
15B	2.51	4.31	5.46	-
16A	2.97	4.84	6.40	5.08
16B	3.03	3.92	5.52	4.00
17A	2.61	3.84	5.11	-
17B	3.51	4.10	6.19	5.08

Monomer concentration = 0.870 moles l^{-1} .
Initiator concentration = 2.311 x 10^{-3} moles l^{-1} .
Temperature = 343 K.
Ionic strength = 6.933 x 10^{-3}.

It can be seen that the latices were very monodisperse and the final diameters and conversions of all six reactions were very similar. The average diameter was 477 nm, with no latex varying by more than 2% from this figure, demonstrating the highly reproducible nature of the polymerisation process (141,170). All the latices were found to have both strong ($-SO_4^-$) and weak ($-COO^-$) acid groups on the surface, the charge densities being very similar to each other and of the same order of magnitude as those observed by other workers (133,141,145, 155). Oxidation of three of the latices revealed the presence of hydroxyl groups, the amounts being similar from latex to latex.

C) Multisampled Kinetic Reactions.

The reactions were all carried out on a large scale (>1 l) and the sampling technique was as described in Chapter II. A series of reactions was carried out at different temperatures (64B (323 K), 62B (333 K), 142 (343 K), 62A (353 K) and 66A (333K)), and a number of small (2 ml) samples were removed at regular intervals for weights analysis and diameter determination by electron microscopy. A series of reactions was also carried out at 343 K from which much larger samples, > 10 ml, were removed for analysis by gas adsorption, conductometric titration and gel permeation chromatography. The results obtained for changes in particle diameter, degree of conversion and the number of particles ml^{-1} (N) are summarised in Tables 30 to 42 (Appendix I).

D) Particle Nucleation.

1) Observed Variation in N.

The variation in N during the course of the polymerisation is shown graphically in Figs 22-26 . The effect of removing samples from the reaction was taken into account in their determination. It can be seen that in all cases except one (18A) a decrease in N occurred during the early stages of the reaction, the value then remaining relatively constant for the rest of the reaction (except in the cases of reactions 19, 35A, 62B and 64B, where a

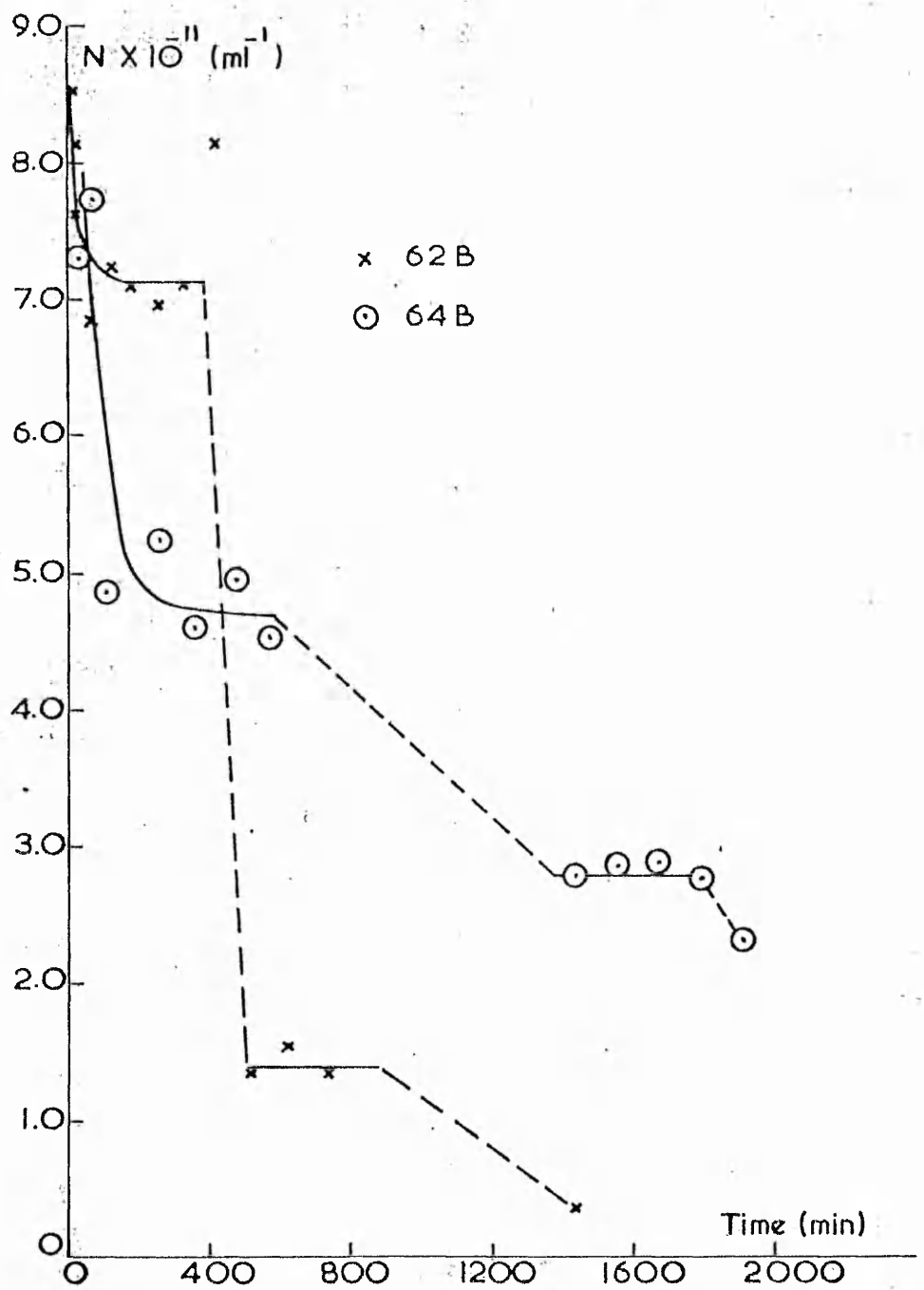

VARIATION OF N WITH TIME FOR REACTIONS 62B & 64B

FIG.22.

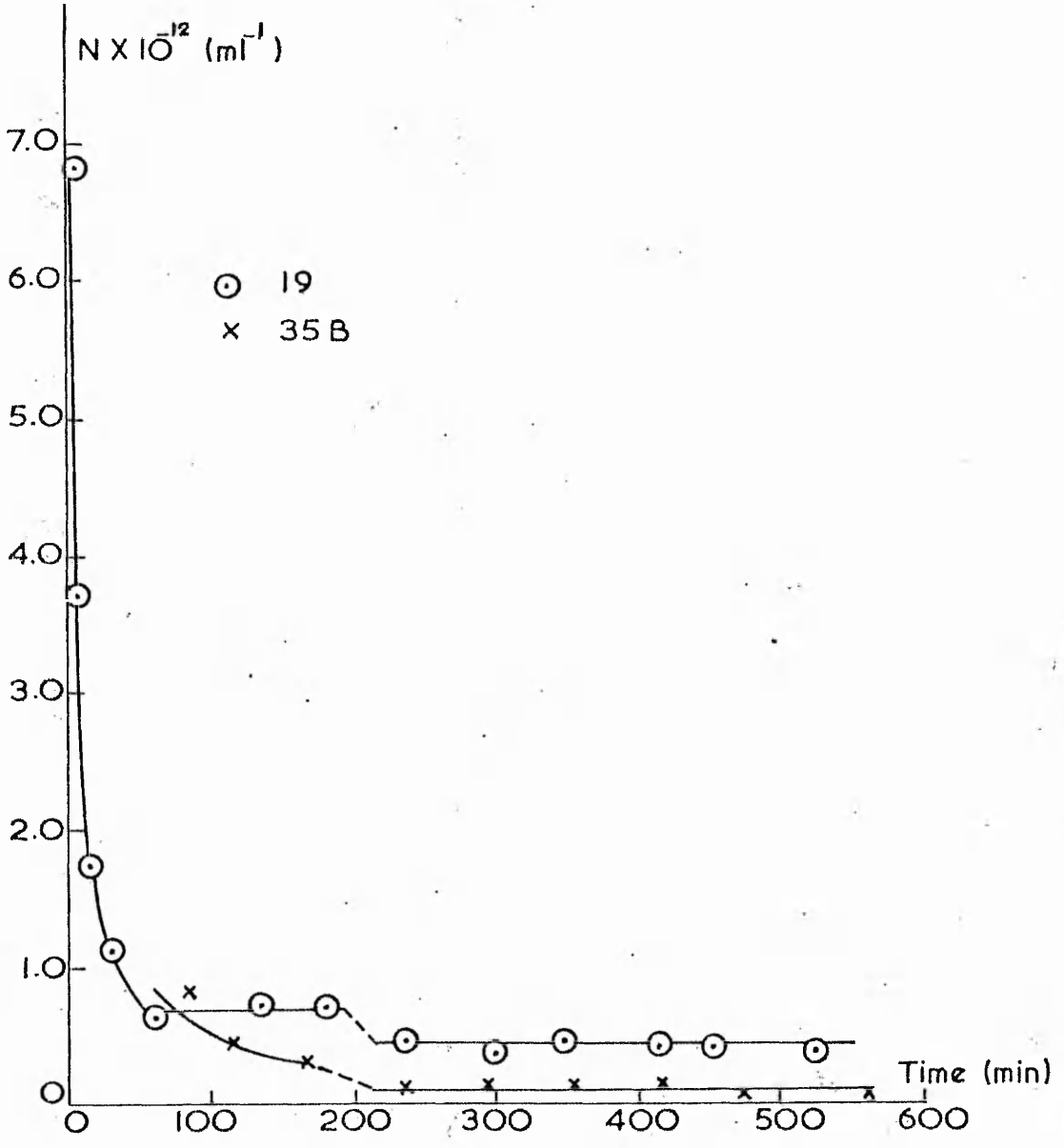

VARIATON OF N WITH TIME FOR REACTIONS 19 & 35B

FIG. 23.

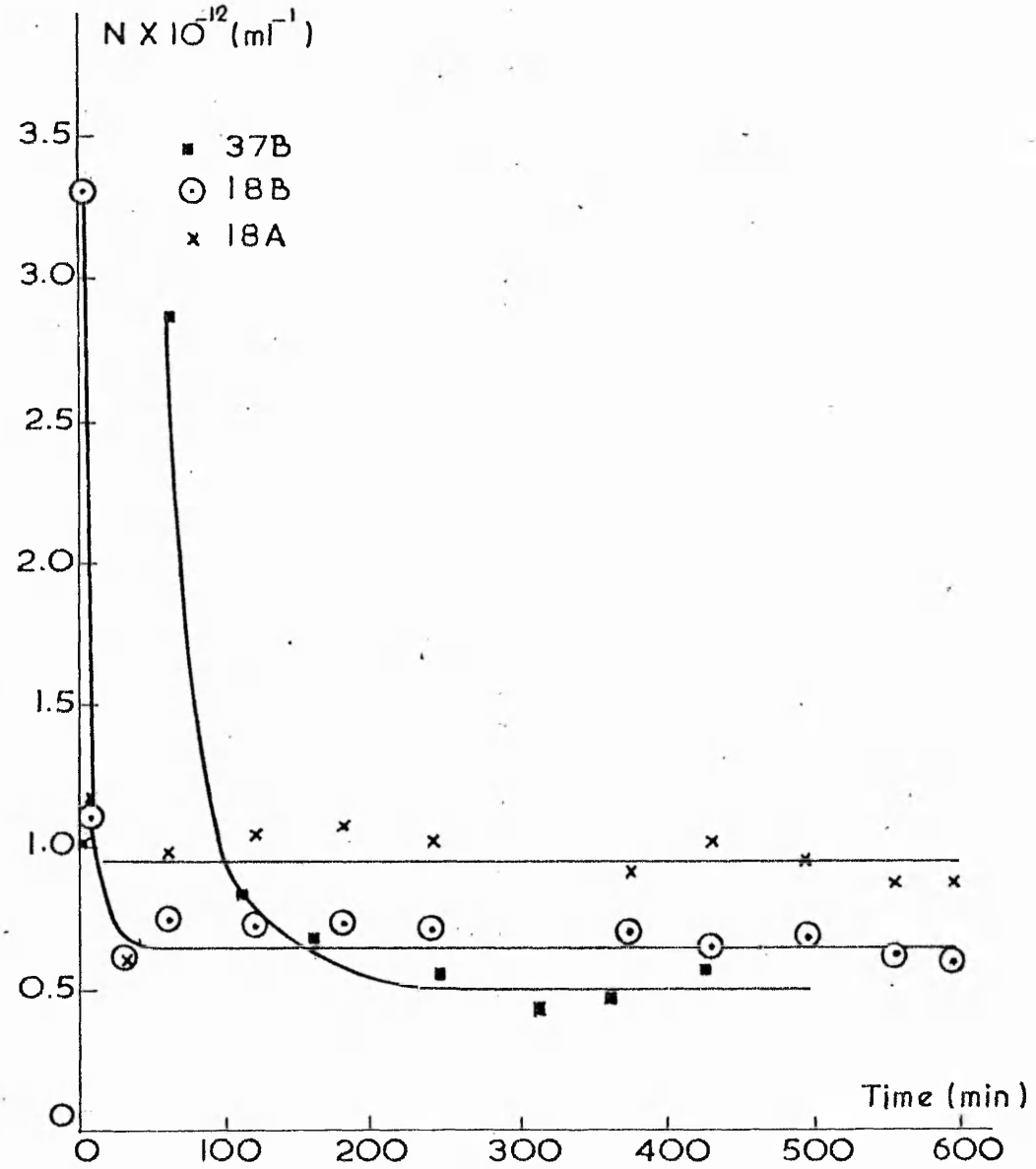

VARIATION OF N WITH TIME FOR REACTIONS 37B, 18B & 18A

FIG. 24.

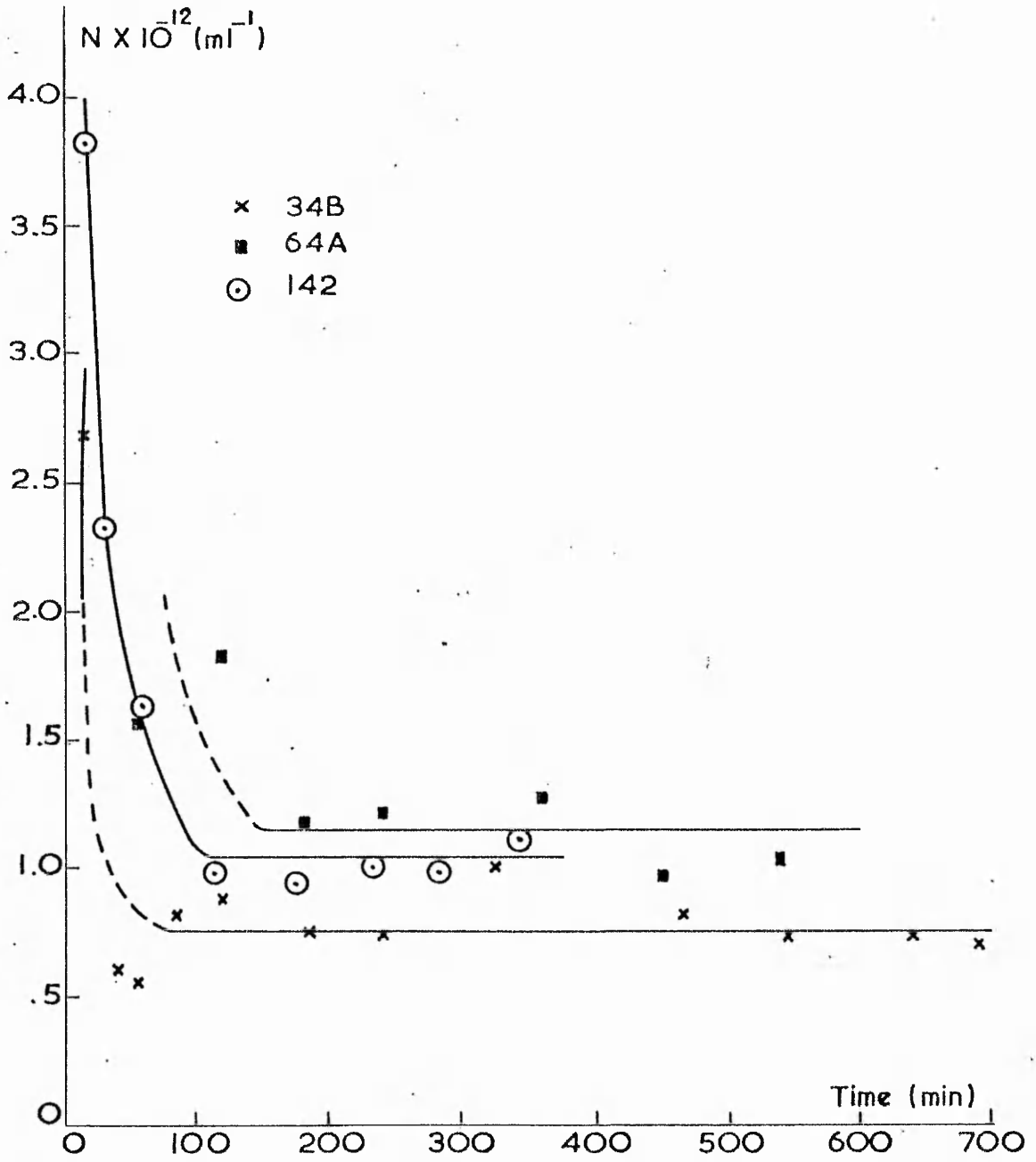

VARIATION OF N WITH TIME FOR REACTIONS 34B, 64A & 142

FIG. 25.

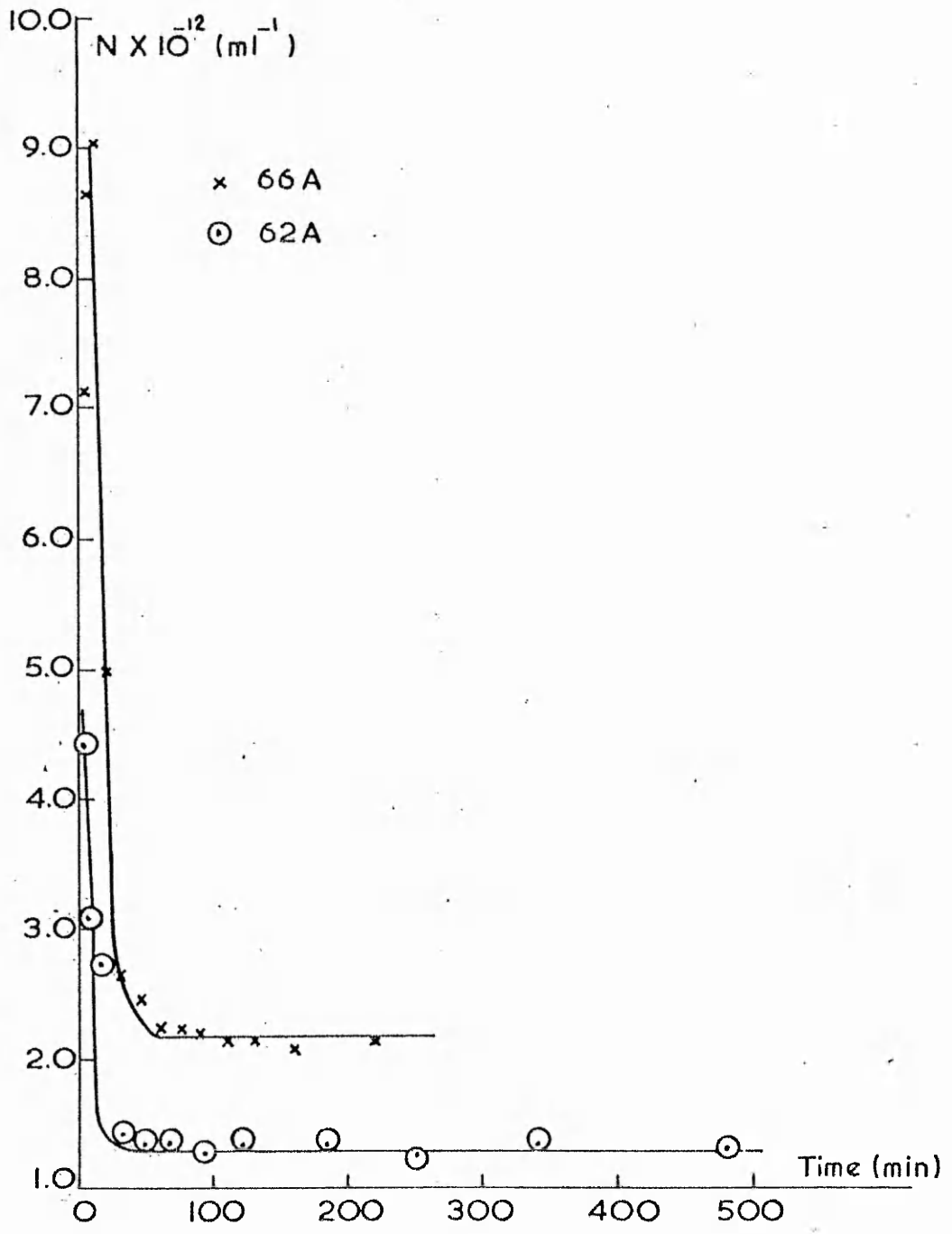

VARIATION OF N WITH TIME FOR REACTIONS 66A & 62A

FIG. 26.

further decrease in N ml^{-1} occurred at a later time). The slight variation in N during the rest of the reaction probably reflects the error involved in the determination of N since it is determined from the % conversion and the weight per particle (the latter involves r^3 which, if it is assumed that the maximum error incurred in determining the particle diameter by electron microscopy is 5%, could well be as much as 15% in error).

The time taken for the initial rapid decrease in N to occur before it became constant depended on the reaction temperature: being ca 100 min at 323 K (~ 1% conversion), 50 min at 333 K (~ 2% conversion), ~ 60 min at 343 K (~2-5% conversion), 20 min at 353 K (~1% conversion) and 20 min at 363 K (~ 5% conversion). The diameters at the end of particle coagulation were all in the range of 70-140 nm. Only in the case of the reaction at 363 K was there a definite observed initial increase in N. The variation in time for N to reach a constant value at a particular temperature is probably due to a varying induction period of the reaction. Although every effort was made to exclude atmospheric oxygen and other impurities capable of reacting with free radicals, it is possible that complete removal was never achieved, thus different reactions might be likely to have different induction periods.

The lack of data concerning the initial increase in N indicates that particle nucleation is a very rapid process with a very large number of particles being formed in a very short time interval. These particles then coagulate together due to colloidal instability caused by growth of the initial nuclei. Fitch and Tsai (30), in their studies on methyl methacrylate emulsion polymerisation in the absence of added surfactant, detected an initial increase in N followed by a decrease. These workers added surfactant to their samples taken from the reaction in order to prevent coagulation. It is therefore possible that the initial increase of N in the present work was not detected due to coagulation of unstable

particles on sampling.

The results are in agreement with the postulate of Goodwin et al of a decrease in N during the early stages of reaction, but in disagreement with the results obtained by workers using styrene in the presence of surfactant (73,83) and with the sodium salt of styrene sulphonic acid (249) in the absence of surfactant, since in these systems N increased during the early stages to a constant value.

2) Variation in N with Temperatures.

The parameters from the kinetic runs (Table 21) and the variation in particle diameter with temperature (Table 22) show that there is a slight variation in N within any one set of identical reactions. This is probably due to variation in the induction periods. Although the small scale reactions were very reproducible, it is possible that by increasing the reaction volume 4 - 6 times, the preflushing with nitrogen was insufficient to completely remove all dissolved atmospheric oxygen. Different induction periods could well result in slight variations in the number of particles produced, although it is thought unlikely that the length of the induction period would significantly alter the characteristics of subsequent particle growth, if it occurred according to the Harkins mechanism (15).

The variation in particle diameter (calculated at 100% conversion) with temperature are plotted in Fig 27 , the slope and intercept being obtained by the least squares method. It can be seen that a reasonable straight line can be drawn through the points, and the resulting equation:

$$\log d = \frac{608.7}{T} + 0.981, \qquad -- \quad (137)$$

is capable of predicting, to within 10%, the experimentally obtained diameters at 100% conversion. (The plotted diameters of reactions 19,35A,64B and 62B were calculated from the observed N before the second coagulation stage). The above equation is similar in form to that given in Chapter IV for peroxydiphosphate/metabisulphite initiated systems.

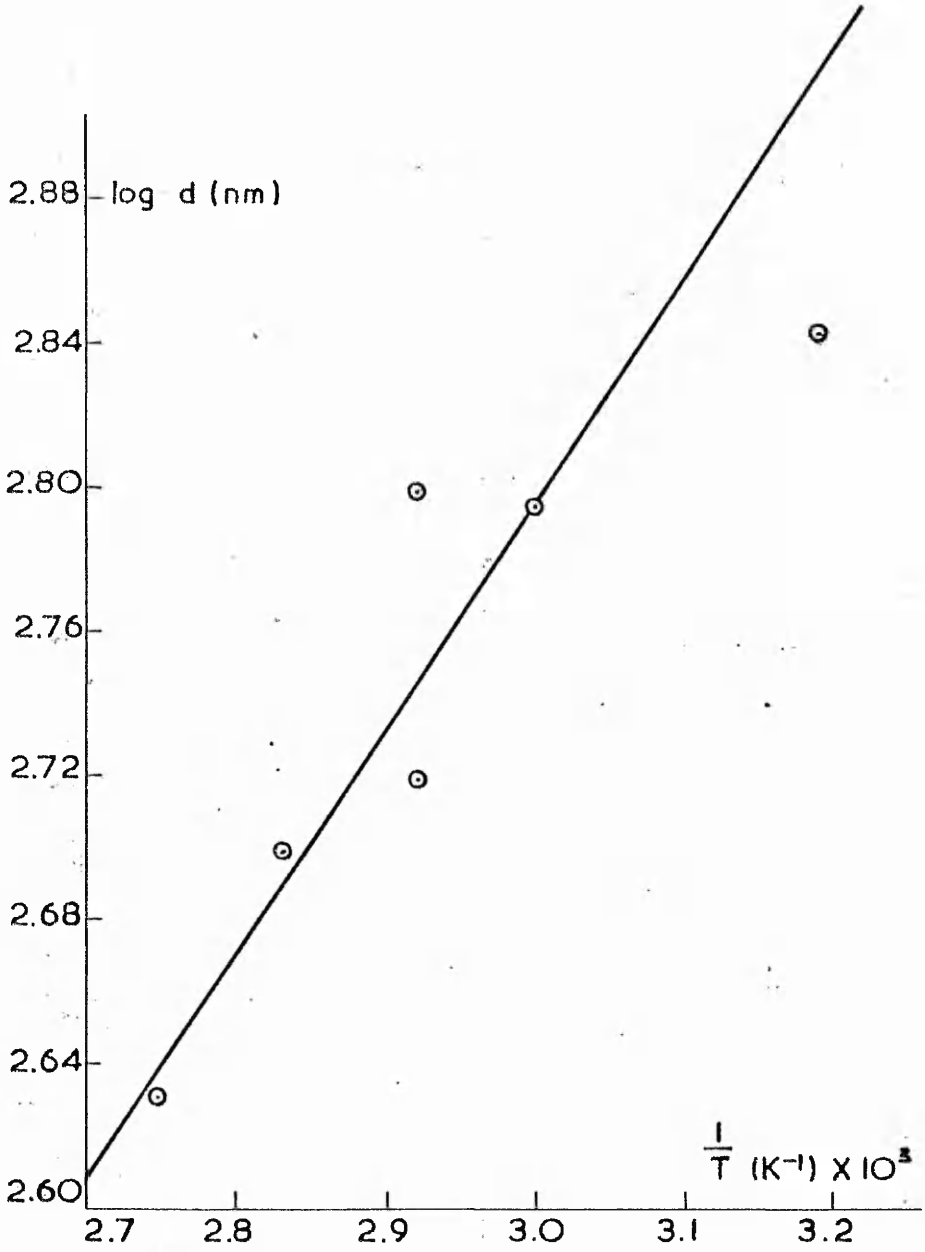

VARIATION OF PARTICLE DIAMETER WITH TEMPERATURE FOR KINETIC RUNS

FIG.27.

TABLE 21

PARAMETERS OF KINETIC RUNS

Reaction	(M) (l^{-1})	(I)x10^{3} (l^{-1})	T (K)	Final Diameter (nm)	Conversion (%)	N(ml^{-1}) x 10^{-11}
64B*	0.870	3.69	323	1060	-	-
62B*	0.870	3.69	333	1428	63.31	0.36
14B	0.870	3.70	343	504	90.64	11.6
34B	0.870	3.69	343	596	88.70	6.9
64A	0.869	4.11	343	634	98.65	11.5
19*	0.870	3.69	343	844	95.01	3.2
35A	0.870	3.71	343	1082	96.02	1.2
37B	0.932	4.01	343	670	92.10	5.4
18A	0.931	4.11	343	558	81.46	8.5
18B	0.931	4.11	343	634	80.98	5.8
62A	0.870	3.70	353	488	92.40	13.2
66A	0.870	3.71	363	416	92.20	21.3

* These reactions showed a second sharp decrease in N during the course of the reaction.

TABLE 22

VARIATION IN PARTICLE DIAMETER WITH TEMPERATURE FOR KINETIC RUNS

Latex	Temperature (K)	N(ml^{-1}) x 10^{-11}	$^{\square}$d(100%) (nm)	*d(calc) (nm)	$\frac{d(100\%) - d(calc)}{d(100\%)} \times 100\%$
64B	323	4.9*	695	734	-6
62B	333	7.5*	623	644	-3
142	343	11.6	522	570	-9
34B	343	6.9	620	570	+8
19	343	6.*.	620	570	+8
35A	343	6.6*	629	570	+9
62A	353	13.2	500	507	-1
66A	363	21.3	426	455	-7

*N (ml^{-1}) taken as the value before the second coagulation

$^{\square}$d(100%) diameter calculated at 100% conversion.

*d(calc) diameter calculated from the equation relating log d to temperature.

Monomer concentration = 0.870 moles l^{-1}.

Initiator concentration = 3.70 x 10^{-3} moles l^{-1}.

Ionic strength = 11.1 x 10^{-3}.

c) Second Coagulation.

Four polymerisations, 19,35A,64B,62B, showed a second coagulation during the course of the reaction, and in the case of reaction 62B it resulted in an 80% decrease in N. The observed decrease did not appear to be due to the coalescence of particles, but to a certain percentage of particles which coagulated out of the reaction. (In the case of 62B there was a very large lump of bulk polymer on the stirrer at the end of the reaction, and the percent conversion of monomer into latex/dispersion of this reaction was only ~ 6%). This loss of particles from the reaction would result in the remaining particles growing to a larger size than would normally be expected.

The coagulations must have been due to colloidal instability of the particles. In the cases of 64B and 62B, the reactions were carried out at 323 and 333 K, i.e. temperatures lower than normally employed. A lower temperature would result in a slower rate of free radical production, which in turn would result in the molecular weight of the polymer produced being greater due to the larger time interval between successive free radical entries. A higher molecular weight would cause the minimum in the surface charge density predicted by equation (144)(occurs on p.163) to be lowered further and the particles may thus be liable to undergo a second coagulation. Whether this usually occurs in reactions at lower temperatures is unknown. It did not appear to occur with potassium peroxydiphosphate/sodium metabisulphite initiator systems.

The relationship ($\log D = \frac{1173}{T} - 0.578$) obtained by Goodwin et al (170) for the variation of particle diameter with temperature was based on observed results at three temperatures, 328 K, 343 K and 358 K, and the results interpolated from the variation in particle diameter with ionic strength plots at different temperatures. The observed results are rather scattered, and it is difficult to determine from them whether the diameter at 328 K is too large, which would indicate a second coagulation

during the reaction. However, if a straight line is drawn through the points at 343 and 358 K then the diameter at 328 K is certainly too large.

In the cases of reactions 19 and 35A, however, no explanation is apparent since they were identical in composition to other reactions which did not exhibit the phenomenon. This decrease in N would not appear to be due to an error in the weights analysis, since the decrease is accompanied in both cases (also with 62B and 64B) by an increase in the radius squared versus time plot. It is possible that the stability conferred by the initial coagulation was not sufficient to confer stability during further particle growth. Also, the samples removed from the reactions immediately prior to the coagulation were very large (~ 100ml) in both cases and removal of samples of this size necessitated the stirrer being stopped for 1 - 2 minutes. The ingress of a certain amount of atmospheric oxygen may also have occurred despite the nitrogen bleed. The combination of these two factors may have resulted in particle coagulation, although the mechanism is not apparent. No other reactions were carried out from which such large samples were removed.

E) Laser Light Scattering.

1) Introduction.

Watson et al (253) have used a light scattering technique to follow the early stages of the photoinitiated emulsion polymerisation of methyl methacrylate, both in the presence and absence of sodium dodecysulphate emulsifier. They determined that $\frac{I_{90}}{I_0}$, the ratio of the unpolarised light intensities at 0° and 90° to the incident light, was proportional to time. They interpreted their results by assuming that each free radical produced formed a primary particle which then underwent coagulation with others according to the Smoluchowski (254) fast rate of particle coagulation. This was accompanied by mutual termination as proposed by Baxendale (179). The methyl

methacrylate was present as a 0.1 mole l^{-1} solution.

The work described here was carried out in collaboration with Capt. D. Munro and Dr. K. Randall of the Royal Military College of Science, Shrivenham, England. It was a preliminary study of the applicability of laser light scattering and photon correlation spectroscopy, using an apparatus designed by the above workers, to the early stages of the emulsion polymerisation of styrene in the absence of added emulsifier. It was hoped to study directly the dynamics of the polymerisation process and demonstrate that growth and coagulation occur until a stable size particle is reached, after which the total number of particles essentially remains constant.

It may be thought that the use of styrene monomer would introduce difficulties due to monomer starvation caused by its solubility in water (3.6×10^{-3} mole dm^{-3} at 323 K (77)). However, it is to be noted that this concentration of styrene is equivalent to 10^{12} particles ml^{-1} of ca. 90 nm diameter. The values for N and the particle diameter being similar to those observed in large scale reactions at the end of the initial period of particle coagulation.

The scattering of light by particles whose radii are small compared to that of the wavelength of light being used (i.e., particles in the early stages of emulsion polymerisation < 100 nm, the wavelength of the light used in this work being 632.8 nm) is termed Rayleigh scattering (255) and can be described by (256):

$$I = \frac{9\pi^2}{2R^2}\left(\frac{m^2 - 1}{m^2 + 2}\right)\frac{V^2}{\lambda^4} \qquad -- (138)$$

where: I is the intensity of the perpendicularly polarised light.

R is the distance of the particle from the point of observation.

V is the volume of the particle.

λ is the wavelength of the light.

m is the ratio of the refractive index of the disperse phase to the solvent.

The light scattered by N particles is thus:

$$I = \frac{N\,9\pi^2}{2R^2}\left[\frac{m^2+1}{m^2+2}\right]\frac{V^2}{\lambda^4} \qquad \text{-- (139)}$$

provided that the region from which the scattering is observed is small, i.e. R for all values of N is almost constant.

Therefore:

$$\frac{I}{I_o} \propto NV^2 \qquad \text{-- (140)}$$

where I_o is the intensity of the incident light.

2) Experimental.

The reactions were carried out in P.T.F.E. capped 10 mm quartz or silica glass cuvettes maintained at 333 K. The total volume of water present was 1 ml in most cases. This was covered with a layer of styrene. It was not possible to stir the reaction since the resulting monomer droplets significantly affected the light scattering. The He/Ne laser beam was passed through the cell at approximately 1mm beneath the styrene meniscus in order to reduce any possible effects of monomer starvation on the reaction.

The water and monomer were both passed through a .10 µm filter before addition to a cuvette. This had been previously cleaned with nitric acid. A P.T.F.E. cap with a small hole in it was used as a stopper. The water and styrene were then degassed using a combination of bubbling with filtered nitrogen and exposure to vacuum. The cuvettes were then placed in the thermostatted compartment of the apparatus and left to equilibrate for 40 minutes. The initiator was then added, (.03 - .08 ml of 0.148 mole l^{-1} potassium persulphate, made up in filtered water), using an Agla micrometer syringe. The scattered light (90^o) was measured every 12.5 seconds and plotted as a function of $\log \frac{I_{90}}{I_o}$ versus time.

An initial series of reactions was carried out to determine the shape and reproducibility of the curves obtained (using different initiator concentrations), and a series of experiments was then carried out to determine

the effect of adding hydroquinone inhibitor to the reaction at various times. Typical plots of log $\frac{I_{90}}{I_o}$ versus time are shown in Fig 28a, and the effect of adding inhibitor in Fig 28b,c.

3) Results.

The log $\frac{I_{90}}{I_o}$ versus time curves were all very similar in shape. The light scattered initially remaining unchanged (A) for about 10 minutes. It then increased slowly (B) and then more rapidly (C), the rate eventually decreasing again (D). It is thought that the initial slow increase in stage (B) is due to either the formation of the initial nucleii or to their growth. The latter seems more likely since the initial nucleii would be very small (~ 10 nm), and hence the light scattered using a 30 mW laser as light source may well have been below the limits of detectability. The very rapid increase (C) is thought to be a combination of growth and coagulation, and the much slower increase (D) mainly due to particle growth alone.

The effect of added inhibitor supports this interpretation since addition of inhibitor (Fig. 28b) between regions (C) and (D) resulted in the amount of light scattered remaining constant with time after an initial drop. Thus, the increase in the amount of scattered light at this stage of the reaction (in the absence of inhibitor) was due to particle growth only. The drop in the amount of light scattered upon addition of the hydroquinone (the hydroquinone also acts as absorber) was probably due either to a dilution effect, (expected to be small since the volume added was only 0.06 ml), or to the reaction mixture being agitated. The hydroquinone was added, using an Agla micrometer syringe, below the styrene layer and if, because of monomer starvation, the reaction was proceeding more rapidly just below the styrene layer than at the bottom of the cuvette then the effect of agitation would be to reduce the number of particles just below the styrene layer. It was found that, if at the end of a reaction

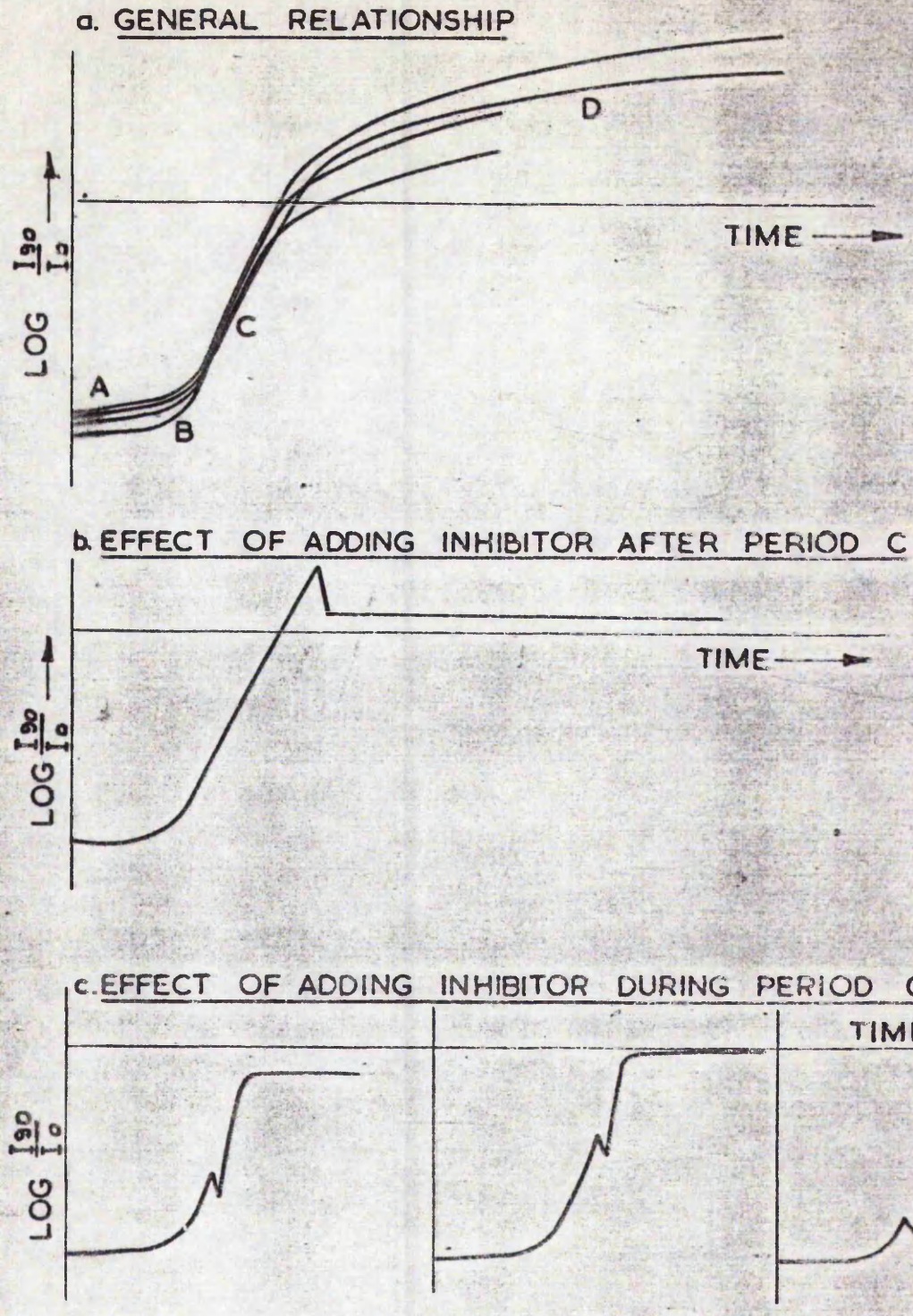

PLOTS OF LOG $\frac{I_{90}}{I_0}$ v TIME FOR REACTIONS RUN IN CUVETTES

FIG. 28.

the laser beam was passed through the cuvette about 10 mm below the styrene layer, then the amount of light scattered decreased. This is almost certainly due to the variation in size and rate of growth at different distances from the styrene/water interface. Experiments carried out by sampling (T.E.M. examination) from test-tube reactions (no mixing) showed a distinct size gradient as the distance from the interface increased. The small particles at relatively large distances from the interface (50 mm) scatter light far less effectively.

If the inhibitor was added during stage (C), it can be seen that although the initial drop occurred, the light scattered continued to increase rapidly until a point was reached when it became constant. Thus, although the polymerisation reaction had been stopped the amount of light scattered still increased, indicating that at this stage particle coagulation was taking place.

It can be seen that in the absence of any growth due to polymerisation, any fractional decrease in N, $\times$, would be accompanied by an identical fractional increase in V.
i.e. as $N \longrightarrow \frac{N}{x}$ then $V \longrightarrow x V$.

Before coagulation $\frac{I_{90}}{I_o} \propto NV^2$ -- (141)

and after coagulation:

$$\frac{I_{90}}{I_o} \propto \frac{N}{x}(xV)^2 = Nx V^2 \quad -- (142),$$

i.e. the amount of scattered light increases on coagulation.

The time taken for the onset of stage (C) appears to be independent of the initiator concentration. Watson et al (253) observed a similar effect in that although the concentration of biacetyl (the light activated initiator used in their study) was varied over a six-fold concentration range, there were no significant differences in the kinetic behaviour.

The total amount of light scattered at the end of period (C) was unrelated to the amount of initiator added.

This could have been due to a number of causes. A higher initiator concentration would result in a larger number of initial nucleii being formed, as well as a larger amount of coagulation occurring due to the increased ionic strength. Also, slight variations in the distance of the laser beam from the styrene layer from reaction to reaction could have been the cause. It is thought likely that the results obtained concerning the coagulation of the particles during the early stages of reaction are applicable to large scale stirred reactions, since there is sufficient monomer present in the water phase to produce a system of particles almost identical to that observed in large scale reactions. Also, the effect of monomer starvation is likely to be minimal just below the styrene layer as evinced by the fact that the particles just below the monomer layer continue growing (part (D) of the curves).

F) The Presence of Low Molecular Weight Material within the Latices.

It has been found that samples removed early in reactions contained appreciable amounts of material of molecular weight ca.1000 (121,122) Fig 29)*, and that the amount of this material did not appear to increase significantly as the reaction proceeded.

1) Experimental

a) Presence of Low Molecular Weight Material within the Particles.

Two samples of latex 35A7 were extracted by shaking with isooctane for 24 hours; one sample was the latex dispersion whilst the other had been freeze-dried. The resulting extracts were rotary evaporated to remove the isooctane and the residue was analysed using gel permeation chromatography (G.P.C.). The G.P.Cs of the extracts and

*The author is grateful to Dr. M.C. Wilkinson for carrying out the experiment depicted in this figure.

GEL-PERMEATION CHROMATOGRAPH OF POLYSTYRENE LATEX

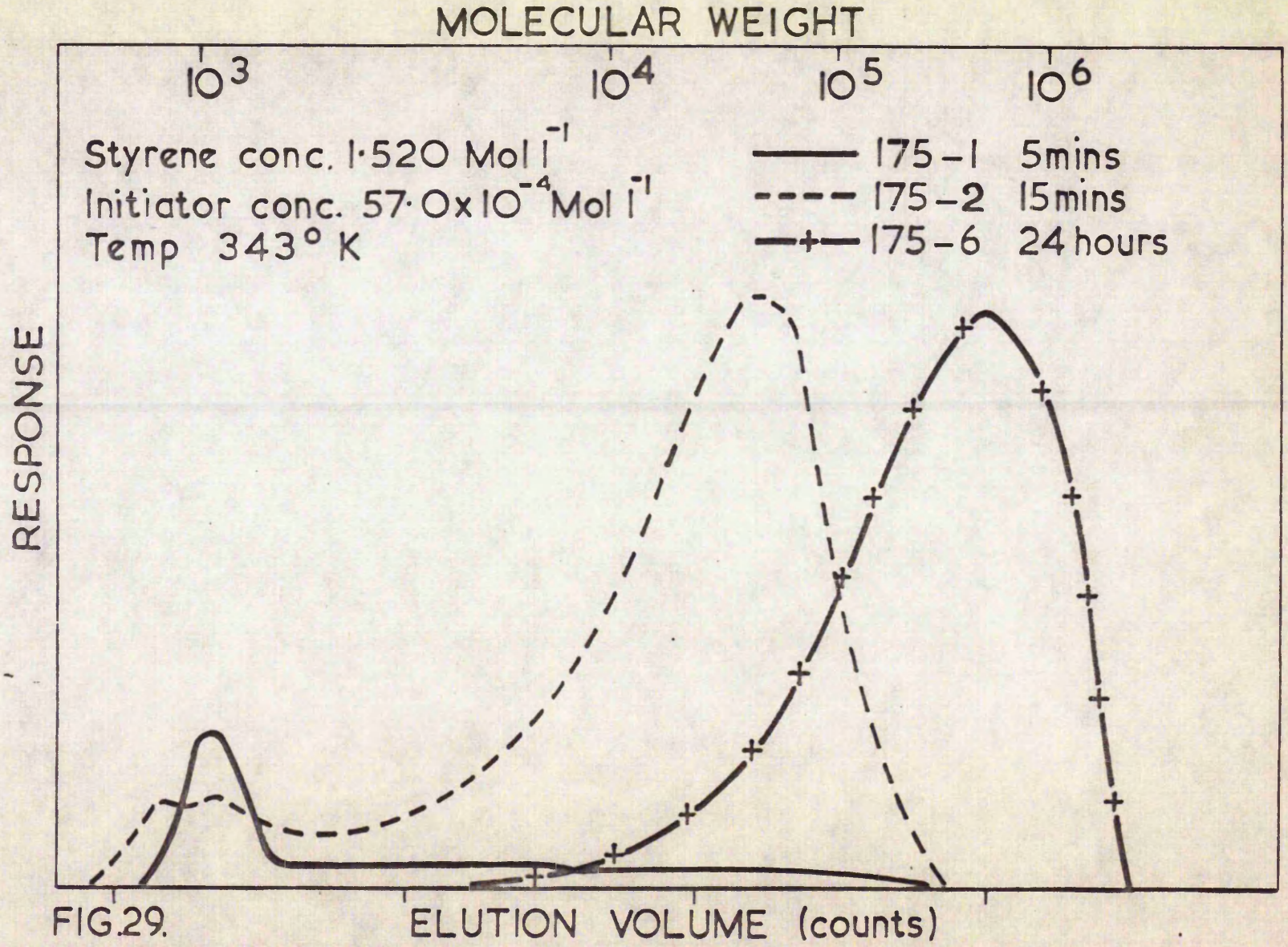

FIG.29.

of a sample of freeze-dried 35A7 are compared in Fig.30 . It can be seen that the material extracted from the freeze-dried latex had a molecular weight of ~ 1000. The extract from the latex dispersion had a slightly lower molecular weight (~ 700) than that extracted from the freeze-dried sample (~ 1000), where it appears as a shoulder on the main peak. It can also be seen that the relative amounts of this material to that of the high molecular weight polymer forming the bulk of the particles is low compared to the amount present in the sample removed from reaction 17% after 5 minutes. The cut-off point of the peaks in all cases occurs at a molecular weight of ~ 500.

The difference between the isooctane extract from the dispersed and the freeze-dried sample is probably due to the slightly different solubilities of the two molecular weight fractions in the aqueous phase. For low molecular weight material to be extracted from the dispersed latex, it must leave the particle and be transported through the water phase into the isooctane. It is reasonable to assume that, the lower the molecular weight of the material (if it consists of a polymer chain with ionic sulphate or perhaps hydroxyl or carboxyl end groups), then the more soluble it is in the aqueous phase, and thus the more efficient the extraction.

b) Analysis of the Material Present in the Aqueous Phase.

A sample of latex was passed through an unltrafiltration unit (Amicon Thin Channel TCF10 unit, Amicon Ltd., 57 Queens Road, High Wycombe, Bucks., U.K.) to remove the latex and the water phase extracted using isooctane which was subsequently evaporated off (room temperature). The material left behind was analysed using G.P.C. A sample of the same latex was also dialysed, the first change of dialysis water rotary evaporated and the remaining solid analysed by G.P.C. It was found that not all of this latter sample was soluble in tetrahydrofuran, the insoluble part presumably being electrolyte. The G.P.Cs of the soluble material are shown in Fig. 31 . It can be seen that both peaks are almost identical (M.Wt. ~ 520) and

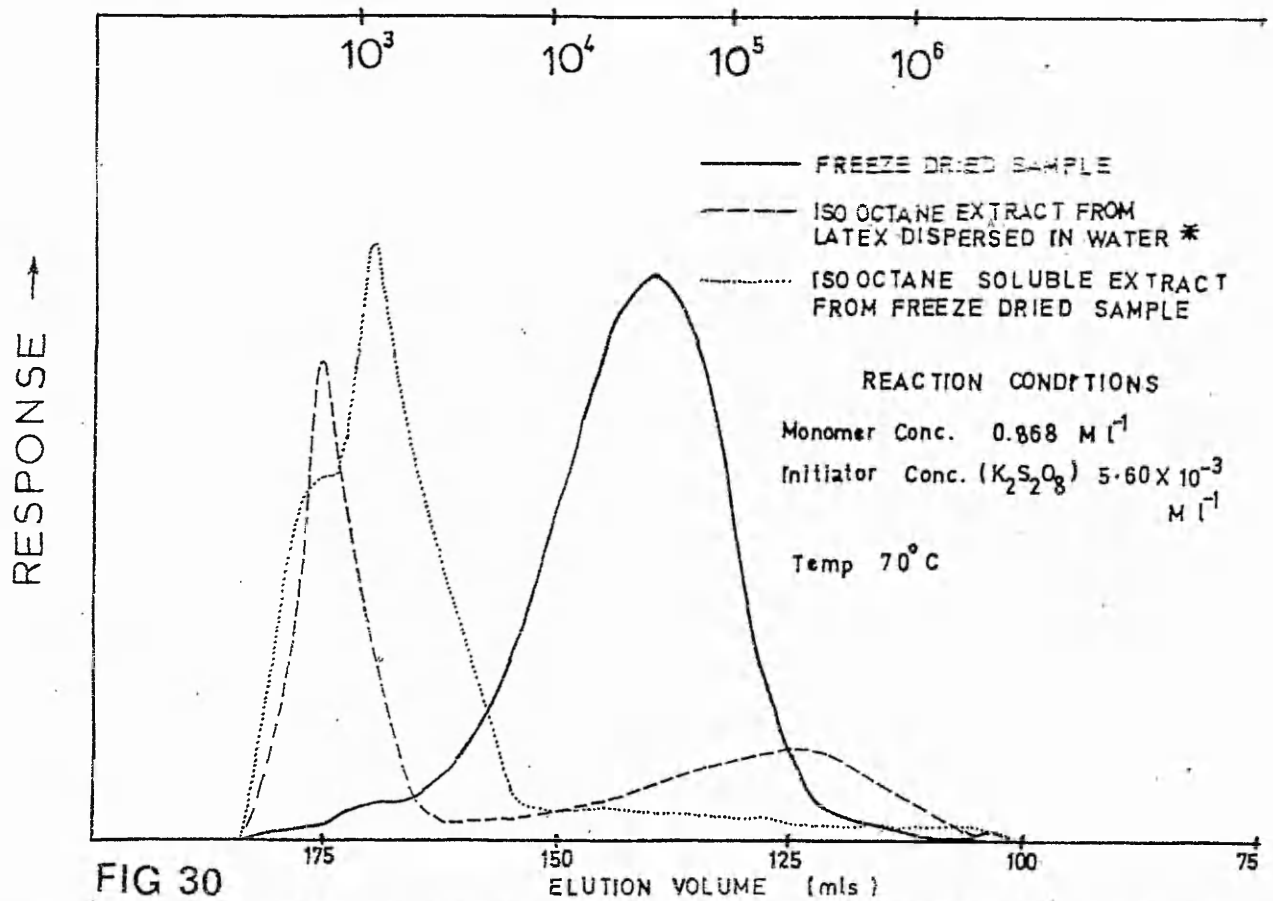

FIG 30

GEL PERMEATION CHROMATOGRAPHS OF PS 35A. SAMPLE TIME 150 mins. * HIGH MOLECULAR WEIGHT PEAK DUE TO SMALL NUMBER OF LATEX PARTICLES TAKEN UP IN THE ISOOCTANE

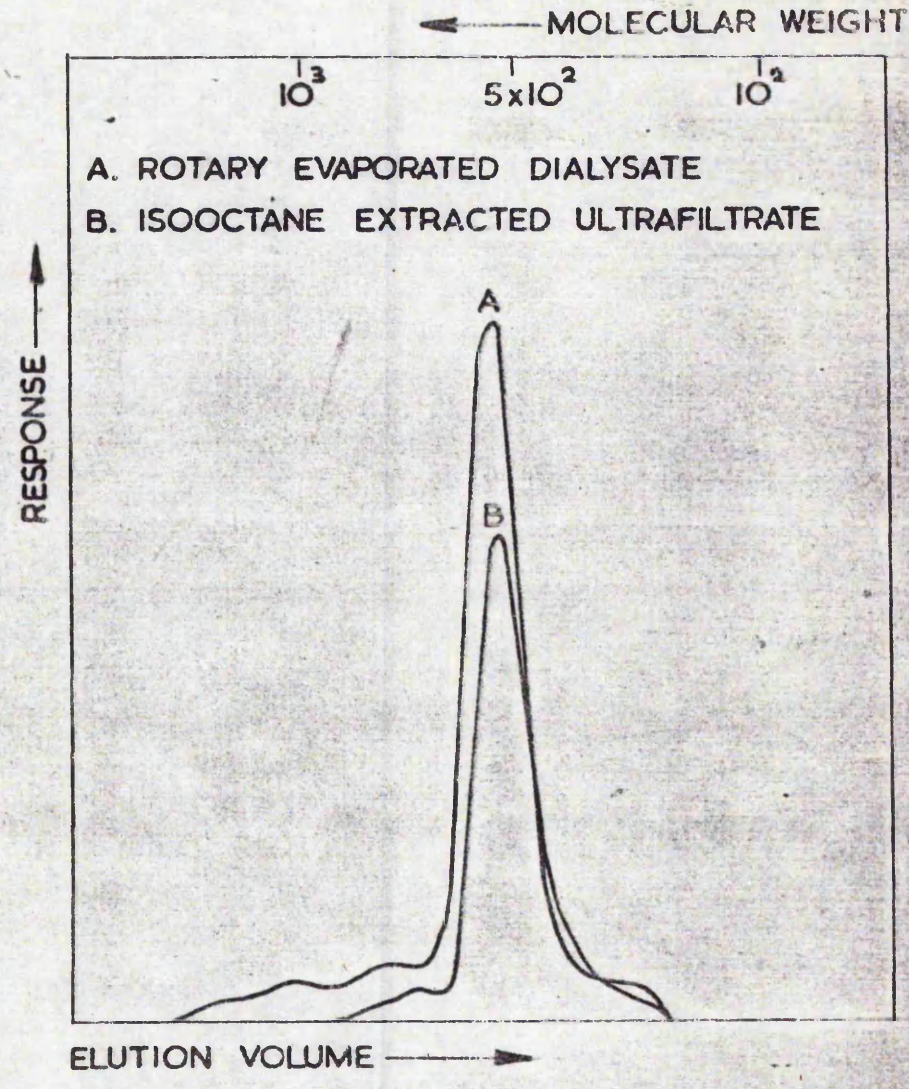

GEL PERMEATION CHROMATOGRAPHS OF WATER SOLUBLE OLIGOMERIC MATERIAL

FIG.31.

that in both cases there is a low leading edge to higher molecular weights, peaking at ~ 700. For the rotary evaporated dialysis sample there is a further peak at ~ 1000. These results indicate that polystyrene containing either one or two sulphate (hydroxyl, carboxyl) groups and molecular weight up to 520 is soluble in water. The sharp cut-off on these chromatographs at low molecular weights is probably due to loss of some material (MW < 120) with solvent on rotary evaporation.

2) Discussion.

It appears that low molecular weight material is present in polystyrene latices in two loci; material ~ 1000 within the particles and material of ~ 520 in the aqueous phase. It would be thought that small amounts of low molecular weight material would be formed throughout the course of the reaction due to termination of low molecular weight oligomeric radicals. Hence, the presence of large amounts of this material in samples removed from early in reactions must be due to some other cause, such as particle nucleation.

G) Proposed Mechanism of Particle Nucleation.

In order that a large amount of low molecular weight material can be formed, it is necessary that a large amount of rapid termination of short chain oligomers takes place. It is unlikely that this material could be formed within the particles, since even in the early stages of a reaction, when the particles are very small, there will, on average, be an appreciable time interval between the entry of one free radical and its termination by another. For instance, if it is assumed that every free radical produced in solution enters a particle, then, at the concentrations employed in this work, there are about 10^{14} free radicals produced ml^{-1} sec^{-1} in a system containing about 10^{13} particles (before initial coagulation). Hence, a free radical enters a particle every 0.1 second. Assuming that the monomer concentration within the particles is 5 mole l^{-1} , then each free radical adds on ~1300 monomer units

sec^{-1}, indicating a molecular weight of at least 13,500. Thus, taking into consideration that in the very early stages N is probably $> 10^{13}$ and that not all the free radicals produced enter the particles it is unlikely that large amounts of material of molecular weight ~ 1000 are produced within the particles.

It seems likely that this material is formed during particle nucleation. The mechanism of Fitch et al (30,71), for the more water-soluble monomer methyl methacrylate, predicts that free radicals grow in solution until, at a certain chain length, the chains collapse upon themselves forming a primary nucleus. These nucleii continue to grow until they coagulate and undergo mutual termination, the process being described by solution kinetics. It is not thought that this mechanism would be applicable to styrene since the monomer and presumably the polymer is far less soluble than methyl methacrylate. Indeed, the G.P.C. data indicates that species of ~ 520 molecular weight (i.e. 3-4 styrene units + end groups) are almost insoluble in water. It thus appears likely that either a precipitation mechanism occurs, or that the growing free radicals reach a concentration and chain length at which they become surface-active and micellise.

The precipitation mechanism would involve the growing free radical concentration in solution being such that supersaturation occurred. It is likely that the addition of a sulphate group to a styrene molecule would increase its solubility beyond 5×10^{-3} mole l^{-1}. However, subsequent additions of styrene units to this species would act to decrease its solubility eventually to the point where the species precipitated out.

A micellar mechanism would involve the free radical oligomers reaching a chain length sufficient to confer surface-active properties before precipitation. Vanderhoff et al (3) postulated that this would be about 4-5 monomer units. (i.e., molecular weight 500 - 600). Indeed, it is generally accepted that if the Harkins model of particle growth is correct then the oligomer must become surface-

active to be able to adsorb at the particle/water interface, due to the charge repulsion forces which exist between the negatively charged particle and the SO_4^- radical. If the oligomer becomes surface-active upon the addition of 4-5 monomer units, then assuming the monomer concentration in the aqueous phase to be 5×10^{-3} mole l^{-1}, one monomer unit is added to a free radical every 0.6 second, i.e. in about 3 seconds there would be 4×10^{-7} mole l^{-1} of surface-active oligomeric species. If micellisation occurs at this concentration then some 10^{12} micelles ml^{-1} sec^{-1} would be formed (assuming 100 oligomers micelle $^{-1}$). Thus, micellisation would occur until the number of particle nucleii produced was such that the concentration of free radical oligomers in solution was reduced below that of the C.M.C. due to adsorption by the growing nucleii. The above calculation is also applicable to the precipitation mechanism.

It is to be noted that although the oligomers may be said to undergo a micellisation-type process, the structures they form are not strictly micelles, which only exist in dynamic equilibrium with surfactant in solution and continually break down and reform. The structures formed in this case would not break down due to termination by combination of the free radicals.

Either of the above mechanisms would lead to large numbers of low molecular weight oligomeric species being brought into close proximity. This would result in a large amount of rapid termination to produce species of molecular weight ~1000. It is interesting to note that the nucleii formed by this mechanism would not be initially unstable since they would consist of large numbers of low molecular weight polymer chains each of which would have a sulphate group at both ends. However, it can be seen from Fig. 29 that once the particle is nucleated further growth proceeds by the formation of polymer of molecular weight up to 10^6. Assuming that the molecular weight of first polymer chain incorporated into the initial nucleii consisting of 100 oligomers is 50,000,

it doubles the volume and increases the surface area by a factor of 1.6, with the addition to the surface charge density of only two charges. Thus, the surface charge density during initial growth of the particle decreases rapidly. The variation of surface charge density can be described as follows:

Let the volume of the initial particle containing N_o polymer chains (M.W.1000) be V, then the surface area per sulphate group on the initial nucleii ($S_{SO_4^-}$) is given by:

$$S_{SO_4^-} = \frac{kV^{\frac{2}{3}}}{2N_o}, \text{ where } k = \frac{4\pi}{(4/3\pi)^{\frac{2}{3}}} \qquad -- (143)$$

Then as the particle grows:

$$S_{SO_4^-} = \frac{k\,(V + N_1V_1 + N_2V_2 + N_3V_3 \ldots\ldots + N_iV_i)^{\frac{2}{3}}}{2N_o + \sum_1^i N_i}, \qquad -- (144)$$

where $N_i\ V_i$ is the volume increase due to chains of increasing molecular weight being incorporated into the particle. If it is assumed that the initial nuclei contain fifty 1000 MW chains with a sulphate group at each end, growth occurs solely by incorporation of 50,000 MW polymer and that all the sulphate groups remain on the surface, then the effect on $S_{SO_4^-}$ of incorporating an increasing number of these high MW chains can be calculated (Table 23). From the above it can be seen that the surface charge density decreases rapidly in the early stages. In reality it would decrease more rapidly due to the molecular weight of the polymer formed increasing as the particle size increases.

H) Conclusions.

The decrease in N observed by both electron microscopy in conjunction with weights analysis and by light scattering is due to the colloidal instability of the particles. This is caused by the incorporation into an initial nuclei consisting of low molecular weight polymer of high molecular weight material. These initial nuclei are formed

TABLE 23

VARIATION IN $S_{SO_4^-}$ WITH THE NUMBER (N) OF HIGH M.W. CHAINS INCORPORATED INTO THE PARTICLE

$S_{SO_4^-}$ $cm^2 \times 10^{14}$	N (50000)	$S_{SO_4^-}$ $(cm^2) \times 10^{14}$	N (50000)
1.78	0	8.15	40
3.72	1	8.12	60
5.63	2	7.94	80
4.01	3	7.73	100
4.49	4	6.79	200
4.90	5	5.70	400
5.29	6	5.08	600
5.57	7	4.66	800
5.84	8	4.35	1000
6.08	9	2.06	10000
6.29	10	0.96	100000
7.53	20		

either by a micellar or a supersaturation and precipitation mechanism involving short chain (~ 500 M.W.) free radical oligomers.

I) Variation of Particle Diameter and Per cent Conversion with Time.

1) Variation in Particle Diameter.

In all the kinetic runs a plot of the radius squared versus time was found to give a straight line (Figs 32-38.) In the four reactions which exhibited a marked decrease in N sometime after the initial decrease, the slopes of the plots were found to change at the point of coagulation, becoming greater in all cases. This indicates that when N decreased during a reaction, the rate of growth per particle increased.

The equations describing the curves (obtained using least squares) are given in Table 30 Appendix I, and have the general form:

$$r^2 = k_1 t - k_2 \qquad \text{--- (145)}$$

The factor k_2 is proportional to both k_1 and the time taken for the initial decrease in N to occur,

i.e.,

$$\frac{dr^2}{dt} = k_1 \qquad \text{-- (146)}$$

Now the rate of polymerisation per particle can be expressed in terms of the rate of volume increase of the particle:

$$\frac{dr^3}{dt} = R_p \quad , \qquad \text{--- (147)}$$

Thus: $$\frac{dr^3}{dt} = 1.5\, k_1 r = R_p \quad , \qquad \text{--- (148)}$$

with the rate of polymerisation being proportional to the particle radius.

The values of k_1 determined at different temperatures can be used to determine the activation energy of the reaction. The values of k_1 (Table 24) are plotted versus temperature in Fig. 39 and in the form of the Arrhenius equation (in Fig. 40):

$$\log k_1 = \log A - \frac{Ea}{RT} \quad . \qquad \text{--- (149)}$$

⊙ 64B SLOPE A = 5.12×10^{-17} M^2 min^{-1}
SLOPE B = 6.20×10^{-17} M^2 min^{-1}
SLOPE C = 1.44×10^{-16} M^2 min^{-1}

X 62B SLOPE A = 8.30×10^{-17} M^2 min^{-1}
SLOPE B = 4.98×10^{-16} M^2 min^{-1}

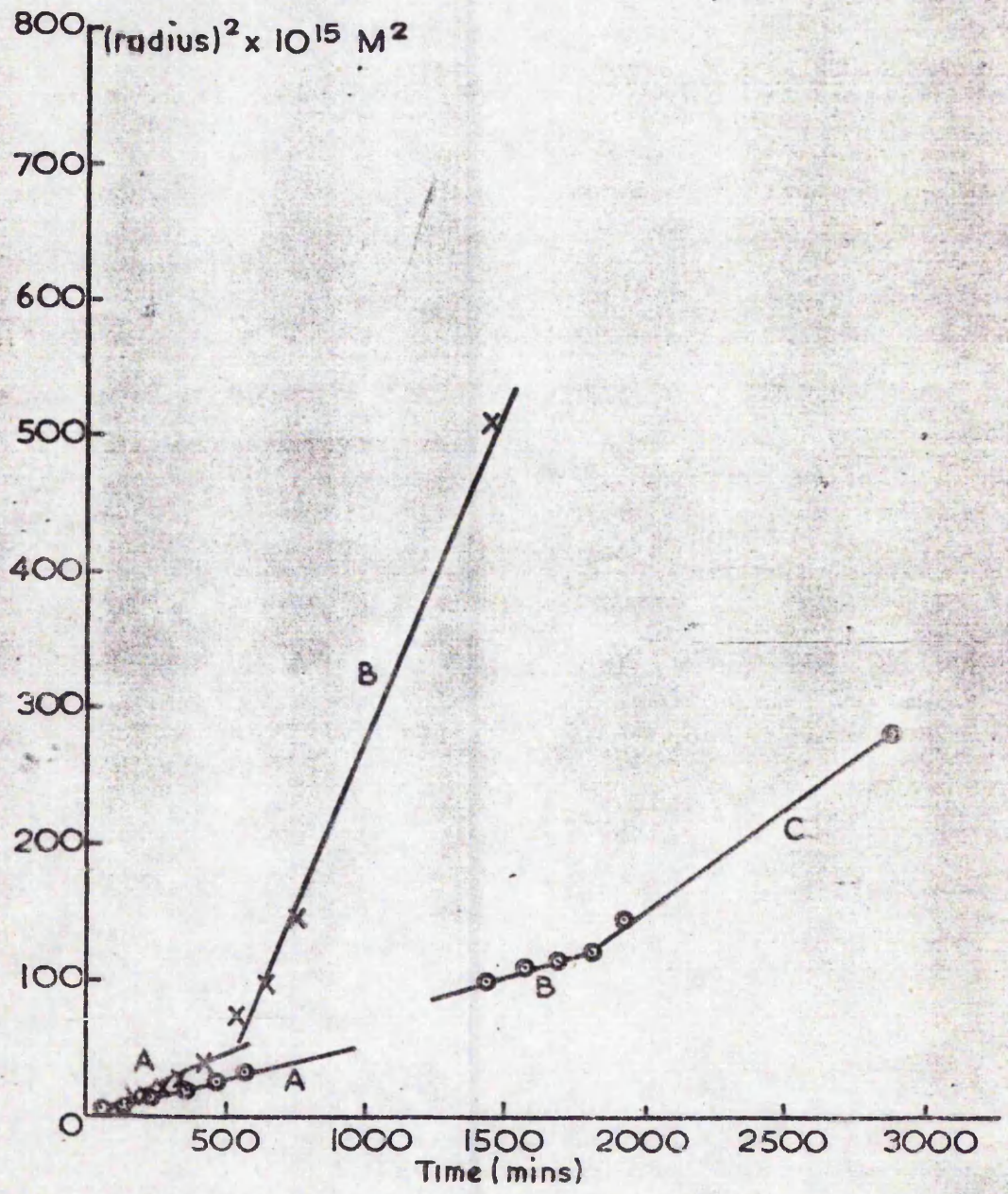

RADIUS SQUARED vs TIME PLOTS FOR 62B and 64B

FIG. 32.

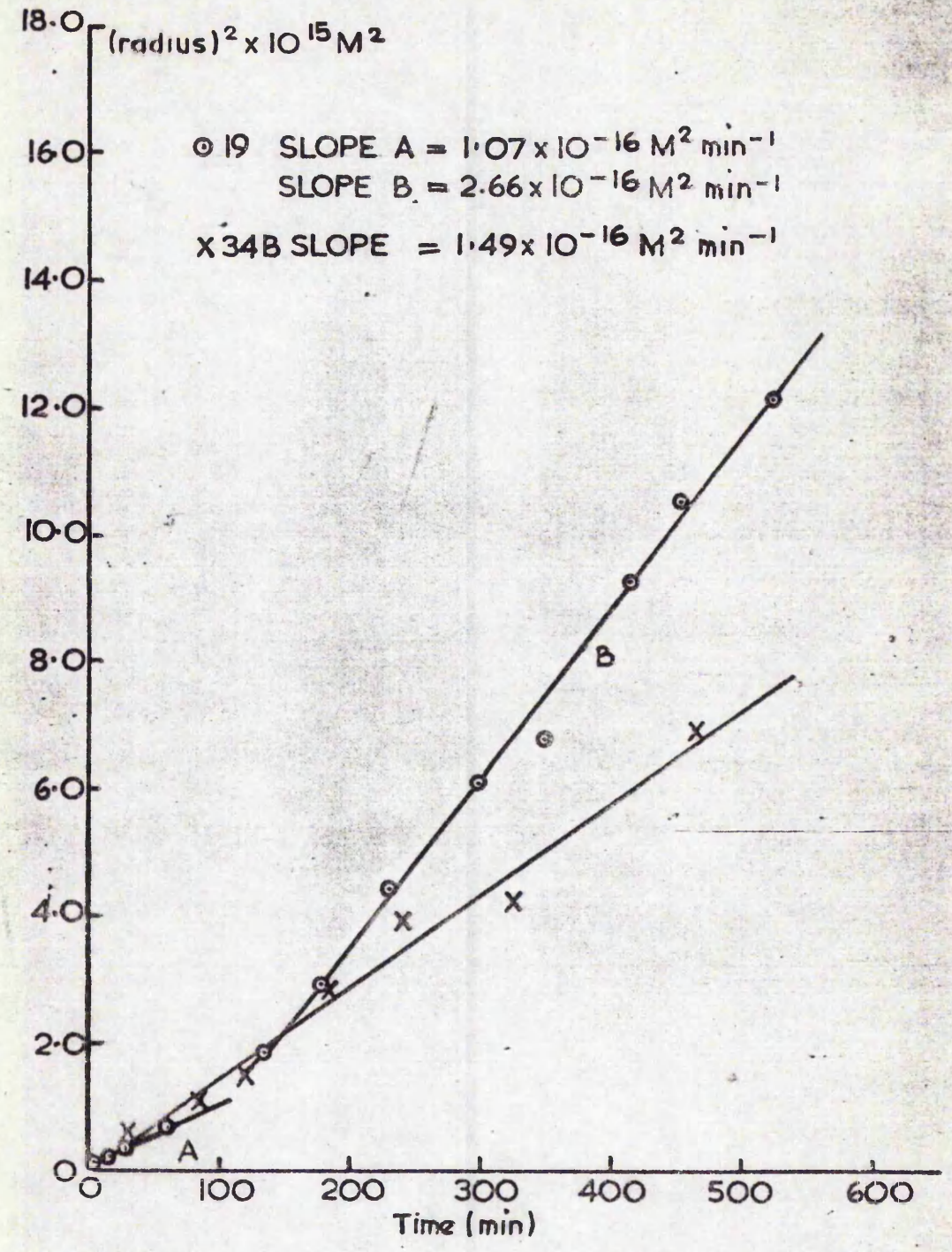

RADIUS SQUARED vs TIME PLOTS FOR 19 and 34 B

FIG. 33.

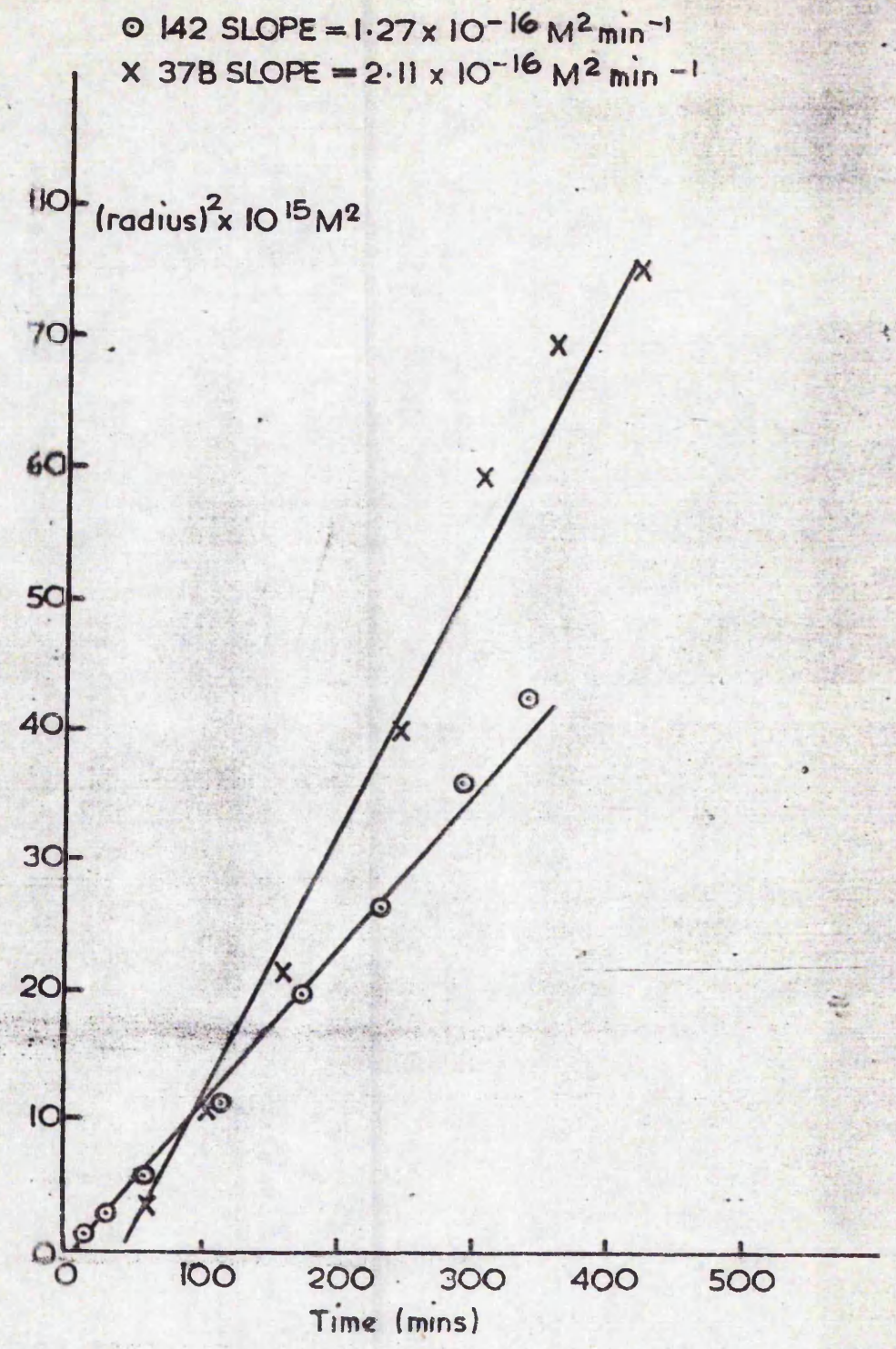

RADIUS SQUARED vs TIME PLOTS FOR 378 and 142

FIG.34.

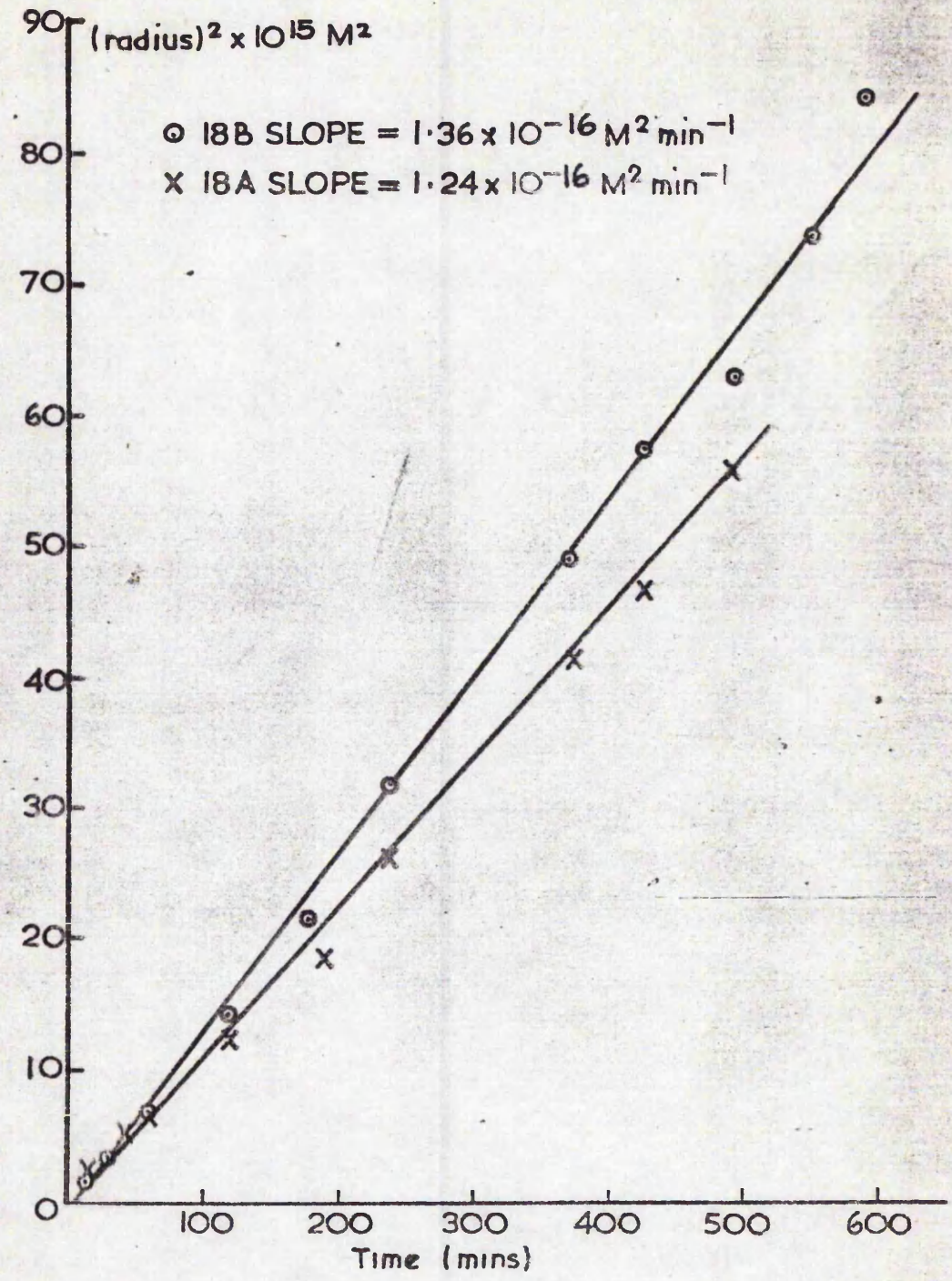

RADIUS SQUARED vs TIME PLOTS FOR 18A and 18B

FIG. 35.

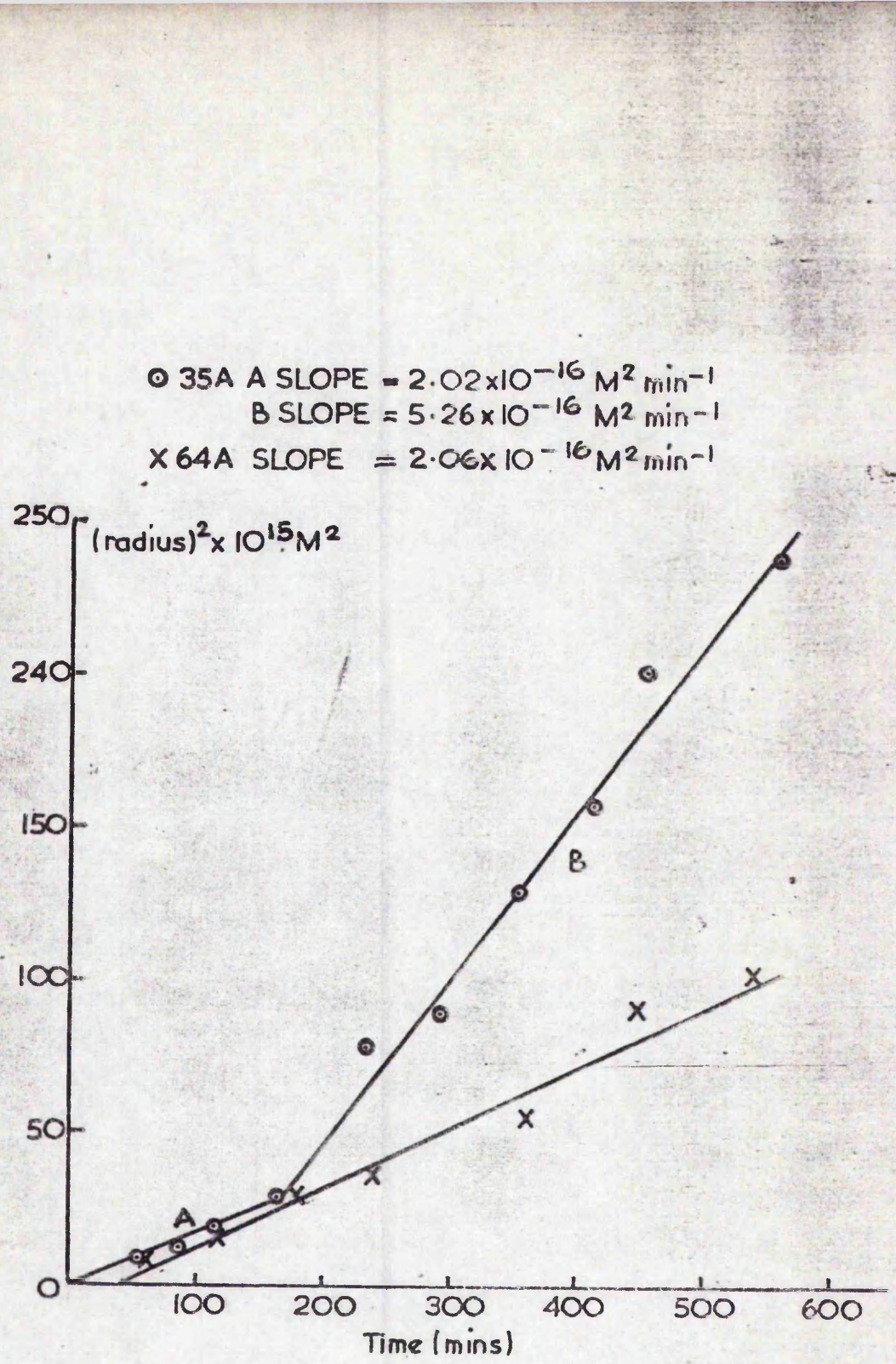

RADIUS SQUARED vs TIME PLOTS FOR 64A and 35A

FIG. 36.

⊙ 62A SLOPE = $1.95 \times 10^{-16} M^2 min^{-1}$

X 66A SLOPE = $2.90 \times 10^{-16} M^2 min^{-1}$

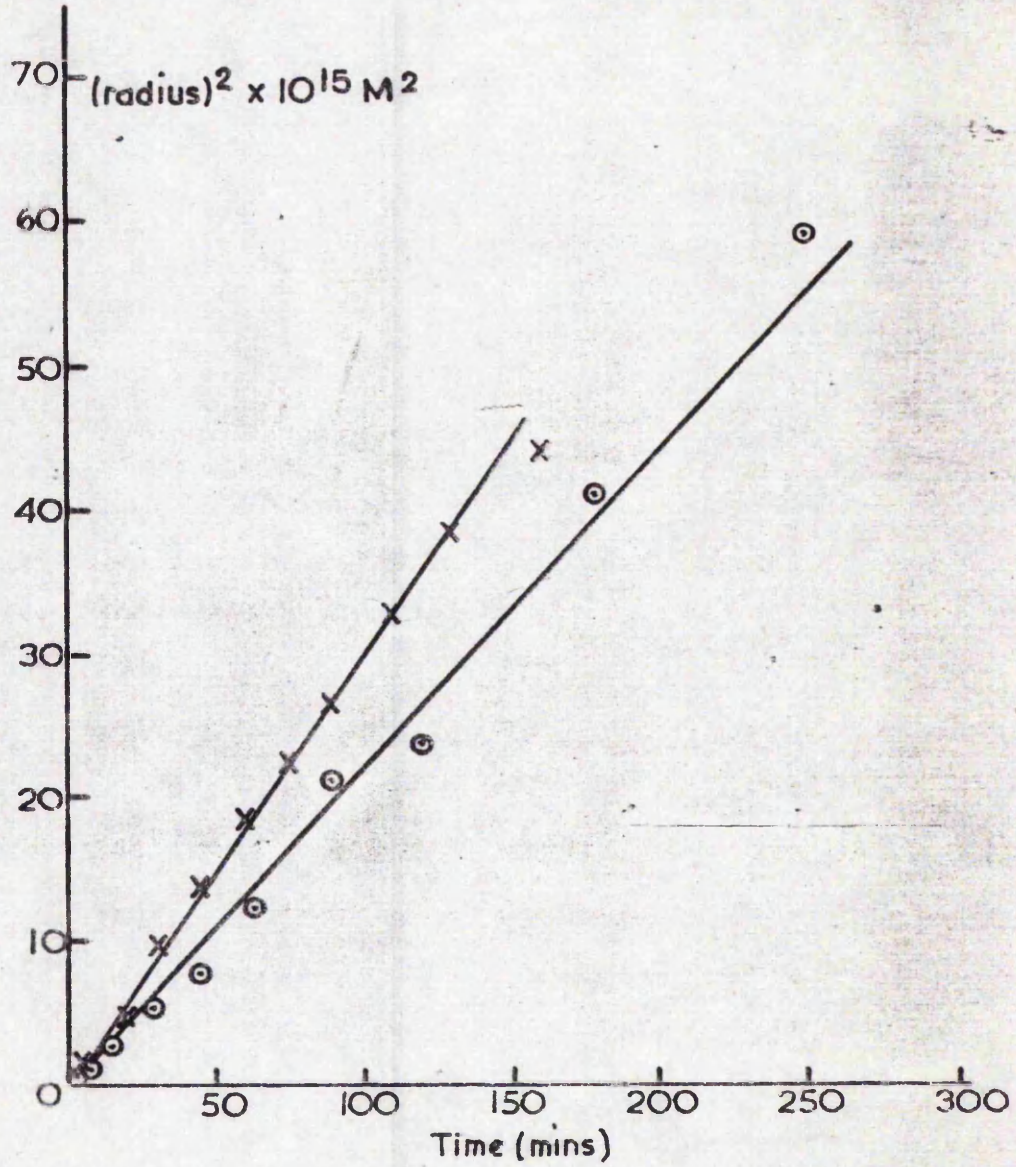

RADIUS SQUARED vs TIME PLOTS FOR 62A and 66A

FIG.37.

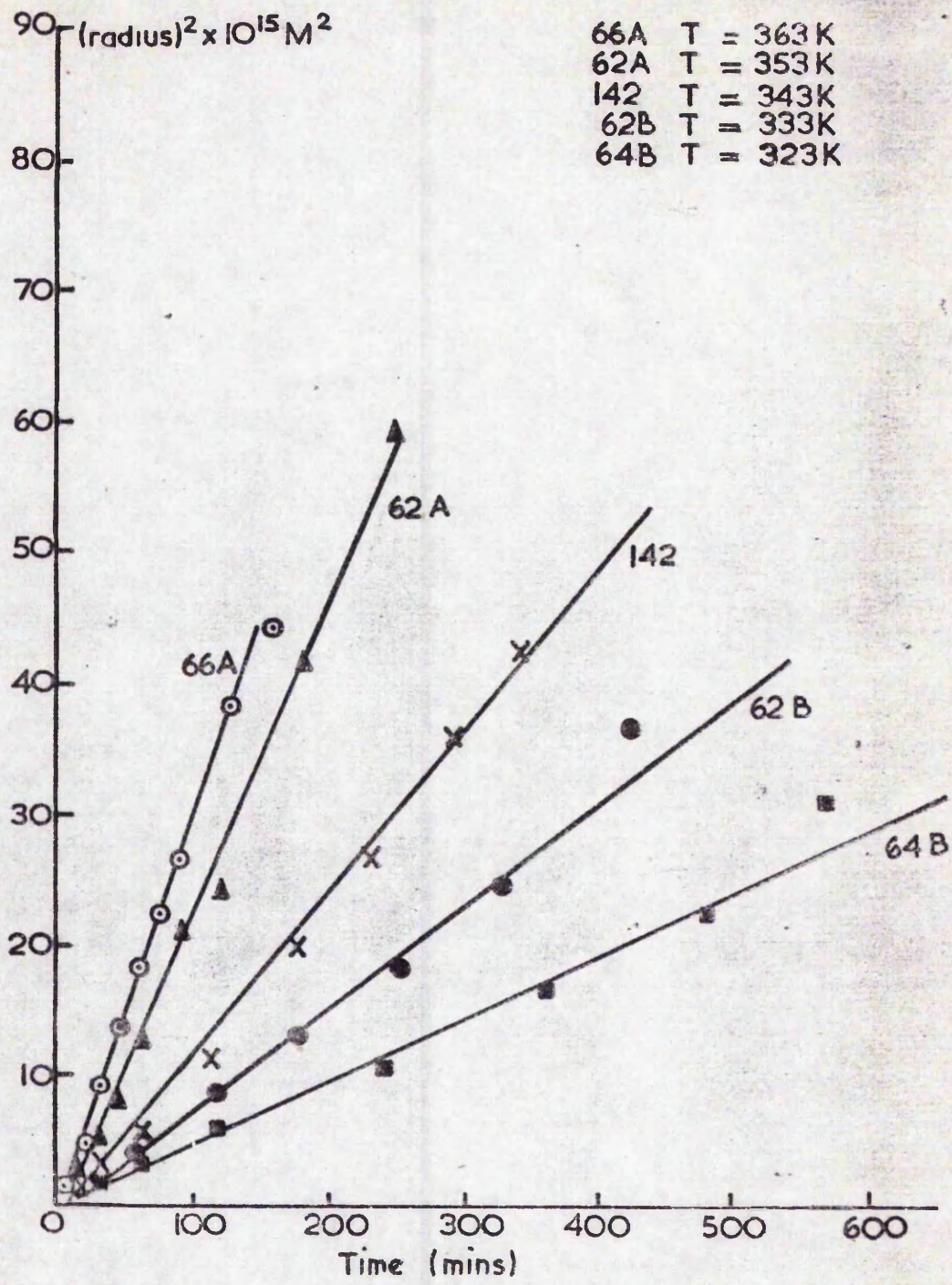

PLOTS OF RADIUS SQUARED vs TIME

FIG. 38.

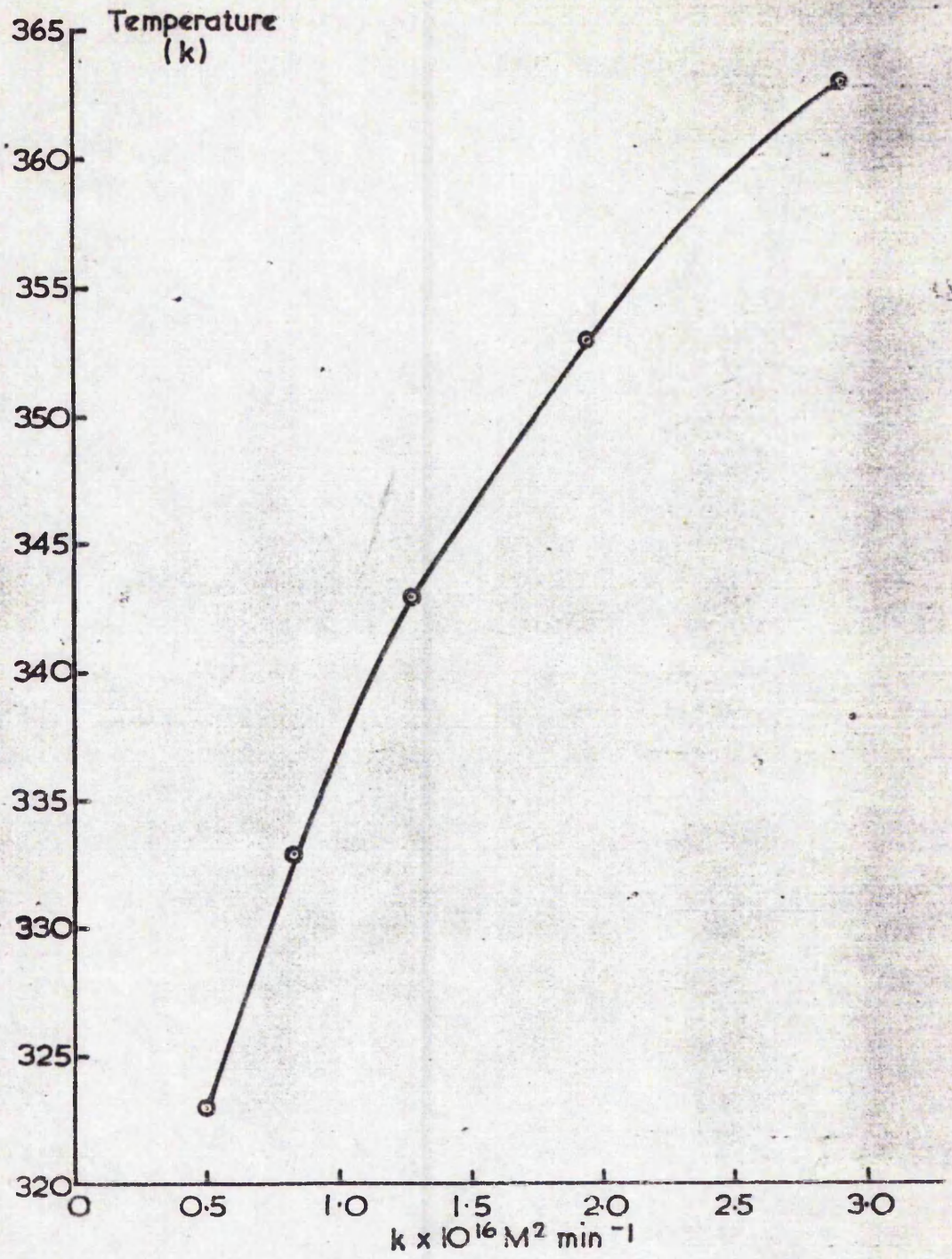

k vs TEMPERATURE

FIG.39.

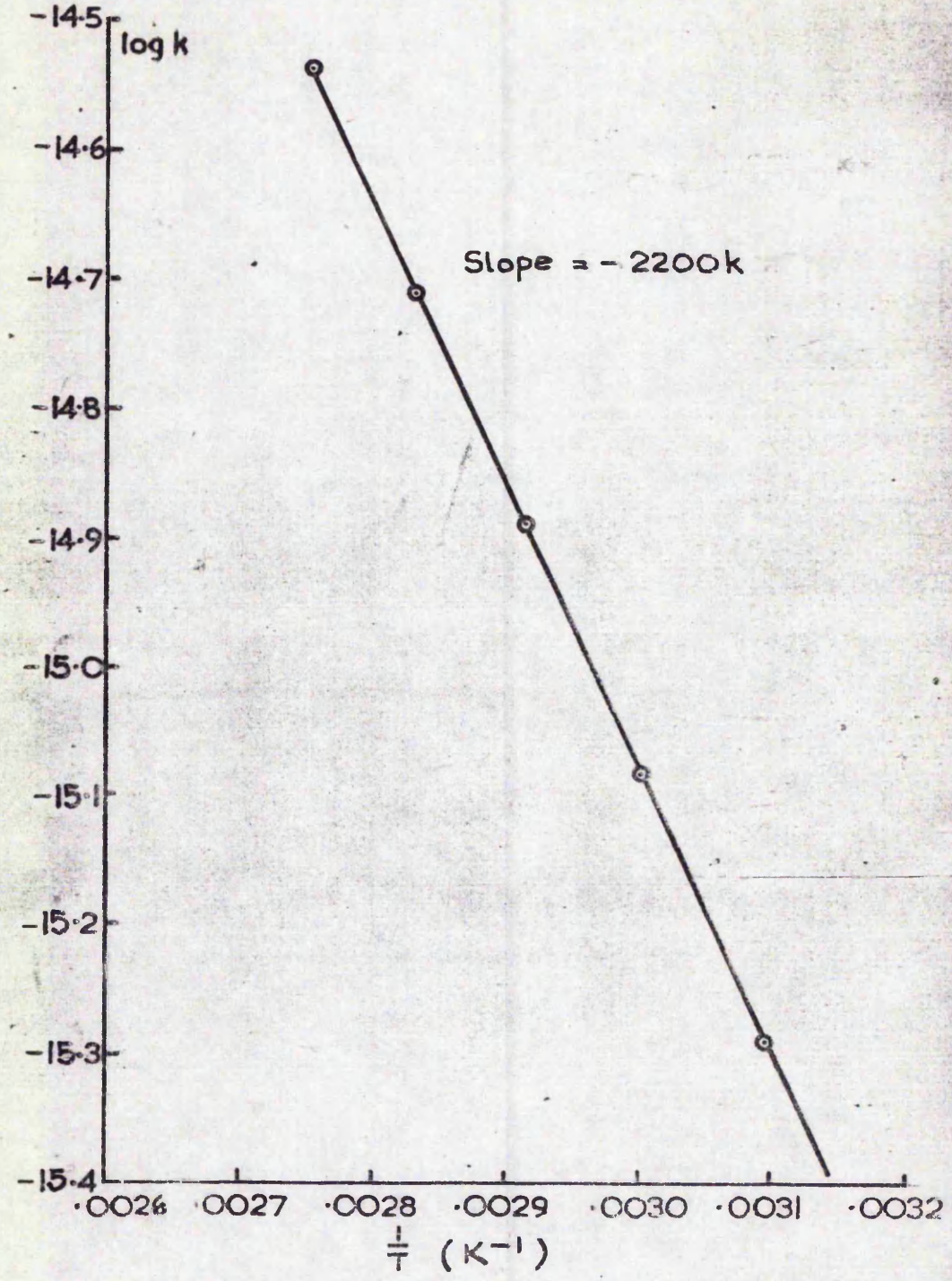

PLOT OF ARRHENIUS EQUATION FOR k

FIG. 40.

TABLE 24

VALUES OF k_1 AT DIFFERENT TEMPERATURES

Temperature (K)	k_1 (M^2 min^{-1})
323	5.12×10^{-17}
333	8.30×10^{-17}
343	1.38×10^{-16}
353	1.95×10^{-16}
363	2.90×10^{-16}

It is evident that the plot of the Arrhenius equation gives a very good straight line and that the activation energy is 2.406 kJ $mole^{-1}$. This value is 36% higher than the activation energy calculated from the variation of literature values of k_p (20) with temperature which gives an activation energy of 1.772 kJ $mole^{-1}$. The values of k_1 used in the case of reactions 62B and 64B were those determined before the second coagulation. The value of k_1 at 343 K was the average value from reactions 142 and 34B.

To obtain the rate of polymerisation of the reaction it is necessary to multiply the rate of polymerisation per particle by the total number of particles, i.e:

$$Rp = 1.5\, k_1 r\, N \quad . \qquad \text{--- (150)}$$

The factor 1.5 k_1 N for the reactions at different temperatures are given in Table 25.

TABLE 25

VARIATION IN 1.5 k_1N FOR REACTIONS AT DIFFERENT TEMPERATURES

Latex	Temperature (K)	1.5 k_1N (M^2 min^{-1} ml^{-1})
64B	323	3.72×10^{-5}
62B	333	9.27×10^{-5}
142	343	19.62×10^{-5}
34B	343	16.76×10^{-5}
62A	353	38.90×10^{-5}
66A	363	98.31×10^{-5}

2) Variation in the Value of k_1 with N.

It was noted that in the cases where a second coagulation took place the slope of the radius squared versus time plot increased, and it is also interesting to note that in the case of repeat reactions at 343 K the value of k_1 also increases with decreasing N from reaction to reaction (Table 26).

TABLE 26

VARIATION OF k_1 WITH N ml^{-1} FOR REACTIONS AT 343 K

Latex	k_1 (m^2 min^{-1})	N ml^{-1} x 10^{-12}	1.5 k_1 N (m^2 min^{-1} ml^{-1})
35A(B)	5.26×10^{-16}	.12	9.47×10^{-5}
19 (B)	2.66×10^{-16}	.40	15.96×10^{-5}
35A(A)	2.02×10^{-16}	.57	17.27×10^{-5}
19A(A)	1.07×10^{-16}	.69	11.07×10^{-5}
34B	1.49×10^{-16}	.75	16.76×10^{-5}
142	1.03×10^{-16}	1.27	19.62×10^{-5}

The values of $1.5\ k_1 N$ are all similar indicating that although the rates/particle are different, the rate/ml or the overall rate of polymerisation of the reaction remains relatively constant.

Now at constant N: $$\frac{dr^3}{dt} = 1.5\ k_1 r \ , \qquad -- \quad (151)$$

but from reaction to reaction $k_1 = f(N)$.

Both the Smith-Ewart (16) (Case III) and the Gardon (258) theories predict that if the rate of entry of free radicals into the particles increases during Interval II then $\bar{n}$, and hence the rate of polymerisation per particle also increases. The effect of reducing N during a reaction is to increase the rate of radical entry and hence $\bar{n}$ in the remaining particles. According to Gardon $\bar{n}$ can be represented as:

$$\bar{n} = 0.5 \left(1 + \left[\frac{4A}{B^2}\right] P_v\right)^{0.5}$$

A fractional decrease in N (i.e. x) would result in P_v being decreased by a factor x, and B^2 being decreased by a factor x^2, i.e. the term $\left[\frac{4A}{B^2}\right] P_v$ is increased by a factor of x.

If $1 \ll \left[\frac{4A}{B^2}\right] P_v$ then the maximum increase in $\bar{n}$, i.e. the maximum increase in the rate of reaction per particle is $x^{0.5}$. It can be seen from Table 26 (and also considering reactions 62B and 64B) that the increase in the rate of reaction in nearly all cases is greater than the square root of the decrease in N. This indicates that either:

a) the equilibrium value of $\bar{n}$ for any r is reached slowly,

b) M is variant with N,

c) Particle growth occurs via two mechanisms (i) by 'normal' polymerisation within the particle and (ii) by

the continuous formation of nuclei in solution which then undergo heterocoagulation with the primary latex particles.

It is generally assumed that $\bar{n}$ reaches an equilibrium value at any value of r rapidly and it would thus appear that process b and/or c are in operation.

It is interesting to consider the mechanism proposed by Chung li et al (175), who found that the observed rate of growth during emulsifier-free seeded polymerisations of styrene could not be explained in terms of the rate of monomer imbibition by the particles. They proposed that nucleation of fresh particles was occurring continuously in the aqueous phase and that these nuclei (monomer saturated) underwent heterocoagulation with the seed particles.

It is important to note that the system studied by Chung li et al (175) is not necessarily equivalent to the system under consideration here. Their results were based on seeded growth processes where the original seed was not initially saturated with monomer. The systems in this work, however, were nucleated in the monomer saturated aqueous phase and hence would probably be swelled with monomer. However, consideration of the equation for the variation in surface charge with particle growth of an initially highly charged nucleii indicates that as the reaction proceeds the surface charge density undergoes an initial decrease. This decrease in charge density would result in a decrease of the saturation-monomer-concentration of the particles due to the increase in the interfacial free energy (Chapter V). Typical areas/charged group obtained by Goodwin et al (141) are in the range $\sim 2 - 7$ nm^2 whereas in a soap-containing system (assuming monolayer coverage by the soap), the area per charged group is $\sim 0.2 - 0.4$ nm^2 (257). It seems likely, therefore, that soap-free polymer latices would imbibe, at equilibrium, considerably less monomer than soap stabilised latices.

An indication that the monomer concentration within the growing particles in soap-free systems is lower than

that in soap-containing systems is apparent from both the radius squared and % conversion versus time plots (Figs. 41-45). In soap-containing systems there is an inflection in the % conversion curve at ca. 55% conversion, since after this time there is sufficient polymer available to imbibe all the remaining monomer. The monomer concentration within the particles at this point is in close agreement with the saturation monomer concentration as determined by other methods such as soap titration. The rate after this point usually begins to decrease, (although a Trommsdorff gel effect could reverse this trend (52)), due to the decreasing monomer concentration at the site of reaction. In all the reactions studied in this work, however, the rate of increase of the % conversion increases throughout the reactions, and the radius squared versus time plots are linear almost up to the final conversion. This indicates that a separate monomer phase is in existence throughout the major part of the reaction and that the monomer concentration within the particles is low. It would be thought that a low monomer concentration would facilitate desorption of free radical oligomers, since a radical is only adsorbed irreversibly if, upon adsorption, it adds on sufficient monomer units to make it insoluble.

It is generally accepted that the phenomenon of secondry nucleation is due to the oligomers in solution reaching a critical chain length (in the case of homogenous nucleation) or a critical concentration (in the cases of a precipitation or micellisation type mechanism), and forming a new set of particles. For either of the above mechanisms to be in operation, either the number of particles multiplied by the radius (radical capture controlled by diffusion theory) or by the radius squared (radical capture controlled by collision theory) decreases, or the rate of desorption of free radicals is high, such that the rate of capture of oligomers is less than their rate of formation, i.e. their concentration in the aqueous phase increases.

These initial nuclei, once formed, become unstable

upon growth and, in the case of secondary nucleation, undergo coagulation with each other until a second stable set of particles is formed. This implies that the number density of these nuclei is such that they undergo coagulation with each other rather than with the primary particles. A situation can thus be envisaged where a mechanism similar to the above is in operation, but that the number of nuclei formed is such that they are far more likely to undergo heterocoagulation with the primary particles rather than coagulation with each other. This would lead to the rate of reaction being greater than that otherwise expected from a mechanism of polymerisation occurring solely within the particles.

It can be seen that if this mechanism is in operation in the systems being studied here that the number of nuclei formed will depend on both the size and number of the particles, being greater for smaller size and lower number densities, and that particles of identical size will grow faster at lower number densities. This is the trend in fact observed in this work; in the cases where N decreased during a reaction the rate of reaction per particle increased, and also in the repeat reactions at 343K the lower the particle number density, the greater was the rate of reaction per particle.

Chung li et al (175) have suggested that heterocoagulation could lead to an increased monomer concentration within the primary particles and hence an increase in the rate of reaction. There is also the possibility that [M] increases with decreasing N (in the absence of heterocoagulation) but this would involve the reaction being monomer starved as a result of the rate of diffusion of monomer being insufficient to maintain polymerisation. However, Chung li et al (175) have pointed out that this is unlikely.

The growth process in these systems would thus appear to be complex, growth occurring via a combination of two mechanisms, 'normal' polymerisation within the particles and particle nucleation and growth in the aqueous phase

followed by heterocoagulation with the primary particles. The relative contribution of the two being dependent on the size and number concentration of the original particles. The general equation for the rate of polymerisation (expressed as mole m^{-3} min^{-1}) is given by:

$$R_p = k_p [M] [R^\bullet] . \quad -- (152)$$

To obtain the rate of polymerisation per particle it is necessary that [M] and [$R^\bullet$] be multiplied by the particle volume (v) and that k_p be divided by v i.e.:

$$R_p = \frac{k_p}{v} [M] [R^\bullet] \ v^2. \quad -- (153)$$

However, $[R^\bullet] = \frac{\bar{n}}{N_A v}$, -- (154)

and thus, $R_p = k_p[M] \frac{\bar{n}}{N_A}$ (M^3 $particle^{-1}$ min^{-1}), -- (155)

where: k_p is in M^3 $mole^{-1}$ min^{-1}

$\bar{n}$ is in $particle^{-1}$

N_A is in mole

[M] is in mole M^{-3}

To express R_p in terms of volume it is necessary to multiply the right hand side of the equation by the monomer molecular weight and divide it by the polymer density. Thus:

$$R_p = 99.05 \times 10^{-6} \ k_p \ \frac{[M] \ \bar{n}}{N_A} \ (M^3 \text{ particle}^{-1} \text{ min}^{-1})$$

$$R_p = k' [M] \bar{n} \quad \text{where} \quad k' = \frac{k_p \times 99.05 \times 10^{-6}}{N_A} \quad -- (156)$$

-- (157)

It is also necessary to take into account the contribution to growth from heterocoagulation. The increase in the particle volume would be $\frac{P_A}{N}$, where P_A is the total volume of polymer formed outside the particles in the aqueous phase and N is the total number of particles present. The overall equation would thus be:

$$R_p = k' [M] \bar{n} + \frac{P_A}{N} = 1.5\, k_1 r \quad (M^3 \text{ particle}^{-1} \text{ min}^{-1}) \qquad -- (158)$$

3) Variation of % Conversion with Time.

The data for the various kinetic runs is represented graphically in Figs. 41-45,46-52. All the curves obtained were convex to the time axis, in contradiction to Smith and Ewart (16) predictions, but in agreement with the predictions of Gardon (45,258). None of the curves in which data points were obtained up to final % conversion showed an inflection point. In the reactions where a second coagulation occurred, it was only readily apparent in the curve for 62B. That it was not detected in the other reactions was probably a result of a less pronounced decrease in N which occurred at a lower % conversion.

The % conversion was found to fit the relationship:

$$\% C = At^2 + Bt , \qquad -- (159)$$

where A & B are constants and t is time, as predicted by the theory of Gardon. The data was plotted in the form $\frac{\% C}{t}$ vs t, where the slope of the graph (determined using least squares) is A and the intercept B. It should be noted that the constants A and B are not the same as in the Gardon theory since t was taken from the start of the reaction and % conversion was used rather than volume of polymer formed. It can be seen that in most cases the data fits the equation well except during the initial stages of the reaction when N was varying. It may be noted that the scatter of the data points from the line of best fit was greater here than was the case for the radius squared versus time plots.

In the cases of reactions where N decreased a second time the slope of these plots changed as did those of the radius squared versus time plots.

The values of the constants (A and B) for the various reactions are given in Table 30 (Appendix I), in the form in which they could be used for determining the particle radius. They were determined in the following manner:

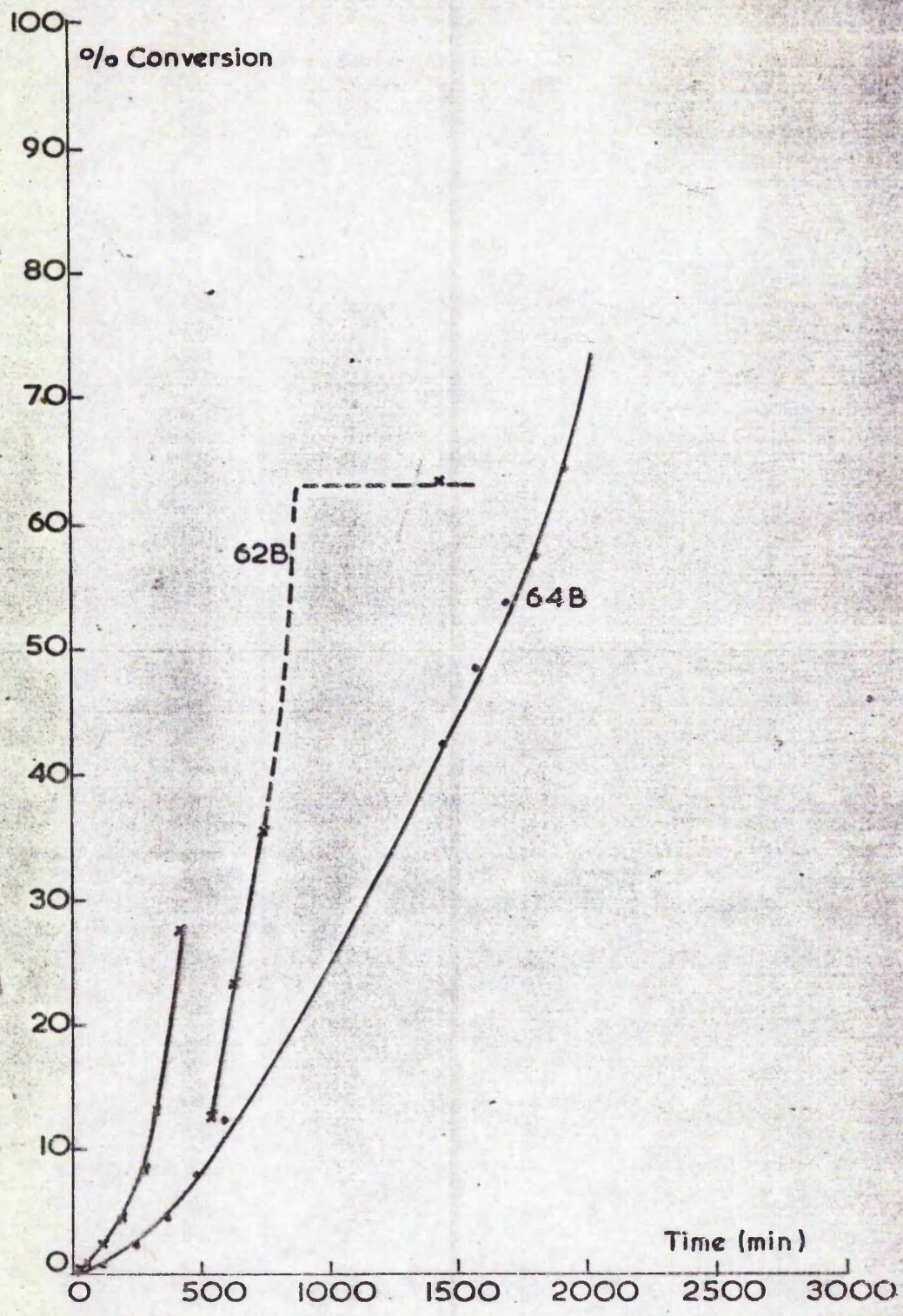

% CONVERSION vs TIME CURVES FOR 64B & 62B

FIG. 41.

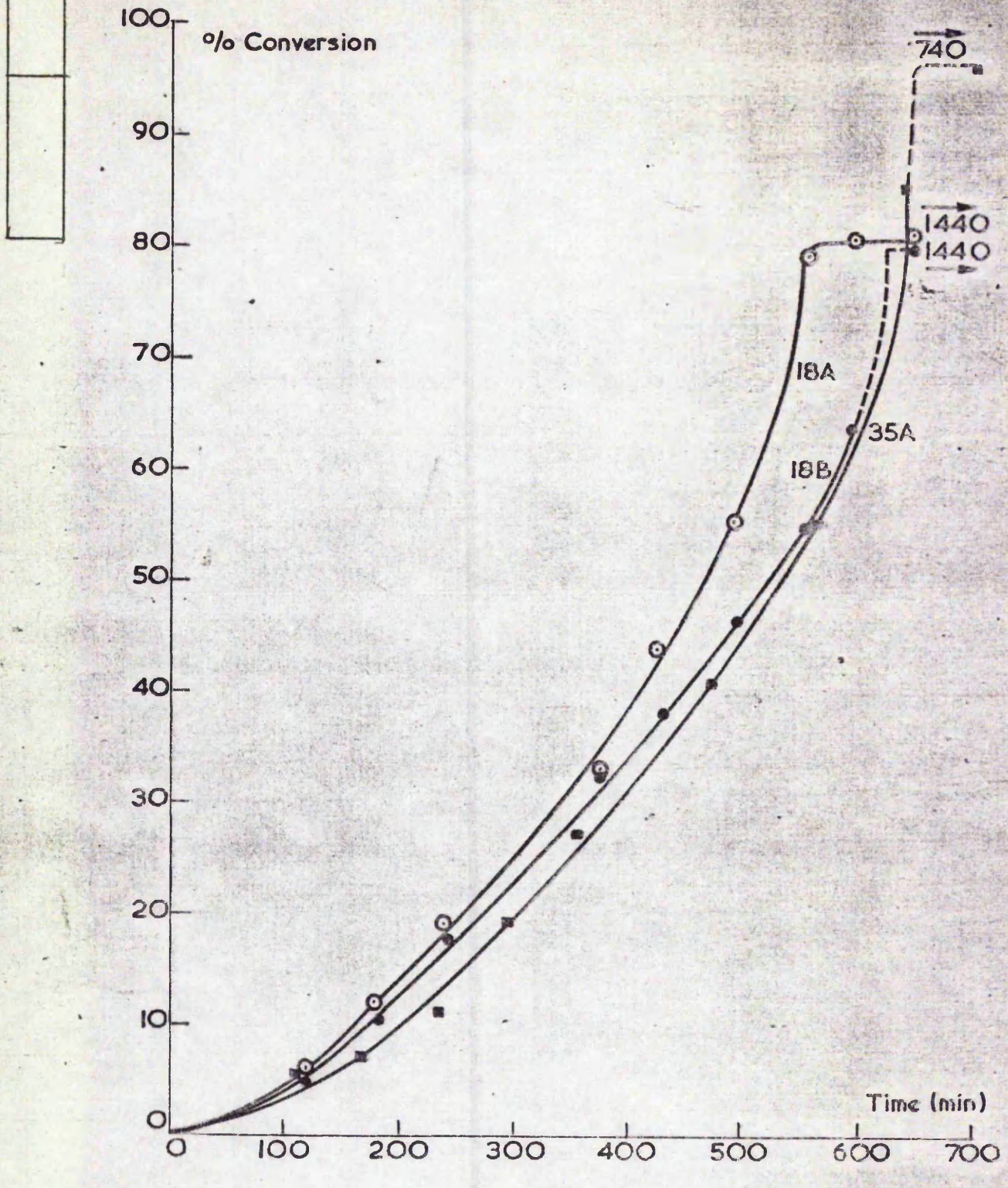

% CONVERSION vs TIME CURVES FOR 18A, 18B & 35

FIG. 42.

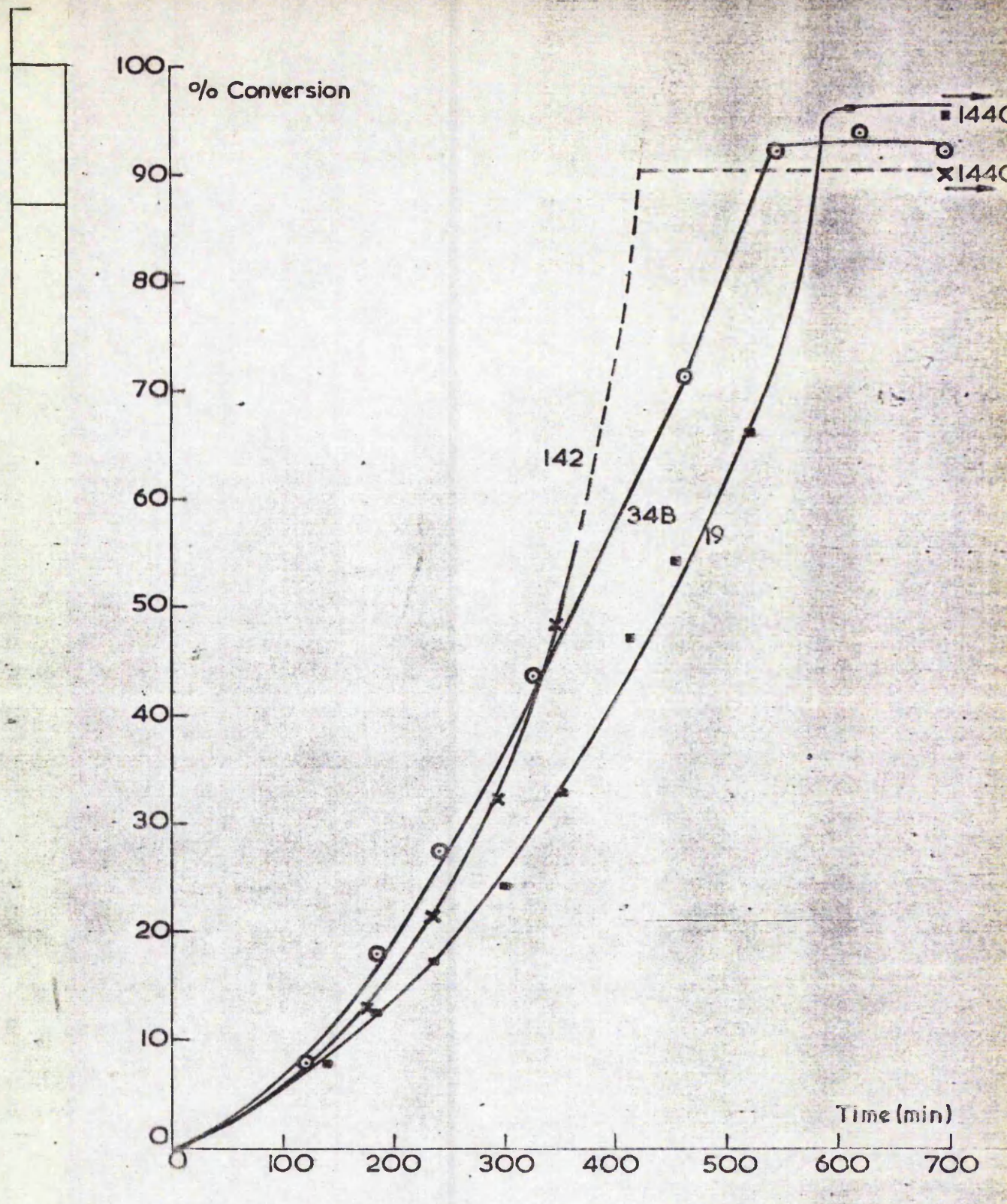

% CONVERSION vs TIME CURVES FOR 34B, 19 & 142

FIG. 43.

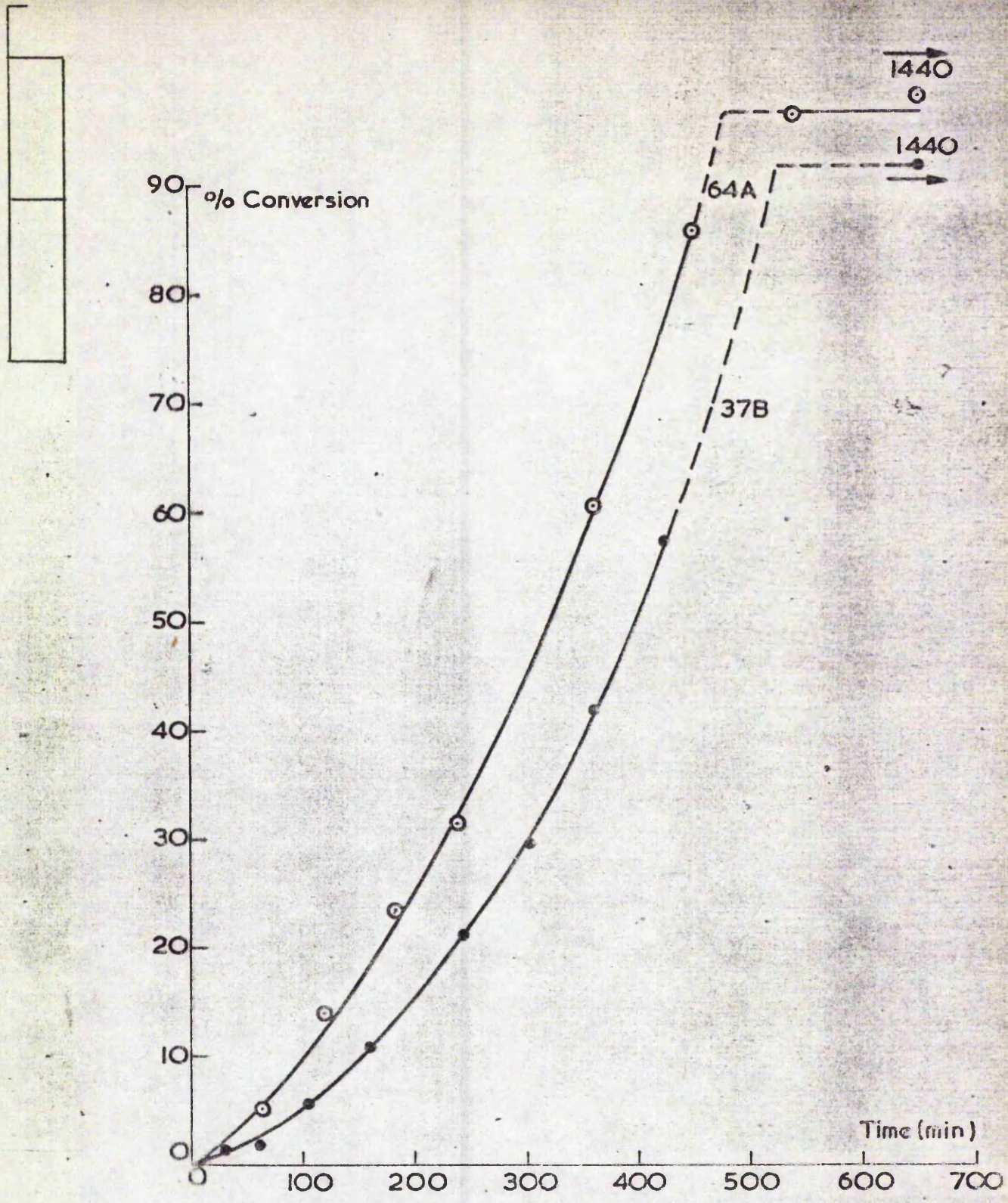

% CONVERSION vs TIME CURVES FOR 64A & 37B

FIG. 44.

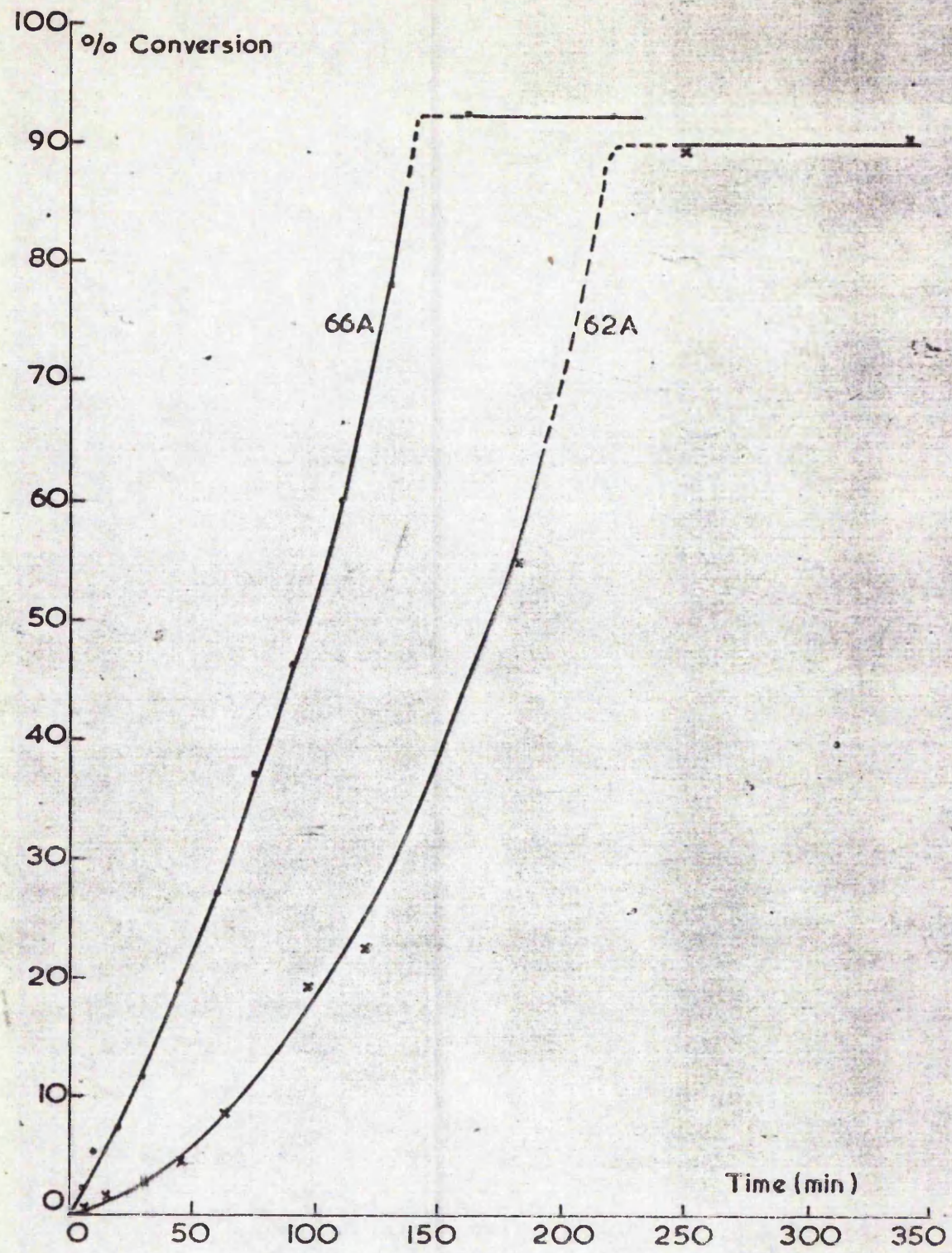

% CONVERSION vs TIME CURVES FOR 62A & 66A

FIG. 45.

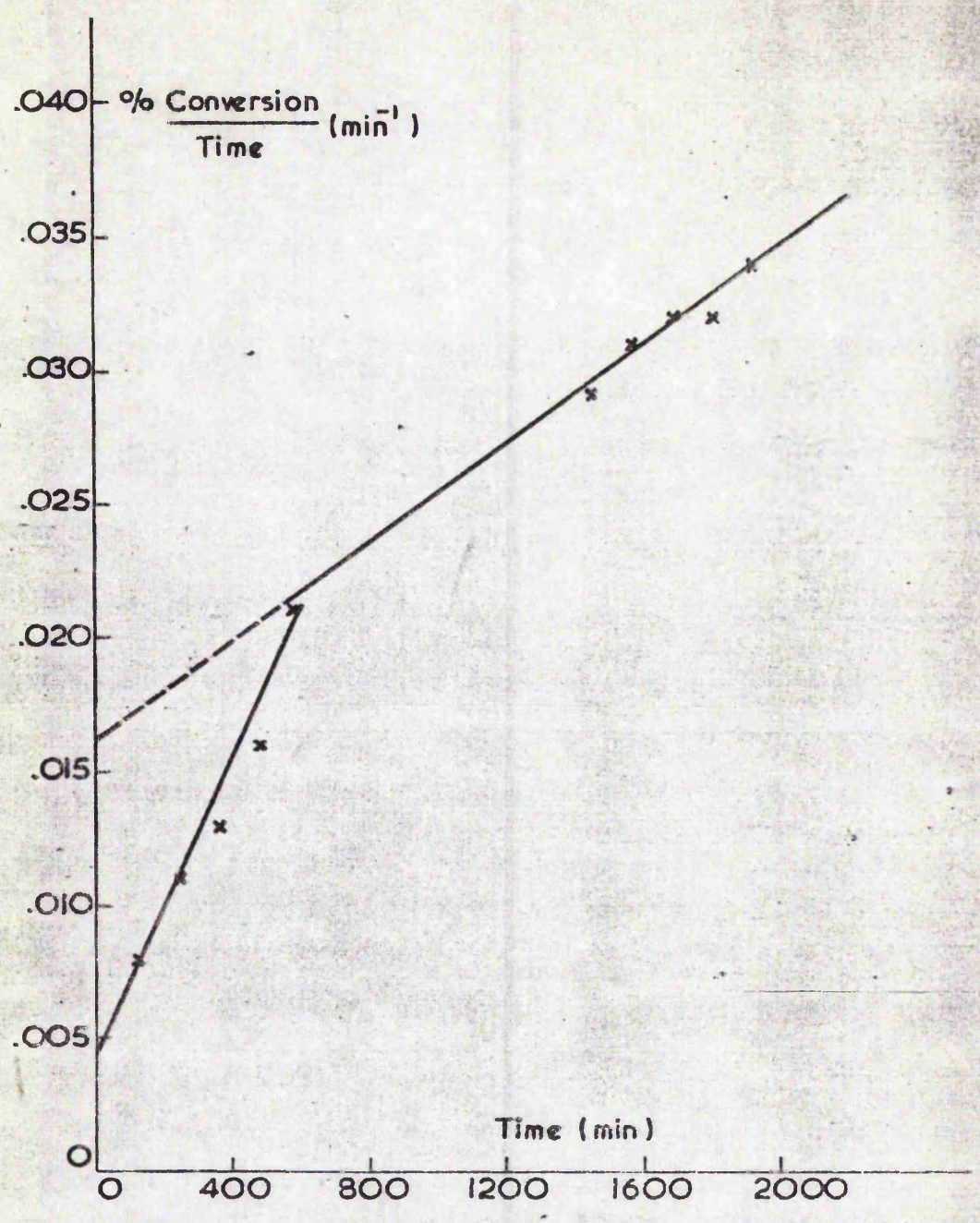

PLOT OF % CONVERSION / TIME vs TIME FOR REACTION 64B

FIG. 46.

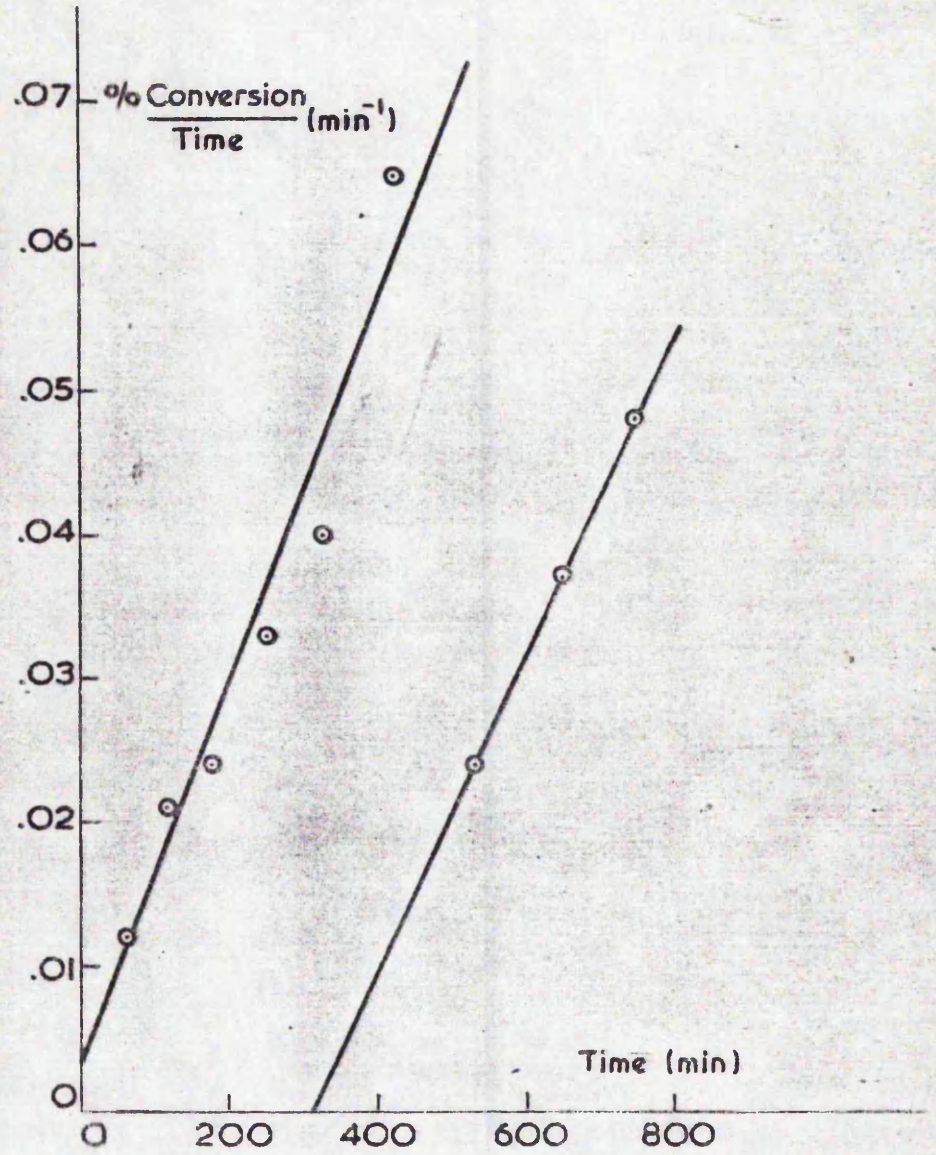

PLOT OF % CONVERSION / TIME vs TIME FOR REACTION 62B

FIG. 47.

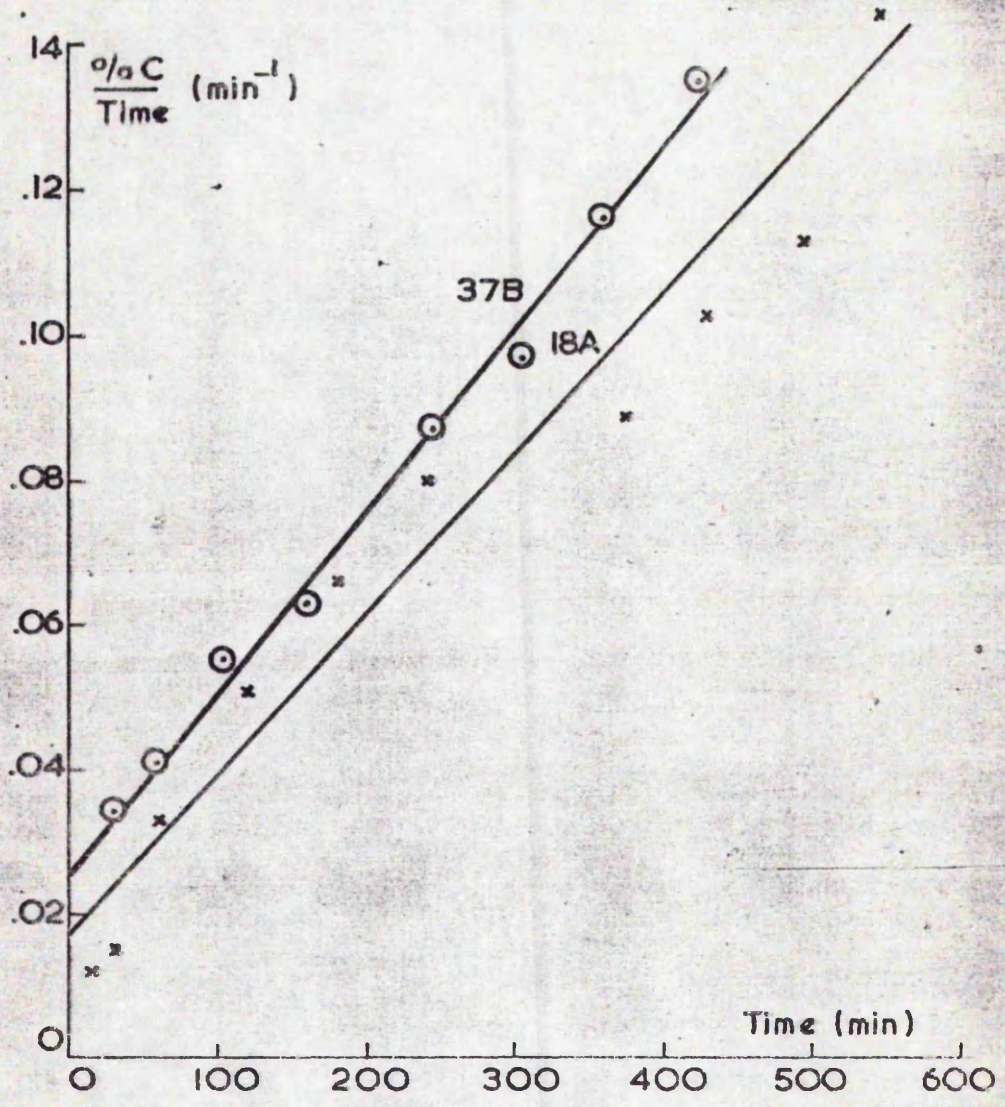

PLOTS OF % CONVERSION / TIME vs TIME

FOR REACTIONS 37B & 18A

FIG. 48.

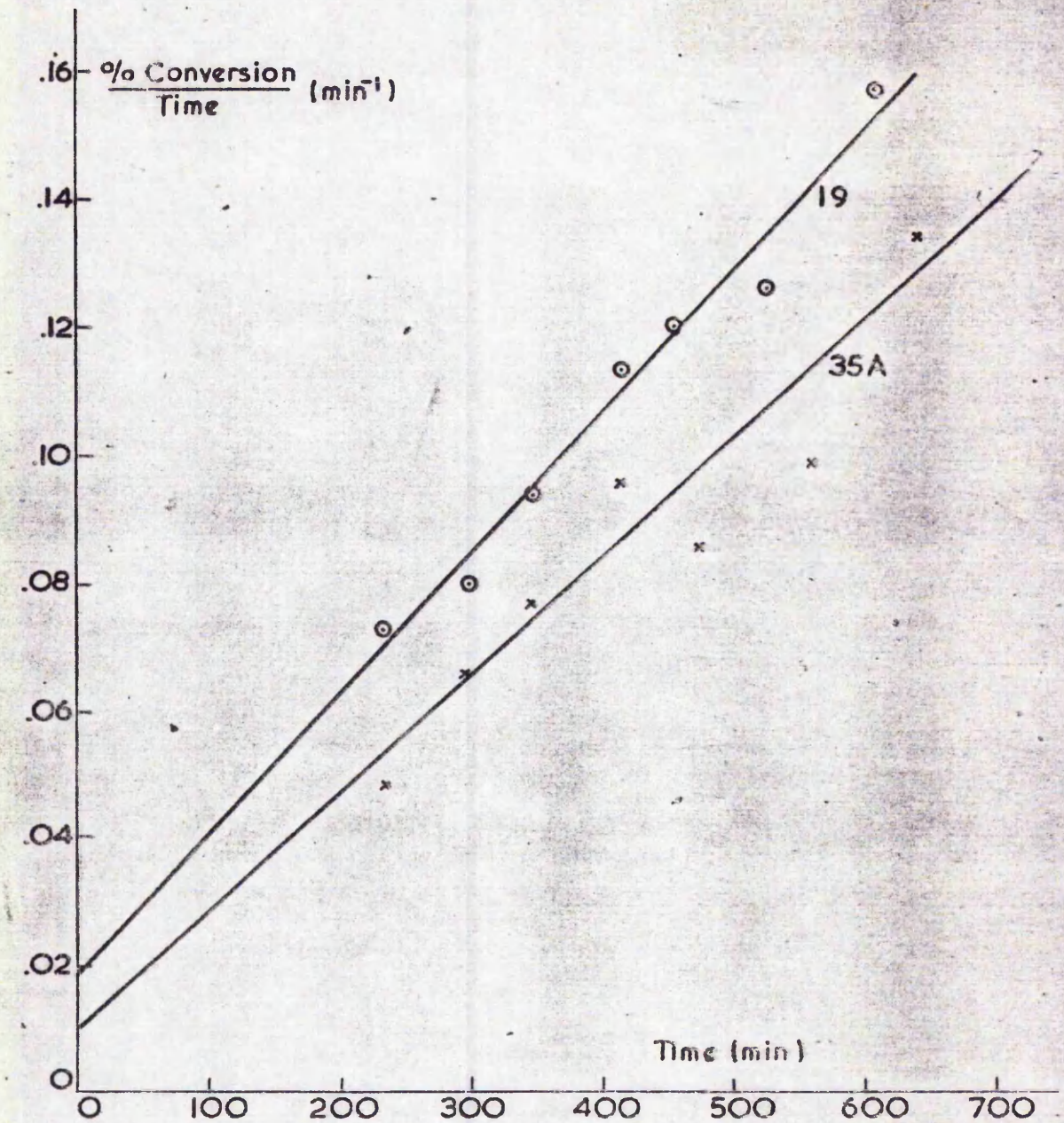

PLOTS OF % CONVERSION / TIME vs TIME FOR REACTIONS 19 & 35A

FIG. 49

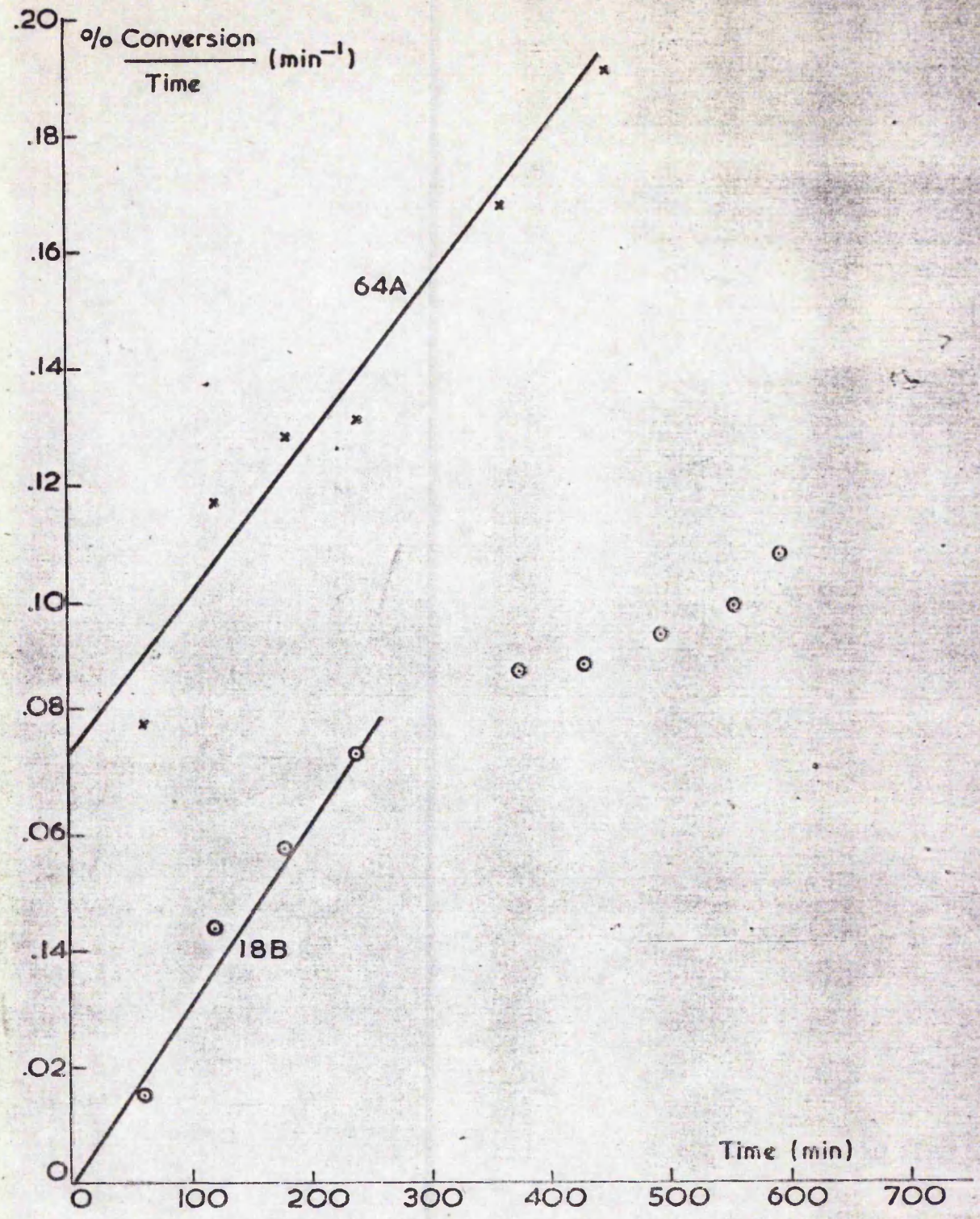

PLOTS OF % CONVERSION / TIME vs TIME FOR REACTIONS 64A & 18B

FIG. 50.

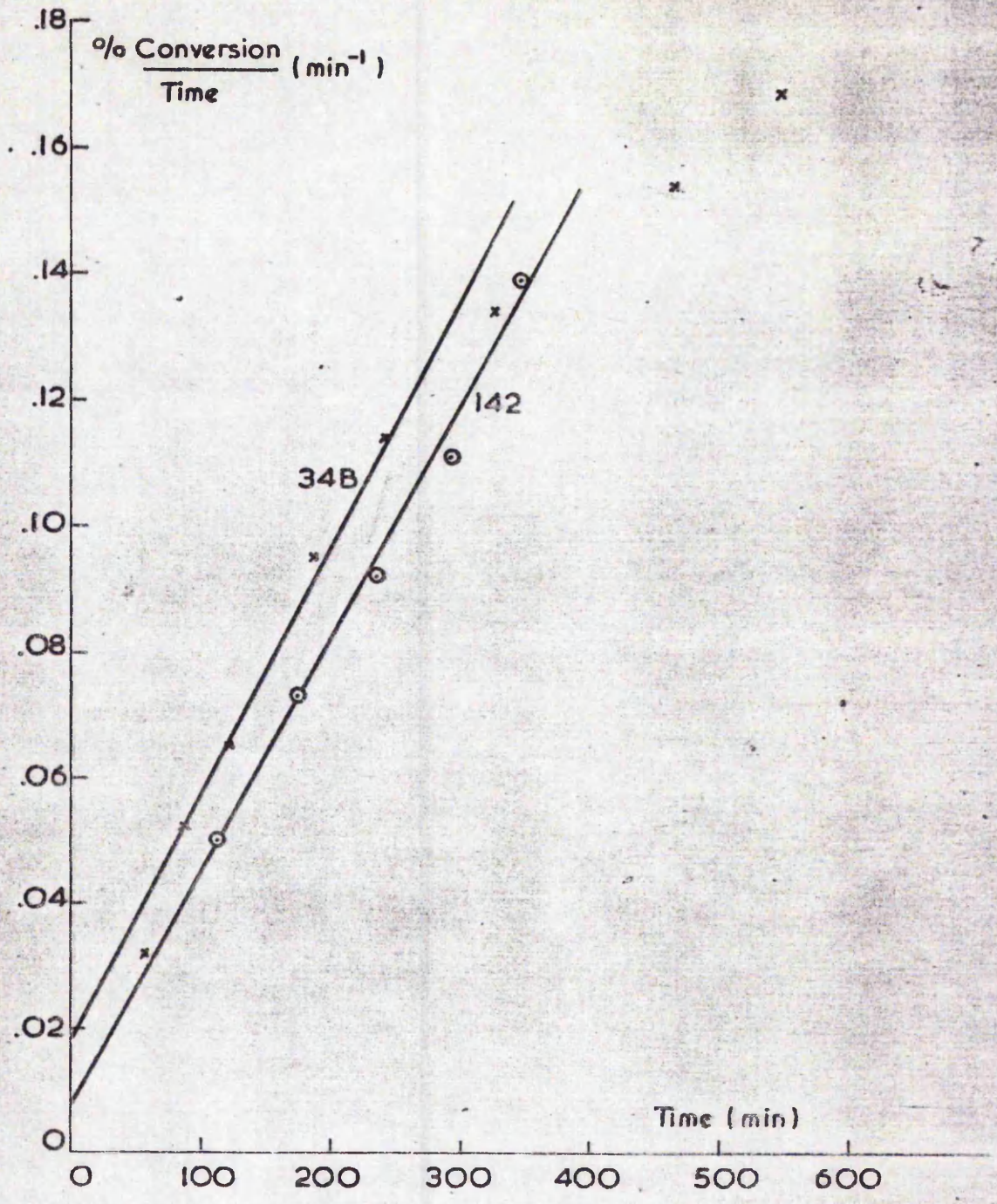

PLOTS OF % CONVERSION / TIME vs TIME FOR REACTIONS 34B & 142

FIG. 51.

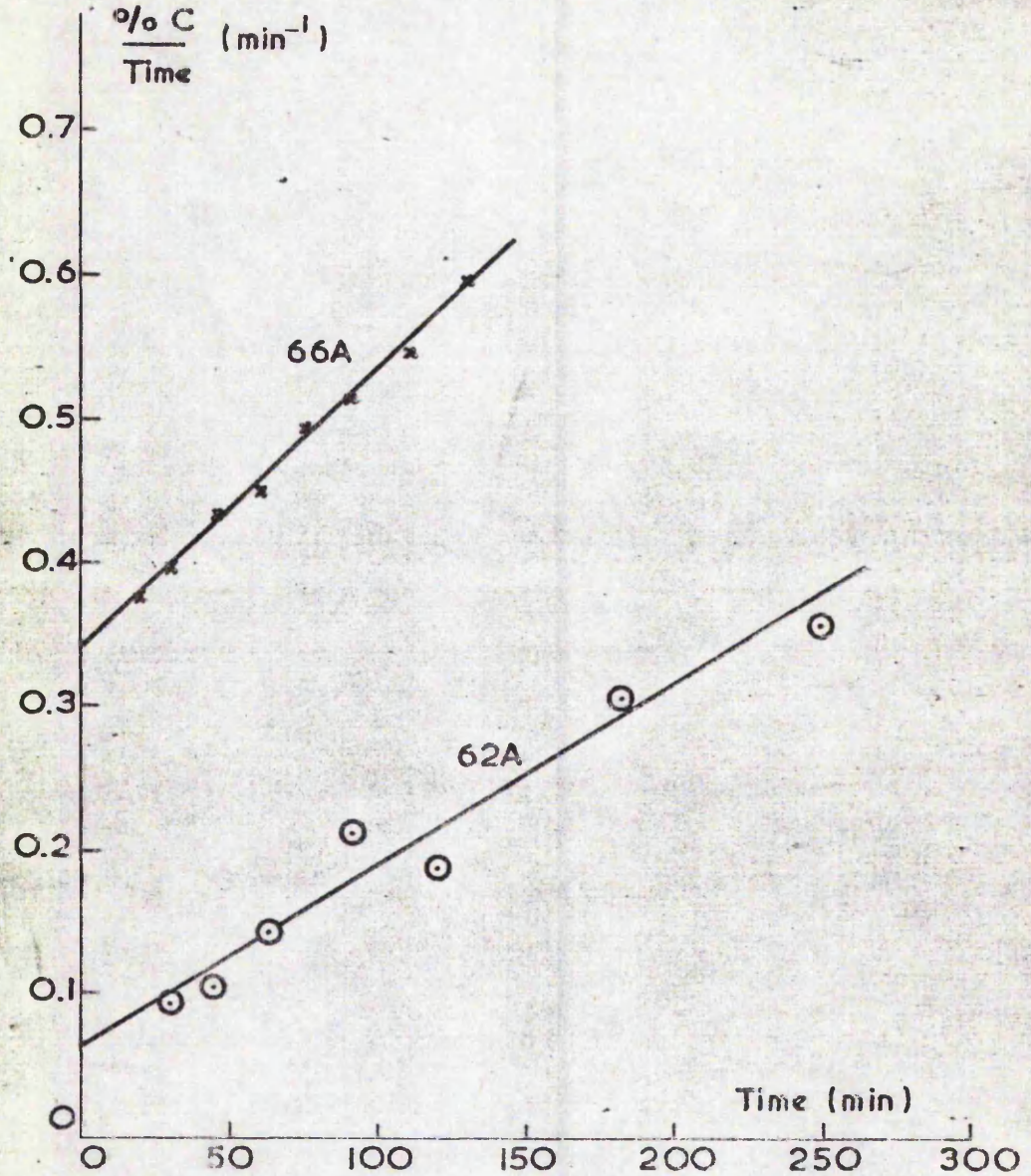

PLOTS OF % CONVERSION / TIME vs TIME FOR REACTIONS 66A & 62A

FIG. 52.

$$\% C = At^2 + Bt \quad , \qquad -- \quad (160)$$

$$\% C = \frac{100\ w}{4/3\ \pi\ r^3 \rho\ N_{total}} \quad , \qquad -- \quad (161)$$

where w is the weight of the monomer charge

ρ is the polymer density.

$$\text{i.e.} \quad r^3 = \frac{300\ w}{4\ N_{total}} \cdot \frac{1}{At^2 + Bt} \qquad -- \quad (162)$$

The value of A derived from the graphs is invariant with time. However, the value of B depends both on A and on the time taken for the initial decrease in N to occur.

J) The Applicability of the Theory of Soap-Present Emulsion Polymerisation to Soap-Free Systems.

Although Gardon states that the equations he derived were only applicable to soap-containing systems, it would be thought that his equations for Interval II (i.e. after particle nucleation) would be applicable to polymerisations carried out in the absence of soap, provided that N remained constant, which, in the majority of cases it did.

The equations of Gardon were derived to describe the polymerisation system from particle initiation to the end of Interval II in terms of variables which could be determined independently. It can be seen that his equations describing particle nucleation are obviously not applicable to soap-free systems since they include parameters dependent upon the added soap. However, upon derivation of equations for $\bar{n}$, the relationship between % conversion and time and molecular weight and time; the parameters involving the surfactant (which are included as the prediction of N) can be replaced by the observed value of N. For example, the equation describing the volume of polymer formed:

$$P = At^2 + Bt \quad , \qquad -- \quad (163)$$

where

$$A = 0.102 \left(\frac{k_p^{1.94}}{k_t^{0.94}}\right)\left(\frac{d_m}{d_p}\right)^{1.94}\left(\frac{\Phi_m^{1.94}}{(1-\Phi_m)^{0.94}}\right)\left(\frac{\rho}{N_A}\right) \qquad -- \quad (164)$$

and B (the Smith-Ewart rate) is given by:

$$B = 0.5 \left(\frac{k_p}{N_A}\right) \left(\frac{d_m}{d_p}\right) \Phi_m \bar{N} , \qquad -- (165)$$

does not contain any parameters associated solely with soap-containing systems.

It was hoped that the applicability of Gardons' theory for Interval II to soap-free systems could be tested during the course of this work. However, from the preceding discussion it would appear that there are two significant differences between soap-free and soap-containing systems during this Interval:

a) That not all the observed growth occurs within the particles, a significant amount occurring in the aqueous phase.

b) That the monomer concentration within the particles is not homogenous and that it is also likely to be considerably lower than that within soap-containing systems, and may even vary as the reaction proceeds.

The main premise for Interval II kinetics is that growth occurs solely within the particles. The growth is a function of $\bar{n}$, the average number of free radicals within a particle, which is itself a function of the rate of entry of radicals into particles, the size of the particles and the monomer concentration within the particles (which affects the rate of termination). It would appear that the rate of growth in soap-free systems is not solely dependent on $\bar{n}$, but also has a contribution from P_A the amount of polymer formed outside the particles which itself will depend on the number and size of the particles in the system, and the rates of radical generation and irreversible capture.

K) The Physical Significance of the Rate of Polymerisation being Proportional to r.

It has been shown in this work that when the particle radius squared was plotted against time a good straight line resulted and also that the radius cubed was equal to $(At^{\frac{1}{2}} + Bt)$, i.e. that:

(1) $r^2 \propto t$ or $r \propto t^{0.5}$, and

$$(2)\quad r^3 = At^2 + Bt \qquad \text{or} \qquad r = (At^2 + Bt)^{.33}.$$

In case (2) the constant A was in general 100 times less than B. Hence after 100 minutes of reaction time the contributions from the two would be about the same and at times greater than 100 minutes the A term would become dominant, i.e:

$$r^3 \propto t^2 \qquad \text{or} \qquad r \propto t^{0.67}$$

Thus, it might be expected that $\frac{r^3}{t}$ vs. t would give a reasonable description of the experimental data. However, since the 'classical' theories of emulsion polymerisation would not appear to be applicable to these systems, it is likely that $r^3 = At^2 + Bt$ is a reasonable approximation of $r^3 \propto t$ rather than vice-versa.

That R_p is proportional to r may reflect a diffusion controlled mechanism of transfer of reactant, and polymeric material from the aqueous phase to the particles.

L) Variation in Molecular Weight with Reaction Time.

Molecular weight determinations were carried out on freeze-dried samples using both membrane osmometry and gel permeation chromatography. The results are summarised in Table 27A and Figs. 53 54 , and a typical set of gel permeation chromatographs are shown in Fig. 55 . It can be seen that there is a general trend of increasing molecular weight with % conversion (as predicted by the Gardon theory). However, in the cases of reactions 142 and 64A the curve is concave to the time axis, whereas those of 34B and 35A are convex to the time axis.

In the two cases 34B and 35A the polydispersity of the polymer produced as described by $\frac{\bar{M}_w}{\bar{M}_n}$ is quite broad compared to those reported by Kotera et al(140). The number average molecular weight is described by:

$$\bar{M}_n = \frac{\sum_{i=1}^{\infty} M_i N_i}{\sum_{i=1}^{\infty} N_i} \quad , \qquad \text{--- (166)}$$

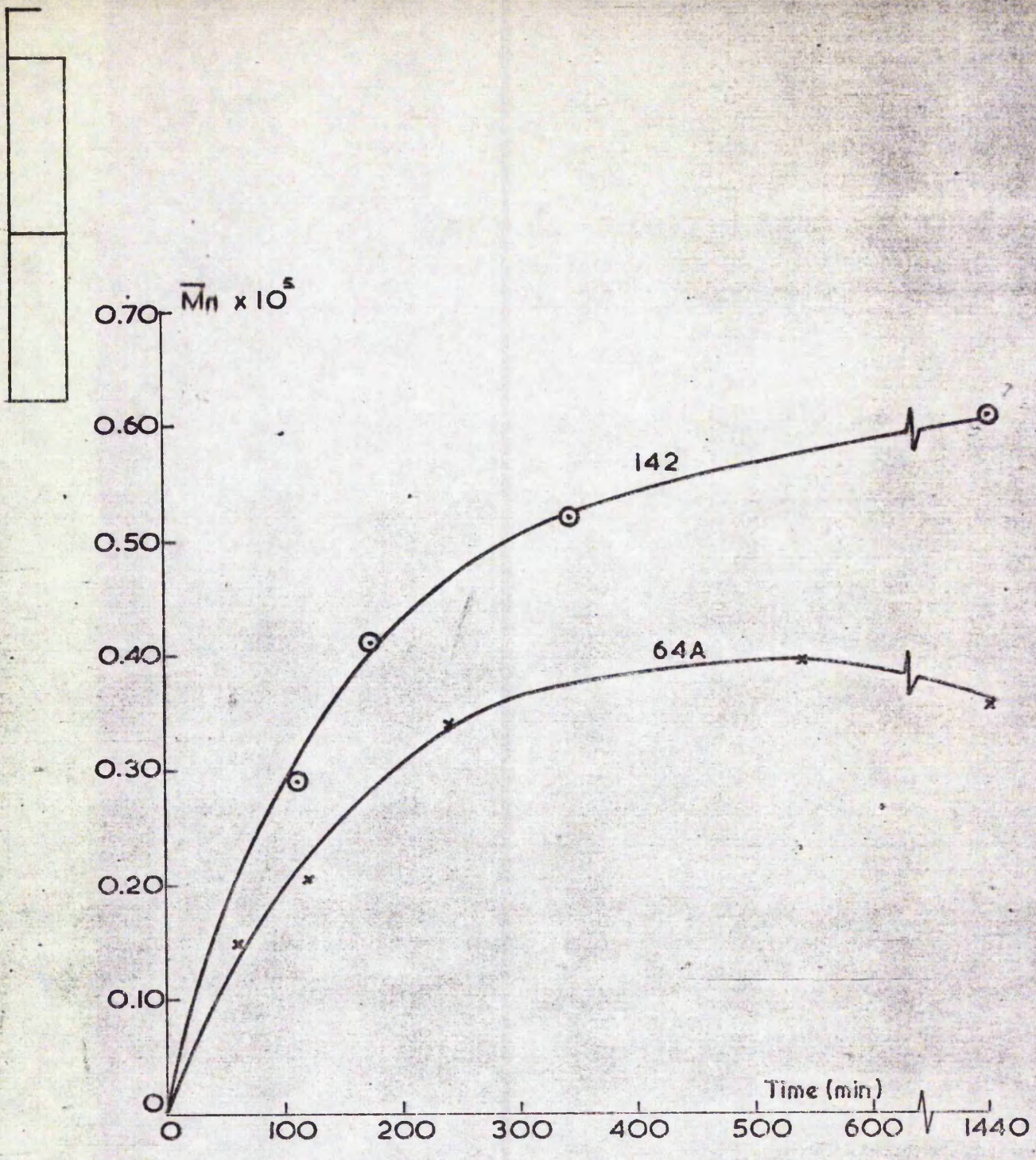

VARIATION OF MOLECULAR WEIGHT ($\overline{Mn}$) WITH TIME FOR REACTIONS 142 & 64A

FIG. 53.

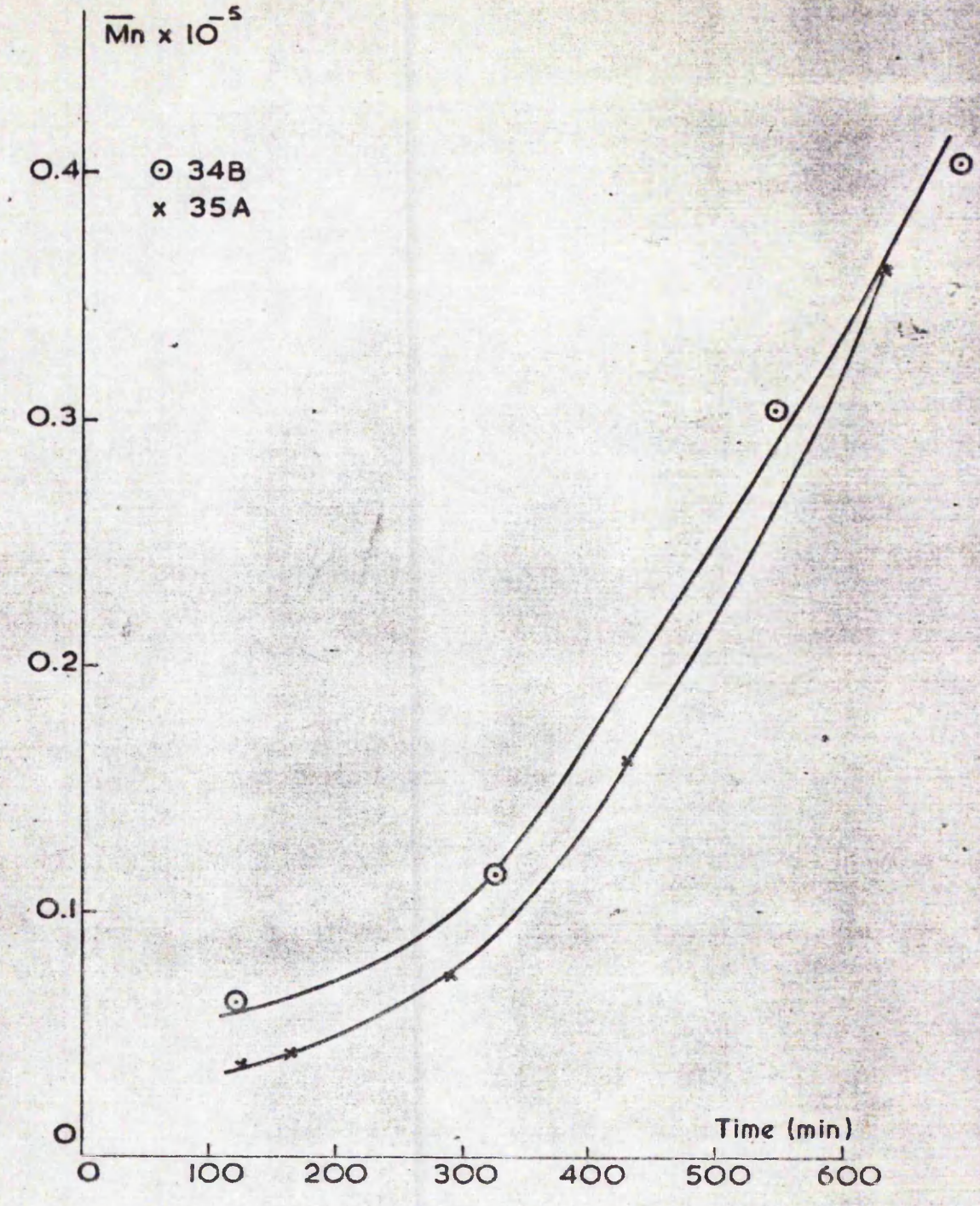

VARIATION OF $\overline{Mn}$ WITH TIME FOR REACTIONS 34B & 35A

FIG.54.

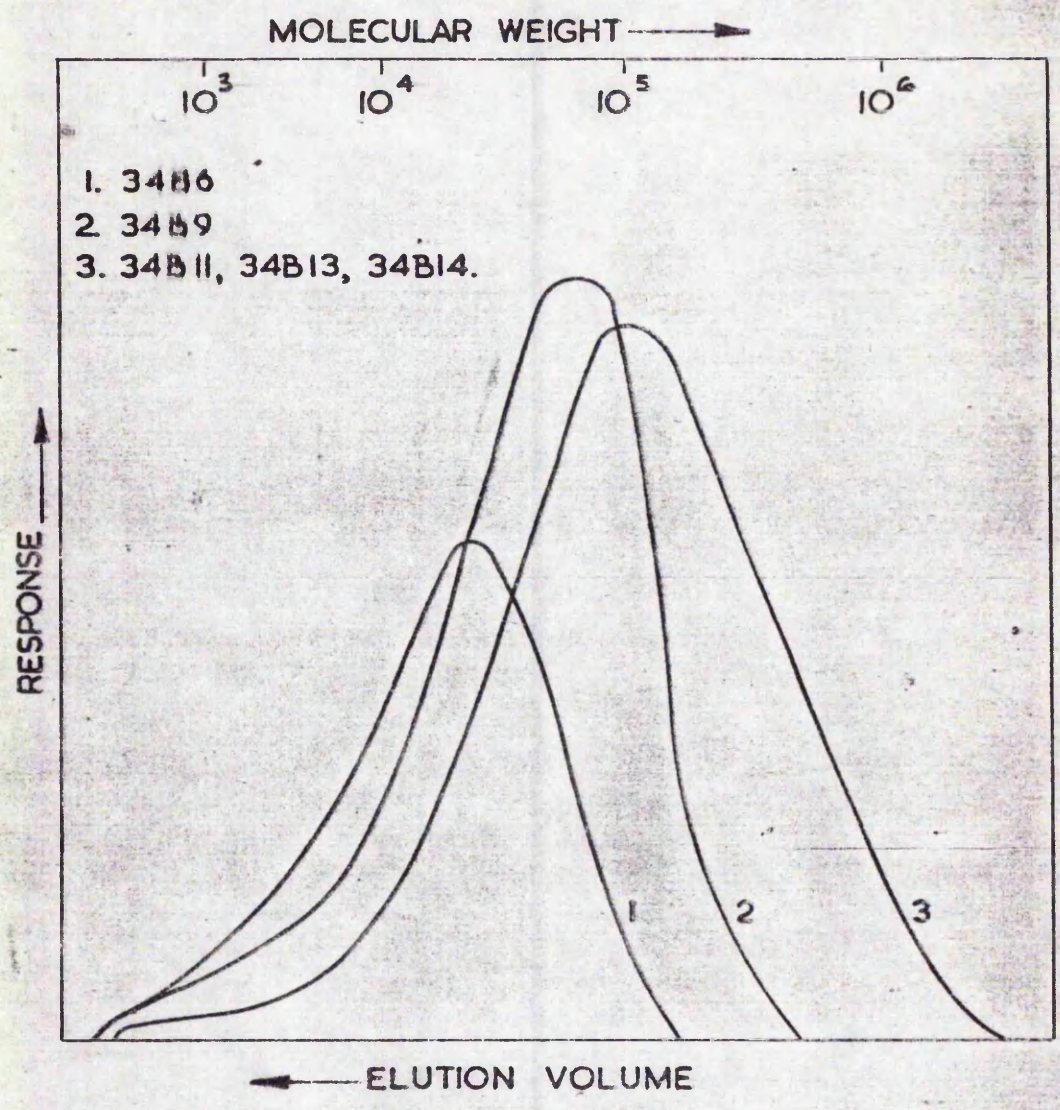

GEL PERMEATION CHROMATOGRAPHS OF FREEZE-DRIED SAMPLES FROM REACTION 34B

FIG. 55.

TABLE 27A

MOLECULAR WEIGHT VARIATION WITH REACTION TIME

Sample	Time (min)	$\bar{M}_n \times 10^{-5}$	$\bar{M}_w \times 10^{-5}$	$\frac{\bar{M}_w}{\bar{M}_n}$
64A1	60	.149	-	-
64A3	120	.203	-	-
64A4	240	.340	-	-
64A7	540	.399	-	-
64A8	1440	.357	-	-
34B6	120	.063	.26	4.2
34B9	325	.115	.61	5.3
34B11	545	.305	2.10	6.9
34B13	690	.405	2.00	4.9
34B14	1440	.283	1.99	7.0
35A6	115	.036	.515	14.3
35A7	165	.037	.310	8.4
35A9	295	.074	.700	9.5
35A11	415	.162	.800	4.9
35A14	640	.362	2.90	8.0
142-5	112	.29	-	-
142-6	175	.41	-	-
142-9	342	.52	-	-
142-10	1440	.61	-	-

where N_i is the number of polymer chains of type i and mass M, i.e., the total mass of the polymer divided by the total number of polymer chains. The weight average molecular weight is described by:

$$\bar{M}_w = \frac{\sum_{i=1}^{\infty} N_i M_i^2}{\sum_{i=1}^{\infty} N_i M_i} \quad . \qquad -- \quad (167)$$

$\bar{M}_w$ will always be greater than $\bar{M}_n$ unless the polymer is monodisperse, in which case they will be equal. The value of $\bar{M}_w$ is affected to a lesser extent by the presence of low molecular weight material than is $\bar{M}_n$. For example, a sample of polymer having 75% of the molecules at M.W. = 50,000 and 25% at M.W. = 1,000 will have a $\bar{M}_n$ of 37,750 and an $\bar{M}_w$ of 49,675. The polydispersity observed in these systems could well be due to the presence of 1000 M.W. material. The values of $\bar{M}_n$ are considerably lower than those reported in soap-containing systems (86) but are of the same order as those reported by Goodwin et al (141) and Kotera et al (140) for soap-free systems.

It is interesting to note that the two reactions which gave a convex curve for molecular weight vs. time contained less particles/ml than the two reactions which showed a concave variation. In the light of the previous discussion this might indicate that in the cases of 34B and 35A (convex) more of the growth was occurring through a heterocoagulation mechanism than in the cases of 142 and 64A.

M) Variation in Surface Area with Sample Time.

1) Experimental.

A series of latex samples from reaction 34B were freeze-dried and used in gas adsorption experiments with krypton, nitrogen and carbon dioxide gases. The krypton and nitrogen isotherms were carried out at liquid nitrogen

temperature (77 K), and the carbon dioxide isotherms at 195 K using solid carbon dioxide/methanol baths to cool the samples. Nitrogen and carbon dioxide isotherms were also carried out upon freeze-dried samples of latex 15A (see earlier this Chapter). The experimental procedure was as described in Chapter II.

2) Results.

The results for nitrogen adsorption are given in Table 18 and Figs. 20,21 (Chapter V). A comparison of the surface areas, determined using the B.E.T. equation, for the krypton and nitrogen adsorption isotherms is given in Table 27, and the uptakes of all three gases at $P/P_o = 0.3$ are compared in Table 28.

TABLE 27

COMPARISON OF KRYPTON AND NITROGEN SURFACE AREAS

Sample	Electron Microscope Surface area ($M^2\ g^{-1}$)	B.E.T. Nitrogen Surface Area ($M^2\ g^{-1}$)	B.E.T. Krypton Surface Area ($M^2\ g^{-1}$)
34B9	13.87	16.82	14.23
34B11	9.65	11.35	10.98

TABLE 28

UPTAKES OF VARIOUS GASES BY POLYSTYRENE LATICES AT $P/P_o = 0.3$

Latex	Uptake N_2 ($mg\ g^{-1}$)	Uptake Kr ($mg\ g^{-1}$)	Uptake CO_2 ($mg\ g^{-1}$)	Electron Microscope Surface Area ($M^2\ g^{-1}$)
34B6	20.0	-	-	26.61
34B7	8.8	-	55.1	16.91
34B8	8.1	-	-	14.43
34B9	5.8	11.8	-	13.87
34B11	4.7	9.6	57.0	9.65
34B12	4.7	-	-	9.65
34B14	4.3	-	57.0	9.59
15A	4.6	-	56.5	11.83

3) Discussion.

a) Nitrogen Adsorption.

It can be seen from Tables 27 and 28 that the surface area determined using the B.E.T. equation on the final samples (34B11 - 34B14, 15A) was in quite good agreement with the surface area determined using electron microscopy, whereas that of the samples removed early in the reaction was considerably larger. This increase in surface area cannot be accounted for by the presence of a smooth walled void within the particles. Vanderhoff et al (152) proposed that latices may well exhibit a certain amount of porosity or surface roughness, and demonstrated that upon heating the latex above its glass transition temperature the surface area determined using the B.E.T. equation corresponded more closely to that obtained by electron microscopy in nearly all cases. It appears to be unlikely, however, that the large discrepancies observed in this work could be attributed to surface porosity alone. It is interesting here to consider the work of Kolbeck et al (259) on the void morphology of polyethylene. They found that when polyethylene was heated under a high pressure of nitrogen, cooled and the pressure reduced, that the nitrogen dissolved in the polyethylene came out of solution and formed voids. Although the size of these voids was very large ($\sim 3 \times 10^{-5}$ cm) compared to those observed in this work, they did observe that the edges of the voids were diffuse, the surfaces consisting of fine fibrils of polymer extending into the interior of the void. It could well be that in latex samples which exhibit voids upon evacuation, a similar phenomena is observed in that as the monomer evaporates from the void it leaves behind a porous system of collapsed polymer filaments. An increase in surface area would also be observed if capillary condensation were taking place in the spaces between touching spheres as proposed by Kiselev et al (208-11). With the size spheres used in this work the effect would be expected to be small, as would the effect of inaccessible surface due to the spheres touching.

b) Krypton Adsorption.

The values obtained for surface area determinations using krypton (area molecule^{-1} 18.5 x 10^{-20} m^2 (260)) were in slightly better agreement with the electron microscope surface area than the corresponding nitrogen surface area. Indeed, Shaw using krypton as adsorbate found the B.E.T. surface area of a latex to be 21.7 m^2 g^{-1} compared to an electron microscope surface area of 21.4 $\pm$ 0.3 m^2 g^{-1}. It might be expected that krypton would give better agreement since the size of the krypton molecule is slightly greater than that of nitrogen. Hence, if a small amount of microporosity were present in the latices the krypton molecule (at the same temperature) would have more difficulty penetrating the pores than a nitrogen molecule.

c) Carbon Dioxide.

It can be seen from the results that the amount of carbon dioxide adsorbed is independent of the particle size, being practically constant for all the samples studied. This indicates that the sorption of carbon dioxide is a bulk phenomenon and could be due to several causes:

i) The isotherms were carried out at a higher temperature (195 K) than the nitrogen and krypton isotherms (77 K). The carbon dioxide molecule is slightly larger than the nitrogen molecule, but its kinetic energy at this higher temperature would be greater, enabling it to penetrate either into pores, or more likely, between the polymer chains more easily.

ii) It is known that polystyrene undergoes multiple transitions, one occurring at 163 K. (nitrogen isotherms were carried out at 77 K., carbon dioxide at 195 K). This transition could result in the spacings between the polymer chains being greater(261)

4) Conclusions.

It appears that (nitrogen and krypton isotherms) for final latex samples give good agreement both with each other and with the electron microscope surface area. However, with early samples considerable deviations become apparent due to either the presence of voids within the

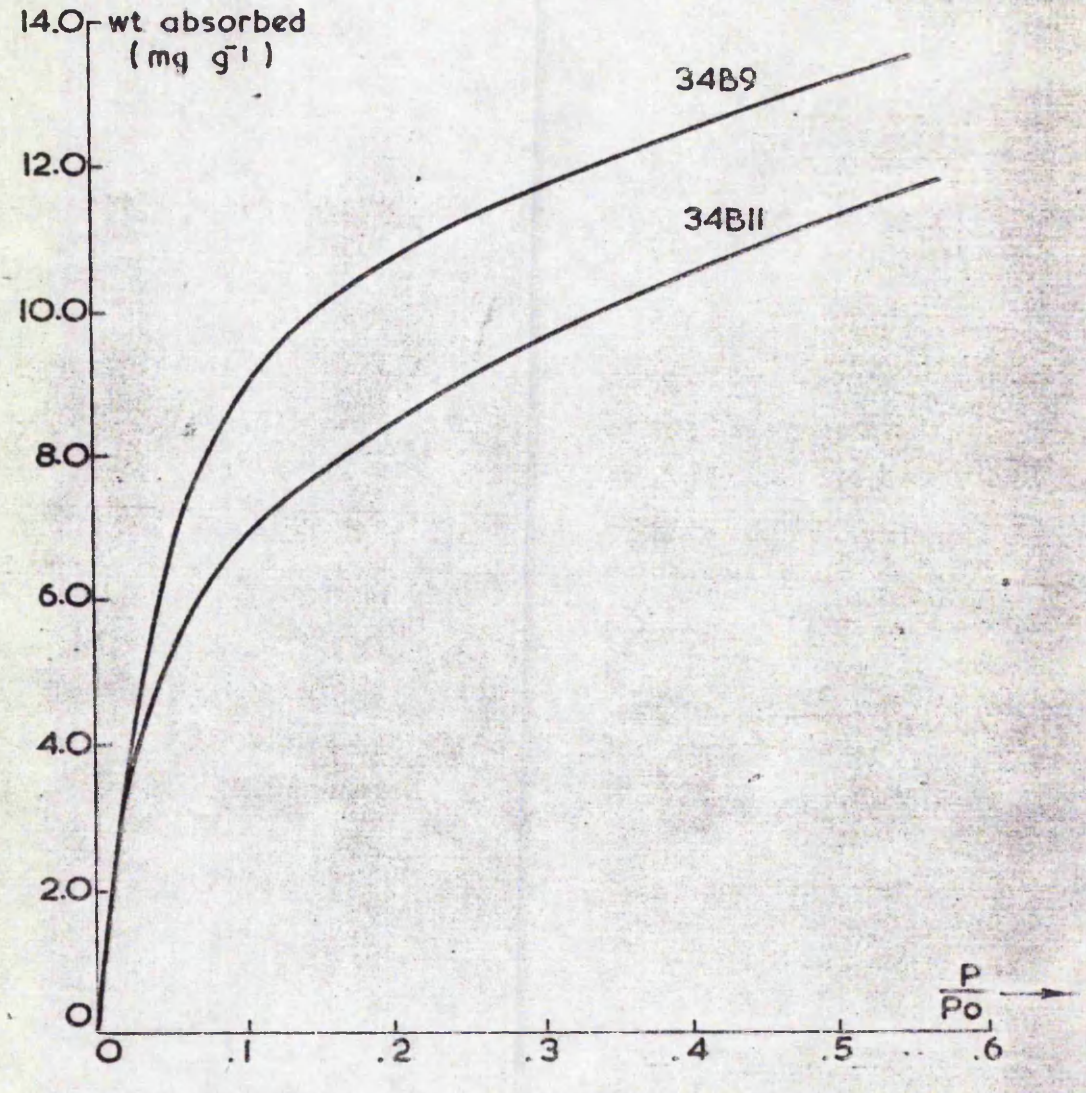

KRYPTION ADSORPTION ISOTHERMS ON SAMPLES 34B9 & 34B11

FIG. 56.

particles or to the removal of monomer resulting in a porous surface structure. Carbon dioxide appears to be absorbed by the latices, the amount being independent of size or sample time.

N) The Effect of a Stainless Steel Stirrer on the Thermal Decomposition of Potassium Persulphate.

1) Introduction.

As a result of the observation that the use of a stainless steel stirrer appeared to act as a catalyst to polymerisation when potassium peroxydiphosphate was used as initiator, and experiment was carried out to determine its effect on the rate of decomposition of potassium persulphate.

2) Experimental.

A 2 l reaction vessel was charged with 0.9 l of doubly distilled water, the vessel was then immersed in a water bath maintained at 343 K and left to equilibrate whilst the contents were bubbled with 'white-spot' nitrogen. A solution of potassium persulphate was then made up in 100 ml of water such that when added to the reaction vessel the solution would be 0.1 mole l^{-1}. This solution was then added (room temperature) to the flask and a stop clock started. In two experiments the vessel was stirred with an all-glass stirrer and in another two a stainless steel stirrer was used. 25 ml samples were removed at regular intervals and 2 ml aliquots of 3 mole l^{-1} sulphuric acid and 7 ml aliquots of 5 mole l^{-1} sodium bromide were added. The mixture was shaken, a known excess of ferrous ammonium sulphate added, and then allowed to stand for 20 min. After this time the excess ferrous ion was titrated with 0.02 mole l^{-1} ceric sulphate made up in 1 mole l^{-1} sulphuric acid, using ferroin as indicator (colour change orange $\longrightarrow$ yellow) (204).

3) Results and Discussion.

The decomposition of persulphate in the aqueous phase can be represented as:

$$S_2O_8^{2-} + H_2O \xrightarrow{\Phi} 2\,H\,SO_4^- + \tfrac{1}{2}\,O_2$$

and the reactions occurring during the titration as:

$$S_2O_8^{2-} + 2\ Fe^{2+} \longrightarrow 2\ SO_4^{2-} + 2\ Fe^{3+}$$

$$Fe^{2+} + Ce^{4+} \longrightarrow Fe^{3+} + Ce^{3+}$$

The decomposition of persulphate is adequately expressed by the first order rate law:

$$-\frac{d[S_2O_8^{2-}]}{dt} = k[S_2O_8^{2-}] \qquad -- (168)$$

Now if the initial concentration at time t = 0 is C_o and at some later time, t, the concentration has fallen to c, then:

$$-\int_{C_o}^{C} \frac{dC}{C} = k \int_{0}^{t} dt\ , \qquad -- (169)$$

$$\text{i.e., } -\ln \frac{C}{C_o} = \ln \frac{C_o}{C} = kt, \qquad -- (170)$$

$$\text{and } \log C = -\frac{k}{2.303} t + \log C_o\ . \qquad -- (171)$$

Thus, a plot of 2.303 log C versus t gives a straight line of negative slope equal to k. The determined values of k are shown in Table 29 .

TABLE 29

FIRST ORDER RATE CONSTANT FOR THE DECOMPOSITION OF POTASSIUM PERSULPHATE

Type of Stirrer	k (min^{-1})	Average k (min^{-1})	% difference
Glass	1.580×10^{-3}	1.575×10^{-3}	2
	1.570×10^{-3}		
Stainless Steel	1.596×10^{-3}	1.608×10^{-3}	
	1.620×10^{-3}		

It can be seen that the difference between the two rates is only 2% which is within experimental error. The literature value of k under these conditions is 1.45×10^{-3} min^{-1} (262) which is slightly lower than these values.

However, it would be expected that values obtained in the manner described above would be slightly higher due to difficulty in obtaining an accurate value of t at which the samples were taken, further decomposition occurring before the addition of the ferrous ammonium sulphate. This indicates that when potassium persulphate is used as initiator, the rate of decomposition remains virtually unaffected by the use of a stainless steel stirrer.

CHAPTER VII

CONCLUSIONS

A number of general conclusions can be drawn from the work described in this thesis.

1) The use of persulphate initiated polymer latices as model colloids should be approached with caution, since hydrolysis of the sulphate stabilising groups (when they are not protected by a layer of surfactant) appears to be a rapid process. Also the nature of the surface groups may be affected by the presence of monomer oxidation products within the final latex samples.

2) Potassium peroxydiphosphate is not capable of initiating styrene emulsion polymerisation but in the presence of trace amounts of heavy metal ions polymerisation is initiated with the production of latices having phosphate surface groupings which appear to be more stable to storage at elevated temperatures than sulphate groups. The final particle sizes and per cent conversions in these reactions are not reproducible.

3) Potassium peroxydiphosphate used in conjunction with sodium metabisulphite (sodium hydrogen sulphite) is an efficient initiator for styrene emulsion polymerisation, the reactions being reproducible. The end groups stabilising these latices are predominantly sulphonate which are very stable to hydrolysis.

4) The monomer concentration within a particle during a soap-free emulsion polymerisation is heterogenous and results in the formation of a void within the particle upon exposure to vacuum. Also the monomer concentration is probably lower than in soap-containing systems.

5) That particle nucleation occurs either by a precipitation or micellisation mechanism involving oligomeric material of ~520 molecular weight. The ~1000 molecular weight material formed by the mutual termination of these oligomers is probably the cause of the monomer heterogeneity within the particles.

6) The mechanism of particle growth occurs via two mech-

anisms in the absence of surfactant: growth within the particles themselves and growth by continuous nucleation of particles in the aqueous phase which undergo hetero-coagulation with the primary particles. Thus, the growth process of these systems cannot be adequately described by the current kinetic theories of emulsion polymerisation. The rate of polymerisation per particle in these systems is directly proportional to the particle radius.

REFERENCES

1) Van der Hoff, B.M.E., "Solvent Properties of Surfactant Solutions", K. Shinoda, Ed., N.Y., 1967.

2) Wachtel, R.E., LaMer, V.K., J. Colloid Sci., 17, 531, 1962.

3) Vanderhoff, J.W., Van den Hul, H.J., Tausk, R.M.J., Overbeek, J. Th. G., "Clean Surfaces", G. Goldfinger, Ed., Marcel Dekkar, N.Y., 1970.

4) Ottewill, R.H., Walker, T., Kolloid z-u-z Polymere, 227, 108, 1968.

5) Ottewill, R.H., private communication quoted in reference (1).

6) Hofmann, F., Delbrück, K., Ger. Offen., 250,690 (Sept 12 1909).
Ibid 254,672 (Jan 26 1912).
Ibid 255,129 (March 12 1912).

7) Gottlob, K., U.S. Pat., 1,149,577 (Jan 6 1913).

8) Fikentscher, H., Gerrens, H., Schuller, H., Angew Chem., 72, 856, 1960.

9) Dinsmore, R.P., U.S. Pat., 1,732,795 (Sept 13 1927).

10) Luther, M., Heuck, C., Ger. Offen., 558,890 (Jan 8 1927).

11) Kaufman, M., "The History of PVC", Maclaren, London, 1969.

12) British Association of Synthetic Rubber Manufacturers, "Not From Trees Alone", 1970, 2nd Edition.

13) Fikentscher, H., Angew Chem., 51, 433, 1938.

14) Yurzhenko, A.I., Kolechkova, M., Dokl. Akad. Nauk. SSSR., 47, 354, 1945.

15) Harkins, W.D., J.A.C.S., 69, 1428, 1947.
Ibid J. Polym. Sci., 5, 217, 1950.

16) Smith, W.V., Ewart, R.H., J. Chem. Phys., 16, 592, 1948.

17) Van der Hoff, B.M.E., "Polymerisation and Polycondensation Processes", Advances in Chemistry Series 34, A.C.S., Washington, D.C., 1962.

18) Bennion, B.C., Tong, L.K.J., Holmes, L.P., Eyring, E.M., J. Phys. Chem. 73, 3288, 1969.
19) Morton, M., Kaizerman, S., Altier, M.W., J. Coll. Sci., 9, 300, 1954.
20) Matheson, M.S., Auer, E.E., Bevilacqua, E.B., Hart, E.J., J.A.C.S., 73, 1700, 1951.
21) Bartholomé, E., Gerrens, H., Herbeck, R., Weitz, R.M., Z. Elektrochem. 61, 522, 1957.
22) Van der Hoff, B.M.E., J. Phys. Chem., 60, 1250, 1956.
23) Medvedev, S.S., "International Symposium on Macromolecular Chemistry", Pergamon Press, N.Y., 1959.
24) Sheinker, A., Medvedev, S.S., Dokl. Akad. Nauk. SSSR., 97, 111, 1954.
Ibid Zh. fiz. khim., 29, 250, 1955.
25) Medvedev, S., "Simposio Internazionale di Chimica Macromolecolare", Milano-Torino, 1954. Ricerca sci., Suppl., 25, 1955.
26) Gardon, J.L., J. Polym. Sci., 6(A1), 2859, 1968.
27) Herzfield, S.H., Roginsky, A., Corrin, M.L., & Harkins, W.D., J. Polym. Sci., 5, 207, 1950.
28) Ugelstad, J., & Hansen, F.K., Nato Advanced Study Institute, "Polymer Colloids Preprints", 1975.
29) Gardon, J.L., J. Polym. Sci., 6(A1), 623, 1968.
30) Fitch, R.M., & Tsai, C.H., "Polymer Colloids", R.M. Fitch, Ed., N.Y., 1971.
31) Fick, A., Ann. Physik, 94, 59, 1855.
32) Fitch, R.M., Shih, Lih-bin, Progr. Coll. Polym. Sci., 56, 1, 1975.
33) Fitch, R.M., Nato Advanced Study Institute, "Polymer Colloids Preprints", 1975.
34) Reiss, H., LaMer, V.K., J. Chem. Phys., 18, 1, 1950.
35) Reiss, H., J. Chem. Phys., 19, 482, 1951.
36) Parts, A.G., Moore, D.E., Watterson, J.G., Makromol. Chem., 89, 156, 1965.
37) Alexander, A.E., Napper, D.H., "Progr. in Polymer Sci., Vol. 3", A.D. Jenkins, Ed., N.Y., 1971.

38) Harada, M., Nomura, M., Kojimu, H., Eguchi, W., Nagata, S., J. Appl. Polym. Sci., 16, 811, 1972.
39) Nomura, M., Harada, M., Eguchi, W., Nagata, S., "ACS Polymer Preprints", Philadelphia, April, 1975.
40) Barrett, K.E.J., "Dispersion Polymerisation in Organic Media", J. Wiley and Sons, 1975.
41) Hansen, F.K., Ugelstad, J., To be published.
42) Haward, R.M., J. Polym. Sci., 4, 273, 1949.
43) Stockmayer, W.H., J. Polym. Sci., 24, 314, 1957.
44) O'Toole, J.T., J. Appl. Polym. Sci., 9, 1291, 1965.
45) Gardon, J.L., J. Polym. Sci., 6(A1), 665, 1968.
46) Gardon, J.L., "Symposium on Emulsion Polymers, Preprints", Manchester, 1969.
47) Ugelstad, J., Mørk, P.C., Brit. Polym. Sci., 2, 31, 1970.
48) Hearn, J., Ph.D. Thesis, University of Bristol, 1971.
49) Hare, K., Mita, I., Kambe, H., J. Polym. Sci., 6(A1), 2663, 1968.
50) Norrish, R.G.W., Smith, R.R., Nature, 150, 336, 1942.
51) Schultz, G.V., Harborth, G., Makromol. Chem., 1, 106, 1947.
52) Trommsdorff, E., Köhle, H., Lagally, P., Makromol. Chem., 1, 169, 1947.
53) Friis, N., Hamielec, A.E., J. Polym. Sci., 12, 251, 1974.
54) Balke, S.T., Hamielec, A.E., J. Appl. Polym. Sci., 17, 2311, 1973.
55) Zimml, W.S., J. Appl. Polym. Sci., 1, 323, 1959.
56) Friis, N., Nyhagen, L., J. Appl. Polym. Sci., 33, 487, 1973.
57) Friis, N., Hamielec, A.E., J. Polym. Sci., 19, 97, 1975.
58) O'Toole, J.T., Polymer Preprints, 7(2), 765, 1966.
Ibid J. Polym. Sci., C.27, 171, 1969.
59) Ewart, R.H., Carr, C.I., J. Phys. Chem., 58, 640, 1954.
60) Saidel, G.M., Katz, S., J. Polym. Sci., C.27, 149, 1969.

61) Katz, S., Shinnar, R., Saidel, G., "Addition and Condensation Polymerisation Processes", Advances in Chemistry Series, 91, A.C.S., Washington D.C., 1969.
62) Min, K.W., Ray, W.H., J. Macromol. Sci., Rev. Macromol. Chem., C11(2), 177, 1974.
63) Brodnyan, J.G., Kelley, E.L., J. Coll. Sci., 20, 7, 1965.
64) Vanderhoff, J.W., Vitkuske, J.F., Bradford, E.B., Alfrey, T. Jnr., J. Polym. Sci., 20, 255, 1956.
65) Smith, W.V., J.A.C.S., 70, 3695, 1948.
66) Smith, W.V., J.A.C.S., 71, 4077, 1949.
67) Van der Hoff, B.M.E., J. Polym. Sci., 44, 241, 1960.
68) Saha, N.G., Nandi, U.S., Palit, S.R., J. Chem. Soc. p 12, 1968.
69) Gardon, J.L., J. Polym. Sci., 6(A1), 2853, 1968.
70) Priest, W.J., J. Phys. Chem., 56, 1077, 1952.
71) Fitch, R.M., Prenosil, M.B., Sprick, K.J., J. Polym. Sci., C.27, 95, 1969.
72) Moore, D.E., J. Polym. Sci., 5(A1), 2665, 1967.
73) Roe, C.P., Ind. and Eng. Chem., 60(9), 20, 1968.
74) Morriss, C.E.M., Alexander, A.E., Parts, A.G., J. Polym. Sci., 4(A1), 985, 1966.
75) Peppard, B.D., "Particle Nucleation Phenomena in Emulsion Polymerisation of Styrene", Univ. Microfilms, 1974.
76) Robb, I.D., J. Polym. Sci., 7(A1), 417, 1969.
77) Bovey, F.A., Kolthoff, I.M., J. Polym. Sci., 5, 487, 1950.
78) Young, L.J., Brandrup, G., Brandrup, J., "Polymer Handbook", J. Brandrup and E.H. Immergut, Eds., Interscience, N.Y., 1966.
79) Flory, P.J., "Principles of Polymer Chemistry", Cornell Univ. Press, Ithaca, 1953.
80) Gerrens, H., Advan. Polym. Sci., 1, 234, 1959.
81) Gerrens, H., Kohnlein, E., Z. Elektrochem, 64, 1199, 1960.
82) Bartholomé, H., Gerrens, R., Herbeck, B., Weitz, H.M., Z. Elektrochem, 60, 334, 1956.

83) Roe, C.P., Brass, P.D., J. Polym. Sci., 24, 401, 1957.
84) Vanderhoff, J.W., Bradford, E.B., Tappi, 39, 650, 1956.
85) Goodall, A.R., Wilkinson, M.C., Hearn, J., To be published in J. Polym. Sci.
86) Williams, D.J., Bobalek, E.G., J. Polym. Sci., 4(A1), 3065, 1966.
87) Kolthoff, I.M., Miller, I.K., J.A.C.S., 73, 3055, 1951.
88) Bartlett, P.D., Cotman, J.D., J.A.C.S., 71, 1419, 1949.
89) Froneaus, S., Ostman, C.O., Acta Chem. Scan., 9, 902, 1955.
90) House, D.A., Chem. Rev., 62, 185, 1962.
91) Kolthoff, I.M., O'Connor, R.R., Hansen, J.L., J. Polym. Sci., 15, 459, 1955.
92) Bovey, F.A., Kolthoff, I.M., Medalia, A.I., Meehan, E.J., "Emulsion Polymerisation", Interscience, N.Y., 1955.
93) Meehan, E.J., Kolthoff, I.M., Carr, E.M., J. Polym. Sci., 13, 113, 1954.
94) Ivanchov., S.S., Yurzhenko, A., Izv. Vysshy, Uchebn. Zavedenic Khim. i Khim. Tekhnol., 4, 13, 1958.
95) Ivanchov, S.S., Yurzhenko, A., Kolloid-Zh., 22, 120, 1960.
96) Morris, C.E.M., Parts, A.G., Makromol. Chem., 119, 212, 1968.
97) Allen, P.W., J. Polym. Sci., 31, 206, 1958.
98) Friend, J.P., Alexander, A.E., J. Polym. Sci., 6(A1), 1833, 1968.
99) Smitham, J.B., Gibson, D.V., Napper, D.H., J.C.I.S., 45(1), 211, 1973.
100) Patsiga, R.A., Ph. D. Thesis, Syracuse University, 1962.
101) Wilmarth, W.K., Haim, A., "Peroxide Reaction Mechanisms", J.O. Edwards, Ed., Interscience, N.Y., 1962.
102) Sturzenhofecker, F., Angew. Chem., 71, 198, 1959.
103) Grancio, M.R., & Williams, D.J., J. Polym. Sci., 8(A1), 2617, 1970.

104) Ibid J. Polym. Sci., 8(A1), 2733, 1970.
105) Keusch, P., & Williams, D.J., Polymer Preprints, 12(1), 464, 1971.
106) Ibid J. Polym. Sci. Polym. Chem. Ed., 11, 143, 1973.
107) Williams, D.J., J. Polym. Sci., 11, 301, 1973.
108) Keusch, P., Prince, J., Williams, D.J., J. Macromol. Sci. Chem., A7(3), 623, 1973.
109) Williams, D.J., J. Elastoplast., 3, 187, 1971.
110) Keusch, P., Williams, D.J., J. Polym. Sci., 11, 193, 1973.
111) Keusch, P., Graff, R.A., Williams, D.J., Macromolecules, 7, 304, 1974.
112) Williams, D.J., J. Polym. Sci., 12, 2123, 1974.
113) Napper, D.H., J. Polym. Sci., 9(A1), 2089, 1971.
114) Bradford, E.B., Vanderhoff, J.W., J. Polym. Sci., C.3, 41, 1963.
115) Gardon, J.L., J. Polym. Sci. Polym. Chem. Ed., 2, 241, 1973.
116) Gardon, J.L., J. Polym. Sci., 12, 2133, 1974.
117) Piirma, I., Kamath, V.R., Morton, M., A.C.S. Meeting, Philadelphia, Preprints, 1975.
118) Morton, M., Kamath, V.R., Piirma, I., Paper Presented at the 17th Canadian High Polymer Forum, St. John, Quebec, 1973.
119) Wilkinson, M.C., Cox, R.A., Polym. Preprints, 16(1), 781, 1975.
120) Cox, R.A., Creasey, J.M., Wilkinson, M.C., Nature, 252, 468, 1974.
121) Goodall, A.R., Wilkinson, M.C., Hearn, J., J.C.I.S., 53, 327, 1975.
122) Goodall, A.R., Wilkinson, M.C., Hearn, J., Nato Advanced Study Institute, "Polymer Colloids Preprints", 1975.
123) Edelhauser, H.A., Polymer Preprints, 7, 843, 1966.
124) Force, C.G., Matijevic, E., Kratohvil, J.P., Kolloid Z u Z Polymere, 223, 31, 1968.

125) Fryling, C.F., J. Colloid Sci., 18, 713, 1963.
126) Ottewill, R.H., Shaw, J.N., Kolloid Z u Z Polymere, 215, 161, 1967.
127) Shaw, J.N., J. Polym. Sci., C.27, 237, 1969.
128) Brace, R., M.Sc. Thesis, University of Bristol, 1970.
129) Schenkel, J.H., Kitchener, J.A., Nature, 182, 131, 1958.
130) Van den Hul, H.J., Vanderhoff, J.W., J. Electroanal. Chem., 37, 161, 1972.
131) Van den Hul, H.J., Vanderhoff, J.W., J.C.I.S., 28, 336, 1968.
132) Roy, G., Mandel, B.M., Palit, S.R., "Polymer Colloids", R.M. Fitch, Ed., Plenum Press, N.Y., 1971.
133) Van den Hul, H.J., Vanderhoff, J.W., Brit. Polym. J., 2, 121, 1970.
134) McCann, G.D., Bradford, E.B., Van den Hul, H.J., Vanderhoff, J.W., "Polymer Colloids", Plenum Press, N.Y., 1971.
135) Wilkinson, M.C., Private communication.
136) Gultepe, M.E., Private communication.
137) Shaw, J.N., Marshall, M.C., J. Polym. Sci., 6(A1), 449, 1968.
138) Greene, B.W., J.C.I.S., 43(2), 449 and 462, 1973.
139) Fitch, R.M., "Polyelectrolytes and their Applications", A. Rembaum and E. Sélégny, Eds., D. Reidel Publ., Dordrecht, Holland, 1975.
140) Kotera, A., Furusawa, K., Takeda, Y., Kolloid Z.u Z. Polymere, 229(2), 677, 1970.
141) Goodwin, J.W., Hearn, J., Ho. C.C., Ottewill, R.H., Br. Polym. J., 5, 347, 1973.
142) Dunn, A.S., Chem. and Ind., 49, 1406, 1971.
143) Chen, S.F., Ph. D. Thesis, University of Bristol, 1974.
144) Everett, D.H., Gultepe, M.E., Nato Advanced Study Institute, "Polymer Colloids Preprints", 1975.
145) Van den Hul, H.J., Vanderhoff, J.W., "Polymer Colloids", R.M. Fitch, Ed., Plenum, N.Y., 1971.

146) Yates, D.E., Nato Advanced Study Institute, "Polymer Colloids Preprints", 1975.

147) Laaksonen, J., Le Bell, J.C., Stenius, P., J. Electroanal. Chem., 64, 207, 1975.

148) Palit, S.R., Chem. and Ind., p.1531, 1960.
Palit, S.R., Saxena, G.K., Nature, 209, 1127, 1966.
Palit, S.R., Ghosh, P., J. Polym. Sci., 58, 1225, 1962.
Palit, S.R., Pure and Appl. Chem., 4, 459, 1962.
Palit, S.R., Anal. Chem., 33, 1441, 1961.

149) Smith, W.V., J.A.C.S., 71, 4077, 1949.

150) Connor, P., Ottewill, R.H., J.C.I.S., 37(3), 642, 1971.

151) Ottewill, R.H., Shaw, J.N., Kolloid Z.u Z. Polymere, 218, 34, 1967.

152) Vanderhoff, J.W., Van den Hul, H.J., J. Macromol. Sci. - Chem., A7(3), 677, 1973.

153) Stone-Masui, J., Watillon, A., J.C.I.S., 52(3), 479, 1975.

154) Van den Hul, H.J., Vanderhoff, J.W., "Preprint to Symposium on Emulsion Polymerisation", Manchester, 1969.

155) Furusawa, K., Norde, W., Lyklema, J., Kolloid Z. u Z. Polymere, 250, 208, 1972.

156) Wu, W.C., El-Aasser, M.S., Vanderhoff, J.W., To be published.

157) Ghosh, P., Chadha, S.C., Mukherjee, A.R., Palit, S.R., J. Polym. Sci., A2, 4433, 1964.

158) Dainton, F.S., Private communication cited in Ref. 157.

159) Read, R.R., Fredell, W.G., Proc. Sci. Section, Toilet Goods Assoc., 30, 11, 1958.

160) Arnett, L.M., Peterson, J.H., J.A.C.S., 74, 2031, 1952.

161) Bevington, J.C., Melville, H.W., Taylor, R.P., J. Polym. Sci., 12, 449, 1954; 14, 463, 1954.

162) Bamford, C.H., Jenkins, A.D., Nature, 176, 78, 1955.

163) Kammerer, H., Schmeider, W., Steinfort, K-G., Makromol. Chem., 72, 86, 1964.

164) Mayo, F.R., Gregg, R.A., Matheson, M.S., J.A.C.S., 73, 1691, 1951.

165) Overberger, G.G., Finestone, A.B., J.A.C.S., 78 1638, 1956.

166) Hearn, J., Ottewill, R.H., Shaw, J.N., Brit. Polym. J., 2, 116, 1970.

167) Ghosh, P., Mukherjee, A.R., Palit, S.R., J. Polym. Sci., A2, 2807, 1964.

168) Bitsch, B., Thesis, University of Strasbourg, 1968. Bitsch, B., Parmeland, G., Reiss, G., Banderet, A., "Preprint IUPAC International Symposium on Macromolecular Chemistry", Budapest, Vol.II, 1969.

169) Dunn, A.S., Chem. and Ind., 49, 1406, 1971.

170) Goodwin, J.W., Hearn, J., Ho. C.C., Ottewill, R.H., Colloid and Polymer Sci., 252, 464, 1974.

171) Homola, A.M., Inoue, M., Robertson, A.A., J. Appl. Polym. Sci., 19, 3077, 1975.

172) Hohenstein, W.P., Mark, H., J. Polym. Sci., 1, 127 and 549, 1946.

173) Matsumoto, T., Ochi, A., Kobunshi - Kagaku, (Tokyo), 22, 481, 1965.

174) Kotera, A., Furusawa, K., Kudo, K., Kolloid Z. u Z. Polymere, 240, 837, 1970.

175) Chung-li, Y., Goodwin, J.W., Ottewill, R.H., Progr. Colloid and Polymer Sci., 60, 163, 1976.

176) Dunn, A.S., Taylor, P.A., Makromol. Chem., 83, 207, 1965.

177) Lim, D., Kolinsky, M., Symposium on Macromolecules, Wiesbaden, "Communications", No.III, B.14, 1959.

178) French, D.M., J. Polym. Sci., 32, 395, 1958.

179) Baxendale, J.H., Evans, M.G., Kilham, J.K., J. Polym. Sci., 1, 466, 1946.

Ibid Trans. Farad. Soc., 42, 668 and 675, 1946.

Ibid J. Chem. Soc., p.266, 1947.

180) Fiquet - Fayard, F., J. Chim. Phys., 56, 692, 1959.
181) Whitby, G.S., Gross, M.D., Miller, J.R., Constanga, A.J., J. Polym. Sci., 16, 549, 1955.
182) Sheriff, A.I.M.D., Santappa, M., J. Polym. Sci., A3, 3131, 1965.
183) Patsiga, R., Litt, M., Stannet, V., J. Phys. Chem., 64, 801, 1960.
184) Crescentini, L., Gechele, G.B., Pizzoli, M., Europ. Polym. J., 1, 293, 1965.
185) Biswas, E.M., Palit, S., J. Sci. Ind. Res., 20B, 160, 1961.
186) Ley, G.J., Schneider, C., Hummel, D.O., Am. Chem. Soc. Polym. Preprints, 7, 725, 1960.
187) Dainton, F.S., Seaman, P.H., James, D.G.L., Eaton, R.S., J. Polym. Sci., 34, 209, 1959.
Ibid
J. Polym. Sci., 39, 279, 1959.
188) Fitch, R.M., Tsai, C.H., J. Polym. Sci., B8, 703, 1970.
189) Gatta, G., Benetta, G., Talamani, G.P., Vianello, G., Adv. Chem. Ser., 91, 158, 1969.
190) La Mer, V.K., & Dinegar, R.H., J.A.C.S., 72, 4847, 1950.
191) Dunn, A.S., & Chong, L. C-H., Br. Polym. S., 2, 49, 1970.
Ibid "Preprint Symposium on Emulsion Polymerisation", Manchester, 1969.
192) Deryaguin, B.V., Landau, L.D., Acta Phys. - Chim., U.R.S.S., 14, 633, 1941.
193) Vervey, E.J.W., Overbeck, J. Th. G., "Theory of The Stability of Lyophobic Colloids", Elsevier, Amsterdam, 1948.
194) Hamakar, H.C., Rec. Trav. Chim., Pay-Bas Belg., 55, 1015, 1936.
Ibid 56, 727, 1937.
195) Hamakar, H.C., Physica, 4, 1058, 1937.
196) Fuchs, O., Z. Phys., 89, 736, 1934.

197) Palit, S.R., Guha, J., J. Polym. Sci., 34, 243, 1949.

198) Napper, D.H., Alexander, A.E., J. Polym. Sci., 61, 113, 1962.

199) Alfrey, T. Jnr., Bradford, E.B., Vanderhoff, J.W., J. Opt. Soc. Amer., 44, 603, 1954.

200) Bradford, E.B., Vanderhoff, J.W., J. Appl. Phys., 26, 864, 1955.

201) Bradford, E.B., Vanderhoff, J.W., Alfrey, T. Jnr., J. Coll. Sci., 11, 135, 1956.

202) Vanderhoff, J.W., Bradford, E.B., Takowski, H.L., J. Polym. Sci., 50, 265, 1961.

203) "Handbook of Chemistry and Physics" 47th Edition, Chemical Rubber Company, Cleveland, Ohio, 1966.

204) Vogel, A.I., "Quantitative Inorganic Analysis, 3rd. Ed., Longman, London.

205) Brunauer, S., Deming, L.S., Deming, W.S., & Teller, E., J.A.C.S., 62, 1723, 1940.

206) Brunauer, S., Emmet, P.H., Teller, E., J.A.C.S., 60, 309, 1938.

207) Halsey, G.D., Disc. Farad. Soc., 8, 54, 1950.

208) Karnaukhov, A.P., Kiselev, A.V., Russ. J. Phys. Chem., 34, 1019, 1960.

209) Aristov, B.G., Karnaukhov, A.P., Kiselev, A.V., Ibid 36, 1159, 1962.

210) Aristov, B.G., Davydov, V. Ya., Karnaukhov, A.P., Kiselev, A.V., Ibid 36, 1497, 1962.

211) Karnaukhov, A.P., Kiselev, A.V., Ibid 31, 2635, 1957.

212) Barb, W.G., J. Polym. Sci., 37, 515, 1959.

213) Claver, G.C., Farnham, W.H., Powder Technol., 6(6), 313, 1972.

214) Bradford, E.B., Vanderhoff, J.W., J. Appl. Phys., 26, 864, 1955.

215) Karamata, D., J. Ultrastructure Res., 35, 201, 1971.

216) Madelaine, G., Marel, C., Am. Occupational Hyg., 9, 135, 1966.

217) Wilkinson, M.C., Ellis, R., Callaway, S., The Microscope, 22(3), 229 (1974)
218) Vanderhoff, J.W., Private communication, quoted in ref. 139.
219) Read, R.R., Fredell, W.G., Proc. Sci. Section, Toilet Goods Assoc., 30, 11, 1958.
220) Kurz, J.L., J. Phys. Chem., 66, 2239, 1962.
221) Bunton, C.A., Kamego, A., Scpulveda, G.L., J. Org. Chem., 36(17), 2571, 1971.
222) Fuller, E.J., Kurz, J.L., Unpublished results quoted in ref. 220.
223) Van Senden, K.G., Koningsberger, C., Tetrahedron Letters, 1, 7, 1960.
224) Mukherjee, A.R., Ghosh, P., Chadha, S.C., Palit, S.R., Makromol. Chem., 97, 202, 1966.
225) Warson, H., Nato Advanced Study Institute, "Polymer Colloids Preprints", Trondheim, Norway, 1975.
226) Haynes, B., "Qualitative Organic Analysis", 2nd Ed., MacMillan, London.
227) Cram, D.J., Hammond, G.S., "Organic Chemistry", 2nd Ed., McGraw-Hill, N.Y., 1964.
228) Ghosh, P., Chadha, S.C., Palit, S.R., Indian J. Appl. Chem., 3, 197, 1965.
229) Castrantas, H.M., Mackellan, D.G., Polym. Preprints, A.C.S. Div. Polym. Chem., 10(2), 1381, 1969.
230) Castrantas, H.M., Harry, M., Mucenicks, P.R., Cohen, B., Mackellar, D.G., Ger. Offen., 2,002,865, 1970.
231) Crutchfield, M.M., Ph.D. Thesis, Brown University, 1960.
232) Crutchfield, M.M., Edwards, J.D., J.A.C.S., 82, 3533, 1960.
233) Fordham, J.W.L., Williams, H.L., J.A.C.S., 73, 4855, 1951.
234) Fritzche, P., Ulbricht, J., Faserforsch Text. Techn., 14, 517, 1963.
235) Bacon, R.G.R., Trans. Farad. Soc., 42, 140, 1946.
236) Kern, A., Makromol. Chem., 1, 209, 1948.
Ibid 1, 249, 1948.
Ibid 2, 48, 1948.

237) Rodriguez, F., Givey, R.D., J. Polym. Sci., 55, 713, 1961.
238) Berry, K.L., Peterson, J.H., J.A.C.S., 73, 5195, 1951.
239) Kolthoff, I.M., Medalia, A.I., Raaen, H.P., J.A.C.S., 73, 1733, 1951.
240) Collinson, E., Swallow, A.J., Quart. Rev., 9, 311, 1955.
241) Parreira, H.C., Ph. D. Thesis, Cambridge Univ., 1965.
242) Bacon, R.G.R., Quart. Rev., 9, 287, 1955.
243) Wright, H.J., Bremmer, J.F., Bhimani, N., Fitch, R.M., U.S. Pat., 3,501,432, 1970.
244) Uri, N., Chem. Revs., 50, 375, 1952.
245) Sully, R.D., J. Chem. Soc., 1498, 1950.
246) Bunn, D., Trans. Farad. Soc., 42, 190, 1946.
247) Sorum, C.H., Edwards, J.O., J.A.C.S., 74, 1204, 1954.
248) Brasted, R.C., "Comprehensive Inorganic Chemistry", Vol.8, Van Nostrand, New York, 1966.
249) Pelton, R., Private communication.
250) Ottewill, R.H., Private communication.
251) Rupar, W., Mitchell, J.M., Rubber Chem. Tech., 35, 1028, 1962.
252) Juang, M.S., Kreiger, I.M., Polym. Preprints, 16(1), 120, 1975.
253) Watson, R., Fitch, R.M., Bakker, D., Polym. Preprints, 16(1), 109, 1975.
254) Smoluchowski, M.V., Z. Physik. Chem., 92, 129, 1918.
255) Strutt, J.W., Phil. Mag., 41, 107, 274, 447, 1871.
256) Sinclair, D., "Handbook on Aerosols", Atomic Energy Commission, Washington D.C., 1950.
257) Maron, S.H., Elder, M.E., Ulevitch, I.N., J. Coll. Sci., 9, 89, 1954.
258) Gardon, J.L., J. Polym. Sci., 6, 687, 1968.
259) Kolbeck, A.G., Uhlmann, D.R., J. Appl. Polym. Sci., 17, 679, 1973.
260) Livingston, H.K., J. Coll. Sci., 4, 447, 1949.
Haynes, J.M., J. Phys. Chem., 66, 182, 1962.
261) Brydson, A.B., Polymer Science, A.D. Jenkins, Ed., North Holland, 1972.
262) Kolthoff, I.M., Meehan, E.J., Carr, E.M., J.A.C.S., 75, 1439, 1953.

APPENDICES

TABLE 30

EQUATIONS FOR DETERMINING r FROM r^2 PLOTS (r_A) AND % CONVERSION PLOTS (r_B)

Reaction	Temperature (K)	r_A (m)	r_B (m)
64B(A)	323	$(5.12\times10^{-17}t - 0.745\times10^{-15})^{0.5}$	$(1.799\times10^{-24}t + 1.130\times10^{-26}t^2)^{.333}$
(B)	323	$(6.20\times10^{-17}t + 9.923\times10^{-15})^{0.5}$	$(1.209\times10^{-23}t + 6.839\times10^{-27}t^2)^{.333}$
62B(A)	333	$(8.30\times10^{-17}t - 1.259\times10^{-15})^{0.5}$	$(9.162\times10^{-25}t + 3.754\times10^{-26}t^2)^{.333}$
(B)	333	$(4.98\times10^{-16}t - 211.400\times10^{-15})^{0.5}$	$(1.547\times10^{-25}t^2 - 4.641\times10^{-23}t)^{.333}$
142	343	$(1.27\times10^{-16}t - 1.280\times10^{-15})^{0.5}$	$(1.789\times10^{-24}t + 7.276\times10^{-26}t^2)^{.333}$
37B	343	$(2.11\times10^{-16}t - 9.737\times10^{-15})^{0.5}$	$(9.188\times10^{-24}t + 8.83\times10^{-26}t^2)^{.333}$
18A	343	$(1.24\times10^{-16}t - 2.78\times10^{-15})^{0.5}$	$(3.897\times10^{-24}t + 4.695\times10^{-26}t^2)^{.333}$
34B	343	$(1.49\times10^{-16}t - 1.176\times10^{-15})^{0.5}$	$(5.053\times10^{-24}t + 1.0302\times10^{-25}t^2)^{.333}$
18B	343	$(1.36\times10^{-16}t - 1.413\times10^{-15})^{0.5}$	$(0 + 9.789\times10^{-26}t^2)^{.333}$
64A	343	$(2.06\times10^{-16}t - 9.280\times10^{-15})^{0.5}$	$(1.329\times10^{-23}t + 4.672\times10^{-26}t^2)^{.333}$
19(A)	343	$(1.07\times10^{-16}t - .006\times10^{-15})^{0.5}$	—
(B)	343	$(2.66\times10^{-16}t - 18.374\times10^{-15})^{0.5}$	$(9.362\times10^{-24}t + 1.131\times10^{-25}t^2)^{.333}$
35A(A)	343	$(2.02\times10^{-16}t - 6.090\times10^{-15})^{0.5}$	—
(B)	343	$(5.26\times10^{-16}t - 56.300\times10^{-15})^{0.5}$	$(1.792\times10^{-24}t + 3.061\times10^{-25}t^2)^{.333}$
62A	353	$(1.95\times10^{-16}t + 1.739\times10^{-15})^{0.5}$	$(9.591\times10^{-24}t + 1.887\times10^{-25}t^2)^{.333}$
66A	363	$(2.90\times10^{-16}t + 0.171\times10^{-15})^{0.5}$	$(3.081\times10^{-23}t + 1.745\times10^{-25}t^2)^{.333}$

TABLE 31

KINETIC CHARACTERISTICS OF REACTION 64B

Sample	Time (min)	Conversion (%)	radius (nm)	σ (%)	Number of particles (ml^{-1})
64B1	30	0.21	39	12	7.30×10^{11}
64B2	60	0.63	55	5	7.75×10^{11}
64B3	120	0.99	75	4	4.87×10^{11}
64B4	240	2.67	102	3	5.25×10^{11}
64B5	360	4.67	128	2	4.60×10^{11}
64B6	480	8.00	149	3	4.99×10^{11}
64B7	570	12.11	176	4	4.54×10^{11}
64B8	1440	42.53	315	3	2.80×10^{11}
64B9	1560	48.61	327	4	2.87×10^{11}
64B10	1680	53.87	338	4	2.88×10^{11}
64B11	1800	57.54	349	3	2.79×10^{11}
64B12	1920	64.61	385	4	2.32×10^{11}
64B13*	2880		530	3	

Styrene concentration: 0.870 moles l^{-1} .

Potassium persulphate concentration: 3.69×10^{-3} moles l^{-1} .

Temperature: 323 K.

* Reaction had coagulated.

TABLE 32

KINETIC CHARACTERISTICS OF REACTION 62B

Sample	Time (min)	Conversion (%)	radius (nm)	σ (%)	Number of particles (ml^{-1})
62B1	18	0.21	37	5	8.53×10^{11}
62B2	30	0.41	48	6	7.63×10^{11}
62B3	60	0.72	60	5	6.86×10^{11}
62B4	120	2.57	90	5	7.24×10^{11}
62B5	180	4.98	113	2	7.10×10^{11}
62B6	255	8.50	136	3	6.95×10^{11}
62B7	330	13.12	156	3	7.11×10^{11}
62B8	425	27.74	191	4	8.19×10^{11}
62B9	535	12.75	269	3	1.35×10^{11}
62B10	630	23.21	312	3	1.57×10^{11}
62B11	750	35.42	382	2	1.31×10^{11}
62B12	1440	63.31	714	2	0.36×10^{11}

Styrene concentration: 0.870 moles l^{-1} .

Potassium persulphate concentration: 3.69×10^{-3} moles l^{-1} .

Temperature: 333 K.

TABLE 33

KINETIC CHARACTERISTICS OF REACTION 19

Sample	Time (min)	Conversion (%)	radius (nm)	σ (%)	Number of particles (ml^{-1})
19-1	2	.12	16	14	6.82×10^{12}
19-2	5	.22	24	7	3.71×10^{12}
19-3	15	.45	39	5	1.73×10^{12}
19-4	30	.91	56	4	1.10×10^{12}
19-5	60	1.48	80	4	0.63×10^{12}
19-6	135	8.23	136	4	0.72×10^{12}
19-7	180	12.57	169	3	0.71×10^{12}
19-8	233	17.01	210	6	0.48×10^{12}
19-9	300	24.01	247	4	0.39×10^{12}
19-10	349	32.78	261	9	0.47×10^{12}
19-11	415	47.01	305	2	0.41×10^{12}
19-12	455	54.48	325	5	0.40×10^{12}
19-13	525	66.14	348	2	0.39×10^{12}
19-14	610	95.90	415	2	0.34×10^{12}
19-15	1485	95.01	422	1	0.32×10^{12}

Styrene concentration: 0.870 moles l^{-1} .

Potassium persulphate concentration: 3.69×10^{-3} moles l^{-1} .

Temperature: 343 K.

TABLE 34

KINETIC CHARACTERISTICS OF REACTION 35A

Sample	Time (min)	Conversion (%)	radius (nm)	σ (%)	Number of particles (ml^{-1})
35A1	5	0.10			
35A2	19	0.41			
35A3	40	1.72			
35A4	55	2.44	89	9	$.70 \times 10^{12}$
35A5	85	4.29	103	8	$.81 \times 10^{12}$
35A6	115	5.81	137	4	$.46 \times 10^{12}$
35A7	165	7.20	171	2	$.30 \times 10^{12}$
35A8	235	11.31	280	1	$.11 \times 10^{12}$
35A9	295	19.54	298	4	$.15 \times 10^{12}$
35A10	355	27.32	360	4	$.12 \times 10^{12}$
35A11	415	39.67	395	3	$.13 \times 10^{12}$
35A12	475	41.01	448	5	$.09 \times 10^{12}$
35A13	560	55.30	488	3	$.10 \times 10^{12}$
35A14	640	85.54	-	-	-
35A15	740	96.02	541	10	$.12 \times 10^{12}$

Styrene concentration: 0.870 moles l^{-1} .

Potassium persulphate concentration: 3.71 moles l^{-1} .

Temperature: 343 K.

TABLE 35

Kinetic Characteristics of Reaction 34B

Sample	Time (min)	Conversion (%)	radius (nm)	σ (%)	Number of particles (ml^{-1})
34B3	15	0.33	29	15	2.68×10^{12}
34B5	30	0.55	57	11	0.60×10^{12}
34B4	55	1.77	87	7	0.55×10^{12}
34B6	85	4.43	104	5	0.81×10^{12}
34B6	120	7.75	122	4	0.89×10^{12}
34B7	185	17.61	169	9	0.75×10^{12}
34B8	240	27.46	197	6	0.74×10^{12}
34B9	325	43.63	206	3	1.03×10^{12}
34B10	465	71.50	263	3	0.81×10^{12}
34B11	545	92.14	296	2	0.73×10^{12}
34B12	620	93.80	297	3	0.74×10^{12}
34B13	690	92.25	300	2	0.70×10^{12}
34B14	1440	88.70	298	3	0.69×10^{12}

Styrene concentration: 0.870 moles l^{-1} .

Potassium persulphate concentration: 3.69×10^{-3} moles l^{-1} .

Temperature: 343 K.

TABLE 36

Kinetic Characteristics of Reaction 142

Sample	Time (min)	Conversion (%)	radius (nm)	σ (%)	Number of Particles (ml^{-1})
142-1	5	0.32	-	-	-
142-2	15	0.81	35	10	3.82×10^{12}
142-3	30	1.54	51	3	2.33×10^{12}
142-4	60	3.31	75	5	1.61×10^{12}
142-5	112	5.80	107	3	0.98×10^{12}
142-6	175	12.80	141	2	0.94×10^{12}
142-7	232	21.24	163	2	1.02×10^{12}
142-8	292	32.29	189	2	0.99×10^{12}
142-9	342	47.65	206	2	1.12×10^{12}
142-10	1440	90.64	252	4	1.16×10^{12}

Styrene concentration: 0.870 moles l^{-1} .

Potassium persulphate concentration: 3.70 moles l^{-1} .

Temperature: 343 K.

TABLE 37

Kinetic Characteristics of Reaction 18B

Sample	Time (min)	Conversion (%)	radius (nm)	σ (%)	Number of particles (ml^{-1})
18B1	1	.04	14	53.5	3.31×10^{12}
18B2	5	.10	27	7.4	1.11×10^{12}
18B3	15	.32	40	3.8	1.13×10^{12}
18B4	30	.51	58	3.4	0.60×10^{12}
18B5	60	.88	83	2.4	0.75×10^{12}
18B6	120	5.28	119	3.8	0.72×10^{12}
18B7	180	10.23	147	4.1	0.74×10^{12}
18B8	240	17.82	178	3.4	0.72×10^{12}
18B9	375	33.16	222	1.4	0.69×10^{12}
18B10	430	38.23	240	1.7	$0.64 \times 10_{12}$
18B11	495	46.61	251	1.4	$0.67 \times 10_{12}$
18B12	555	55.12	272	1.7	$0.63 \times 10_{12}$
18B13	595	64.03	290	2.9	$0.60 \times 10_{12}$
18B14	1445	80.98	317	1.4	0.58×10

Styrene concentration: 0.931 moles l^{-1} .

Potassium persulphate concentration: 4.11×10^{-3} moles l^{-1} .

Temperature: 343 K.

TABLE 38

Kinetic Characteristics of Reaction 64A

Sample	Time (min)	Conversion (%)	radius (nm)	σ (%)	Number of particles (ml^{-1})
64A1	60	4.71	88	2	1.59×10^{12}
64A2	120	14.03	122	6	1.83×10^{12}
64A3	180	23.08	168	5	1.19×10^{12}
64A4	240	31.42	190	7	1.21×10^{12}
64A5	360	60.61	235	7	1.29×10^{12}
64A6	450	86.01	303	2	0.97×10^{12}
64A7	540	96.70	320	5	1.02×10^{12}
64A8	1440	98.65	317	4	1.15×10^{12}

Styrene concentration: 0.869 moles l^{-1} .

Potassium persulphate concentration: 4.11×10^{-3} moles l^{-1} .

Temperature: 343 K.

TABLE 39

Kinetic characteristics of Reaction 37B

Sample	Time (min)	Conversion (%)	radius (nm)	σ (%)	Number of particles (ml^{-1})
37B1	5	0.21	-	-	-
37B2	15	0.70	-	-	-
37B3	30	1.03	-	-	-
37B4	60	2.43	57	7	2.71×10^{12}
37B5	105	5.75	112	5	0.84×10^{12}
37B6	160	10.09	146	6	0.67×10^{12}
37B7	245	21.51	200	5	0.55×10^{12}
37B8	305	29.62	244	8	0.42×10^{12}
37B9	360	41.87	264	8	0.47×10^{12}
37B10	425	57.48	275	7	0.57×10^{12}
37B11	1440	92.10	335	4	0.54×10^{12}

Styrene concentration: 0.932 moles l^{-1} .

Potassium persulphate concentration: 4.01×10^{-3} moles l^{-1} .

Temperature: 343 K.

TABLE 40

Kinetic Characteristics of Reaction 18A

Sample	Time (min)	Conversion (%)	radius (nm)	σ (%)	Number of particles (ml^{-1})
18A1	1	0.02	16	8.5	1.01×10^{12}
18A2	5	0.09	25	5.4	1.18×10^{12}
18A3	15	0.18	41	5.6	0.60×10^{12}
18A4	30	0.44	-	-	-
18A5	60	2.00	77	1.8	0.99×10^{12}
18A6	120	6.11	110	2.4	1.05×10^{12}
18A7	180	11.88	136	1.2	1.09×10^{12}
18A8	240	19.18	162	3.8	1.03×10^{12}
18A9	375	33.37	203	2.2	0.91×10^{12}
18A10	430	44.35	216	1.5	1.01×10^{12}
18A11	495	55.48	236	1.5	0.96×10^{12}
18A12	555	79.65	275	1.1	0.87×10^{12}
18A13	595	80.97	278	2.8	0.86×10^{12}
18A14	1445	81.46	279	3.1	0.85×10^{12}

Styrene concentration: 0.931 moles l^{-1} .

Potassium persulphate concentration: 4.11×10^{-3} moles l^{-1} .

Temperature: 343 K.

TABLE 41

Kinetic Characteristics of Reaction 62A

Sample	Time (min)	Conversion (%)	radius (nm)	σ (%)	Number of particles (ml^{-1})
62A1	3	0.20	21	10	4.43×10^{12}
62A2	6	0.55	33	5	3.10×10^{12}
62A3	15	1.68	50	6	2.74×10^{12}
62A4	30	2.72	73	4	1.42×10^{12}
62A5	45	4.57	89	3	1.34×10^{12}
62A6	63	8.94	111	4	1.35×10^{12}
62A7	91	19.15	145	9	1.29×10^{12}
62A8	120	22.45	152	5	1.32×10^{12}
62A9	183	55.03	204	6	1.34×10^{12}
62A10	250	89.01	244	7	1.26×10^{12}
62A11	340	90.42	240	11	1.35×10^{12}
62A12	480	90.90	242	8	1.31×10^{12}
62A13	1440	92.40	244	7	1.32×10^{12}

Styrene concentration: 0.870 moles l^{-1} .

Potassium persulphate concentration: 3.70×10^{-3} moles l^{-1} .

Temperature: 353 K.

TABLE 42

Kinetic Characteristics of Reaction 66A

Sample	Time (min)	Conversion (%)	radius (nm)	σ (%)	Number of particles (ml^{-1})
66A1	2	0.52	24	8	7.13×10^{12}
66A2	5	2.33	38	5	8.67×10^{12}
66A3	10	5.51	50	8	9.06×10^{12}
66A4	20	7.49	68	13	5.00×10^{12}
66A5	30	11.97	97	4	2.67×10^{12}
66A6	45	19.51	117	5	2.47×10^{12}
66A7	60	27.02	135	4	2.27×10^{12}
66A8	75	37.01	149	12	2.27×10^{12}
66A9	90	46.21	163	12	2.20×10^{12}
66A10	110	60.00	180	6	2.13×10^{12}
66A11	130	77.82	196	7	2.13×10^{12}
66A12	160	92.61	210	5	2.07×10^{12}
66A13	220	92.20	208	6	2.13×10^{12}

Monomer concentration: 0.870 moles l^{-1} .

Potassium persulphate concentration: 3.71×10^{-3} moles l^{-1} .

Temperature: 363 K.